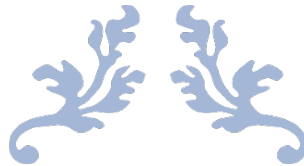# CARDIFF UNIVERSITY

Development of a series of modified acridinium esters for use in clinical diagnostics

BY

Mesfer M Alamri

Thesis submitted to Cardiff University in partial fulfilment of the requirements for the award of the Degree of Doctor of Philosophy (PhD)

بسم الله الرحمن الرحيم

ACKNOWLEDGEMENTS

ABSTRACT

Acridinium esters (AE) have been traditionally used as chemiluminescent reporter molecules in clinical diagnostic assays due to their high quantum yields and detection limits in the attomole range. The aim was to produce a family of novel acridinium esters with modified chemiluminescent properties for use in clinical diagnostics. The hypothesis was that, by changing the substituents on the acridinium ring and the phenoxy ring of the acridinium ester molecule, a series of compounds with distinct chemiluminescent characteristics could be generated which would support dual analyte measurement.

Two series of compounds were synthesized based on the addition of two methoxy (electron donating) or two bromo (electron withdrawing) groups to the 2 and 7 positions of the acridinium ring. Additionally, the effect of adding methyl or methoxy groups to the 2- and 6-positions of the phenoxy ring of the acridinium ester molecule was compared to the unsubstituted state. Five distinct acridinium esters were synthesized and their excitation and emission spectra determined. Two of the compounds were linked to a DNA oligonucleotide and incorporated into a Hybridisation Protection Assay (HPA), a direct and highly specific nucleic acid assay. The performance of these chemiluminescent labelled probes within the HPA (kinetics of light output and the rate of hydrolysis) was characterised.

Major findings included a shift in the fluorometric spectra resulting from the substitution on the acridinium ring, resulting in the peak emission wavelengths of *N*-methylacridone, 2,7-dibromo-10-methyl-9-acridone and 2,7-dimethoxy-10-methyl-9-acridone being observed at 430, 440 and 480 nm, respectively. Furthermore, the optimal pH for discrimination between hybridised and unhybridised probes for the dimethoxy-substituted acridinium ester **34cx** was between 9.2 and 9.6 whilst the pH optimum of the routinely used unsubstituted compound **15** ranged from 7.5 to 8.5.

Theoretically, the differential properties of dimethoxy-substituted AE DNA probes, the shift in emission wavelength and hydrolysis pH, may form the basis for a novel dual analyte HPA format to be developed.

LIST OF ABBREVIATIONS

^{13}C NMR	Carbon-13 nuclear magnetic resonance.
^{1}H NMR	Proton magnetic resonance.
Ab	Antibody.
Ag	Antigen.
ATP	Adenosine triphosphate.
bDNA	Branched nucleic acids.
calc	Calculated
cat	Catalyst.
CCDC	Cambridge Crystallographic Data Centre.
$CDCl_3$	Deuterated chloroform
CL	Chemiluminescence.
CLIA	CL immunoassay .
CT	Charge transfer.
CVs	Coefficient of variations.
DCC	1,3-dicyclohexylcarbodiimide.
DCE	1,2-Dichloroethane.
DCM	Dichloromethane.
DCU	Dicyclohexylurea.
DKA	Dual Kinetic Assay.
DMAP	4-Dimethylaminopyridine.
DMF	N,N-Dimethyl formamide.
DMSO	Dimethyl sulfoxide
DNA	Deoxyribonucleic acid.
ECL	Electrochemiluminescence.
EDTA	Ethylenediaminetetraacetic acid
EIA	Enzyme immunoassay.
EPR	Electron paramagnetic resonance.
ES-MS	Electrospray Ionization Mass Spectrometry.
ET	Electron transfer.
EtOAC	Ethyl Acetate.
GCMS	Gas chromatography–mass spectrometry.
H_2O_2	Hydrogen peroxide.

HIV	Human immunodeficiency virus.
HIV-WT	Human immunodeficiency virus-World type.
HPLC	High-performance liquid chromatography.
HRMS	High-resolution mass spectrometry.
hυA	photon Absorption.
hυF	photon Fluorescence.
hυP	photon Phosphorescence.
IC	Internal conversion.
IR	Infrared spectroscopy.
ISC	Intersystem crossing.
LDS	Lithium dodecyl sulfate.
LE	Locally excited state.
MeCN	Acetonitrile.
MS	Mass spectrometry
NASBA	Nucleic Acid Sequence Based Amplification.
NHS	N-hydroxysuccinimide.
PCR	Polymerase chain reaction .
PL	Photoluminescence.
PO-CL	Peroxyoxalate chemiluminescence.
RIA	Radioimmunoassay.
RLUs	Relative light unit.
RNA	Ribonucleic acid.
s	Second.
S_0, S_1, S_2, T_1	Electron energy levels (singlet, triplet).
SDS	Sodium dodecyl sulfate.
SET	Single electron transfer.
ssDNA	single-stranded DNA.
THF	Tetrahydrofuran.
UV-vis	Ultraviolet-visible absorption spectroscopy.
μs	Microsecond.
Φ_{CE}	Chemiluminescence excitation quantum yield.
Φ_{CL}	Chemiluminescence quantum yield,
Φ_F	Fluorescence quantum yield.

TABLE OF CONTENTS

LIST OF FIGURES

LIST OF TABLES

Chapter 1

Introduction

1. Introduction

1.1 Luminescence

The word luminescence was first used by a German physicist, Eihardt Wiedemann in 1888. He also classified luminescence into six kinds according to the source of energy used to obtain the excited state.[1] The luminescence methods are recognized as a phenomenon of the emission of light because of the chemical reaction.[2] In this reaction product is formed in an electronically excited state. When the electron returns to the ground state, energy is released in form of light as a photon.[3] Wiedemann recognized photoluminescence, thermoluminescence, electroluminescence, crystalloluminescence, triboluminescence, and chemiluminescence. In photoluminescence, light energy absorbed by a material promotes an electron into a higher energy state. This energy is then re-emitted as the electrons fall back into their lower energy state. The light emitted is at a longer wavelength (lower energy) than the light absorbed because some of the energy is dissipated as excited state species relaxes to its vibrational ground state. Luminescence can be induced by generating an excited state species using other sources of energy and the processes are designated according to the source of the energy that delivers the excited state, including electroluminescence, chemiluminescence, bioluminescence, etc. Luminescence can be subdivided into two types: fluorescence and phosphorescence.[4] (Figure 1.1). A major difference between these two types of luminescence is the half-life of the excited state. Fluorescence is different from phosphorescence in that the electronic transition responsible for fluorescence does not involve a change of spin state during the transition from a singlet excited state (such as S_1) to the ground state (S_0), which results in a short-lived ($<10^{-5}$ s) excited state for fluorescence. In terms of phosphorescence, there is

a change of spin state during the transition, from a triplet state (T_1) to the ground state, which results in a longer lifetime of the excited state (seconds).[5] Chemiluminescence (CL) occurs when a chemical reaction results in an excited state product, which then returns to the ground state by emission of light and is used as detection mode.[6,7] Both organic and inorganic chemical reactions may result in such emissions. Chemiluminescence detection has been utilized in a variety of formats including immunodiagnostics [8–10] and DNA probe-based assays.[11–15] Nature uses CL (called bioluminescence) as a subset of chemiluminescence, where the emission of light is based on a chemical reaction that occurs within a living organism such as fireflies, mushrooms, jellyfish, and bacteria.[16,17]

In biological systems, bioluminescence occurs from *in situ* enzyme-catalysed chemical transformations, for example, Luciferin reacts with oxygen in the presence of luciferase enzyme,[18,19] calcium or magnesium ions and adenosine triphosphate (ATP) leading to luminescence.[20,21]
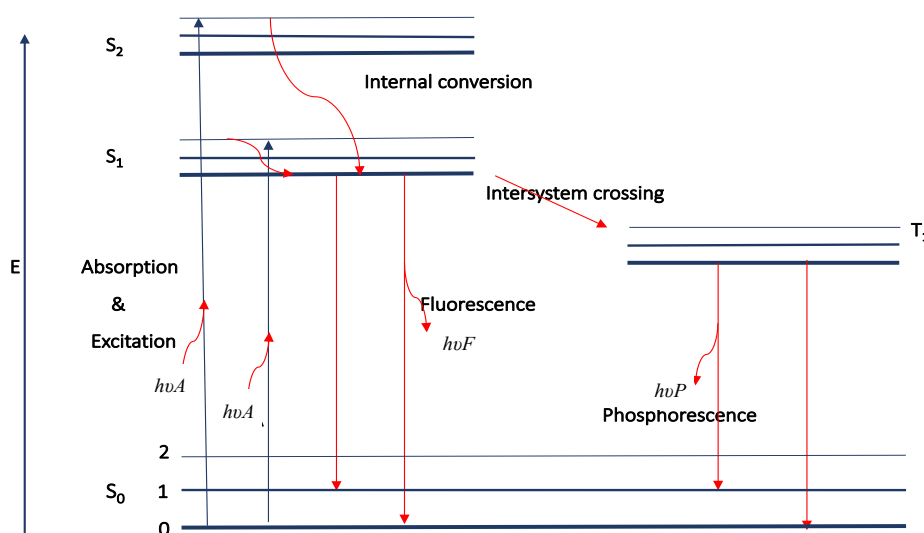
Figure 1. 1: A simplified Jablonski diagram showing photon absorption (hυA), excitation, internal conversion, intersystem crossing, fluorescence (hυF), phosphorescence (hυP). (S_0, S_1, S_2, T_1 are electron energy levels).

In some cases, the chemiluminescent excited species is the product of a reaction between an analyte and an appropriate reagent (usually a strong oxidant). In such a procedure, light emission can be used to measure the amount of analyte present. The basic requirements for measuring the chemiluminescence are very simple; they consist of the analyte, the reagent and the luminometer only. There is no other light source to create background noise and lower the detection limit and sometimes quantum yields can be relatively high.

Two main categories of chemiluminescent reaction have been described in the literature, direct and indirect, depending on whether the initial excited product emits the light (direct chemiluminescence) which can be represented by:

$$\textit{Direct chemiluminescence} \quad A + B \longrightarrow [\ IH\ ]^{*} \longrightarrow Product + Light$$
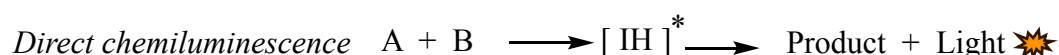
or whether the initial excited product transfers its energy to a fluorescent acceptor which then emits light (indirect chemiluminescence, also referred to as energy transfer chemiluminescence) which is represented by:

$$\textit{Indirect chemiluminescence} \quad A + B \longrightarrow [\ I\ ]^{*} + F \longrightarrow [\ FH\ ]^{*} \longrightarrow F + Light$$
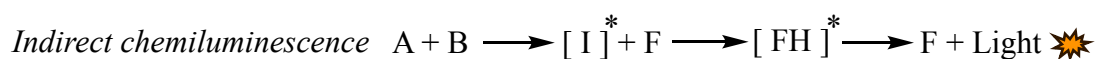
Extensive studies of chemiluminescence have been comprehensively reviewed in number of textbooks and articles in recent years.[22–27] Currently, there are five classes of chemiluminescent used in different fields: acridinium derivatives, acyl hydrazides (luminol & isoluminol), coelenterazine, dioxetanes and peroxyoxalic derivatives. The most known

chemiluminescent reactions involve oxidation by oxygen or hydrogen peroxide. The chemical reactions take place during the chemiluminescence of acridinium ester. A representative example is the oxidation of acridinium derivatives with alkaline hydrogen peroxide (Figure 1.2), which produces *N*-methylacridone (**2**) in its excited state, and this emits light as it decays to the ground state as a final product (**3a**). For organic compounds, the most common luminescence bands are due to $\pi*-\pi$ and $\pi*-n$ transitions. The $\sigma*-\sigma$ transition, although allowed, is not normally seen due to its high energy in most organic compounds.
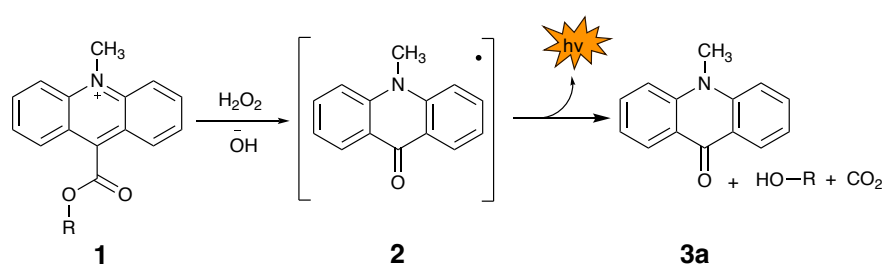
Figure 1. 2: Typical example of direct CL of an acridinium ester.

The nature of the substituents on aromatic rings may increase or decrease both the wavelength and the quantum yield of the emission. For example, in a recent study of substituent effects on absorption and fluorescence of anthracene, halogen and ketone substituents were shown to decrease the fluorescence quantum yield.[28] In photoluminescence, the quantum yield (Φ) is the ratio of the number of photons emitted to the number of photons absorbed. Therefore, the maximum value of Φ is 1. Practically, Φ is always less than 1, because of many non-radiative processes that lead to a decrease in the number of emitted photons.[29]

To achieve a high level of sensitivity, a chemiluminescence reaction must be efficient in producing the excited product molecule and the excited species must be efficient at emitting light. The excited molecules can be either the final product or an intermediate molecule of the reaction. The excited molecule can also relax to its ground state without a photon emission *via* dark routes based on chemical reaction, collisional deactivation, transition internal conversion or interference system crossing. The intermediate depends on the pH leading to the formation of an excited state and light emission.[30] Unlike luminol and its derivatives, acridine chemiluminescence has no catalytic requirement for production of a high quantum yield, Φ_{CL}, which can be represented by the following equation:

$$\Phi_{CL} = \Phi_R * \Phi_{CE} * \Phi_F$$

Where; Φ_{CL} is the overall probability of generating light in the reaction (the ratio of the number of photons emitted to the number of molecules of reactant reacting);

Φ_R is the reaction yield (proportion of reacting molecules that give the desired product); Φ_{CE} is the chemi-excitation quantum yield (proportion of product molecules that are excited); and. Φ_F is the fluorescence quantum yield (proportion of excited product molecules that emit light in going to the ground state).

The Franck-Condon principle relates to the interaction between electronic and vibrational motions and plays an important role in understanding the nature of electronic transitions and differences in the bonding properties of excited states relative to the ground state (Figure 1.3). According to this principle, absorption is an almost instantaneous process while nuclear movement is relatively slow because nuclear masses are much larger than the electron mass.
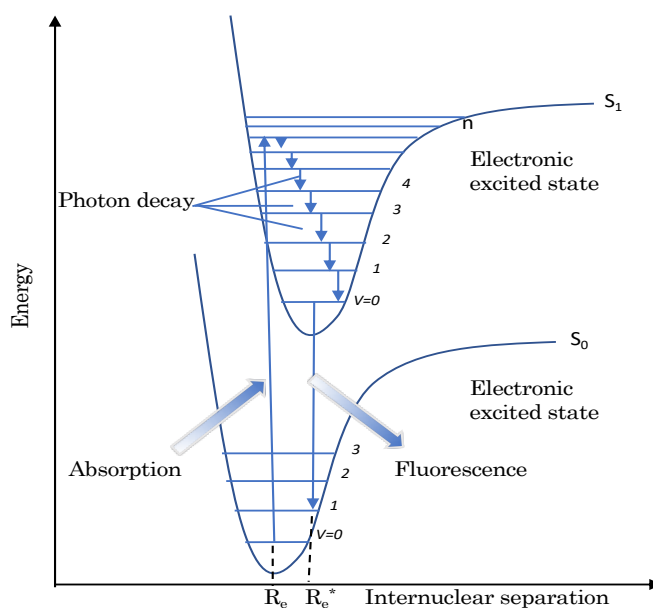
Figure 1. 3: Potential energy curves for the ground state and an excited state of a molecule. (r, interatomic distance; A, the vertical electronic transition is allowed for absorption; B, fluorescence; numbers indicate vibrational states.).

Franck-Condon principle states that electronic transitions between singlet states are so rapid (within femtoseconds) that the nuclei may be assumed to be static during the time scale, which is so fast compared with nuclear motion. Therefore, such transitions are drawn as vertical lines in energy level diagrams of the type shown in Figure 1.3, which illustrates an appropriate vertical transition A (giving a higher vibrational state of the S_1 excited singlet state), and a transition B (giving a higher vibrational level of the ground state S_0).

1.2   Categories and history of chemiluminescence

Chemiluminescent phenomena are observed in a wide spectrum of situations and have been observed for over two thousand years. However, the first chemical description of chemiluminescence was by Radziszewski, who observed yellow light emission when he

mixed 2,4,5-triphenylimidazole (lophine, **4**, Figure 1.4) with a strongly alkaline solution in

the presence of oxygen.[31] The most important observation in the study was that the

lophine does not emit light when heated by itself. This led to the term luminescence being

defined based on the source of the light emitted. The first study of light emission occurs

through a chemical reaction was described by Wiedemann, but the mechanism of the

reaction was not fully described.[32]
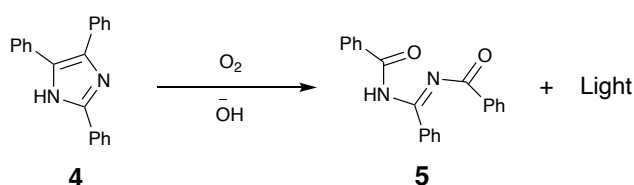
Figure 1. 4: The reaction of lophine (4) with oxygen in a strongly alkaline environment to produce light emission.

Luminol, isoluminol and its derivatives: Chemiluminescence continued to be

studied during the early twentieth century. In 1905, Trautz [33] reported the first review of

known chemiluminescent reactions and attributed them to the action of active oxygen. He

also described the luminescence properties of reactions of several organic compounds with

various oxidants. Another important discovery was the ability of luminol (5-amino-2-3-

dihydro-1,4-phthalazinedione, **6**) to undergo a chemiluminescent reaction on alkaline

oxidation. The first report was described by Albrecht in 1928.[34] He found that blood,

among other substances, enhanced the luminescence of luminol in an alkaline solution of

hydrogen peroxide. The chemiluminescence mechanism of luminol derivatives follows the

scheme shown in (Figure 1.5). The most likely starting point appears to be the oxidation

of the cyclic diacyl hydrazine moiety to give an azaquinone. The intermediate product is

obtained by oxidization of the heterocyclic ring. The first step is strongly dependent on the composition of the medium, the decomposition of the intermediate depends on the pH of the system and leads to the excited state and light emission.[30] The optimum reaction pH varies between 8 and 11, depending on the catalyst. During the 1930's Drew and co-workers [35] established some aspects of the structure of hydrazide derivatives and they found that electron-donated groups increased the quantum yield while electron-withdrawn groups reduce the quantum yield.
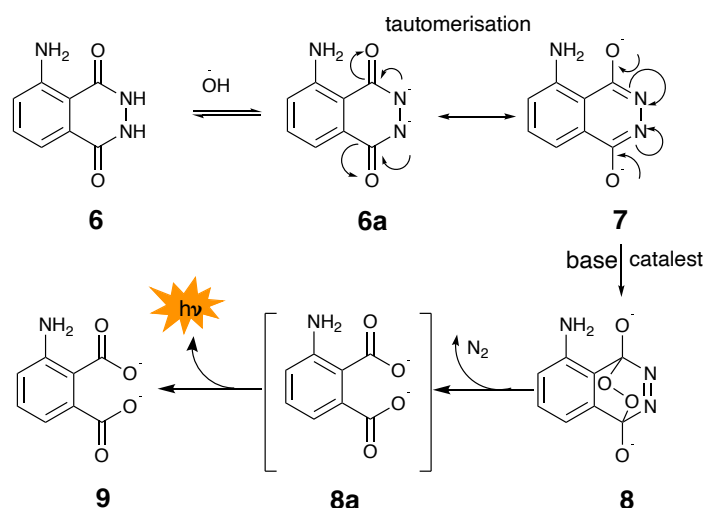
Figure 1. 5: Mechanism of the luminol chemiluminescence reaction.

Since that time, several luminol derivatives have been synthesized and used as chemiluminescent reagents in environmental and medical fields.[36,37] Various studies have been conducted on compounds that are structurally like luminol to improve the overall quantum yield (ϕ_{cl}). Sarabia *et al.*[38] in a recent study, measured the degree of chemiluminescence of luminol in relative light units (RLU) using a luminometer. This method differed from previous studies as that use the luminometer to measure the chemiluminescence reaction caused by the luminol, resulting in an accurate and

quantitative measurement. Luminol and isoluminol were the first chemiluminescence molecule to be tested in immunoassays and have been applied in a broad field including immunoassays or non-immunoassays diagnostics because oxidation of luminol derivatives led to the identification of labelled antigens or antibodies. Rongen in an excellent review [39] suggest more than 60 immunoassays from different classes of luminol derivatives (figure 1.6, compound **6**, **6b** and **6c**). For the application in immunoassays, more isoluminol derivatives were synthesized because the emission intensity of luminol was diminished substantially by alkylation and particularly acylation of the 5-amino-substituent of luminol.[40] They found that 6-aminoisomer, isoluminol, further enhance efficiency on alkylation and finds use in derivative form.
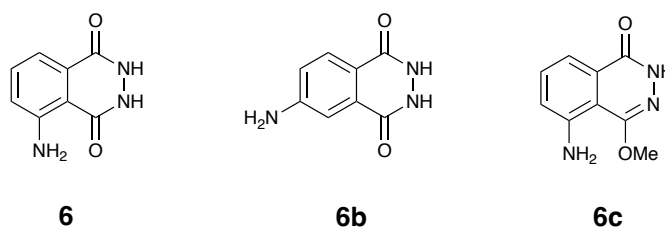
Figure 1. 6: Structure of luminol (6), Isoluminol (6b) and O-methyl luminol

Coelenterazine [41] is a luciferin, a light-emitting biomolecule that serves as a substrate for luciferases or as a constituent of photoproteins, including aequorin. Coelenterazine can take part in chemical reactions outside of biological systems through chemiluminescence. The chemical structure of coelenterazine of natural type (figure 1.7) was determined, it has been synthesized in different ways and used as a chemiluminescence reagent triggered by superoxide anion.[42–44] In contrast with luminol, the coelenterazine reaction is very specific and no need for physical separation to remove hydrogen peroxide

from the median before determination. The oxidation of coelenterazine to coelenteramide is accompanied by the emission of blue light (emission maximum, 460-470 nm).[45]
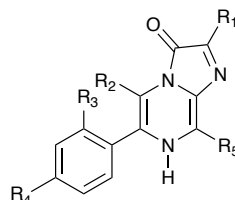
Figure 1. 7:The structure of coelenterazines, (R_1= p-CH$_2$C$_6$H$_4$OH, R_2 = R_3 = R_4 = R_5 = H)

The synthesis of coelenterazine analogues made it possible to prepare various semi-synthetic aequorins, which consequently allowed researchers to investigate the effect of functional groups on the chemiluminescence properties. Several modification substitutions are inserted to different positions of the compound and the result is that; the introduction groups do not significantly affect the CL intensity but in some cases hinder deleterious interaction with bovine serum albumin and allow covalent of the compound.

Dioxetanes are four-membered, organic, saturated oxygen heterocycles comprised of two adjacent oxygen and two carbon atoms in a cyclic system (figure 1.8). The relative stability of dioxetanes depends on the types of substituent groups present.[41,46] Dioxetane derivatives are decomposed thermally or chemically into two carbinolic compounds. One of which is in the excited state, a very high yield obtained during the emission process, but it is rapidly quenched in an aqueous solution because of the predominant are in the T_1 state, therefore, it has poor utility in diagnostics applications.
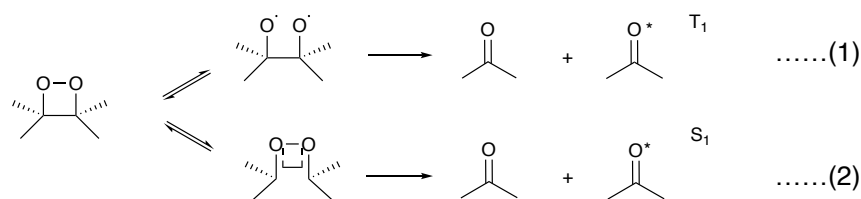
Figure 1. 8: The two modes of 1, 2-dioxetane decomposition; 1) the diradical mechanism (triplet excited state (T_1)), and 2) the chemically initiated electron exchange CL (singlet excited state (S_1)).

Peroxyoxalate chemiluminescence (PO-CL), is a designation used for the reaction between hydrogen peroxide and activated derivatives of oxalic acid in the presence of a fluorescent substance (a sensitized or indirect chemiluminescent reaction).[47] The first example of PO-CL was reported [48] and studied the reaction of oxalyl chloride with hydrogen peroxide in the presence of a fluorescent compound. light is emitted from a sensitizer molecule, or fluorophore, FL, that gains its excitation energy from intermediates appearing along the reaction path, rather than directly from excited species formed in the reaction. The main overall reaction can be summarized as:

$$R\text{-}CO\text{-}CO\text{-}R + H_2O_2 \xrightarrow{FL} 2CO_2 + 2RH + h\upsilon$$
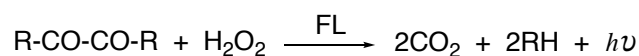
Peroxyoxalic chemiluminescence gives the most efficient high-emitted reactions from a synthetic molecule.[49] In contrast, peroxyoxalate chemiluminescence compounds (figure 1.9) produced a high energy intermediate but no florescent therefore cannot emit light by itself. However, the reaction with hydrogen peroxide emits light through energy transfer to the fluorescer which is exited in the S_1 state. The high background is frequently observed

in peroxalate chemiluminescence because of the decomposition of the intermediate process.
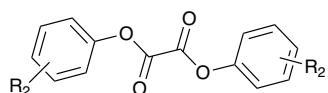
Figure 1. 9: The structure of peroxyoxalic acid derivatives

Acridinium derivatives: The advantages of the chemiluminescent properties of acridinium salts were first noted in a study of lucigenin (**10**), (bis-(*N*-methylacridinium) nitrate) in 1935 by Gleu and Petsch.[50] The compound is oxidized in an alkaline environment to form *N*-methylacridone (**3a**) and generates light emission at 430 nm. After the discovery of the properties of lucigenin, extensive studies were focused on related compounds. These studies led to the recognition that generally acridinium salts such as **11** emit light when oxidized by hydrogen peroxide under alkaline conditions. For example, in the 1960s, several acridinium compounds were synthesized, including 9-cyano-10-methylacridinium nitrate (**12**), 9-carboxy-10-methylacridinium chloride (**13**) and 9-chlorocarbonylacridine hydrochloride (**14**) (Figure 1.10), and used in many investigations at that time.[51–53]

By the second half of the 20th century, scientists were stimulated to study the reaction mechanism which caused chemiluminescence in such acridinium salts. In 1964, McCapra and his co-workers studied the reaction of 9-cyano-10-methylacridinium nitrate (**12**) with H_2O_2 in an alkaline alcoholic solution.[54] They found that the emitted light had a maximal wavelength of 430 nm and the spectrum obtained was identical to the fluorescence spectrum of *N*-methylacridone (**3a**). The proposed mechanism involved an initial

nucleophilic attack by hydroperoxide anion to form an unstable 1,2-dioxetanone derivative before decomposing to form *N*-methylacridone (**3a**).
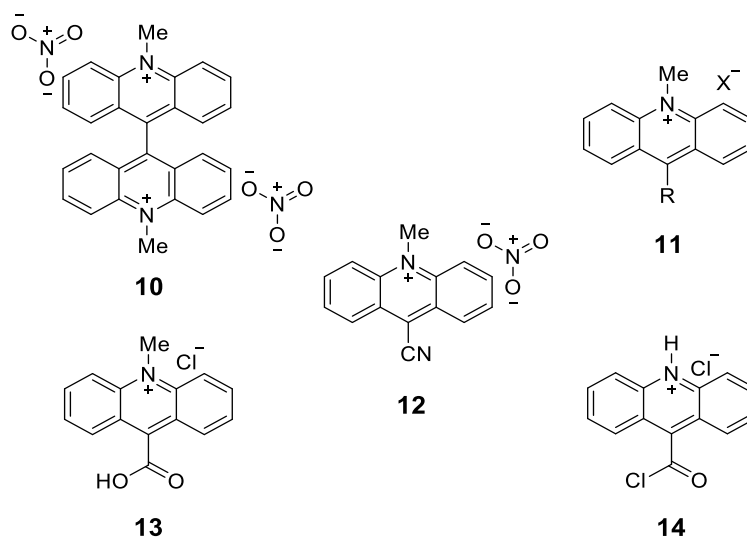
*Figure 1. 10: Examples of chemiluminescent molecules; lucigenin (**10**), a general acridinium salt (**11**), 9-cyano-10-methylacridinium nitrate (**12**), 9-carboxy-10-methylacridinium chloride (**13**) and 9-chlorocarbonylacridine hydrochloride (**14**).*

Extensive studies were continued on acridinium derivatives; for example, Rauhut studied the chemiluminescent reaction of 9-chlorocarbonyl-10-methylacridinium chloride (**14**) in the presence of H_2O_2.[53] The study found that the chemiluminescence intensity and the reaction rate are strongly affected by pH; the reaction at low pH (4.0) provides a weaker light emission than the emission obtained at neutral pH, but at a longer wavelength. From these studies, it is seen that one requirement for chemiluminescence in these systems is the presence of a good leaving group so that aryl esters exhibit the phenomenon better than aliphatic esters.

1.2.1 Acridinium Esters

The discovery of the chemiluminescence properties of acridinium salts started with lucigenin (*bis-N*-methylacridinium nitrate, **10**), which is oxidized to form *N*-methylacridone (**3a**) and emits light at 430 nm in an alkaline environment.[50] A mechanism was proposed for this reaction which is like the CL reaction of acridinium esters. Extensive studies covered classes of acridinium salts including acridinium esters as compounds that emit light when oxidized by hydrogen peroxide in the presence of alkaline species. The synthesis of a commercially useful acridinium ester (AE, **15**, Figure 1.11) has been previously reported by Weeks in seven steps and the reaction mechanism has also been well studied.[55,56] AEs have proven to be useful chemiluminescent labels providing the advantages of stability with a high quantum yield and extremely accurate quantitation. The reactions of AEs are very simple, involving treatment with alkaline peroxide to yield light emission (typically 1 to 5 s, Figure 1.11) with a maximal wavelength 430 nm (from unsubstituted acridinium esters), which can be measured using a standard luminometer. The chemiluminescent wavelengths of AEs are mainly dependent on the nature of functional groups on the acridinium ring.[56] The reaction involves oxidative cleavage in the presence of alkali to yield a dioxetanone intermediate that breaks down to give an excited *N*-methylacridone (**3a**) product. The use of acridinium esters in detection systems offers comparable efficiency and background signal to the use of isotopes, but without the disadvantages associated with handling radioactive materials. Consequently, derivatives of acridinium esters have come to play an important role in chemiluminogenic assays of biological molecules, acid-base and redox titrations, determination of molecular oxygen, organic compound determination and in other areas.[57–59]
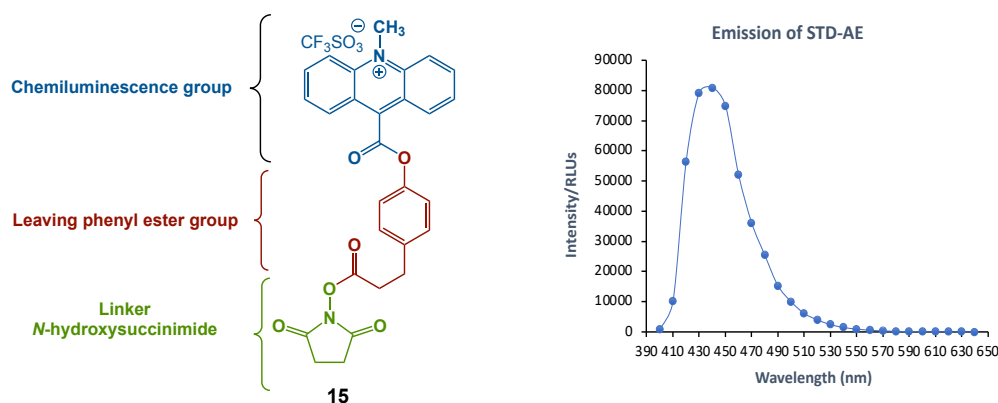
*Figure 1. 11: Chemical structure of an acridinium NHS ester (**15**) to the left; the emission signal of the chemiluminescence reaction of **15** with alkaline peroxide.*

As a result of the effectiveness of acridinium esters in immunoassay, much effort has been devoted to their structural modification, to improve stability and chemiluminescence properties. For example, chemiluminescent acridinium ester labels containing two methyl groups in the 2- and 6-positions of the phenoxy ring of the leaving group are used in clinical diagnostics and show significantly improved hydrolytic stability at neutral pH (7.4) compared to compound **15**. [60–62] Since acridinium esters have relatively strong chemiluminescence intensity among chemiluminescent compounds, various derivatives have been synthesized and used to label antibodies using different strategies to improve the stability and emission properties based on the chemical structure of acridinium compounds.[60] More efficient chemiluminescence compounds have been found in the thiol and sulfonamide derivatives and show five times more luminogenic than EA-NHS.[63,64] Attempts to improve the stability in the phenol leaving group have led to the presence of AE-NHS with leaving group substituted with 2,6-dimethyl, 2,6-dimethoxy and 2,6-dibromo groups.[63,65,66] Electron-withdrawing groups introduced into the phenyl ring increase both the efficiencies and the reaction rates while electron-donating groups have the opposite effect.[67] Moreover, detailed studies have been reported on a family of

acridinium ester-based chemiluminescent labels for proteins that determined some structural and environmental features that affect the emission properties. One study [68] involved the introduction of 2-alkoxy groups onto the acridinium ring. In another study,[69] they described the synthesis and properties of two hydrophilic acridinium dimethylphenyl esters that had differently charged *N*-sulfopropyl functional groups attached to the nitrogen atom of the acridinium ring. Such modifications, along with the use of surfactant, can give improved light output. Recently, Nakazono *et.al.*[70] studied the effect of the introduction of an electron-withdrawing group at the 4-position of the phenyl and biphenyl moieties. They found that inserting cyano, methoxycarbonyl or nitro groups at the 4-position was very effective for increasing the chemiluminescence intensity under natural conditions (pH 7). For example, 3,4-dicyanophenyl-10-methylacridinium-9-carboxylate trifluoromethanesulfonate showed approximately 100 times stronger emission than that of phenyl-10-methylacridinium-9-carboxylate trifluoromethanesulfonate at pH 7. All these studies show significant information about the development of chemiluminescent acridinium esters.

In the presented study, we have focused on the synthesis of families of aryl acridinium esters containing two different groups (Br, OMe) on the 2- and 7-positions of the acridinium ring and alkoxy groups attached to the 2- and 6-positions of the phenoxy ring.

1.2.2 Mechanism of chemiluminescence reaction of AEs

The mechanism of acridinium derivatives has been studied in detail by McCapra.[55,56] The most probable accepted mechanism is presented in figure 1.12 with the alternative routes suggested by McCapra. All intermediate compounds have been isolated and characterized except the dioxotanone.[71] In contrast to lucigenin and luminol, no catalyst

is involved in the acridinium ester chemiluminescence reaction., only hydrogen peroxide and a strong base being required. The reaction of acridinium derivatives is triggered first by the addition of hydroperoxide anion to C-9 of the acridinium ring in an alkaline environment, followed by cleavage of the leaving group to form an unstable intermediate 1,2-dioxetanone compound.[72] The unstable compound decomposes to form an acridone in its electronically excited state. Light emission occurs when the electron reverts to its ground state. The formation of the 1,2-dioxetanone intermediate has not been demonstrated experimentally, but it has been studied theoretically by Rak,[73] who together with his co-workers proposed that the cleavage of the leaving group and the formation of excited 10-methyl-9-acridone occur simultaneously.
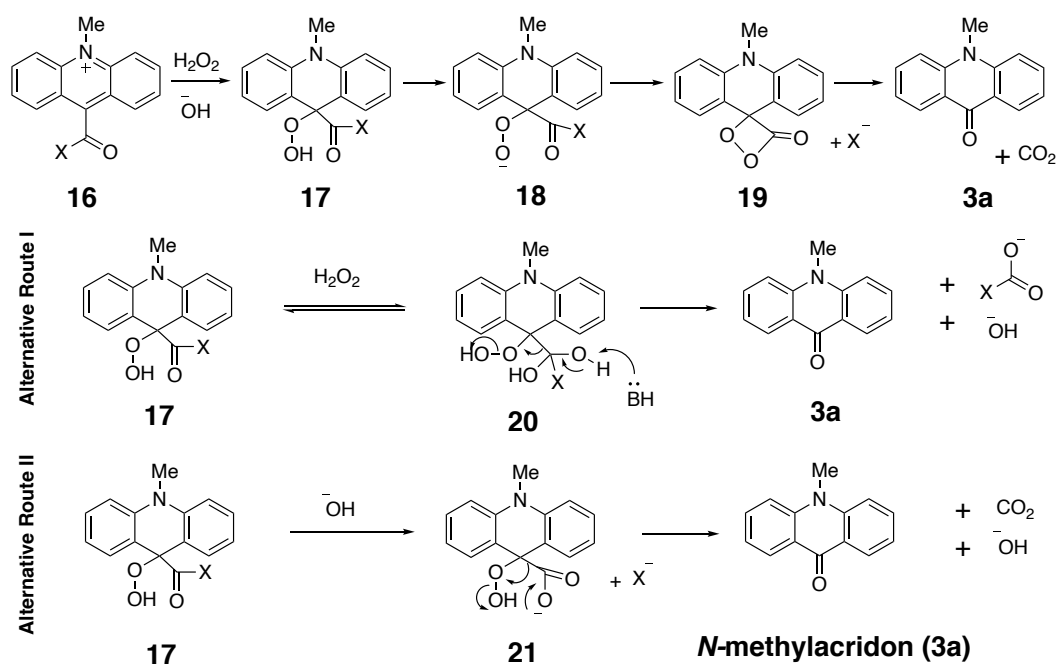
Figure 1. 12: The probable mechanism for acridinium derivatives and possible alternative routes.[41]

In 1964, McCapra and Richardson[54] studied the reaction of 9-cyano-10-methylacridinium nitrate with hydrogen peroxide in ethanolic solution and they found that the emitted light had a maximum wavelength of 430 nm, and the spectrum was identical to the emission spectrum of *N*-methylacridone (**3a**).

1.3   Development of the first immunoassays

The first immunoassay was described by Yelaw and Berson[74] to analyse nanomolar concentrations of hormones in biological fluids using ^{125}I as a label and it was therefore named radioimmunoassay (RIA). RIA is an extremely sensitive method for measuring a very small amount of a substance in many biofluids including urine and blood but requires specialized equipment.[75] RIA methods are reliable and accurate; however, they suffer from the problems associated with radioisotopes, which restrict their use in special laboratories, and from the drawback of the short half-life of ^{125}I as a label.

Radioimmunoassay is based upon the competition between radio-labelled antigens and unlabelled antigens to high-affinity specific antibody binding sites, with which they form antigen-antibody complexes.[76] In one form of this assay, a quantity of the antigen of interest is tagged with a radioactive isotope (e.g. ^{125}I) and mixed with a known amount of its antibody, excess antigen is then removed by washing (figure 1.13). Subsequently, the unlabelled antigen is added and competes with the radio-labelled antigen to bind the antibody. Thus, displacing the radioactive antigen in proportion to the amount of unlabelled antigen present. After separation, the precipitated antibodies and/or the supernatant solution can then be measured for radioactivity. The standard curve, which can be generated using unlabelled antigens of known concentrations, shows the relationship between the unlabelled antigen and radioactivity, and from that plot, the concentration of

the antigen can be determined. RIA techniques are still used, especially for peptide quantitation, because of their extremely low picomolar detection limits and sometimes because it is useful to obtain data for comparison with historical data from previously approved peptide drugs. Most alternative methods to RIA have not been adopted since they display reduced sensitivity, and stability, or exhibit molecular size restriction when compared to RIA. However, chemiluminescence immunoassay using acridinium esters does provide a direct replacement of isotopes in immunoassays, showing equivalent properties in most respects and therefore offering a practical alternative. They exhibit a long shelf life, wide analyte applicability, display attomolar sensitivity and can be used on robust technological platforms.[77]
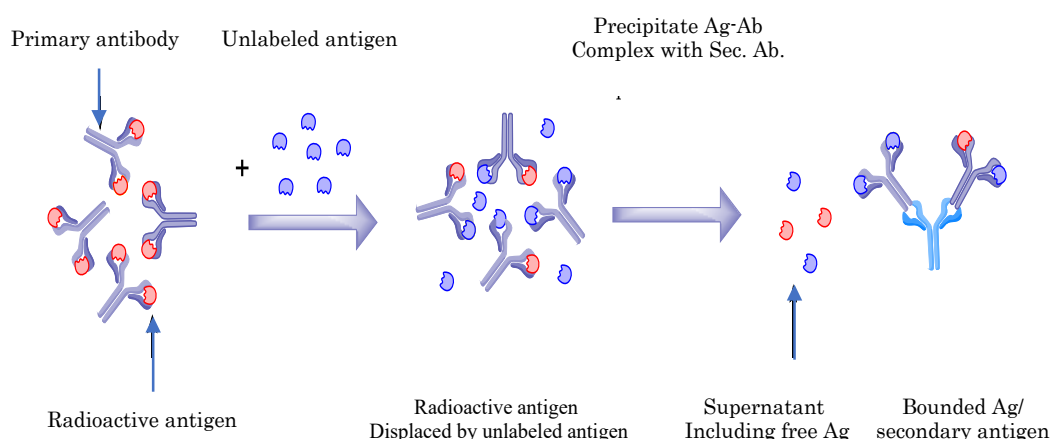
Figure 1. 13: Schematic for RIA assay. The radioactive antigen is added to the antibody, followed by the addition of an unlabeled antigen. The antigen-antibody complex is precipitated using a secondary antibody to separate bonded antigens. From the data obtained, a standard curve can be drawn, and the antigen's concentration can be read directly from the standard curve.

1.4   The application of chemiluminescence in biomedical detection

Since the development of RIA, many assays that have a similar format based on the binding reaction between antibody and antigen have been developed because of their impressive sensitivity and specificity. Chemiluminescent molecules such as lucigenin, luminol and acridinium esters have all been used in immunoassays.[74,78] The use of luminol and a derivative of isoluminol as chemiluminescent labels depends on the coupling of the immunoassay with enzymatic reactions catalysed by peroxidase. Development of a competitive protein binding assay for biotin using luminol as a chemiluminescent reagent was reported.[79]

Chemiluminescence immunoassays based on the non-radioactive cyclic hydrazide, luminol, dioxetanes and derivatives of oxalic acid have been used as detection methods in clinical fields for many years. The combination of the amplification properties of an enzyme and a chemiluminescence detection reaction provides a highly sensitive analytical system. Despite their high sensitivity and the improvement of stability over the use of radioisotopes, there are some drawbacks, including (i) oxalic acid and its derivatives have poor solubility in water; (ii) in the case of aryl hydrazides, the chemiluminescence reaction only proceeds in the presence of catalysts; and, (iii) luminol chemiluminescence is prone to interference by a large number of factors, such as a high background arising from the catalytic requirements of the reaction, which subsequently results in a lower sensitivity compared to acridinium esters. Research over the last three decades has shown acridinium esters to be superior practical alternatives to luminol as labels for immunoassay because the chemiluminescence reaction of acridinium esters does not require a catalyst. Acridinium esters offer significant advantages such as a very low background light level combined with high quantum yield, the simplicity of the light emission process and rapid kinetics (1-5 s). The first acridinium ester synthesised for this purpose was described by

Weeks.[80] The molecule consisted of three parts, the chemiluminescent acridinium ring, the phenoxy leaving group and the succinimide linker group, which is replaced by the reaction of a free amine group of an antibody/protein and therefore does not exist in the final labelled antibody. A similar reaction is involved when labelling a nucleic acid probe.

Weeks coupled the acridinium ester spontaneously to antibodies under mild aqueous conditions to yield stable derivatives with high specific chemiluminescence activity without affecting the antibody activity. The acridinium esters usually contained functional groups such as *N*-hydroxysuccinimidly (NHS) esters in the phenyl ring to enable the labelling of antibodies and DNA probes. Chemiluminescence in DNA hybridization assays emerged as an alternative technique to the use of radioactive tags, which are discussed in the next section. In 1989, Arnold developed several hybridization assay formats involving acridinium ester labelled DNA probes with high sensitivity (10^{-18} mol/L) of the target.[11] Sarrazin described a highly sensitive hepatitis C virus RNA detection method using a hybridisation protection assay with amplicon-specific acridinium ester labelled probes.[81] Recently, the application of chemiluminescence techniques has grown in a variety of areas, including environmental monitoring, [82,83] biomedical research, [39,84–88] and biological marker assays, including both nucleic acid assays and immunoassays processes for the detection of nucleic acids.[89–92]

1.5 Nucleic acid assays based on AE

Chemiluminescent acridinium esters have been synthesized and used as labels, which are covalently attached to a suitable synthetic DNA oligonucleotide through coupling to a free primary amine group in the DNA probe without any change in luminescence properties [93] An amine linker arm can be inserted at various positions during synthesis of the

oligonucleotide at positions that do not affect the hybridization characteristics of the DNA probe resulting in DNA probes with high specific activity acridinium ester derivatives.[11,86,88] Chemiluminescent labels are easy to control, require no special handling or disposal and have an excellent shelf life. Furthermore, assay formats have been developed that are simple to perform and very rapid including novel homogeneous formats which require no physical separation.[94] Recently, acridinium esters have been employed in several clinical assays in manual kit-based tests as well as in formats compatible with automated clinical analysers. The first nucleic acid test cleared for use by the Food and Drug Administration (FDA) in 1988 was the Gen-Probe PACE test which used chemiluminescent detection to monitor the presence of Chlamydia and Gonococci. These approaches have become extensively used, providing the preferred platform for monitoring donated blood for the presence of HIV-1, HIV-2 and other viruses.[95]

The development of an acridinium ester based nucleic acid test was mainly performed within a commercial environment at Gen-Probe (which merged with Hologic in 2012 and is based in San Diego, USA). The family of assays exploiting the chemiluminescent endpoint has expanded substantially with many of the innovations being captured within the patent literature rather than in research publications.[96] Many of the innovations relate to the approaches used to separate AE-labelled probe that has bound to their specific target from the non-hybridized material as well as amplification methods that increase the sensitivity of the technique.[72,88,92] Approaches to the separation of the chemiluminescent labelled probe from that hybridized to its target have included: solid phase separation (PACE 2); quencher and hydrolysis approaches, whilst branched DNA and transcription-mediated amplification (TMA) have been used in combination with these separation techniques to enhance the sensitivity.

1.5.1 Solid Phase

Separating hybridized target from the excess labelled probe can be performed using a secondary probe modified to bind to a solid phase, for example, the incorporation of biotin into the secondary probe facilitates binding to a streptavidin-coated solid phase, or by exploiting the intrinsic biochemical properties of the single-stranded (ss) excess probe and the double-stranded (ds) hybridized product. Gen-Probe developed a proprietary approach that exploited the higher affinity of hydroxyapatite for dsDNA by using a magnetic bead coated with hydroxyapatite to separate dsDNA from ssDNA (Figure 1.14).

The incorporation of the solid phase separation in conjunction with AE-labelled oligonucleotides led to the development of a series of essays, namely PACE, that were compatible with automation and have become extremely widely used.

Gen-Probe PACE 2 exploits acridinium ester-labelled, single-strand DNA probes complementary to *C. trachomatis* and *N. gonorrhoea* ribosomal RNA found in urogenital specimens.[97] This version of the assay exploits both solid phase and hydrolysis separation steps, resulting in an assay automatable and straightforward. The advantages of this assay are the ability to detect both *C. trachomatis* and *N. gonorrhoea* in a single assay format, ease in transport and storage of specimens, ease in the detection of dual infections, and objective reporting of results.[98] Gen-Probe PACE 2 assays for *C. trachomatis* (PACE 2 CT) and *N. gonorrhoea* (PACE 2 NG) which use nucleic acid hybridization for the detection of rRNA are now among the most widely used clinical assays for these pathogens.
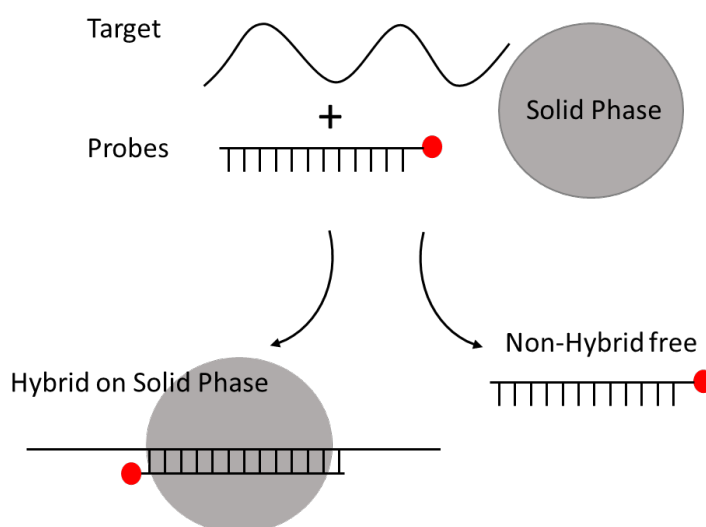
Figure 1. 14: Solid phase separation used in PACE 2 assays. A magnetic particle (grey circle) coated with hydroxyapatite, which has a higher affinity for double-stranded DNA, and thus selectively removes the probe that has hybridized with its target. This allows excess probe which remains single-stranded to be washed away. The red circle denotes the acridinium ester label on the probe.

1.5.2   Use of Quenchers

Dyes have been used in concert with chemiluminescent compounds to 'quench' or modify the light generated dependent on their proximity to the chemiluminescent molecule. The principles are the same whether the light emission is stopped completely (quenched) or whether the emission wavelength is modified to that corresponding to the fluorescence of the dye, but in this review, only the situation of a quencher is considered. A few different formats have been exploited that use DNA hybridisation to change the spatial arrangement of the quencher and chemiluminescent compound: molecular beacons, non-competitive and competitive hybridisation approaches (Figure 1.15).

An example of this approach to exploiting acridinium esters is the molecular beacon format using hairpin-shaped oligonucleotide probes where the quencher and chemiluminescent molecules are attached to opposite ends of the probe but are close when

the probe is in its hairpin formation. The loops of molecular beacons serve as probes while the stems serve to bring the chemiluminescent label and quencher together (Figure 1.15A).[99] The luminescence of the AE-labelled probe is quenched when unhybridised to its complementary target. When the probe binds to a specific target DNA or RNA strand, the quencher and chemiluminescent molecules are separated. Removing the chemiluminescent label from the vicinity of the quencher restores its chemiluminescence. The loop typically consists of 15-25 nucleotides while the stems are only 5-7 nucleotides long, allowing ease of opening in the presence of a specific target oligonucleotide that can hybridise with the longer loop strand.

For example, a new probe type, the Hybridisation Induced Chemiluminescence Signal (HICS) probe was developed.[66] These new HICS probes involve an AE conjugated through the N-linker (*N*-acridinium position) positioned on one terminus of a stem-loop oligonucleotide and a methyl red quencher attached to the opposite end, similar to the format used in molecular beacons. On hybridization of the HICS probe to a complementary target nucleic acid, the stem separates, removing the chemiluminophore from the vicinity of the quencher and permitting detection of the emitted light produced by the chemiluminescent reaction.
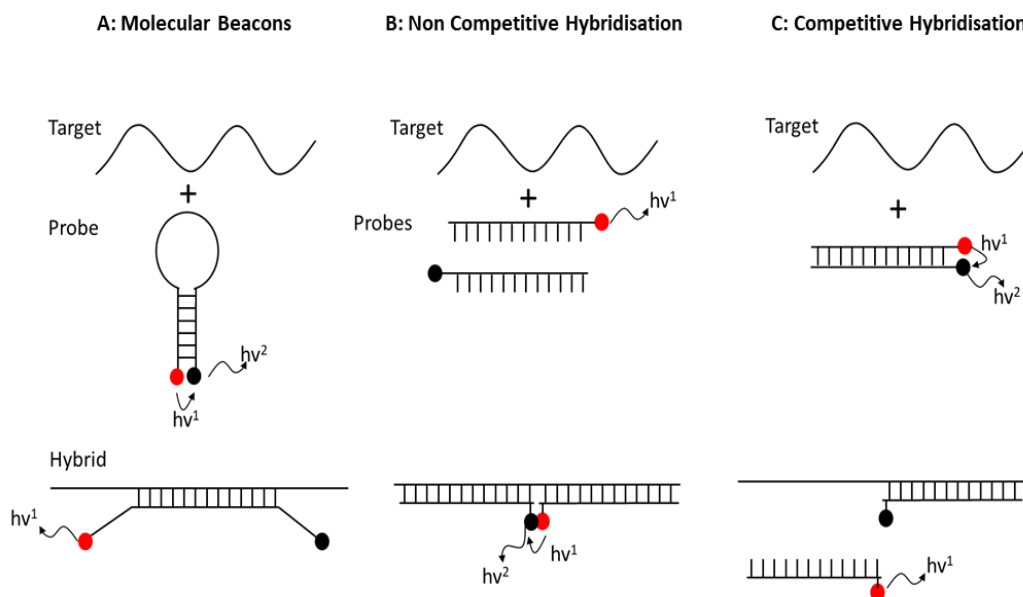
Figure 1. 15: Incorporation of dyes (black spheres) in chemiluminescent nucleic acid detection. Chemiluminescent compounds (red spheres) and dyes are covalently attached to DNA oligonucleotides. If the dye is a quencher, no light output is observed. When the dye is a 'modifier' and the chemiluminescent compound is distal from it, the light output is wavelength hv1, but close proximity to the dye changes this output to wavelength hv2. Three formats where hybridisation changes the light output are depicted: Panel A showing Molecular Beacons; Panel B Non-Competitive Hybridisation; and Panel C Competitive Hybridisation.

1.5.3   Probe hydrolysis

The Hybridisation Protection Assay (HPA) technique described by Arnold *et al*.[11] consists of synthesizing an acridinium-ester-labelled DNA probe which can be differentially hydrolysed based upon selective chemical degradation of the acridinium ester label. Acridinium esters, like other aryl esters, are easily hydrolysed in basic conditions. When the acridinium ester is linked to a single-strand nucleic acid, hydrolysis of the acridinium ester probe is similarly easily hydrolysed by the action of the base (figure 1.16). However, if the acridinium ester probe complexes with a complementary strand of nucleic acid, the acridinium ester sits in the minor grove of the double helix and the hydrolysis of the AE is protected by the low water activity within the groove.[100]
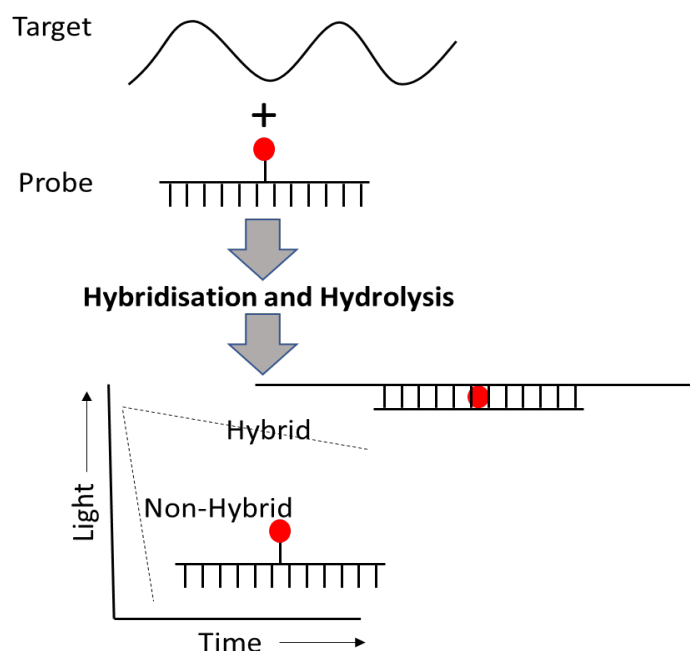
Figure 1. 16: Underlying principle of Hybridisation Protection Assay. Differential hydrolysis is observed between the hybridized and non-hybridized probe when acridinium esters are covalently attached via an internal linker. Red spheres indicate the chemiluminescent AE molecule.

In another word, the chemiluminescence associated with the unhybridised probe is rapidly reduced to a low background level, but the chemiluminescence associated with the hybridized probe is reduced in rate due to the protective effect of duplex formation (Figure 1.16).

Differential hydrolysis is typically carried out at $60^{o}C$ in sodium tetraborate buffer over 30 min time at a chosen pH (based on the chemical properties of the particular acridinium esters). Thus, this "Hybridisation Protection Assay" (HPA) uses an oligonucleotide bound acridinium ester that in its unhybridised single-stranded form is deactivated by the chemical treatment, but when the probe hybridizes with its target oligonucleotide to form a double strand nucleic acid, the AE intercalates and is protected

from deactivation.[100] In this format, triggering the chemiluminescence reaction leads to the production of light only from the AE protected by the double-stranded product.

The assay allows the measurement of specific single-stranded target levels in a sample in a quick, quantitative, and homogeneous way. The remaining chemiluminescence after hydrolysis indicates the amount of target nucleic acid. To allow quantitation, a dilution series (standard curve) of ssDNA target of a known concentration can be prepared and measured alongside the samples. As there is a linear relationship between the target that is present in the initial sample and the amount of light that is generated, the measured light output can be used to calculate the concentration of the original level of the target from a standard curve.

1.5.4 Signal Amplification by Branched Nucleic Acids

Branched nucleic acids (bDNA) can provide a signal amplification approach, which was developed in the early 1990s by Chiron Corporation (Emeryville, CA, USA), while an improved version of the assay was generated for viral quantification and improved for the detection of viral loads (HIV-1 and HCV) in the following years.[101,102] The signal generated is in proportion to the amount of target and thus nucleic acid concentration can be determined from a calibration curve. The bDNA approach is less sensitive than direct target amplification, but it has several advantages, including the minimal risk of contamination.

Therefore, it provides a reliable means for direct quantification of viral load in clinical specimens. Molecular diagnostic assays using bDNA technology for the detection of nucleic acid target molecules are sensitive, specific, and reliable tools and examples of their use include monitoring disease and viral or bacterial infections or monitoring the

effectiveness of a patient's treatment. The two major current applications are viral load quantification for HIV and HCV. The sensitivity of bDNA is achieved by signal amplification on the bDNA probe after binding it to the target sequence. The purposes of the large, branched DNA are to allow the complex to bind many molecules of the AE probe, which magnifies the signal. The bDNA method uses a 96-well microplate format based on a series of specific hybridisation reactions and chemiluminescence detection of the hybridized probe. The bDNA technology employs multiple capture extenders (oligonucleotides) that hybridise to complementary regions of the target nucleic acid of interest through hybridisation. A schematic diagram of the bDNA assay for direct quantification of nucleic acid molecules is shown in Figure 1.17.[103] The first step is to release viral RNA from the serum (A). Specific nucleotides (label extender and capture extender) are hybridised to the target nucleic acid. The next step (B) involves the target RNA molecules being captured into the microwell by another set of synthetic oligonucleotides known as capture probes, which bind to both the well surface and the capture extenders.
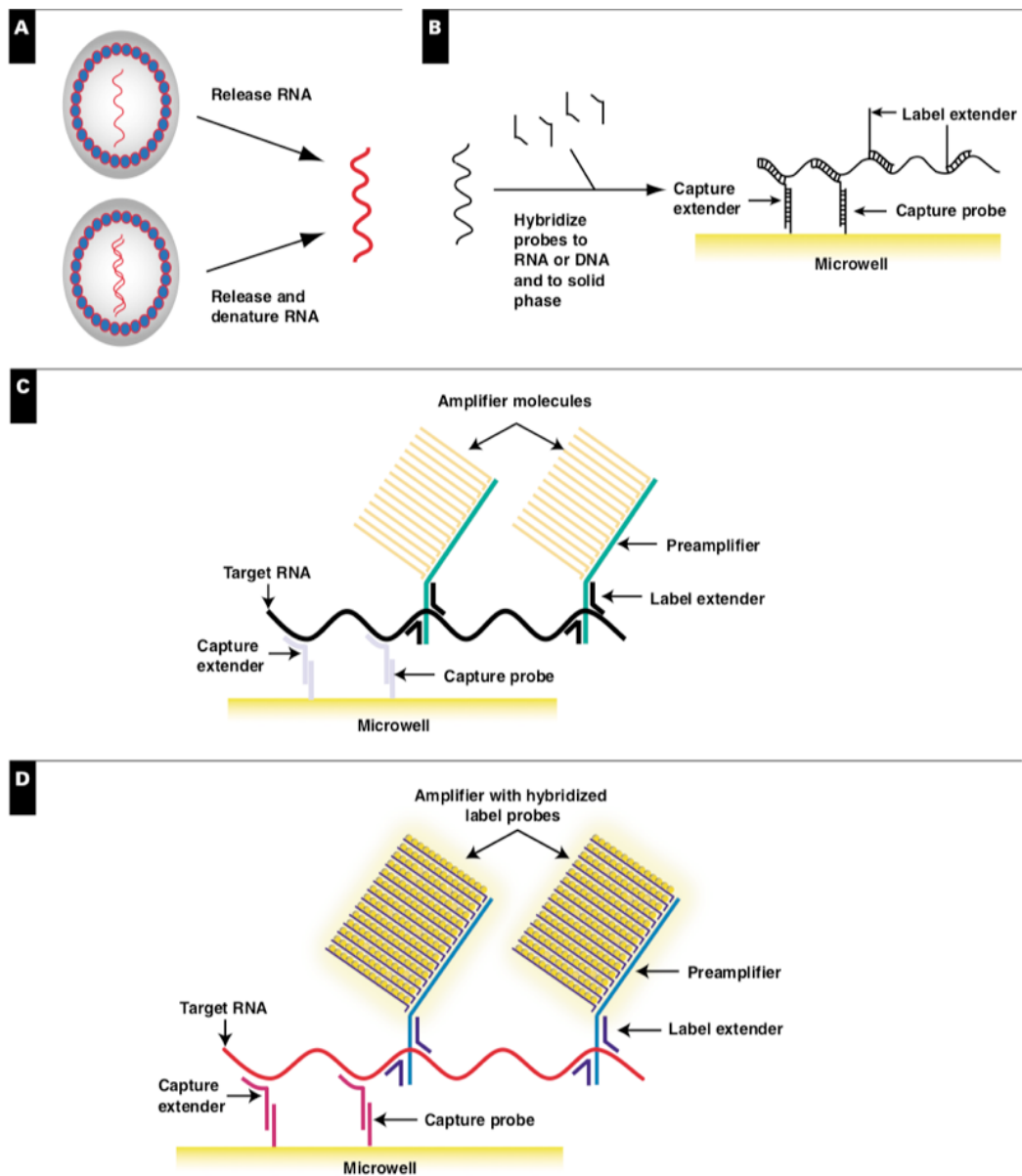
Figure 1. 17: Branched chain DNA (bDNA) specimen processing. Capture stage: disruption of microorganism. (A) disruption of microorganisms, (B) target capture, (C) bDNA incorporation, and (D) detection through attached chemiluminescent probes.[103]

The bDNA (also known as a pre-amplifier) is then hybridised to the label extender, by which it also becomes attached to the target (C). In the first generation, the label extender probes bind bDNA which in turn binds many alkaline phosphate probes. In the second and third generations the label extender binds the amplifier and this in turn binds to many amplifiers, thereby becoming an amplifier containing multiple copies of labelled

probe per unit of the target (D). The result is stronger signal amplification and lower detection limits. Light emission is directly related to the amount of target RNA present in the sample. Results are recorded as relative light units (RLUs) by the luminometer, and the concentration of the viral RNA can be obtained from a standard curve based on known concentration.

1.5.5   Transcription-Mediated Amplification (TMA)

Transcription-based amplification methods are modelled on the replication of DNA in the host cells. These methods are known by various names including Gen-Probe's TMA.[104] Nucleic Acid Sequence Based Amplification (NASBA) [105] and Self-Sustained Sequence Replication (3SR) [106] and are alternatives to PCR. All these techniques depend on RNA polymerase instead of DNA polymerase. The technique amplifies the captured HIV-1 and HCV viral RNAs.[101,102] These methods utilize two primers, RNA polymerase and reverse transcriptase, to rapidly amplify either the target RNA or DNA and produce RNA amplicon, in contrast to most other nucleic acid amplification methods that produce only DNA amplicons.

TMA enables the simultaneous detection of multiple pathogenic organisms in a single tube. TMA is isothermal, which contrasts with other amplification reactions such as PCR which require a thermal cycler instrument to rapidly change the temperature to drive the reaction. The mechanism of TMA is shown in Figure 1.18. A combined promoter-primer which contains a T7 RNA polymerase promotor anneals and hybridizes to the target RNA (step 1). This promoter-primer is extended via reverse transcriptase (RT) (step 2) to produce a DNA:RNA hybrid (step 3).
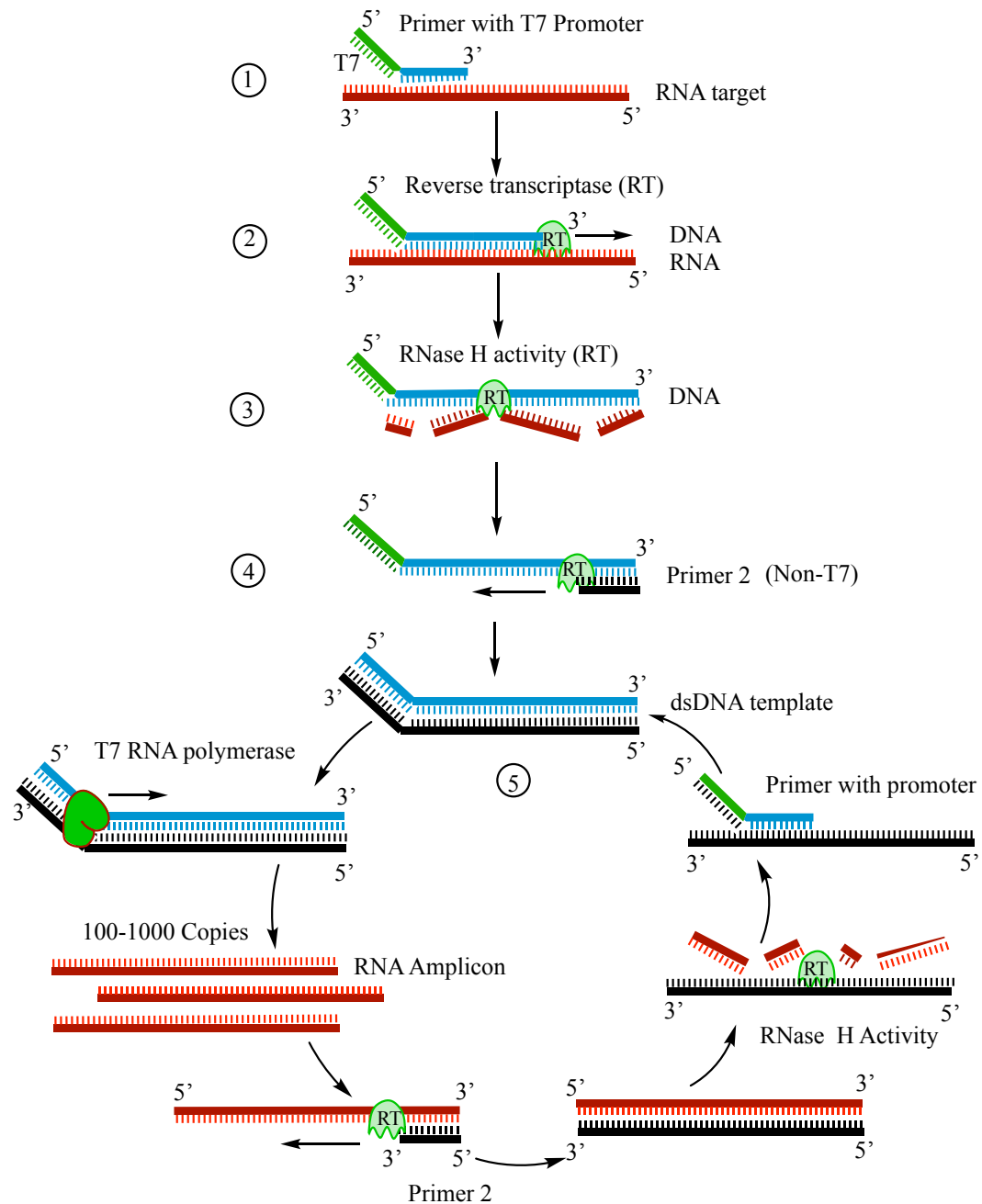
Figure 1. 18: Workflow for Transcription-Mediated Amplification (TMA).

RNase H digests the RNA strand of RNA:DNA hybrid leaving only single-stranded complementary DNA (cDNA, step 4). Following the degradation by the RNAse H activities of the RT, a second primer then binds to the cDNA (Step 5). This primer is then extended by the RT to produce second-stranded DNA that contains an active double-

stranded T7 RNA polymerase promoter (step 6). The action of T7 RNA polymerase then produces between 100 to 1000 RNA copies of the template (steps 7, 8), which contains the sequence that will bind the AE probe used for amplicon detection. TMA is a powerful amplification tool as every RNA amplicon produced in steps 7, and 8 can pair to the second primer (step 9) and re-enter the amplification cycle. The RT then catalyses the formation of cDNA by extending the 3' end of the primer to produce another RNA:DNA hybrid duplex (step 10) as in step 5, allowing the cycle to be repeated and more RNA amplicons to be generated. The addition of an acridinium ester labelled DNA probe which specifically binds to the target amplicon is often used in conjunction with TMA as the detection methodology. The HPA assay format is discussed in more detail in the next section.

1.6 Hybridization Protection Assay Technology

Hybridization protection assay (HPA) is a detection methodology (see 1.5.3) utilizing a chemiluminescent marker which was initially developed for detecting pathogens.[11] It involves the hybridisation of acridinium ester labelled probe with target nucleic acid (RNA or single-stranded DNA targets) followed by a differential hydrolysis step which involves alkaline hydrolysis of free and unhybridised acridinium ester probes while the hybridised acridinium ester probe is protected as a result of intercalation of the acridinium ester in the cavity of the nucleic acid duplex. This is thought to be due to the intercalation of the acridinium ester into the minor groove of the double-stranded product of hybridisation.[100] After the hybridisation of the acridinium ester probe with its target nucleic acid under conditions that do not promote ester hydrolysis, the reaction conditions are adjusted; at this stage, separation of the hybridized from the unhybridised probe is simple and rapid due to the action of hydrolysis reagents. The free acridinium ester or unhybridised probe is hydrolysed rapidly, while the hybridized probe is minimally affected under the

experimental conditions. Following this differential hydrolysis process, any remaining chemiluminescence is a direct measure of the amount of target present. The chemiluminescence reaction is triggered at this stage and the light is emitted from the hybridized probes, measured by a luminometer, and reported as Relative Light Units (RLUs).

1.6.1 Advantages of HPA

The main advantages of HPA include i) the absence of enzymic steps; ii) homogeneous format; iii) ease of probe design; iv) high level of specificity; and v) the potential to measure multiple analytes. The absence of enzymic steps means the assay is less prone to inhibition from factors present in the sample, allowing it to be performed directly on clinical specimens after minimal sample preparation. Due to the hydrolysis step, the HPA assay format is completely homogeneous, requiring no physical separation of the free probe from hybridized probe nor washing steps, making the HPA format as easy to perform as the simplest immunoassay. However, in contrast to immunoassays, another advantage is that it is straightforward to make a DNA probe for any target nucleic acid sequence as long as the relevant sequence has been characterised. The mechanism underpinning the specificity and potential to support multi-analyte measurement is explored in detail below.

1.6.2 Assay Specificity

The HPA technique is based on the sequence-specific hybridization of short oligonucleotide probes covalently labelled with a chemiluminescence acridinium ester. The basis of HPA specificity is the steric protection of the AE from alkaline hydrolysis

when a hybrid is formed between probe and target. The difference in acridinium ester hydrolysis rates allows discrimination between hybridized and unhybridized AE probes. Furthermore, it also has an inherent ability to provide discrimination between closely related target sequences, primarily due to the chemical degradation of any unprotected AE that is not fully intercalated and protected in the duplex, something that occurs when the AE is incorporated proximal to a DNA mismatch. This feature of the hydrolysis step allows the technique to detect single-base mismatches rapidly and sensitively, as well as multi-mismatches, in a DNA target derived from closely related bacteria such as meningococcus and gonococcus.[11,88]

A detailed investigation into the specificity of the HPA format revealed that 12 single-base mismatches could be distinguished from the corresponding matching duplex. In this study,[107] the researchers looked at the effect on the hydrolysis rate of perfectly and imperfectly matched duplexes, where the position of the mismatch was only one place away from the AE linker site (the effects were smaller when the mismatch was further away). Sixteen probes were synthesized with every combination of nucleotides on either side of the AE linker site, i.e. N (AE) N, where N can be any nucleotide (A, T, C or G) Then 96 possible targets were synthesized which had a single nucleotide mismatch on the 3' or the 5' side of the site of the AE linker. In other words, for each mismatch, there was one of four possible nucleotides on the other side of the AE linker. The hydrolysis performance was compared to the 16 possible oligonucleotide targets with a perfect match at these two sites and the ratio of the matched / mismatched was reported. This study proved that when an AE-labelled probe hybridizes to a complementary target, AE is protected from hydrolysis relative to the unhybridized conformation. Single-base mismatches in the duplex adjacent to the site of AE attachment disrupt this protection resulting in more rapid AE hydrolysis, thus providing a basis for discrimination between

matched and mismatched targets. The authors [107] reported that this disruption was not caused by a decrease in the overall stability of the duplex, but most likely by a local alteration of the structure of the double helix which renders AE more susceptible to hydrolysis. All 12 single-base mismatches displayed this effect.

1.6.3   Potential for multiple analyte measurements

Another advantage is that the format can be adapted and used as a dual analyte assay to measure one or more targets simultaneously in a single sample. The chemiluminescence properties of 4-(2-(succinimidyloxycarbonyl)ethyl)phenyl 10-methylacridinium-9-carboxylate trifluoromethanesulfonate **(15)** can be altered by chemical modification to exhibit distinct chemiluminescent properties. The addition of electron-withdrawing groups to the *ortho* position of the leaving group of AE such as (di-*o*-Br-, *o*-F-, di-*o*-F-, di-*o*-Cl-, and di-m-F) increased the rate of light emission, while the addition of electron donating groups (*O*-OCH$_3$-, di-*o*-OCH$_3$-, *o*-Me-, and di-*o*-Me) to the leaving group of the AE decreased the rate of chemiluminescence.[108] Steric effects appear to be rather small since substitution with two relatively large bromine atoms at *ortho* positions still yielded a rapidly reacting AE. These studies also found that the introduction of two m-F groups into the leaving group had little effect on the hydrolysis rate, but significantly enhanced the light emission. By utilising oligonucleotide probes labelled with two modified AEs, two different analytes can be simultaneously detected using the HPA format as described above. The remaining chemiluminescence signal from either or both labels after hydrolysis can be measured over multiple time intervals and the signal of each label can be resolved mathematically to quantitate the amount of each target present.

This simultaneous discrimination of chemiluminescence signals based on the speed of light output, i.e. one AE which emits light at a faster rate than the other within the HPA format, resulted in the development of the Dual Kinetic Assay (DKA).[87,88,96] An example of its application is the detection and resolution of *C. trachomatis* and *N. gonorrhoea* in a single specimen.[98] In this assay, sample preparation, amplification and detection steps exploited the TMA-HPA workflow, but the detection step was adapted to use DKA to allow the simultaneous detection of two closely related amplification products representing the two microbes in question. Moreover, the sample processing can be modified to amplify more than one target at a time. For example, this adaptation of TMA-HPA has been used in a quantitative mode to assess two viral targets, HIV-1 RNA and HBV DNA, in plasma, exhibiting a high dynamic range [104] The outcomes of these studies illustrate that the sensitivity, specificity and versatility of these technologies allow adaption to many applications.

1.6.4   Limitations of HPA

As mentioned above, arguably the biggest disadvantage of HPA is that it does not have the sensitivity of approaches that incorporate an inbuilt amplification step, such as PCR, which increases the quantity of target before detection. However, HPA can be combined with pre-amplification; a process that is exploited in workflows such as TMA which can be used to measure low copy numbers of targets. As described in Section 1.5.5, TMA is an isothermal method, which when used upstream of the HPA, amplifies DNA or RNA targets sufficiently to be detectable by HPA. An example of its use is the detection of *Mycobacterium tuberculosis* in sputum samples and *Chlamydia trachomatis* in male and female urogenital swabs and urine samples.[109,110] A TMA/HPA assay for simultaneous detection of HIV and HCV in blood samples has also been described.[95]

On the other hand, the disadvantages of using AE as the endpoint detection system is that the chemiluminescence reaction is irreversible, so the sample cannot be reanalysed, nor can the reaction be re-measured as the AE is transformed to a non-chemiluminescent compound. Acridinium esters have low stability at extremes of pH and temperature. This means they need to be used within a specific pH range (~pH 7-10) and a relatively narrow temperature range.[93] They do not retain their integrity when heated to 95-96°C, therefore cannot be incorporated during amplification processes, such as PCR, which require such high temperatures to denature the amplicon, allowing primer binding and the continuation of the amplification reaction. A temperature of 60°C has been recommended for any assay as it allows a good compromise between the kinetics and specificity of hybridisation, the stability of the chemiluminescent compound and the performance of the hydrolysis reaction.

1.7   Applications of the HPA format.

The technical advantages of HPA (see 1.6.1) have led to this approach being applied to a range of high-throughput clinical assays. Selection of the HPA application was initially driven by the abundance of target molecules which would allow HPA to be applied without the requirement for initial amplification of the target. The high copy numbers of ribosomal RNAs and the ability of these sequences to identify organisms were utilised to generate a suite of applications to detect clinically relevant pathogens.[97]

Coupling HPA with the amplification provided by TMA allowed both detection and quantification of pathogens in high-throughput assays from small clinical samples.[111–114] Furthermore, amplification allowed assays to be developed for viral pathogens and transcripts whose targets were not as abundant as the ribosomal RNAs.[101,102,104] Key to

many of these assays was the specificity that allowed closely related sequences to be measured in the same sample.[88,98]

1.7.1 Quantitation of Ribosomal RNA

Nucleic acid hybridization formats have a wide range of applications for the detection, identification, and quantification of microorganisms in clinical diagnostics and environmental studies.[89,115] rRNA was the target of choice for non-amplified HPA assays as there are thousands of copies per cell providing natural 'amplification' compared to a nuclear gene, where there may only be 1-2 copies per cell. Using the rRNA as the target in the HPA allows the pathogens to be detected when there are lower numbers of cells present when compared to using a nuclear gene as the target. The HPA technique employs chemiluminescent acridinium ester-labelled single-strand DNA probes complementary to highly conserved ribosomal RNA (rRNA) regions and can distinguish between closely related target sequences, allowing accurate identification and discrimination of mycobacterial species. The labelled DNA probe combines with complementary rRNA to form a stable DNA-RNA hybrid; any remaining unhybridized probe is then selectively hydrolysed. The probe hybridizes with target rRNA in the version of the method without an amplification step. However, combining the specificity of HPA with isothermal enzymatic amplification of rRNA (TMA) substantially increases the dynamic range provided by the HPA assay.[88,116] One of the earliest reports of the detection and the quantitation of purified ribosomal RNA was by Arnold and his co-workers.[117] Shortly after, applications of discrimination of a single base pair mismatch between the probe and its target sequence were reported by Nelson *et al.*[107]

1.7.2 Viral detection

The combination of HPA and TMA allowed the detection of viral pathogens within clinical samples. Furthermore, combined with the multiple analyte capabilities of Dual Kinetic Assay, it allowed simultaneous detection of HIV-1 RNA and HBV DNA in plasma, assays which exhibited a high dynamic range leading to the adoption of this assay as the screening approach of choice for the US blood and organ donation service.[104]

1.7.3 Quantitation of Messenger RNA

The HPA format has been used without an amplification step to measure highly abundant transcripts. For example, the technology is capable of measuring highly abundant messenger RNA transcripts, such as those coding for the beta-actin, vitellogenin and zona radiata proteins, sensitively and quantitatively. It can also identify single nucleotide differences in RNA transcripts with high specificity.[57,118]

The technology has been adapted further by developing more sensitive chemiluminescent methods capable of measuring medium abundance genes such as those that would be useful for a genotoxicity screen *in vitro*. A study by Morris *et al.* describes the use of the HPA with and without initial amplification of the target in conjunction with *in vitro* models to measure toxicologically relevant gene expression changes and demonstrates that the HPA can in certain circumstances, measure genes with lower levels of expression.[119,120] The change in expression of an averagely abundant gene, cystatin A, was detected by directly measuring a specific RNA transcript, i.e. without the need for cDNA synthesis or amplification; this was possible due to a large change in expression in response to doxorubicin exposure.

This study also looked at combining the HPA technology with a linear amplification step, which has several consequences: it adds enzymic steps, increasing the cost, the time to result and the observed coefficient of variations (CVs), but it lowers the limit of detection and, by doing so, increases the number of genes that can be measured to an extent that it is now a viable option for research with *in vitro* cell lines. However, the disadvantage of introducing any form of target amplification is the probability of increasing the error associated with measurement and as such, the precision of the assay decreases.

1.7.4   Further development of multiple analyte measurements

The simple model acridinium ester (**15**), is susceptible to hydrolyse in solution at room temperature reducing the stability. Such modified AEs characteristically have a good quantum yield and increased rate of chemiluminescence.[121] For the esters to exhibit chemiluminescence, phenyl leaving group pKa must be < 11 for bright emission to be observed, and there is a strong correlation between the pKa and the kinetic of the light emitting reaction and its quantum yield. Different strategies for increasing the stability of acridinium compounds have been described in the prior art.[60] However, the addition of electron-withdrawing groups to the phenyl ring lowers the pKa of the phenol, making it a better leaving group, which results in increased quantum yield and an increased rate of the chemiluminescent reaction. In contrast, the addition of electron-donating groups raises the pKa of the phenol, making it a worse leaving group, which results in decreased quantum yield and a decreased rate of the chemiluminescent reaction.[88] for example; Law *et al*. introduced methyl groups to the 2,6-position of the phenyl ring, and the resulting sterically stabilized acridinium ester, DMAE-NHS [2',6'-dimethyl-4'-(N-succinimidyloxycarbonyl)phenyl l0-methylacridinium-y-carDoxyiate] which provides shielding from hydrolysis and improve its stability and was found to have the same light

output as an acridinium ester lacking the two methyl groups. while electron-donating groups decrease the efficiencies and reaction rate. They reported that the stability of the former compound when conjugated to an immunoglobulin showed no loss of chemiluminescent activity even after one week at 37^0C at pH 7. In contrast, the unsubstituted acridinium ester only retained 10% of its activity when subjected to the same treatment.

Where these modifications lead to a change in the chemiluminescent properties, these can be exploited in various ways. For example, the dual analyte system based on two different AEs with different kinetics of light output i.e. a 'flasher' and 'glower', mentioned in Section 1.6.1.2, has been used to successfully measure and discriminate a number of targets e.g. two different regions of the HIV (*gag* and *pol*), the discrimination of HIV and HCV viruses from an internal control [104] and the discrimination of rRNAs from *C. trachomatis* and *N. gonorrhoea* in a single specimen.[65] the hydrolysis characteristics of two AE derivatives differing only in the presence of two *meta* fluorine substituents in the phenol ring of one of them were similar, while the kinetics of the chemiluminescent reaction was very different, allowing signal resolution when the chemiluminescent reactions were triggered simultaneously.

An alternative approach exploited a new class of hybrid luminophore probes that emit light of distinct wavelength ranges and intensities upon energy transfer (ET) from an acridinium ester chemiluminophore to a covalently conjugated fluorophore.[65,122] This system was designed to facilitate rapid generation of different chemiluminescent probes with altered emission wavelengths for dual or multi-analyte assays. These 'wavelength shifted probes' were designed on the molecular beacon probe structure, where a small stretch of self-binding nucleotides at the 3' and 5' ends of an oligonucleotide promote a hairpin structure in the absence of target, thereby bringing a light emitting donor entity and

a molecule that can act as an acceptor, into close proximity. This causes the light emission properties to be those of the acceptor molecule, but in the presence of the specific target sequence, which the probe has been designed to bind to, hybridisation to the target has the effect of increasing the distance between the donor and the emitter and any emitted light is from the donor molecule.

This format was extended to include a chemiluminescent label instead of a fluorescent one by Browne *et. al.*[65] when they developed an assay based on a molecular beacon structure with an AE at the 5' and a quencher on the 3' end of the oligonucleotide probe. Two different AEs were synthesized, including a 2,7-dimethoxy AE, and the addition of the 2,7-dimethoxy groups was shown to shift the wavelength of emission by ~60 nm from the un-substituted AE. Adapting a luminometer and using filters with different wavelengths (<450 nm over the first 12 s and >550 nm between 12-184 s), allowed sufficient resolution of the two signals for dual analyte measurement.

Browne *et al.*[122] further extended this technology by labelling the 5' end of the oligonucleotide probe with AE and a variety of different fluorophores that could re-emit the light gained through electron transfer from the AE molecule. The fluorophores tested were 6-carboxyfluorescein, 5-carboxytetramethylrhodamine (TAM) and cyanine dye. The quenchers tested were dabcyl and Black Hole Quencher 2. This study used an oligonucleotide probe, which had the advantage that any sequence could be synthesized, and in this study, it was shown that between 2 and 200 fmol of a bacterial and a fungal target could be quantitatively measured. After triggering the chemiluminescent reaction, the resulting light output was shown to have an altered wavelength, intensity, and kinetic profile from that of AE on its own. The resulting TAM-AE labelled probes were shown to emit wavelengths between 540−670 nm with a maximum at ∼580 nm, over a 60 s period. This was considerably slower than unmodified AE probes that decayed over 20 s with a

wavelength range of between 400-520 nm. These differing properties were exploited in a dual assay format by measuring the shorter wavelengths over the first time points (0-12 s, <450 nm, unmodified AE signal) before measuring the longer wavelengths at the later time points (12-10 s, 550 nm, AE-TAM signal), which allowed sufficient resolution to discriminate the signal for both probes. The optimised assay was capable of accurately measuring 2-200 fmol of their specific targets, even in the presence of 50 fmol of a non-specific target, within an hour. This format allowed direct measurement of the target sequence, without amplification by either culture or enzymatic methods, of environmentally relevant targets without the requirement for physical separation of the excess probe. However, the sensitivity achieved with this format was not as low as possible with the HPA format where the excess probe is removed by chemical hydrolysis.

The ability to measure more than one analyte in a single sample has several advantages, e.g. different targets can be measured in a single specimen, the amount of clinical sample required is reduced and the number of samples that can be handled is increased. This format also allows the introduction of a positive control measurement, e.g. the measurement of a second target which has either been introduced (external control) or is an integral part of the sample (internal control). This gives a method of standardisation of the technique by taking a second measurement within the same sample and reduces the potential for error or contamination. However, the accurate detection of a second target in each sample requires clear discrimination of both signals, the challenge of which is demonstrated by the examples discussed above.

N-Alkylation of acridine esters is an important step in the synthesis of AEs. It can be achieved in variable yields using different alkylating reagents such as alkyl iodides and benzyl bromide.[123] However, more powerful alkylation reagents such as trifluoromethanesulfonates have been reported to afford better yields.[67] In principle,

modification of the alkyl group could influence the chemiluminescent properties of the AE generated, but alkylation with more complex alkyl groups is a challenge because of steric hindrance. In a recent study, the *N*-sulfopropyl group was reported to be an easy group to introduce to the acridine nitrogen and gave excellent yields on alkylation of a wide range of acridinium esters.[61,124] The study also reported how the polarity of the *N*-alkyl group affected the properties of the chemiluminescent labels.

Given the advantages of dual analyte measurements, the initial aim of the present study was to explore further the work started by Nelson *et al*. [88] and Browne *et al*.[65] and to make modified AE molecules that would react at different rates, by changing the nature of the phenol leaving group, and/or offer different wavelengths of emission, by changing the substituents on the acridine ring. If two AEs with similar hydrolysis properties, but different kinetic and/or spectral properties were used in conjunction, the HPA format, incorporating a chemical hydrolysis step, could lead to a dual or multi-analyte assay with improved sensitivity. A series of novel AE were therefore synthesized to investigate their properties specifically with a dual or multi-analyte system in mind.

1.8   Aims and Objectives

Chemiluminescence (CL) and bioluminescence (BL) are the detection techniques of choice for the development of highly sensitive analytical methods, from immunoassays and nucleic acid hybridization assays to whole-cell biosensors. Nevertheless, basic and applied research on CL and BL aimed at further improving their analytical performance is still very active. The acridinium ester 4-(2-succinimidyloxycarbonylethyl)phenyl-10-methylacridinium 9-carboxylate trifluoromethane sulfonate (AE-**15**), which reacts rapidly with alkaline hydrogen peroxide to produce visible light emission (wavelength 430 nm), has been used as a detection label in several assay procedures, including nucleic acid probe-based systems.[93,125] Chemiluminescent acridinium esters (AEs) permit the development of high sensitivity ligand binding assays due to a combination of high intensity light emission and very low backgrounds. Ligand binding assays can be "heterogeneous" or "homogeneous" depending respectively on whether the binding complexes formed between the target molecule and binding reagent need to be physically separated from non-bound reagent, for example by solid-phase adsorption, before end-point measurement.[66] Esters with steric hindrance are difficult to hydrolyse. Improving acridinium ester stability conceivably should enable substitution using a methyl or similar group near the ester. When a substitutional group is introduced at the 2,6-position of phenol, this tendency is markedly reinforced.[126] For example, Law *et al*. introduce two methyl groups to the acridinium ester moiety to stabilize this linkage. The resulting sterically stabilized acridinium ester, DMAE-NHS [2',6'-dimethyl-4'-(*N*-succinimidyloxycarbonyl)phenyl l0-methylacridinium-y-carDoxyiate] was found to have the same light output as an unsubstituted acridinium ester. The compound was used in immunoassay and shows an excellent stability after binding, even after one week at 37^0C at pH 7. [60] In contrast with the unsubstituted acridinium ester which retained 10% of its activity when subjected to the

same treatment. Moreover, Law *et al*. disclose a hydrophilic version of DMAE termed NSP-DMAE-NHS-AE [3-[9-[4-(2,5-dioxopyrrolidin-1-yl)oxycarbonyl-2,6-dimethylphenoxy]carbonylacridin-10-ium-10-yl]propane-1-sulfonate].[127]

Extended studies by Natrajan *et al.,* on the NSP-DMAE derivatives with hydrophilic modifiers attached to the phenol shows aqueous solubility when diamino hexa(ethylene) glycol attached to the phenol leaving group.[128] Moreover, a different class of stable chemiluminescent acridinium compounds has been described by Kinkel *et al.* and Mattingly *et al*.[63] In this class of compounds, the phenolic ester leaving group is replaced by a sulfonamide moiety, which is reported to understand hydrolytic stability without compromising the light output.

Based on these studies and to combine the advantages of substituted acridinium ester we decided to synthesise two series of novel acridinium ester compounds according to the following objectives:

Objective 1: *To synthesize a family of novel acridinium esters.*

One objective was to synthesize a series of compounds based on the addition of two methoxy (electron-donating) or two bromo (electron-withdrawing) groups to the 2 and 7-positions of the acridinium ring. Additionally, we wished to produce compounds with methyl or methoxy groups at the 2 and 6-positions of the phenoxy ring of the acridinium esters to test the effect on the kinetics of both hydrolysis and the chemiluminescent reaction. The hypothesis was that changing the substituents on the acridinium ring and the phenoxy ring of the acridinium ester molecule could be generated which would expect to influence, the stability, the chemiluminescent properties of the products by a combination of steric and electronic effects from the substituents and would support dual analyte

measurement. We also wanted to produce an unsubstituted reference compound with a modified linker configuration to facilitate comparison with previously used AE molecules.

Objective 2: *To characterise the emission properties of modified acridinium esters*

The second objective was to characterise the excitation and emission spectra of the acridone derivatives expected to be the products of the chemiluminescent reactions of the synthesized AEs.

Objective 3: To *determine the optimal conditions for the use of the modified acridinium esters in a DNA diagnostic assay format*.

The third objective was to link the novel AE compounds to a DNA oligonucleotide and incorporate them into the Hybridisation Protection Assay (HPA), a direct and highly specific nucleic acid assay. We then wished to characterise the performance of these chemiluminescent labelled probes within the HPA, by measuring the kinetics of light output and the rate of hydrolysis.

Chapter 2

Materials and methods

2 Materials and Methods

2.1 Materials

All materials used in this research are commercially available and listed in Table 2.1 with the exception of the chemiluminescence material, acridinium ester, and its modified versions. These were synthesized and purified in a chemistry laboratory as described in Chapter 3 using materials listed in section 2.1.1. The addresses of companies listed in Table 2.1 from which materials were routinely bought include Sigma Aldrich (Gillingham, U.K.), Life Technologies (Carlsbad, CA, USA) and Thermo Fisher (Newport, U.K.).

2.1.1 Materials used in the synthesis of Acridinium Ester

The materials used in this study were of the highest grade, purchased from established commercial sources, and were used as received unless otherwise stated. Several were dried where required using laboratories recommended methods. Thionyl chloride was freshly distilled and added from the dropping funnel. Tetrahydrofuran (THF) and dichloromethane (DCM) were distilled and kept over 3A molecular sieves. Anhydrous dimethyl sulfoxide (DMSO), obtained from Sigma Aldrich Ltd, UK, is a highly polar solvent that was used in the labelling reactions. This solvent needed to be anhydrous, so it was bought fresh when required.

A reference compound was bought in for comparison purposes: The *N*-methylacridone (**3a**) was purchased from Sigma Aldrich Ltd (UK). The 4-(2-succinimidyloxycarbonylethyl)-phenyl 10-methylacridinium-9-carboxylate trifluoromethanesulfonate (STD AE **15**) was purchased from CatCelt (Swansea, UK).

Table 2. 1: List of materials used in the biochemistry assays

No.	Materials	Form	Suppliers
1.	Acetonitrile		Sigma-Aldrich, UK.
2.	DMSO	Anhydrous	Sigma-Aldrich, UK.
3.	EDTA (Ethylenediaminetetraacetic acid)		Sigma-Aldrich, UK.
4.	EGTA (Ethylene glycol tetraacetic acid)		Sigma-Aldrich, UK.
5.	Ethanol		Sigma-Aldrich, UK
6.	Glycogen	20 mg / mL. ultrapure	Life Technologies
7.	HEPES buffer 2-[4-(2-hydroxyethy)piperazine-1-yl]ethanesulfonic acid	1 M, pH 8.0	Thermo Fisher
8.	Hydrogen peroxide	3%	Sigma-Aldrich, UK.
9.	Lithium hydroxide	monohydrate	Sigma-Aldrich, UK.
10.	Lithium lauryl (dodecyl) sulphate		Sigma-Aldrich, UK.
11.	Lysine		Alfa Aeser
12.	Nitric acid	1 N	Sigma-Aldrich, UK.
13.	Sodium acetate	3 M, pH 5.2	Sigma-Aldrich, UK.
14.	Sodium lauryl (dodecyl) sulphate		Sigma-Aldrich, UK.
15.	Sodium hydroxide		Sigma-Aldrich, UK.
16.	Sodium tetraborate		Fisher Scientific, UK.
17.	Succinic acid		Sigma-Aldrich, UK.
18.	Triton X102		Sigma-Aldrich, UK.
19.	Water	Nuclease-free	Life Technologies (Ambion)

2.1.2 Materials used in the preparation of labelled probe

The use of acridinium ester as a means for labelling DNA, antibodies, and antigen has been described in number of studies. These studies described the use of these chemical materials to generate a sensitive assay for a variety of acridinium esters. All reagents used were analytical grade reagents. l-Lysine monohydrochloride, sodium acetate, sodium dodecyl sulfate (SDS), lithium dodecyl sulfate (LDS), succinic acid, lithium hydroxide monohydrate, mono-potassium phosphate, di-potassium phosphate, urea, potassium chloride and sodium hydroxide were obtained from Sigma-Aldrich, UK. Sodium tetraborate, acetonitrile and 2-[4-(2-hydroxyethyl)piperazin-1-yl]ethanesulfonic acid (HEPES) were analytical grade and were obtained from Fisher Scientific, UK (Table 2.1). Glacial acetic acid was analytical grade and was obtained from Across Organic. All glassware and bottles were autoclaved at 115ºC for 20 minutes.

2.1.2.1 HEPES Buffer (0.125 M, pH 8.0)

2-[4-(2-Hydroxyethy)piperazin-1-yl]ethanesulfonic acid (HEPES; 1.49 g: 6.25 mmol) was dissolved in nuclease-free water (45 mL) and the pH was adjusted to 8.0 by the addition of sodium hydroxide solution. The volume was made up to 50 mL with distilled water. The buffer solution was autoclaved, the pH was readjusted if necessary and then the mixture was filtered through a 0.20 µm filter.

2.1.2.2 Lysine in HEPES (0.125 M, pH 8.0)

l-Lysine monohydrochloride (0.57 g: 3.1 mmol) was dissolved in HEPES buffer (pH 8.0; 20 mL). The pH of the solution was readjusted to pH 8.0 and the total volume was

made up to 25 mL using HEPES buffer. The mixture was then filtered through a 0.20 µm filter.

2.1.2.3   Sodium acetate buffer (3 M, pH 5.0) (stock solution)

Sodium acetate buffer (3 M, pH 5.0) was obtained from Thermo Fisher (Table 2.1). In some cases, it was diluted in nuclease-free water to the required concentration, adjusted to the volume and the pH required, using a few drops of acetic acid.

2.1.2.4   Sodium acetate buffer (1.0 M, pH 5.0)

Sodium acetate buffer (0.1 M) was prepared by adding 3.33 mL of stock solution (3M) to 90 ml of nuclease-free water and made up to a total volume of 100 mL, the pH was adjusted to 5.0 by the addition of glacial acetic acid.

2.1.2.5   Potassium dihydrogen phosphate (KH_2PO_4, 0.5 M) (stock solution)

Potassium dihydrogen phosphate (34.0 g: 250 mmol) was dissolved in distilled water (450 mL) and the pH was adjusted to 7.0 by the addition of sodium hydroxide solution. The volume was made up to 500 mL with distilled water, then autoclaved and the pH was readjusted if necessary.

2.1.2.6   Buffer A (Potassium dihydrogen phosphate 20 mM, 20% *v/v* acetonitrile, pH 7.0)

Potassium dihydrogen phosphate (0.5 M, 32 mL) was added to 450 mL of distilled water and the volume was made up to 800 mL. The buffer was adjusted to pH 7.0 and

autoclaved. Acetonitrile (200 mL) was added to complete 1000 mL as a total volume. The

buffer then was filtered through 0.20 μm filter.

2.1.2.7 Buffer B (20 mM dipotassium monohydrogen phosphate, 1 M potassium chloride, 20% *v/v* acetonitrile, pH 7.0).

To prepare a 20 mM solution of K_2HPO_4, potassium chloride (59.6 g, 800 mmol) was

dissolved in distilled water (700 mL), and dipotassium monohydrogen phosphate (0.5 M,

32 mL) in distilled water. The pH was adjusted to 7.0, the buffer was autoclaved and then

200 mL of acetonitrile was added to make up to 1000 mL, and finally, the buffer was

filtered through 0.20 pum filter.

2.1.3   Materials used for HPA assay

2.1.3.1   Hybridization buffer

A mixture of succinic acid (1.18 g, 100 mmol), lithium hydroxide (0.25 g, 100 mmol),

EDTA (58.5 mg, 2 mmol), EGTA (76.1 mg), and lithium dodecyl sulfate (10% *w/v*) was

dissolved in 100 mL of nuclease-free water and stirred until completely dissolved. The pH

was adjusted to 4.8 and the solution was then filtered through a 0.2 μm filter.

2.1.3.2   Hydrolysis buffers

A series of hydrolysis buffers were prepared at various pH values as required based

on the following method: Triton X102 (10 mL) was added to nuclease-free water (190 mL)

and then sodium tetraborate (11.5 g, 150 mmol) was added. The mixture was stirred in a

water bath at 60˚C until completely dissolved. The solution was allowed to cool to room temperature and the pH was adjusted to the required pH (in the range of 7-10).

2.1.3.3   Detection reagents

Detection Reagent 1: hydrogen peroxide (3% wt, 14.4 mL) was added to an autoclaved solution of nitric acid (384.6 mL, 1mM) to make up 400 mL of Reagent 1 (32 mM in hydrogen peroxide). Detection Reagent 2: sodium hydroxide (30 g) was dissolved in autoclaved water (500 mL) to prepare a 1.5 M solution.

2.1.4   Oligonucleotides

Modified DNA oligonucleotides that included an internal non-nucleotide linker containing a free primary amine attached to the oligonucleotide via a six carbons aliphatic spacer arm were used for labelling with acridinium-ester (figure 2.1).   These oligonucleotides were designed to our specifications and purchased from Integrated DNA Technologies (IDT, Coralville, USA). Oligonucleotides with the reverse complement sequence were purchased from Eurofins MWG Operon (Ebersberg, Germany).
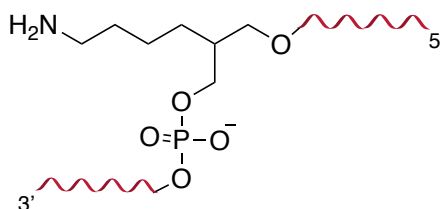
Figure 2. 1: Modified DNA oligonucleotides that included an internal non-nucleotide linker containing a free primary amine attached to the oligonucleotide via a six carbons aliphatic spacer arm.

2.1.5   Equipment list

2.1.5.1   High Performance Liquid Chromatography (HPLC)

High-performance liquid chromatography (HPLC) was conducted using a Thermo Separation Product instrument (Waltham, MA, USA) with automatic gradient elution. It was equipped with a diode array detector capable of measurement of the complete spectrum from 200-600 nm.   Moreover, it has the ability to separate and purify synthetic oligonucleotides of a similar size and has an efficient separation of chemical compounds. A Nucleogen-DEAE 60-7 ion exchange column was used for nucleic acid separation (Fisher Scientific, Loughborough, U.K).

2.1.5.2   Leader 50i Luminometer

A Leader 50i Luminometer (Gen-Probe, San Diego, USA), capable of automatically injecting Detection Reagent 1 (32 mM hydrogen peroxide in 1 mM nitric acid) followed by Detection Reagent 2 (1.5 M sodium hydroxide) into the sample tube in the luminometer chamber, was used for the immediate measurement of the rapid chemiluminescence output. The luminometer sample chamber, which holds a 12 x 75 mm polystyrene tube (Sarstedt, West Germany), presents the luminescent sample to the detector.

2.1.5.3   Tristar Luminometer

For the kinetic analysis, a TriStar 2 multiplate reader from Berthold Technologies Harpenden, U.K.), configured for luminescence readings and capable of dual injection of the Detection Reagents and able to measure the chemiluminescence output in milliseconds was used. Data were captured using the ICE software. The microplates used in the

experiments were white, hard-shell 96-well microplates also purchased from Berthold Technologies. To trigger the chemiluminescent reaction, Detection Reagent 1 (200 μL) was injected followed by Detection Reagent 2 (200 μL) after one second delay (0.5 second delay, followed by 0.5 second shake). The chemiluminescence intensity in Relative Light Units (RLU) was obtained over the required time.

2.1.5.4 Fluorimeter

A SpectraMax Gemini EM (Molecular Devices, Wokingham, U.K.) was used to determine the excitation and emission wavelengths. The instrument parameters are bandwidth slit 2 nm, temperature 25°C. All measurements were performed in 96 well microplates, Softmax pro- 7, (Molecular Devices, LLC, Sunnyvale, USA).

2.1.5.5 Nanodrop Spectrophotometer

The Nanodrop-1000 (Thermo Fisher Scientific, V 3.6.0) was used to determine the concentration of DNA and RNA with UV/Vis spectroscopy. The technique measured 260 nm absorbance to determine the nucleic acid concentration, while 230 and 280 nm absorbance was used to calculate purity. Probe Storage Buffer or RNase free water (1.2 μL) was measured to calibrate the instrument before making a measurement. Repeated blank measurements were taken to obtain a straight baseline. The sample (1.2 μL) was placed on the pedestal and the measurements were taken at 230, 260, 280 and 320 nm.

2.1.5.6 Allegra 21R Centrifuge

For any centrifugation steps requiring low temperatures (0 to 4°C), the Allegra 21R refrigerated centrifuge from Beckman Coulter (High Wycombe, U.K) was used with a

F2402H rotor. For precipitating nucleic acids, centrifugation speeds of 13,000 to 14,000

rpm were typically used.

Chapter 3

Synthesis and development of a family of novel acridinium esters

3 Synthesis and development of a family of novel acridinium esters

3.1 Introduction

Chemiluminescent compounds have found wide utility in tests developed for the measurement of a wide range of clinical analytes, providing sensitivity and specificity in immunoassay procedures that are used instead of traditional techniques like radioimmunoassay (RIA) and enzyme linked immunoassay (ELISA). Some chemiluminescent compounds, however, may also have some disadvantages, for example, low solubility in water, which is required for coupling to nucleic acids, and the effect of external additives on sensitivity. Use of acridinium esters as chemiluminescent compounds can overcome or at least reduce all the above drawbacks. The chemiluminescence reaction can be simply triggered by hydrogen peroxide in an alkaline environment.

Since the first report of a chemiluminescent acridinium ester in 1980 at the second international symposium on the application of chemiluminescence and biochemiluminescence, which was held in San Diego,[78] acridinium esters have been synthesized and offered as alternative chemiluminescent materials in medical diagnostics as chemiluminescence labels in immunoassays [80] and nucleic acid hybridization assays.[88] Several acridinium ester derivatives have been synthesized by Nelson and his co-workers, who have studied their chemiluminescence properties, which revealed significant differences in the kinetics of the reactions. These differences allow two or more derivatives to be simultaneously detected and quantified in a single reaction vessel. The first acridinium derivative for practical use was 4-(2-succinimidyloxycarbonylethyl)phenyl 10-methylacridinium-9-carboxylate trifluoromethanesulfonate (**15**; Figure 3.1), which can be coupled to DNA and interacts with hydrogen peroxide in a basic environment to emit a

short burst of light at 430 nm within <5 s. Compound **15** shows low stability, especially at room temperature, but it becomes more stable after coupling to DNA. This property makes the AE derivative a useful tool as a detection label in number of assay procedures, including nucleic acid probe–based procedures [93] and simultaneous detection of multiple nucleic acid targets in a homogeneous format using DNA probes labelled with various AE derivatives.[88]
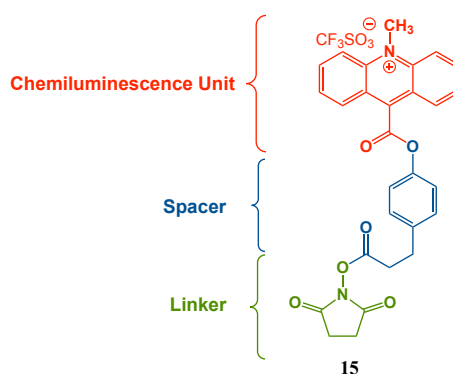
*Figure 3. 1: The structure of the standard acridinium ester (**15**) used in immunoassays.*

Recently, a dimethylphenyl acridinium ester was reported to display significant chemiluminescence efficiency and high stability. Changes in the leaving group and the substituents on the acridine ring can play a major role in the efficiency of chemiluminescence and stability of acridinium esters.[60] The main advantages of acridinium esters as chemiluminescence tools are the high sensitivity in immunoassays, a wide dynamic range, chemical reaction simplicity, rapid reaction kinetics, ease of use, and the lower background signals resulting from the fact that no catalyst is required to ignite the chemiluminescence reaction. Various derivatives of acridinium esters can be synthesized, including the introduction of electron-donating groups such as methyl or methoxy substituents into the acridinium ring, which may enhance the light emission or

lead to a shift of the emission wavelength, which offers the possibility of detecting more than one target in a single reaction.
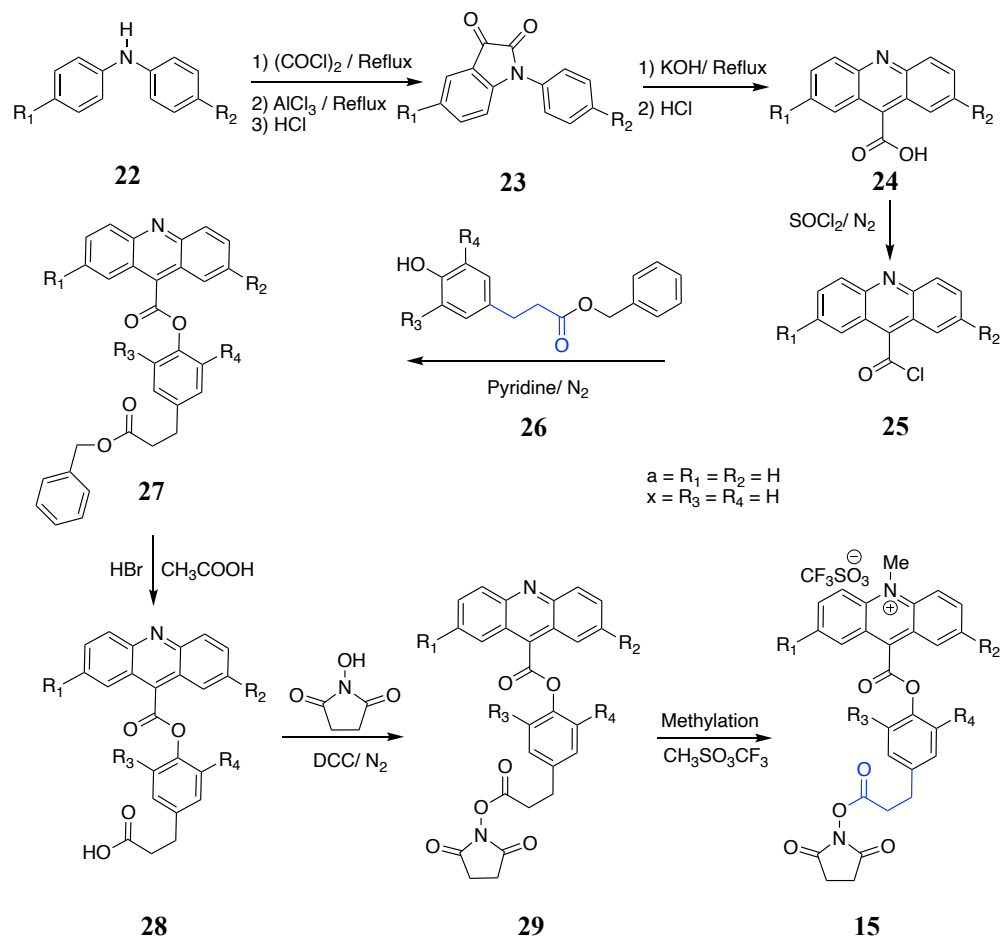
*Figure 3. 2: Published synthesis route for various acridinium esters (AE). The scheme involves 7 steps employed by Weeks et al. In this thesis, letters will be used after the structure number to denote the nature of the substituents on the acridinine unit (**a: unsubstituted acridinium ring** $R_1=R_2 = H$) and on the phenol unit (**x: unsubstituted leaving group** $R_3=R_4 =H$). Therefore, the standard unsubstituted AE **15** becomes **15ax**.*

In a recent study, a new acridinium NHS ester with two bromo substituents on the 2 and 7-positions of the acridinium ring was synthesized in our research group by Dr G. El-Hiti according to the synthetic route reported by Weeks *et al.*, shown in Figure 3.2 (the

standard or STD route). A similar synthetic route was expected to be suitable for the synthesis of the family of compounds needed for our research.

In the present study, the syntheses of a series of novel 10-methyl-9-(aryloxycarbonyl)acridinium trifluoromethanesulfonates bearing two substituents on the 2- and 7-positions of the acridinium ring and three differently substituted (at the 2- and 6-positions) aryl rings were planned. One of the tasks of the current work was to assess the light emission and the binding properties of the novel acridinium esters in comparison to the standard acridinium ester.

3.2 Development of acridinium esters

Chemiluminescent (CL) compounds have found wide utility in tests developed for medical diagnosis providing at least comparable sensitivity to radioimmunoassay (RIA) and enzyme immunoassay (EIA) procedures.[129] The AEs and their chemiluminescent conjugates give a strong fluorescent signal with clear background and no need for a catalyst or any external additives to measure the emitted light. The chemiluminescence reaction can be triggered by hydrogen peroxide in an alkaline solution to emit a flash of light. For use in medical diagnosis, the AE is attached to an active group such as a *N*-hydroxysuccinimide ester (NHS-ester), which can easily be joined to oligonucleotides or proteins under mild conditions. An important consideration for NHS-esters is that, with a few exceptions, they tend to be insoluble in aqueous buffers; this means that generally they must be dissolved in a non-aqueous organic solvent (*e.g.,* DMSO) or such a solvent must be added to the aqueous buffer containing the biological molecules of interest.

Our goal in this study was to produce a range of chemiluminescent acridinium esters with a variety of contrasting chemiluminescent properties for use in clinical diagnostics.

This may allow the detection of more than one acridinium label in the same assay by allowing different signals to be resolved and potentially allowing for multiple targets to be measured simultaneously.

3.3   Materials and Methods

Melting points (Mp) were recorded on a GALLENKAMP apparatus using the capillary method and are uncorrected. ^{1}H-NMR spectroscopy (400 or 500 MHz) and ^{13}C-NMR spectroscopy (100 or 125 MHz) spectra were recorded in deuterated chloroform (CDCl$_3$) or DMSO-d_6 on a Bruker AC 400 or 500 spectrometer. NMR spectroscopy assignments are based on chemical shift values and coupling patterns/constants and have not been rigorously verified. The chemical shifts were recorded in parts per million (ppm) and the coupling constants (J) were measured in Hz. IR spectra were obtained using a Perkin Elmer FTIR spectrometer. Low resolution mass spectra (MS) were recorded on a VG 12/253 mass spectrometer using electron impact (EI), chemical ionization (CI), or electrospray (ES) ionisation techniques. The data are presented as m/z ratios for fragments. Chemicals and reagents were obtained from Sigma Aldrich and Alfa Aesar. Column chromatography was carried out with silica gel 60 Å.

3.4   Synthesis of 4-(succinimidyloxycarbonyl)phenyl 2,7-dibromo-10-methylacridinium-9-carboxylate trifluoromethanesulfonate (34bx)

It was planned to synthesize the AE **34bx** from commercially available *bis*(4-bromophenyl)amine by a route (Figure 3.3) similar to that used by Dr El-Hiti. The first three steps were, in fact, identical to those used by Dr El-Hiti. We used identical

conditions; we obtained very similar results. The procedures and the characterization are

given below.
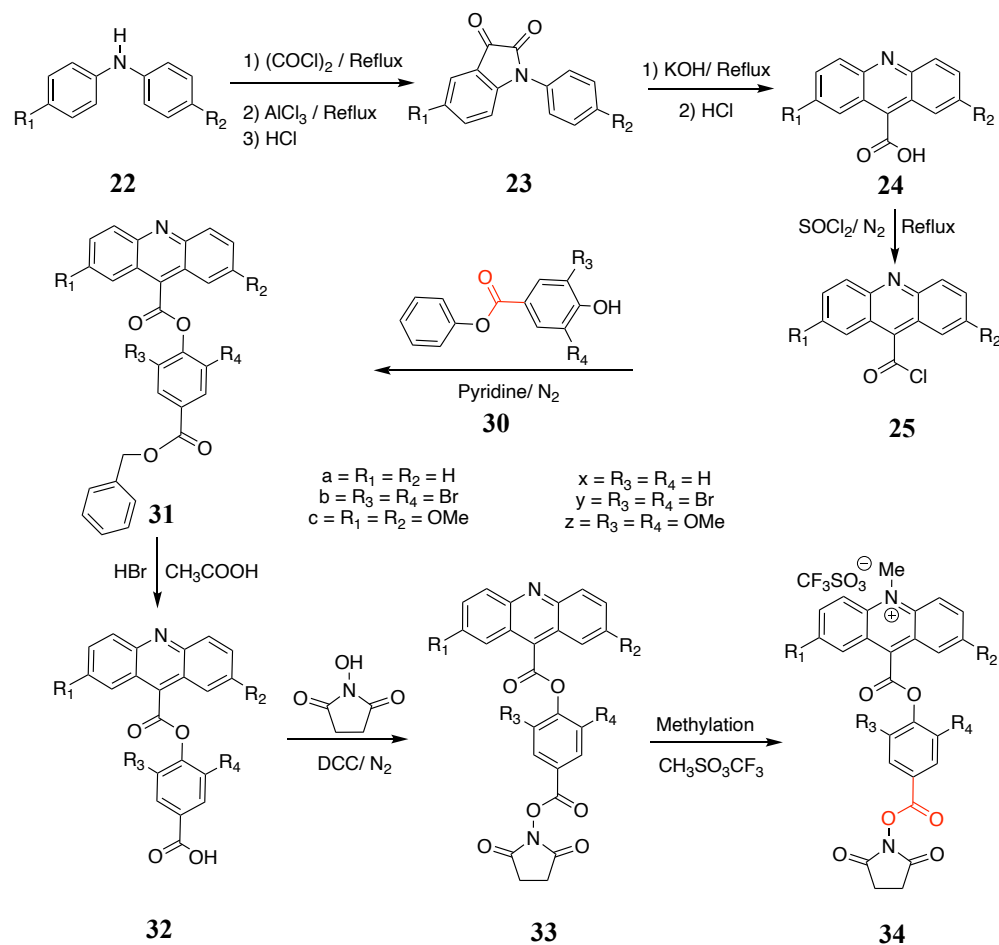
*Figure 3. 3: Proposed synthesis scheme for modified family of acridinium esters based on published route. The scheme includes the use of a benzyl 4-hydroxybenzoate (30) as the phenolic reactant. In acridinium ring; **a: unsubstituted** AE, R₁=R₂ = H. **b: bromo AE compounds**, R₁=R₂ =Br. **c: methoxy AE compounds**, R₁=R₂ =OMe. In the leaving group, the carbonyl group is attached directly to the phenyl ring. The aim was to tune the ease of hydrolysis of the ester bond [(**x:** R₃=R₄ =H). (**y:** R₃=R₄ =Me). (**z:** R₃=R₄ = OMe)].*

3.4.1 Synthesis of *N*-(4-bromophenyl)-5-bromoisatin (23b)
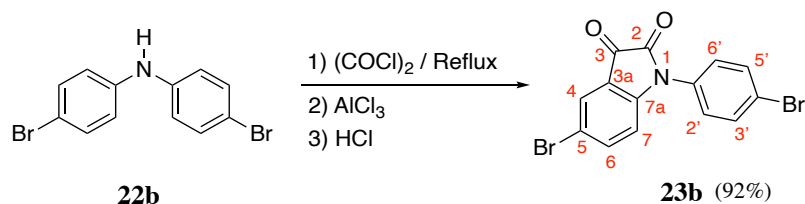
Figure 3. 4: The synthesis of N-(4-bromophenyl)-5-bromoisatin (23b).

bis(4-Bromophenyl)amine (**22b**, 5.01 g, 15.3 mmol) was dissolved in dichloromethane (DCM, 40 mL) and then added dropwise to stirred, refluxing oxalyl chloride (5.5 g, 43.6 mmol) in DCM (70 mL). The mixture was heated under reflux with stirring for 1.5 h. The excess oxalyl chloride and DCM were evaporated under reduced pressure. To the residue, DCM (100 mL) was added followed by anhydrous aluminium chloride (AlCl$_3$, 6.00 g, 45.1 mmol) portion-wise over 10 min. The mixture was refluxed for 1.5 h and the solvent was then removed under reduced pressure. Dilute hydrochloric acid (HCl, *ca*. 1 M, 60 mL) was added to the product and the mixture was stirred for 30 min, and then extracted with DCM (3 × 40 mL). The extract was dried over anhydrous magnesium sulfate and then filtered, and the organic layer was evaporated under reduced pressure. The orange solid obtained was washed with diethyl ether (20 mL) to give pure **23b** (5.36 g, 14.1 mmol, 92% yield). The structure was confirmed by NMR spectroscopy, mass spectrometry and X-ray crystallography (Figure 3.4). Mp: 235-237ºC. ^{1}H-NMR spectroscopy (400 MHz; CDCl$_3$): δ = 7.74 (d, *J* = 2.0 Hz, 1 H, H-4), from 7.64-7.59 (m, 2 H, H-6/H-7), 7.22 (dd, *J* = 2.0 and 8.5 Hz, 2 H, H-2'/H-6'), 6,74 (dd, *J* = 2.0 and 8.5 Hz, 2 H, H-3'/H-5'). ^{13}C-NMR spectroscopy (100 MHz; CDCl$_3$): δ = 186.5 (s, C-3), 162.2 (s, C-2), 154.8 (s, C-7a), 144.8 (s, C-1'), 138.0 (d, C-3'/C-5'), 137.7 (d, C-6), 133.8 (d, C-

2'/C-6'), 132.1 (d, C-4), 126.6 (d, C-7), 124.8 (s, C-3a), 120.6 (s, C-4'), 118.1 (s, C-5). EI-

MS: *m/z* (%) = 384 (8), 383 (49), 382 (20), 381 (100), 380 (10), 379 (51), HRMS (EI): calc

for $C_{14}H_7{}^{79}Br_2NO_2$ (M^+): 378.8844; found: 378.8843.
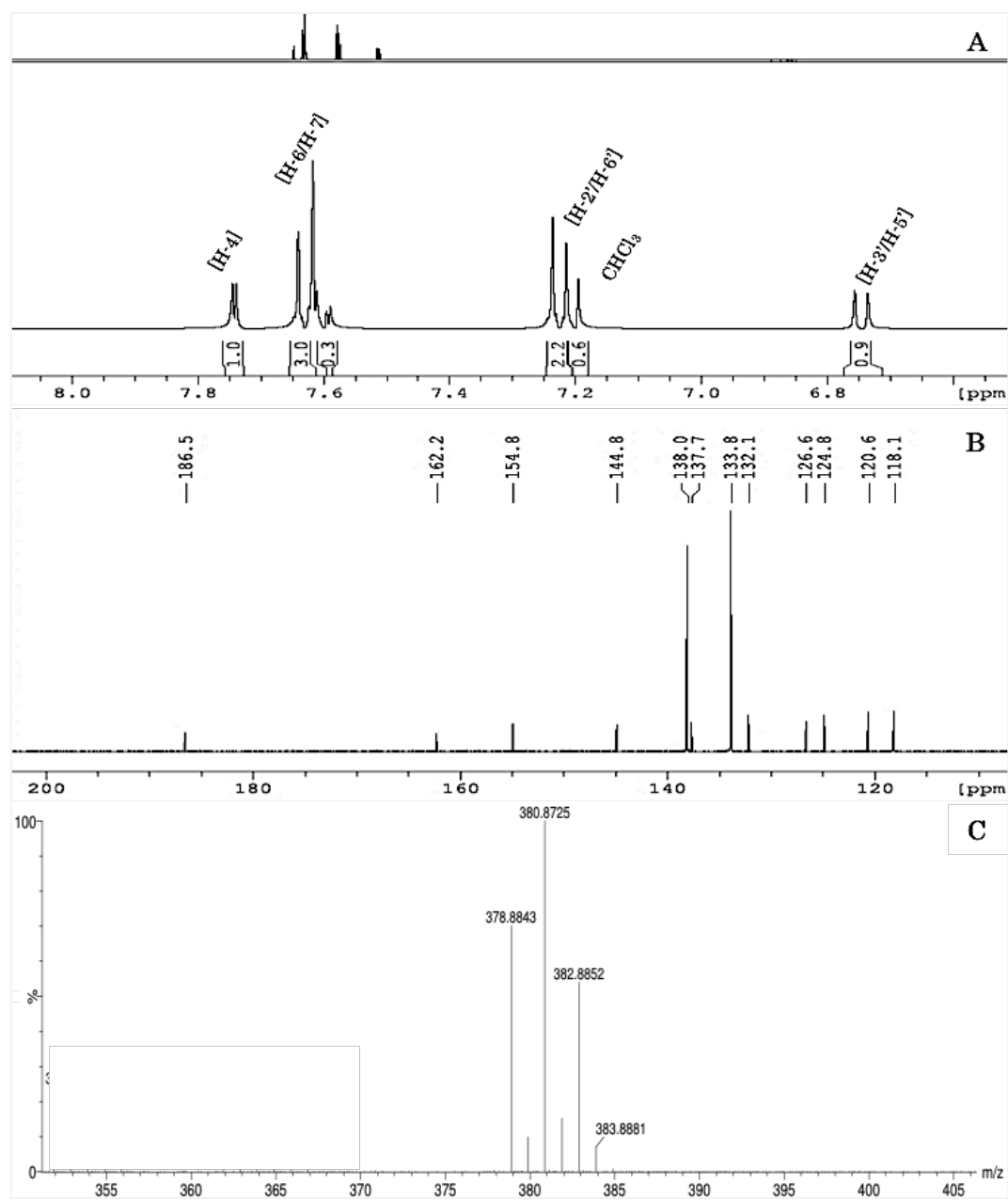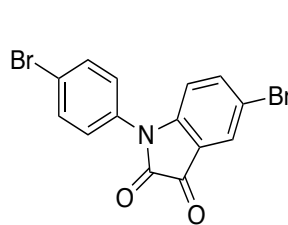
*Figure 3. 5: The ^1H NMR (A), ^{13}C NMR (B) and mass spectra (C) of N-(4-bromophenyl)-5-bromoisatin (**23b**).*

3.4.1.1 Crystal structure of *N*-(4-bromophenyl)-5-bromoisatin (23b)
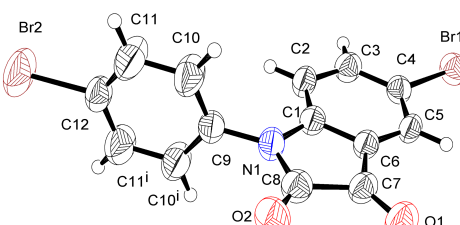
Pure **23b** was crystallised from acetonitrile to give orange crystals (Mp. 235-236 ºC). One crystal was selected for X-ray crystallographic analysis (parameters in Figure 3.6) and the structure and packing arrangements were determined (See Figures 3.6 and 3.7). Full details of the analysis have been lodged with the Cambridge Crystallographic Data Centre (CCDC reference: 1829295) and published (see Appendix).

*Figure 3. 6: Data, data collection and handling for X-ray crystallographic studies of N-(4-bromophenyl)-5-bromoisatin (**23b**), including the X-ray crystal structure*

X-ray crystallography data for compound 23b			
Appearance	Orange crystal	Radiation type	Mo Kα
Crystal size (mm)	0.29 x 0.24 x 0.19	μ (mm^{-1})	6.12
Crystal system	Orthorhombic	Diffractometer	Agilent SuperNova, Dual, Cu at zero, Atlas
Space group	Pnma	Measured reflections	5624
Temperature (K)	293	Independent reflections	1801
a (Å)	15.1160 (14)	Parameters	110
b (Å)	6.8728 (6)	H atom treatment	H atom parameters constrained
c (Å)	12.7492 (11)	Computer programs used	CrysAlis PRO; SHELXS97; SHELXL2018
V (Å³)	1324.5 (2)	Chemical formula	$C_{14}H_7Br_2NO_2$

Chemical Formula: $C_{14}H_7Br_2NO_2$

.
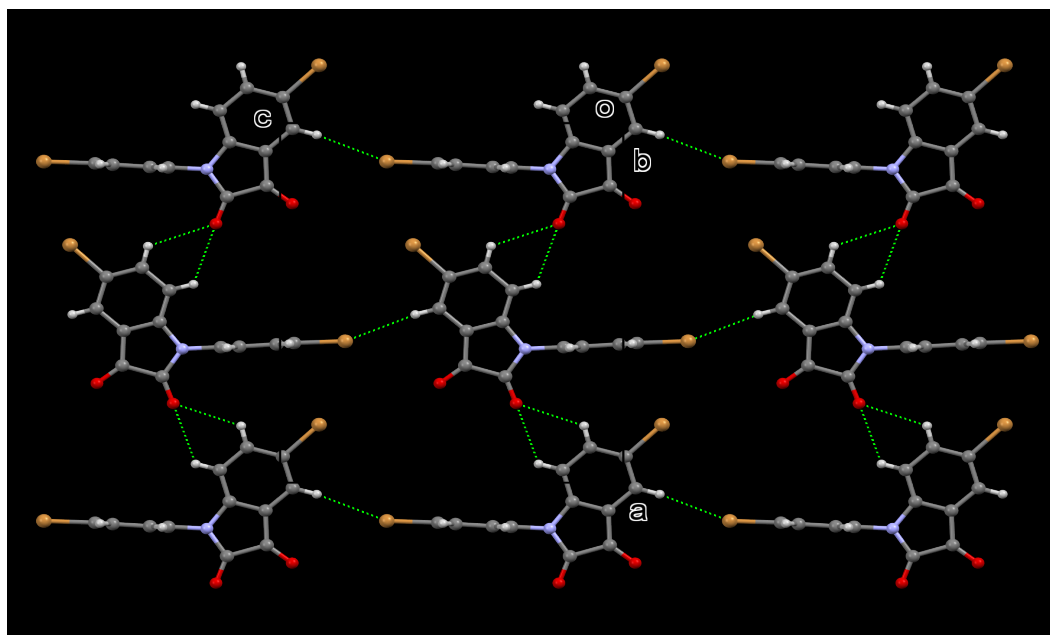
*Figure 3. 7: Three-dimensional arrangement of molecules of **23b** within the crystal.*

3.4.2 Synthesis of 2,7-dibromoacridine-9-carboxylic acid (24b)
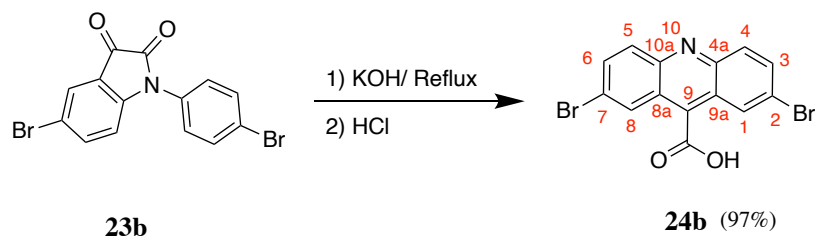
*Figure 3. 8: Synthesis of 2,7-dibromoacridine-9-carboxylic acid (**24b**).*

A mixture of **23b** (3.81 g, 10 mmol) and potassium hydroxide (KOH; 14 g, 250 mmol) in water (280 mL) was refluxed for 72 h (figure 3.8). The orange solid turned to yellow and then dissolved to give a green solution, which turned yellow as the reaction proceeded. The mixture was poured into a mixture of conc. HCl (11 M, 30 mL) and ice (80 g). The

mixture was stirred for 5 min and the solid obtained was collected by filtration, then washed

with water (3 × 50 mL), methanol (2 × 40 mL) and diethyl ether (40 mL).
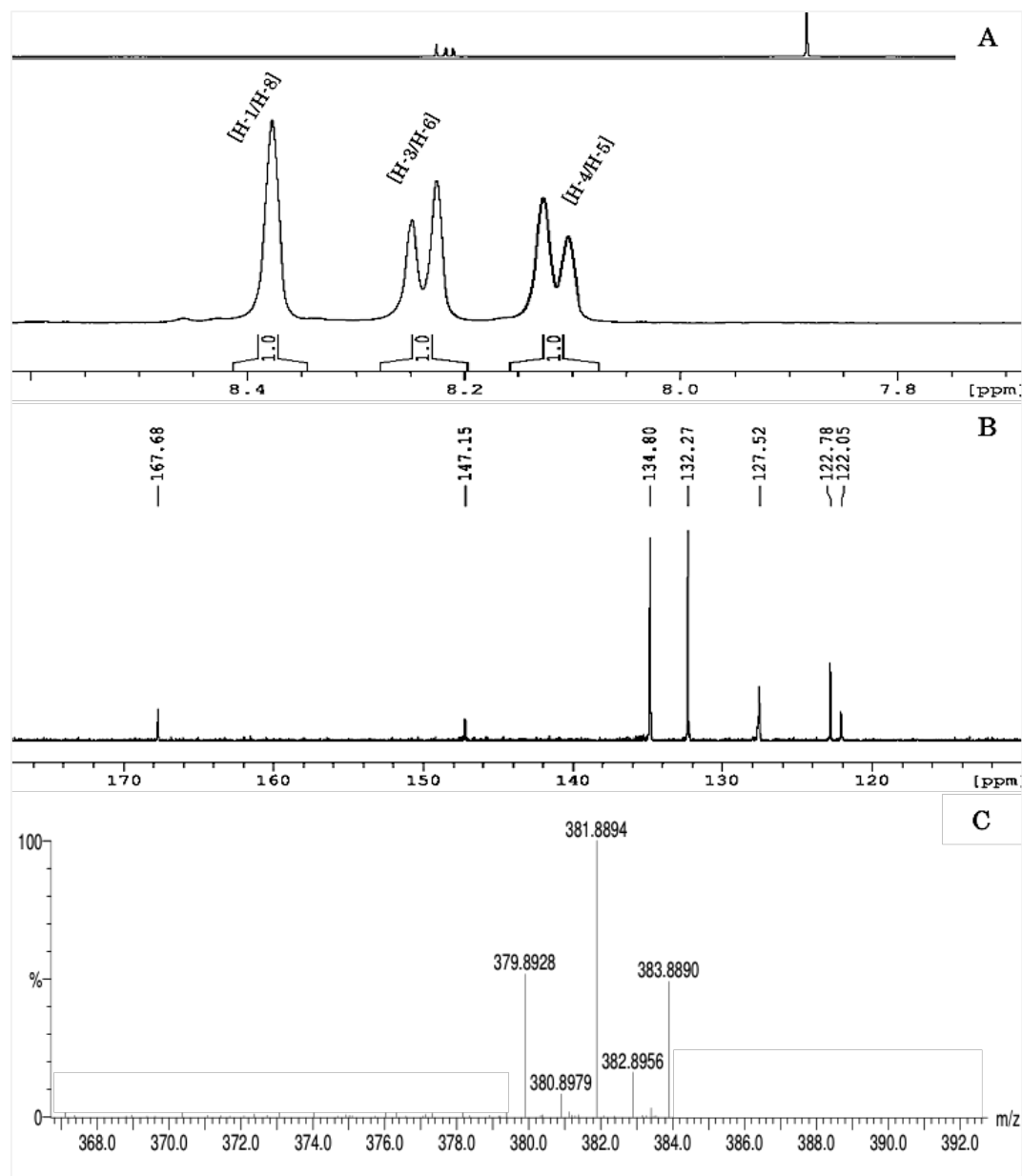
*Figure 3. 9: The ^1H NMR (A), ^{13}C NMR (B) and mass spectra (C) of 2,7-dibromoacridine-9-carboxylic acid (**24b**).*

The solid product was dried to give **24b** as a yellow solid in 97% yield (3.69 g, 9.67 mmol). Mp: 308-310ºC. IR ν_{max}: 3434, 2920, 2856, 1610, 1460, 1320, 1290, 850 cm^{-1}. ^{1}H-NMR spectroscopy (400 MHz; DMSO-d_6): δ = 8.38 (s, 2 H, H-1/H-8), 8.24 (d, J = 8.8 Hz, 2 H, H-3/H-6), 8.11 (d, J = 8.8 Hz, 2 H, H-4/H-5). ^{13}C-NMR spectroscopy (100 MHz; DMSO-d_6): δ = 167.7 (s, C=O), 147.2 (s, C-4a/C-10a), 134.8 (s, C-9), 134.8 (d, C-3/C-6), 132.3 (d, C-4/C-5), 127.5 (d, C-1/C-8), 122.8 (s, C-8a/C-9a), 122.1 (s, C-2/C-7). EI-MS: m/z (%) = 383 ([MH^{81}Br$_2$]$^+$, 75), 381 ([MH^{81}Br^{79}Br]$^+$, 100), 379 ([MH^{79}Br$_2$]$^+$, 87), 366 (6), 364 (13), 362 (8), 339 (42), 337 (88), 335 (44), 303 (22), 301 (23), 274 (12), 272 (13), 257 (33), 255 (32), 246 (19), 244 (20), 221 (11), 207 (14), 177 (61), 150 (23); HRMS (EI) spectrometry: calc for C$_{14}$H$_8$^{79}Br$_2$NO$_2$ (M$^+$+H): 379.8922; found: 379.8928.

3.4.3   Synthesis of 2,7-dibromoacridine-9-carbonyl chloride (25b).
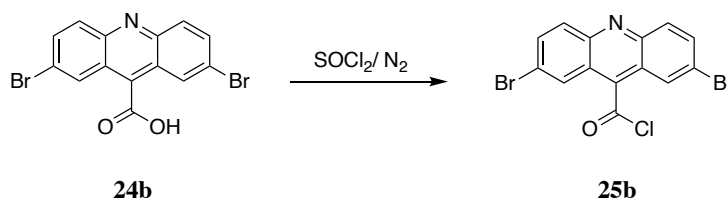
Figure 3. 10: Synthesis of 2,7-dibromoacridine-9-carbonyl chloride (**25b**).

2,7-Dibromoacridine-9-carbonyl chloride (**25b**) was prepared according to a procedure reported by M. Rauhut and his co-workers and other later studies. [66,130]   A mixture of 2,7-dibromoacridine-9-carboxylic acid (**24b**; 2.00 g, 5.24 mmol) and freshly distilled thionyl chloride (30 mL) was refluxed under anhydrous conditions for 1.5 h. Thionyl chloride was removed under reduced pressure to leave a yellow solid (*ca*. 2.10 g,

5.24 mmol), which was used for the next step without any further purification or spectroscopic analysis.

3.4.4 Synthesis of 4-(benzyloxycarbonyl)phenyl 2,7-dibromoacridine-9-carboxylate (31bx)

The next step was to introduce the new leaving group by reaction of benzyl 4-hydroxybenzoate (**30x**), which was commercially available, with 2,7-dibromoacridine-9-carbonyl chloride (**25b**). In this new step, Dr El-Hiti's conditions for the production of **27** were used, except for changing the phenolic reactant from **26** to **30x**. Compound **31bx** was obtained in good yield by the procedure described below.
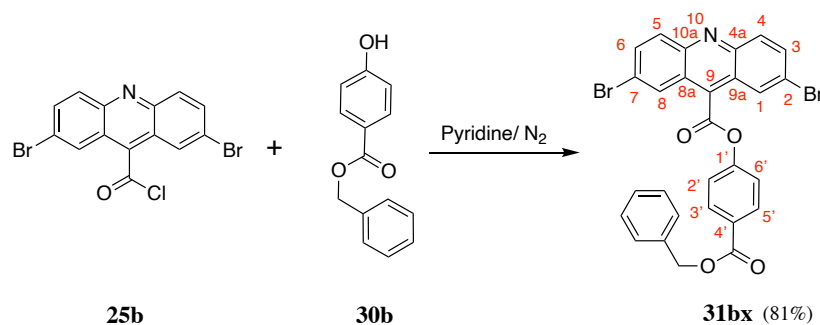
Figure 3. 11: Synthesis of 4-(benzyloxycarbonyl)phenyl 2,7-dibromoacridine-9-carboxylate (31bx).

A mixture of benzyl 4-hydroxybenzoate (**30x**, 1.22 g, 5.28 mmol) in anhydrous pyridine and 2,7-dibromoacridine-9-carbonyl chloride (**25b**, 2.10 g, 5.25 mmol) in anhydrous pyridine (30 mL) was stirred at 70°C and the progress of the reaction was monitored by TLC until completion (5 days). The resulting mixture was cooled in an ice bath for 20 min and then poured into a mixture of hydrochloric acid (1 M, 100 mL) and dry ice (30 g). A yellowish solid product was formed. The product obtained was washed with

diethyl ether (20 mL x 2) to remove the impurities and the solvent was evaporated to give

a pure compound **31bx** in 81% yield (2.55 g, 4.32 mmol, Figure 3.11),

*Figure 3. 12: The ^{1}H NMR (A), ^{13}C NMR (B) and mass spectra (C) of 4-(benzyloxycarbonyl)phenyl 2,7-dibromoacridine-9-carboxylate (**31bx**).*

Mp. 218–220ºC. IR v_{max}: 3321, 3278, 2927, 2850, 1745, 1695, 1624, 1513, 1168, 962 cm^{-1}. ^{1}H NMR spectroscopy (400 MHz; CDCl$_3$): δ = 7.62 (d, J = 2.1 Hz, 2 H, H-1/H-8), 7.52 (d, J = 9.0 Hz, 2 H, H-3'/H-5'), 7.38 (d, J = 9.2 Hz, 2 H, H-4/H-5), 7.14 (dd, J = 2.1 and 9.2 Hz, 2 H, H-3/H-6), 6.76 (d, J = 9.0 Hz, 2 H, H-2'/H-6'), 6.72–6.49 (m, 5 H, Ph), 4.65 (s, 2 H, CH$_2$). ^{13}C-NMR spectroscopy (125 MHz, DMSO-$d6$): 165.3 (s, C=O), 164.3 (s, C=O), 153.7 (s, C-1'), 147.1 (s, C-4a/C-10a), 135.8 (s, C-1 Benz), 134.5 (d, C-3/C-6), 132.6 (s, C-9), 131.9 (d, C-4/C-5), 131.8 (d, C-3'/C-5'). 128.9 (s, C-4'), 128.7 (d, C-3/C-5 Benz), 128.4 (d, C-4 Benz), 128.2 (d, C-1/C-8), 126.8 (d, C-2/C-6 Benz), 123.5 (s, C-9a/C-8a), 123.2 (s, C-2/C-7), 121.5 (d, C-2'/C6'), 67.0 (t, CH$_2$). ES$^+$-MS: m/z (%) = 594 ([MH^{81}Br$_2$]$^+$, 50), 592 ([MH^{81}Br^{79}Br]$^+$, 100), 590 ([MH^{79}Br$_2$]$^+$, 50), 557 (5), 556 (6), 548 (25), 546 (18), 519 (5), 481 (7), 445 (9), 376 (15), 359 (20), 331 (18). HRMS (ES$^+$) spectrometry: calc for $C_{28}H_{18}^{79}Br_2NO_4$ (M+H$^+$): 589.9603; found: 589.9600.

3.4.5   Synthesis of 4-((2,7-dibromoacridine-9-carbonyl)oxy)benzoic acid (32bx)

Hydrolysis of benzyl ester **31bx** with hydrobromic acid and acetic acid was conducted using a procedure identical to that used by El-Hiti for the related system. Compound **32bx** was synthesized in 68% yield according to the procedure described below.
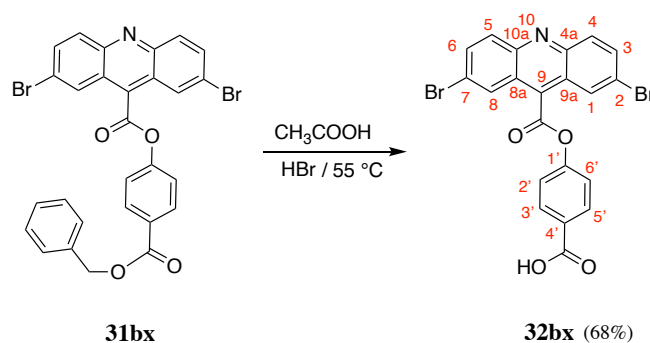
Figure 3. 13: Synthesis of 4-((2,7-dibromoacridine-9-carbonyl)oxy)benzoic acid, (32bx).

A mixture of 4-(benzyloxycarbonyl)phenyl acridine-9-carboxylate (**31bx**, 1.26 g, 2.1 mmol), glacial acetic acid (20 mL) and 48% hydrobromic acid (10 mL) was heated at 55°C for 50 h in an oil bath and then cooled to room temperature. The reaction mixture was poured into cool water (80 mL) and a yellow solid formed. This was collected by filtration and purified by washing with DCM (2 x 20 mL) to give **32bx** in 68% yield (0.72 g, 1.43 mmol, Figure 3.13), Mp: 357–358°C. IR ν_{max}: 3100, 1732, 1604, 1500, 1701, 1604, 1429, 1236, 1159 cm^{-1}.
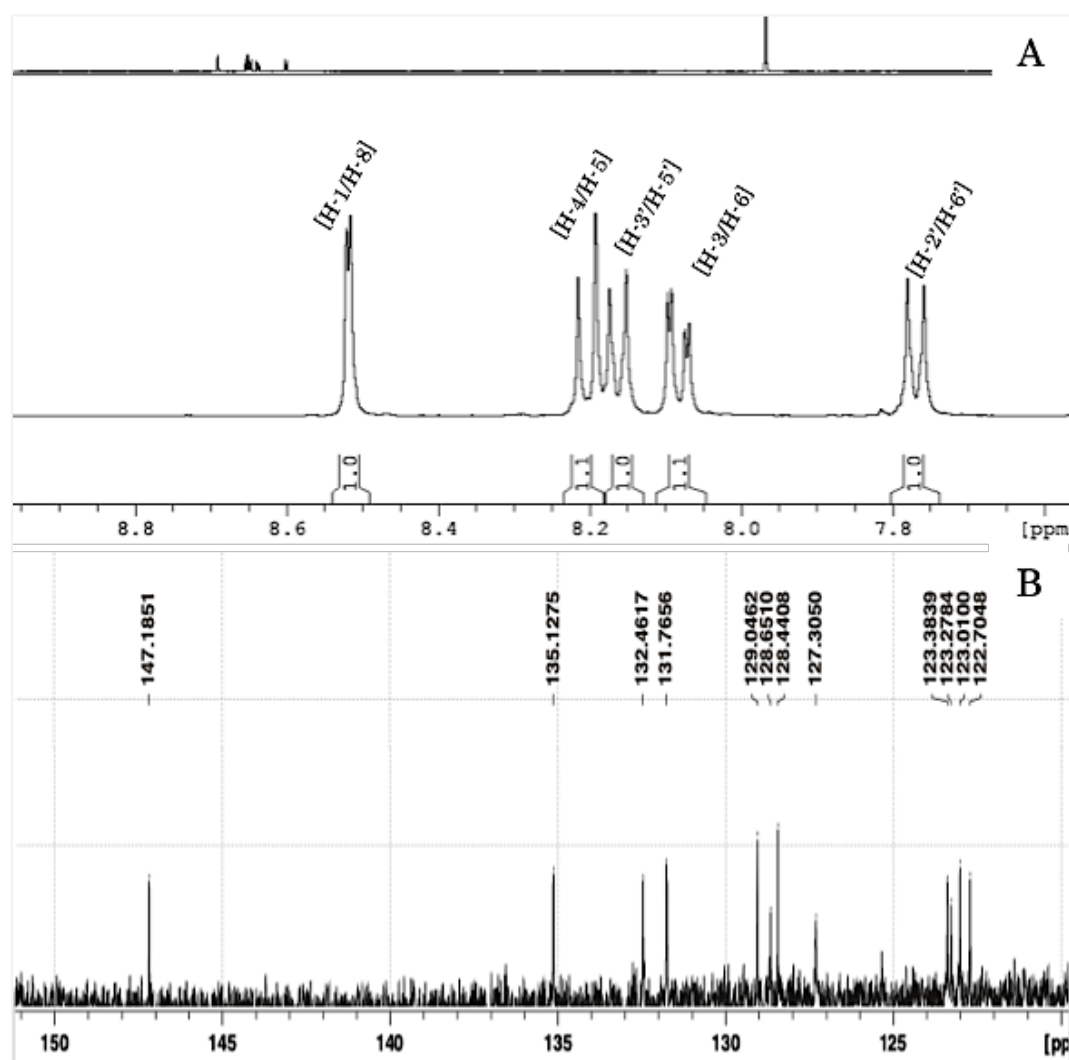
*Figure 3. 14: The ^{1}H NMR (A) and ^{13}C NMR (B) of 4-((2,7-dibromoacridine-9-carbonyl)oxy)benzoic acid, (**32bx**).*

^{1}H NMR spectroscopy (400 MHz; DMSO-d_6): δ = 8.54 (d, J = 2.1 Hz, 2 H, H-1/H-8),

8.23 (d, J = 9.1 Hz, 2 H, H-4/H-5), 8.18 (d, J = 9.0 Hz, 2 H, H-3'/H-5'), 8.10 (dd, J = 2.1

and 9.1 Hz, 2 H, H-3/H-6), 7.78 (d, J = 9.0 Hz, 2 H, H-2'/H-6'). ^{13}C-NMR spectroscopy

(125 MHz, DMSO-$d6$): 147.0 (s, O=C-OH), 135.1 (s, O=C), 132.5 (s, C-1'), 131.7 (s, C-

4a/C-10a), 129.0 (d, C-3/C-6), 128,6 (s, C9), 128.6 (d, C-3'/C-5'), 125.3 (s, C-4'). 127.3

(d, C-1/C-8), 123.4 (d, C-4/C-5), 123.3 (s, C-8a/C9a), 123.0 (d, C-2'/C6'), 122.7 (s, C-2/C-

7). AP$^+$-MS: m/z (%) = 504 ([MH^{81}Br$_2$]$^+$, 49), 502 ([MH^{81}Br^{79}Br]$^+$, 100), 500 ([MH^{79}Br$_2$]$^+$,

51), 369 (20), 339 (21), 337 (37), 335 (30), 262 (40), 260 (45). HRMS spectrometry (AP$^+$):

calc for C$_{21}$H$_{12}$^{79}Br$_2$NO$_4$ [M+H$^+$]: 499.9133; found: 499.9133.

3.4.6 Synthesis of 4-(succinimidyloxycarbonyl)phenyl 2,7-dibromoacridine-9-carboxylate (33bx)

The synthesis of compound **33bx** from compound **32bx** was attempted using conditions similar to those described by Dr El-Hiti. However attempted isolation of **33bx** resulted in almost none of the expected product; instead, a significant quantity of the starting material **32bx** was left unreacted. It seemed likely that the solubility of the acid in the reaction solvent (DCM) was low, resulting in the lack of reactivity. Various conditions were applied to overcome this problem, including a change of solvents, and increasing the reaction time. Under the best conditions found, the product obtained in 33% yield. The procedure is described below. 4-((2,7-Dibromoacridine-9-carbonyl)oxy)benzoic acid (**32bx**, 1.2 g, 2.4 mmol) was added to a mixture of THF and DCM (1:1, 30 mL), and stirred at 60˚C for 10 min under anhydrous conditions until the compound dissolved. The mixture was allowed to cool to room temperature, then *N*-hydroxysuccinimide (NHS) (0.82 g, 7.1 mmol) was added, followed by *N,N*-dicyclohexylcarbodiimide (DCC) (1.5 g, 7.2 mmol). The mixture was placed in an ice bath for one hour and then stirred at room temperature

for 36 hours. The solvents were evaporated under reduced pressure. The solid obtained

was washed with diethyl ether (2 x 20 mL).
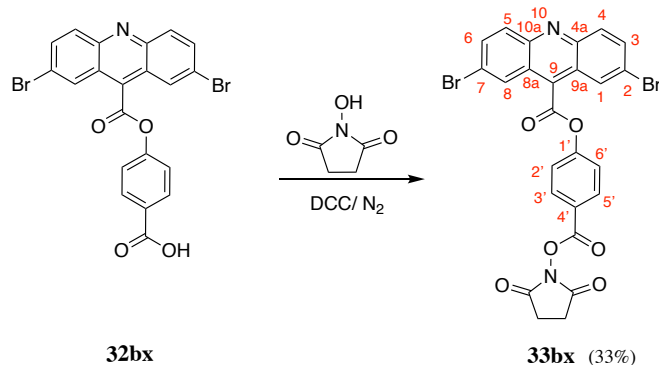
Figure 3. 15: Synthesis of 4-(succinimidyloxycarbonyl)phenyl 2,7-dibromoacridine-9-carboxylate (33bx).

The ^{1}H-NMR spectrum of the crude product showed a small peak at 2.93 corresponding to

NHS and strong signals in the aromatic region. The crude product was purified by column

chromatography, (silica gel; ethyl acetate–hexane, 2:1) to give **33bx** (0.48 g, 0.80 mmol,

33% yield, Figure 3.15), Mp; 242-243ºC, IR ν_{max}: 2929, 1772, 1728, 1336, 1257, 1238,

1199, 1172, 1004, 983. 962 cm^{-1}. ^{1}H-NMR spectroscopy (500 MHz; DMSO-d_6): δ = 8.57

(d, J = 2.0, 2 H, H-1/H-8), 8.34 (d, J = 8.8 Hz, 2 H, H-3'/H-5'), 8.22 (d, J = 9.2 Hz, 2 H,

H-4/H-5), 8.10 (dd, J = 2.0 and 9.2 Hz, 2 H; H-3/H-6), 7.95 (d, J = 8.8 Hz, 2 H, H-2'/H-

6'), 2.93 (s, 4 H, CH$_2$CH$_2$). ^{13}C-NMR spectroscopy (125 MHz; DMSO-d_6): δ = 170.8 (s,

C=O of NHS), 163.8 (s, O-C=O Ar), 161.6 (s, O=C-O-NHS), 155.5 (s, C-1'), 147.1 (s, C-

4a/C10a), 135.1 (d, C-3/C-6), 132.7 (d, C-3'/C-5'), 132.4 (d, C-4/C-5), 132.3 (s, C-9),

127.3 (s, C-4'), 123.9 (d, C-1/C-8), 123.5 (d, C-2'/C-6'), 123.4 (s, C8a/C9a), 123.3 (s, C-

2/C-7), 25.8 (t, CH$_2$CH$_2$). TOF MS EI spectrometry m/z (%) = MS AP$^+$-MS: m/z (%): 601

([MH^{81}Br$_2$]$^+$, 50), 599 ([MH^{81}Br^{79}Br]$^+$, 100), 597 ([MH^{79}Br$_2$]$^+$, 45).   HRMS (EI)

spectrometry: calc for $C_{25}H_{15}{}^{79}Br_2N_2O_6$ (M+H): 596.9297; found: 596.9319 (see figure 3.16).
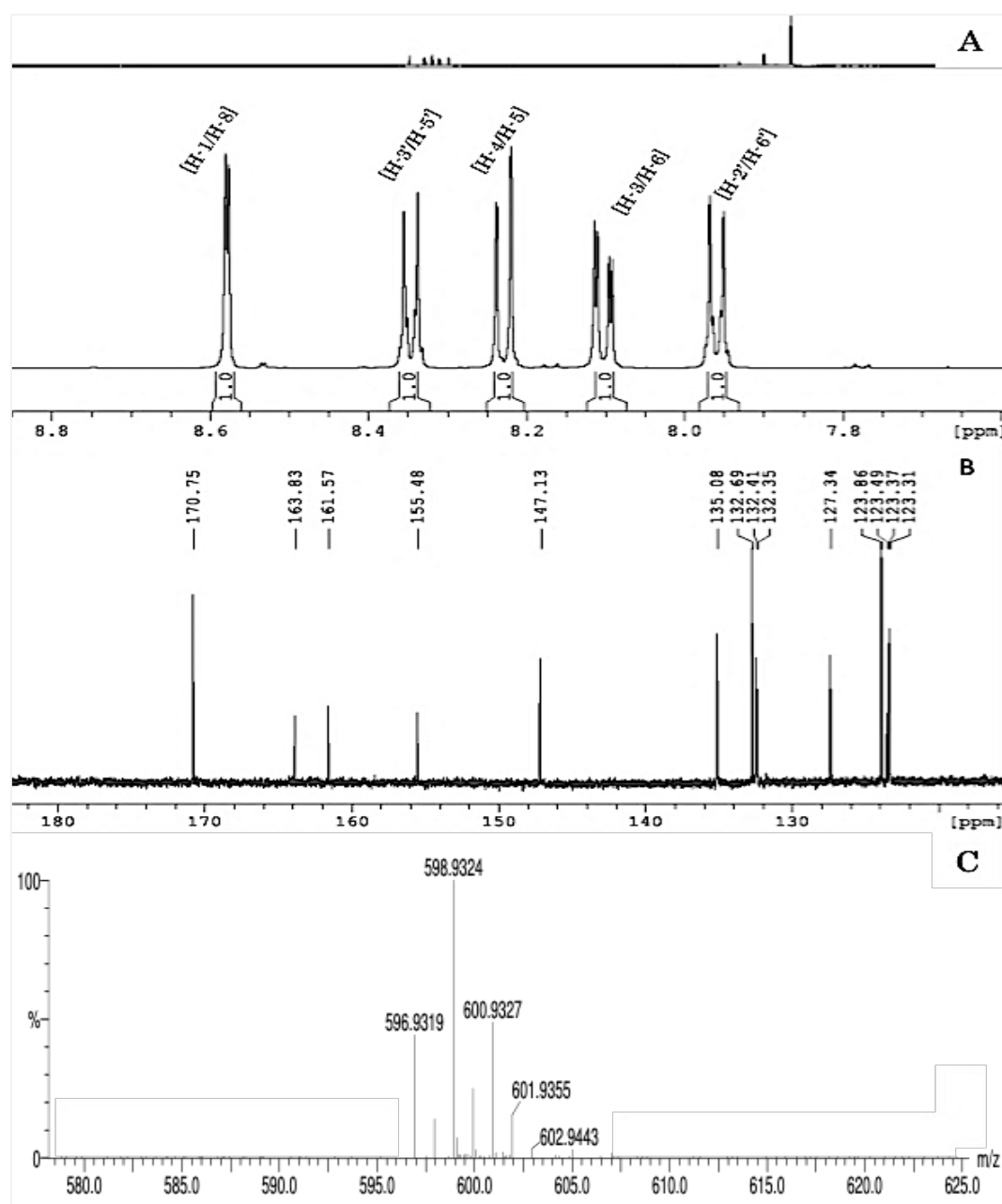
Figure 3. 16 The ^1H-NMR (A), ^{13}C-NMR (B) and mass spectra (C) of 4-(succinimidyloxycarbonyl)phenyl 2,7-dibromoacridine-9-carboxylate (**33bx**).
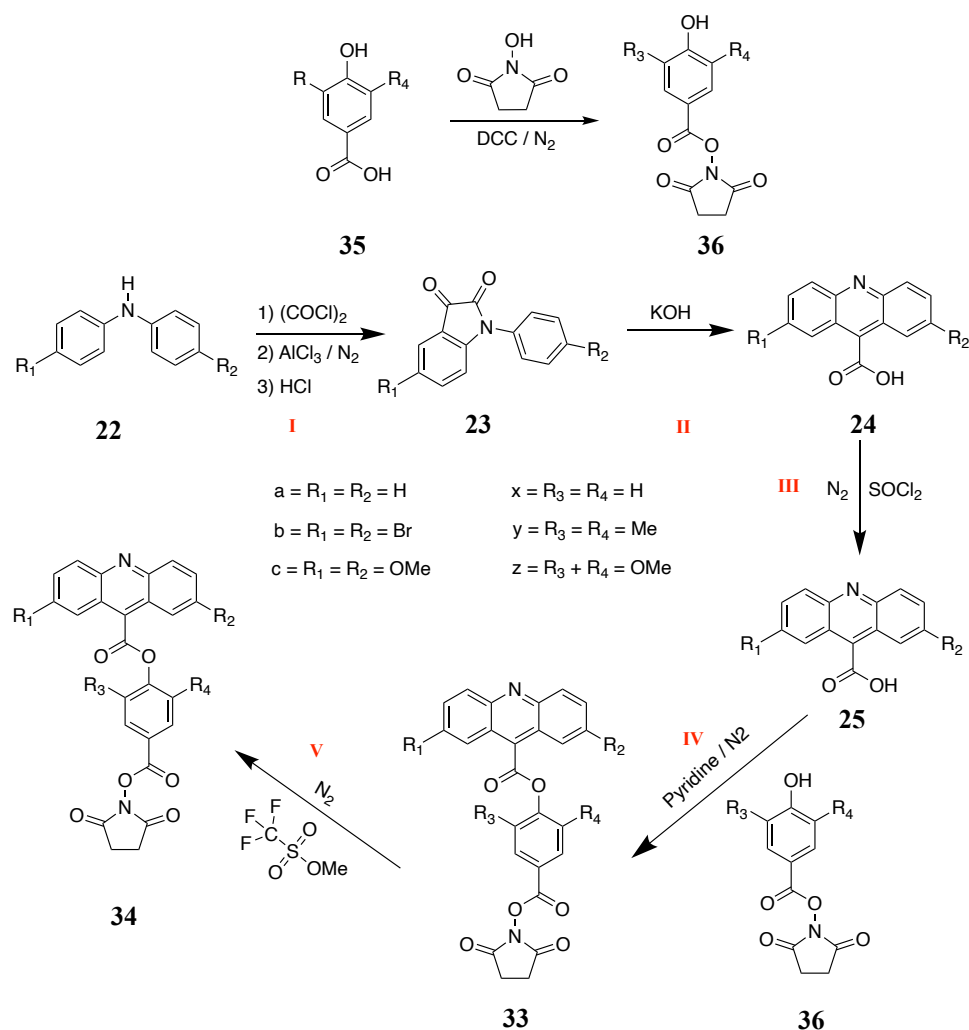
*Figure 3. 17: Alternative synthesis scheme for modified family of acridinium esters. The scheme involves 5 steps using 36 instead of 7 steps using 30 as presented in the published route. In this route, the phenolic succinimidyl ester 36 was first synthesized and attached to the acyl chloride 25, to give 33. In the acridine ring; **a: unsubstituted AE**, R₁=R₂ = H. **b: bromo AE compounds**, R₁=R₂ = Br. **c: methoxy AE compounds**, R₁=R₂ = OMe. In the phenol leaving group; [(x: R₃=R₄ =H), (y: R₃=R₄ =Me) or (z: R₃=R₄ = OMe)].*

Although the above procedure provided a sample of compound **33bx**, the low yield and inconvenient reaction conditions were not considered to be acceptable. To solve this problem an alternative approach was therefore considered (figure 3.17), which would also have the benefit of saving reaction steps (a comparison of the new and published routes is given in Figure 3.18). The first step in the synthesis of **33bx** by the new route was to

synthesise 4-hydroxybenzoic acid NHS ester (**36x**) by treating 4- hydroxybenzoic acid with NHS and DCC in a way similar to that used in the attempted synthesis of compound **33bx** described above.
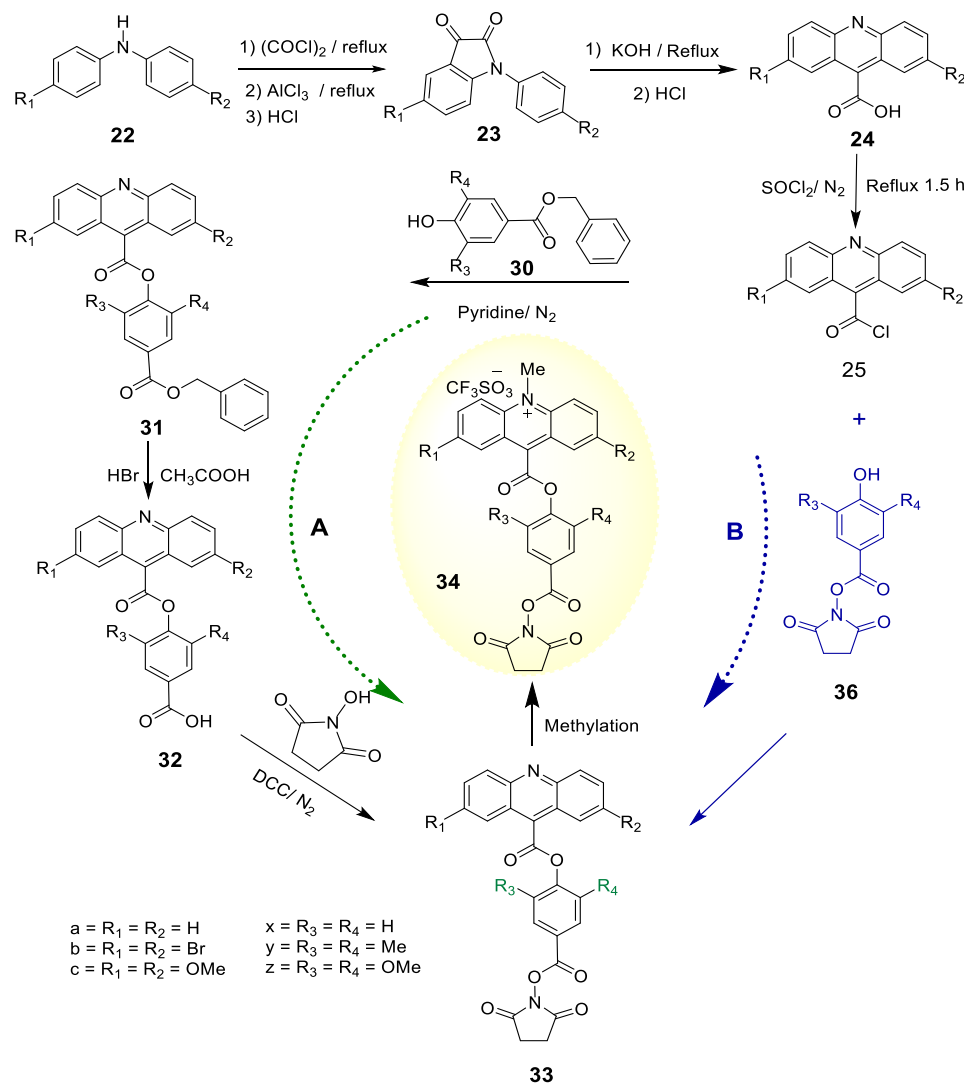
*Figure 3. 18: Comparison of synthesis schemes for modified family of acridinium esters. "**Panel A**" is the synthesis scheme based on the published route in 7 steps. "**Panel B**" is the alternative synthesis scheme for the modified family of acridinium esters in 5 steps.*

The method was applied, and the crude product obtained was analysed by NMR spectroscopy, which showed that the reaction proceeded to only a small extent and that a lot of starting material remained. Various conditions, including varying the solvent,

temperature, and reaction time, were applied and it was found that a good yield could be obtained when using THF as solvent at room temperature for 2 days, as described below.

3.4.7   Synthesis of succinimidyl 4-hydroxybenzoate (36x)
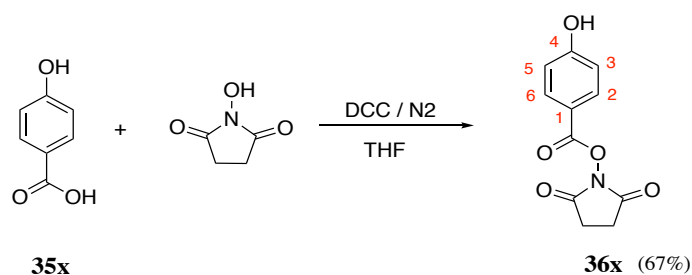
Figure 3. 19: Synthesis of succinimidyl-4-hydroxybenzoate (36x).

To a stirred cold (0ºC) solution of 4-hydroxybenzoic acid (**35**x, 3.5 g, 25.3 mmol) in tetrahydrofuran (150 mL), 1,3-dicyclohexylcarbodiimide (DCC) (5.78 g, 28.0 mmol) was added; the mixture was stirred for 10 min and *N*-hydroxysuccinimide (4.38 g, 38.0 mmol) was then added. The mixture was stirred under a nitrogen atmosphere at 0ºC for 2 h and at room temperature overnight.   The mixture was filtered to remove the insoluble dicyclohexylurea and the filtrate was evaporated to dryness under reduced pressure. The residue obtained was washed with diethyl ether (2 × 30 mL) and then suspended in boiling ethyl acetate (100 mL) and filtered.   The filtrate was washed with saturated sodium bicarbonate solution then water and dried over anhydrous magnesium sulfate. The solution was concentrated, and diethyl ether (30 mL) was added; the mixture was left to precipitate overnight and then filtered to give **36x** as an off-white powder (2.3 g, 17 mmol, 67% yield, Figure 3.19),
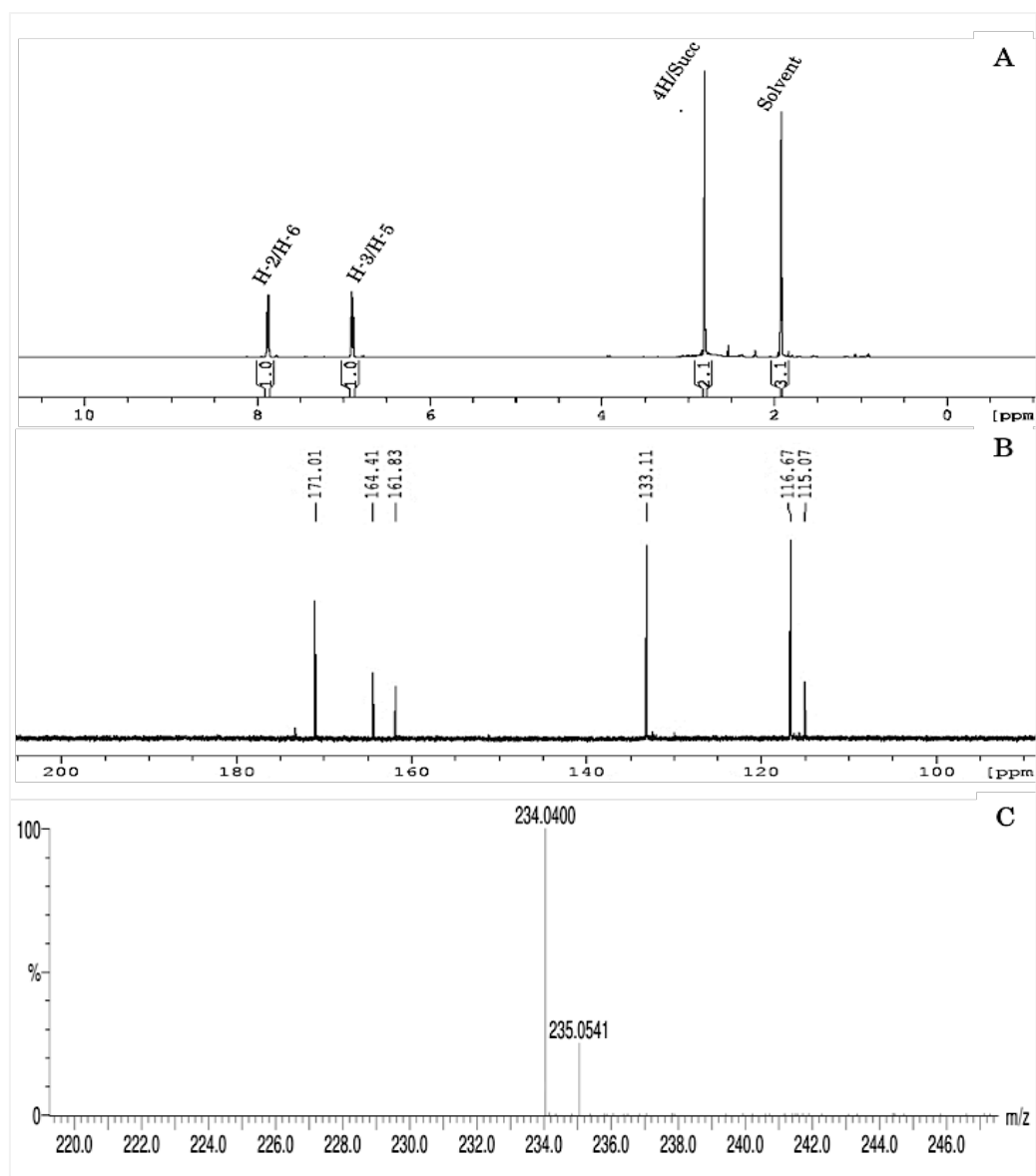
Figure 3. 20: The ^{1}H-NMR (A), ^{13}C-NMR (B) and mass spectra (C) of succinimidyl 4-hydroxybenzoate (36x).

Mp: 198-200ºC, IR v_{max}: 3321, 2920, 2860, 1680, 1598, 1429, 1317, 1230, 1219, 1130, 1074 cm^{-1}. ^{1}H-NMR spectroscopy (400 MHz; DMSO-d_6) δ = 10.24 (s, OH), 7.95 (d, J = 8.8 Hz, 2 H, H-2/H-6), 6.97 (d, J = 8.8 Hz, 2 H, H-3/H-5), 2.87 (s, 4 H, CH$_2$CH$_2$). ^{13}C-NMR spectroscopy (125 MHz; DMSO-d_6) δ = 171.2 (s, 2 O=C-N), 164.4 (s, O=C-O),

161.8 (s, C-4), 132.4 (d, C-2/C-6), 115.7 (d, C-3/C-5), 115.1 (s, C-1), 25.8 (t, CH_2CH_2).

MS-ES: *m/z* (%) = 235 (M$^+$, 26), 234 ([M – 1]$^+$, 100), 222 (15). HRMS spectrometry (EI): calc for $C_{11}H_8NO_5$ ([M – H]$^+$): 234.0403; found: 234.0400.

3.4.8   Synthesis of compound 33bx by the alternative route

The product **36x**, obtained as described above, was then added to 2,7-dibromoacridine-9-carbonyl chloride **25b** and gave compound **33bx** (Figure 3.21) based on the procedure described below.
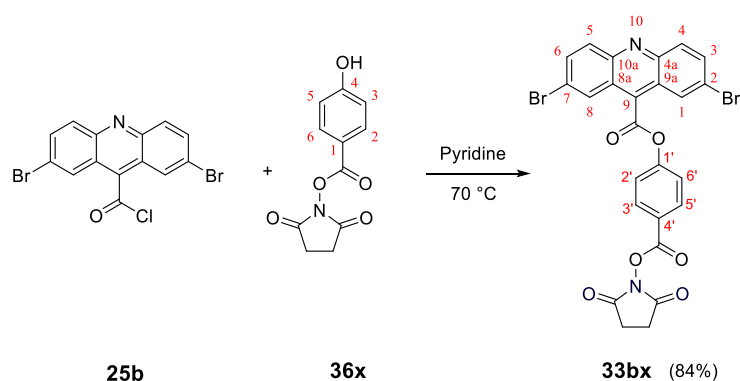
*Figure 3. 21: The alternative approach to synthesis of 4-(succinimidyloxycarbonyl)phenyl 2,7-dibromoacridine-9-carboxylate (**33bx**).*

A solution of 2,7-dibromoacridine-9-carbonyl chloride (**25b**; 2.1 g, 5.27 mmol) in anhydrous pyridine (25 mL) was heated at 40ºC and stirred for 10 min, then cooled to room temperature. A solution of succinimidyl 4-hydroxybenzoate (**36x**: 1.30 g, 5.50 mmol) in anhydrous pyridine (10 mL) was added to the mixture. The mixture was stirred at 60ºC for 36 h under anhydrous conditions. The reaction mixture was cooled to room temperature then poured into 1 M HCl (80 mL) containing ice (50 g) and then filtered to give the crude product, which was washed with a mixture of DCM/diethyl ether (1:1, 30 mL) and then with an excess of diethyl ether to give pure solid yellow product **33bx** (2.64 g, 4.43 mmol,

84% yield). The product was identical to that obtained previously, but the synthesis route was much easier, required a shorter reaction time and gave a much higher yield. This approach was therefore adopted as the approach of choice for the synthesis of other compounds required for the rest of this work.

3.4.9 Synthesis of 4-(succinimidyloxycarbonyl)phenyl 2,7-dibromo-10-methylacridinium-9-carboxylate trifluoromethanesulfonate (34bx)

The final step involved methylation of **33bx** to give compound **34bx** (Figure 3.22). In this step the standard procedure was applied, involving treating **33bx** (0.10 g, 0.167 mmol) with methyl trifluoromethanesulfonate (0.20 mL; 0.33 mg, 2 mmol) in DCM (40 mL) under anhydrous conditions and stirring overnight, based on the approach that was described by Dr El-Hiti. The ^{1}H NMR spectrum of the crude product, however, showed no evidence of a new peak in the region expected for a methyl group attached to a positively charged nitrogen atom (around 5 ppm), even though many attempts were made, including varying the reaction conditions. Even after increasing the reaction time up to 5 days at room temperature, the ^{1}H NMR spectrum still showed no evidence of a new peak around 5 ppm for the expected methyl group. Therefore, the temperature was increased to allow reflux of DCM and after 8 days of reflux the ^{1}H-NMR spectrum showed significant differences in the aromatic region; there were two sets of aromatic signals, one set corresponding to signals expected for the AE and one appearing to be like starting material, suggesting that the crude product was a mixture of two components, the AE and another that was assumed to be starting material. Increasing the reaction time beyond 8 days, even in the presence of further fresh methyl triflate, did not result in any further enhancement of the signals thought to be for the AE.
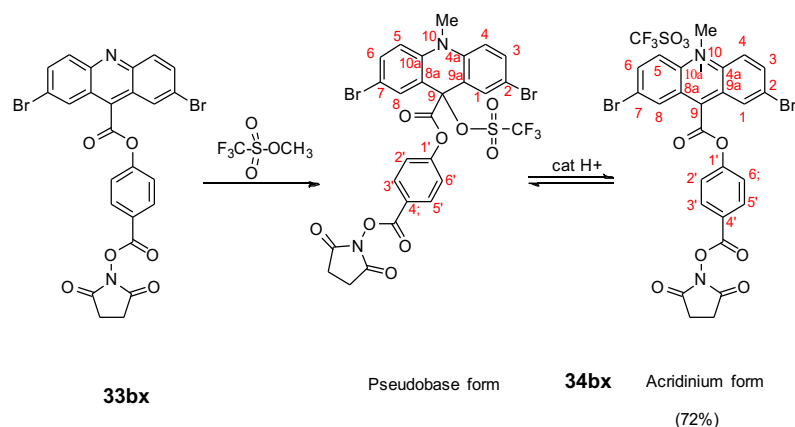
*Figure 3. 22: Synthesis of dibromoacridinium ester (**34bx**) illustrating pseudo-base acridinium equilibrium.*

Attempted isolation of the AE from the mixture by crystallisation using many solvents led to material that was substantially richer in the AE, but always much of the other material remained. However, when the ^{1}H NMR spectrum of this purer material was studied in detail it was seen that there was another extra significant peak at 3.46 ppm integrating correctly for an extra methyl group in the major component, and the peak at 5 ppm, corresponding to the AE, was in fact due to the minor component. This suggested the possibility that the major component was not starting material but was an isomer of compound **34bx** in which the trifluoromethanesulfonate anion had attached to the 9-position of the acridine ring (see Figure 3.22). We refer to this compound as "pseudo-base" by analogy with the corresponding hydroxide adduct, which is derived from the corresponding AE hydroxide, which is indeed basic.
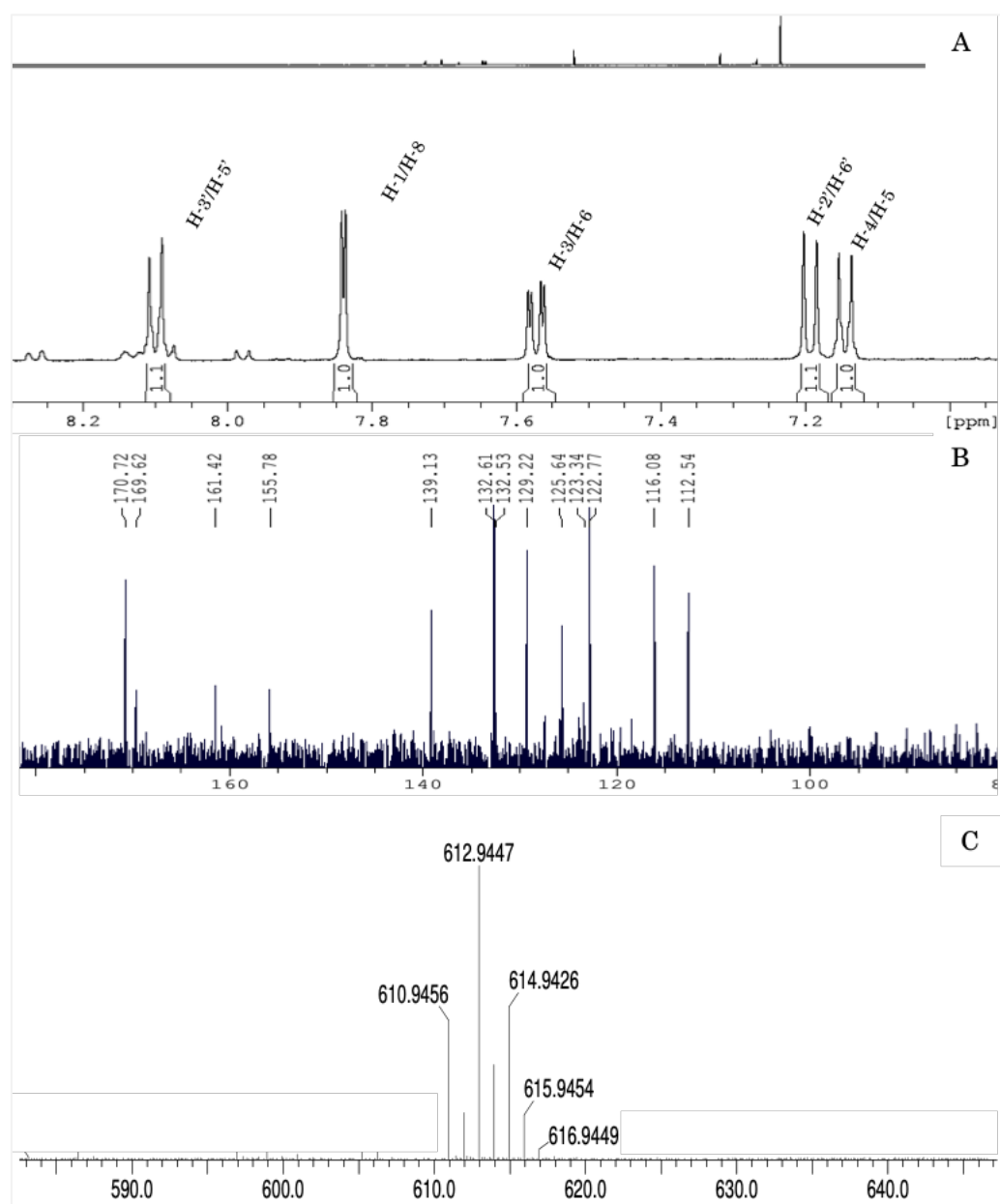
Figure 3. 23: The ^{1}H-NMR (A), ^{13}C-NMR (B) and mass spectra (C) of the pseudo-base corresponding to 4-(succinimidyloxycarbonyl)phenyl 2,7-dibromo-10-methylacridinium-9-carboxylate trifluoromethanesulfonate (34bx).

The yield of this impure pseudo-base was 72% (0.09 g, 0.118 mmol), Mp: 283-285ºC.

IR v_{max}:2910, 2293, 2252, 1714, 1506, 1375, 1039, 918 cm^{-1}. ^{1}H NMR spectroscopy (400

MHz; DMSO-d_6): δ = 8.10 (d, J = 8.9 Hz, 2 H, H-3'/H-5'), 7.83 (d, J = 2.4, 2 H H-1/H-8),

7.57 (dd, J = 2.4, 8.8 Hz, 2 H, H-3/H-6), 7.19 (d, J = 8.9 Hz, 2 H H-2'/H-6') 7.14 (d, J =

8.8 Hz, 2 H, H-4/H-5), 3.45 (s, 3H (N-CH$_3$), 2.87 (s; 4H, CH$_2$ CH$_2$). ^{13}C-NMR

spectroscopy (100 MHz; DMSO-d_6): δ = 170.3 (s, 2C=O of NHS), 169.6 (s, C=O next to

acridine), 161.4 (s, C=O next to Ar), 155.8 (s, C-1'), 139.1 (s, C-4a/C-10a), 132.6 (d, C-

1/C-8), 132.5 (d, C-3'/C-5'), 129.2 (d, C-3/C-6), 125.6 (s, C-8a/C-9a), 123.3 (s, C-4'),

122.7 (d, C-2'/C-6'), 116.1 (d, C-4/C-5), 112.5 (s, C-2/C-7), 72.7 (C-9), 34.0 (q, N-Me),

26.0 (t, CH$_2$CH$_2$). TOF MS AP spectrometry (m/z) (%): 616 (13), 615 (51), 613 (100), 611

(49), 605 (10). HRMS (ES) spectrometry: calc for $C_{26}H_{17}{}^{79}Br_2N_2O_6$ (M$^+$ - CF$_3$SO$_3$):

610.9454; found: 610.9456. (Figure 3.23).

3.5   Synthesis of 4-(succinimidyloxycarbonyl)-3,5-dimethylphenyl 2,7-dibromo-10-methylacridinium-9-carboxylate trifluoromethanesulfonate (34by).

Compound **34by** was synthesized in three steps; the first involved reaction of 2,6-dimethylbenzoic acid (**35y**) with N-hydroxysuccinimide in the presence of DCC to produce succinimidyl 3,5-dimethyl-4-hydroxybenzoate (**36y**); the second step involved esterification of 2,7-dibromoacridine-9-carbonyl chloride **36y** to produce **33b**y. The final step involved methylation using methyl trifluoromethanesulfonate to produce **34by**.

3.5.1 Synthesis of succinimidyl 3,5-dimethyl-4-hydroxybenzoate (36y)
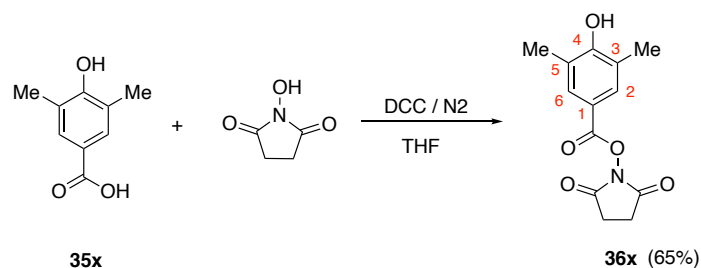
*Figure 3. 24: Synthesis of succinimidyl 3,5-dimethyl-4-hydroxybenzoate (**36y**).*

Having obtained the acridinium ester with an unsubstituted hydroxybenzoate leaving group (albeit that it was in the form of its pseudo-base), we wanted next to form the corresponding esters with different leaving groups. In the first instance, we wished to synthesize the derivative with two additional methyl groups on the phenolic ring and the first task was therefore to produce succinimidyl 3,5-dimethyl-4-hydroxybenzoate (**36y**, see Figure 3.24). This turned out to be straightforward by use of a procedure similar to that used for the preparation of **36x**, as described below.

A stirred cold (0ºC) solution of 3,5-dimethyl-4-hydroxybenzoic acid (**35y**, 5.0 g, 30.0 mmol) in tetrahydrofuran (150 mL), 1,3-dicyclohexylcarbodiimide (6.81 g, 33.0 mmol) was added; the mixture was stirred for 10 min and *N*-hydroxysuccinimide (5.18 g, 45.0 mmol) was then added. The mixture was stirred at 0ºC under nitrogen for 2 h and then at room temperature for 30 h. The mixture was filtered to remove the insoluble dicyclohexylurea and the filtrate was evaporated to dryness under reduced pressure. The residue obtained was washed with diethyl ether (2 × 30 mL) and then suspended in boiling ethyl acetate (100 mL). The suspension was allowed to cool and then filtered, and the solvent was washed with saturated sodium bicarbonate solution followed by water and

dried over anhydrous magnesium sulfate. The suspension was concentrated, diethyl ether

(30 mL) was added, and the mixture was left overnight.
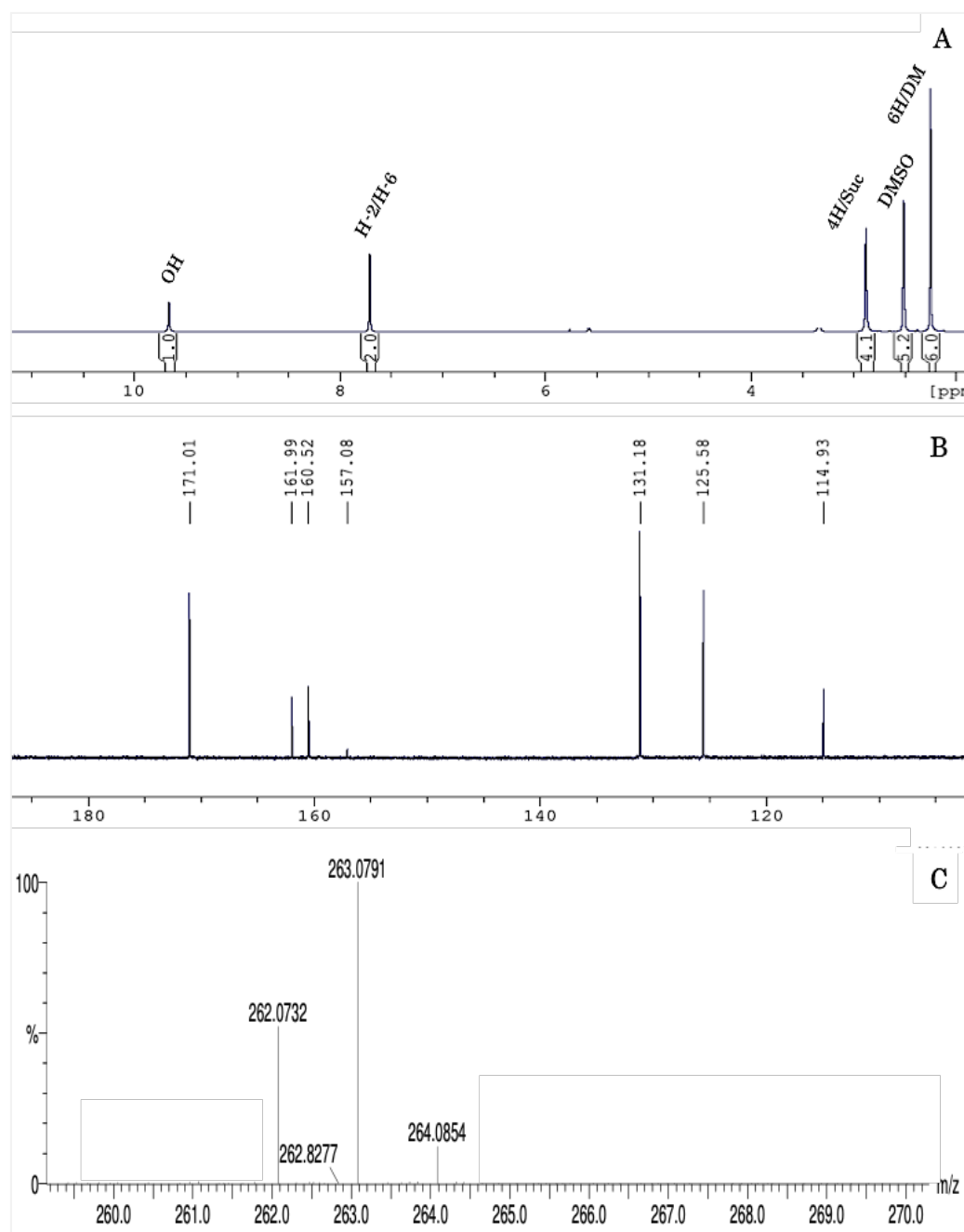
Figure 3. 25: The ^{1}H-NMR (A), ^{13}C-NMR (B) and mass spectra (C) of succinimidyl 3,5-dimethyl-4-hydroxybenzoate (36y).

The solid obtained was filtered to give **36y** as a white powder (5.12 g, 19 mmol, 65%

yield). Mp: 292-294°C. IR ν_{max}: 3321, 2926, 2848, 1697, 1622, 1429, 1317, 1165, 1074

cm^{-1}. ^{1}H-NMR spectroscopy (500 MHz; DMSO-d_6); δ = 9.66 (s, exch., 1 H, OH), 7.70 (s, 2 H, H-2/H-6 of Ar), 2.87 (s, 4H, CH$_2$CH$_2$), 2.24 (s, 6 H, 2 Me). ^{13}C NMR spectroscopy (DMSO-d_6) δ = 171.0 (s, O=C-N), 162.0 (s, O=C-O), 160.5 (s, C-4 of Ar), 131.2 (d, C-2/C-6 of Ar), 125.6 (s, C-3/C-5 of Ar), 114.9 (s, C-1 of Ar), 25.8 (t, CH$_2$ CH$_2$), 16.9 (q, 2 Me). MS EI$^+$ spectrometry m/z (%): 264 (12), 263 (100), 262 (51). HRMS (EI) spectrometry: calc for C$_{13}$H$_{13}$NO$_5$ (M$^+$): 363.0794; found: 263.0791 (Figure 3.25). The product was crystallised from acetonitrile and a crystal was selected for X-ray crystallographic analysis (Figure 3.26).

3.5.1.1 Crystal structure of succinimidyl 3,5-dimethyl-4-hydroxybenzoate (36y)
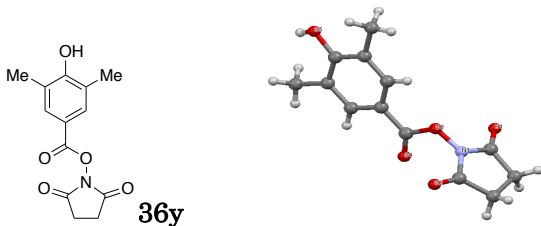
X-ray crystallography data for compound (36y)			
Appearance	Colourless	Radiation type	Mo Kα
Crystal size (mm)	0.315 x 0.246 x 0.126 mm^3	μ (mm^{-1})	0.106 mm^{-1}
Crystal system	Monoclinic	Diffractometer	Atlas
Space group	P2$_1$/c	Measured reflections	12014
Temperature (K)	293 (2) K	Independent reflections	3191
a (A°)	12.3656(10) Å α= 90°.	Parameters	175
b (A°)	9.8337(6) Å	H atom treatment	°
c (A°)	11.6498(10) Å	Computer programs	SHELX,
V (A°^{3})	1277.6(2) Å^3	Chemical formula	C$_{13}$H$_{13}$NO$_5$

Figure 3. 26: Data, data collection and handling for X-ray crystallographic studies of succinimidyl 3,5-dimethyl-4-hydroxybenzoate (36y).

3.5.2 Synthesis of 4-(succinimidyloxycarbonyl)-2,6-dimethylphenyl 2,7-dibromoacridine-9-carboxylate (33by)

The next step was to synthesise the corresponding ester of 2,7-dibromoacridine-9-carboxylic acid. Fortunately, a procedure similar to that adopted for synthesis of compound **33bx** was satisfactory and gave a 74% yield of compound **33by**. The procedure is detailed below. A solution of **36y** (1.00 g, 3.80 mmol) in pyridine (15 mL) was added to a stirred solution of 2,7-dibromoacridine-9-carbonyl chloride (**25b**) (1.50 g, 3.76 mmol) in pyridine (25 mL). The mixture was stirred at room temperature for 2 h and then at 60ºC for 48 h under anhydrous conditions.
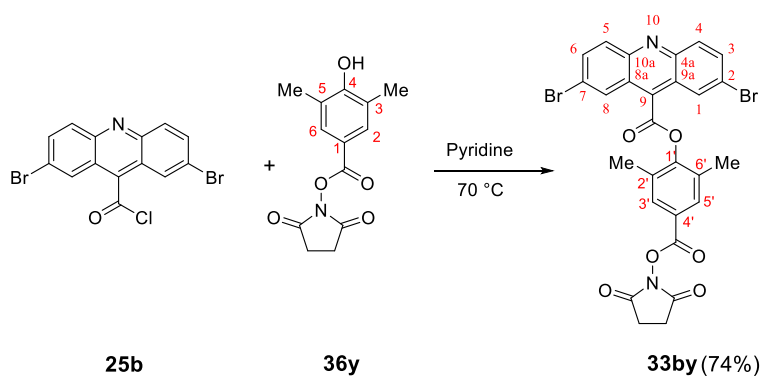
Figure 3. 27: Synthesis of 4-(succinimidyloxycarbonyl)-2,6-dimethylphenyl 2,7-dibromoacridine-9-carboxylate (33by).

The mixture was allowed to cool to room temperature then poured into HCl (1 M, 60 mL) containing ice (50 g) and filtered to leave a yellowish solid material, which was dissolved in chloroform and precipitated with diethyl ether to give **33by** (1.80 g, 2.87 mmol, 74% yield). Mp: 231-232ºC. IR v_{max}:3304, 2949, 2839, 1909, 1753, 1724, 1604, 1433, 1342, 1165, 1132, 958 cm^{-1}. ^{1}H-NMR spectroscopy (500 MHz; DMSO-d_6): δ = 8.61 (d, J =1.9 Hz, 2 H, H-1/H-8), 8.26 (d, J = 7.2 Hz, H-4/H-5), 8.13, (dd, J = 2, 7.2 Hz, 2 H, H-3/H-6), 8.09 (s, 2 H, H-3'/H-5'), 2.94 (s, 4 H, CH$_2$CH$_2$.), 2.09 (s, 6 H, 2 Me). ^{13}C NMR spectroscopy (125 MHz; DMSO-d_6): δ = 170.8 (s, N-C=O), 163.6 (s, O=C-OAr), 161.6 (s,

O=C-ON), 154.5 (s, C-9), 153.5 (s, C-1'), 147.2 (s, C-4a/C-10a), 135.0 (d, C-3/C-6), 132.7 (s, C-8a/C-9a), 132.3 (d, C-4/C-5), 131.8 (s, C-4'), 131.6 (s, C-2'/C-6'), 127.0 (d, C-1/C-8), 123.5 (s, C-2/C-7), 106.0 (d, C-3'/C-5'), 25.8 (t, CH_2CH_2), 17.4 (q, Me). MS AP+ spectrometry m/z (%):629 (51), 627 (100), 625 (49). HRMS AP spectrometry calc for $C_{27}H_{19}{}^{79}Br_2N_2O_6$ (M+H) 624.9610 found 624.9634, (Figure 3.28).
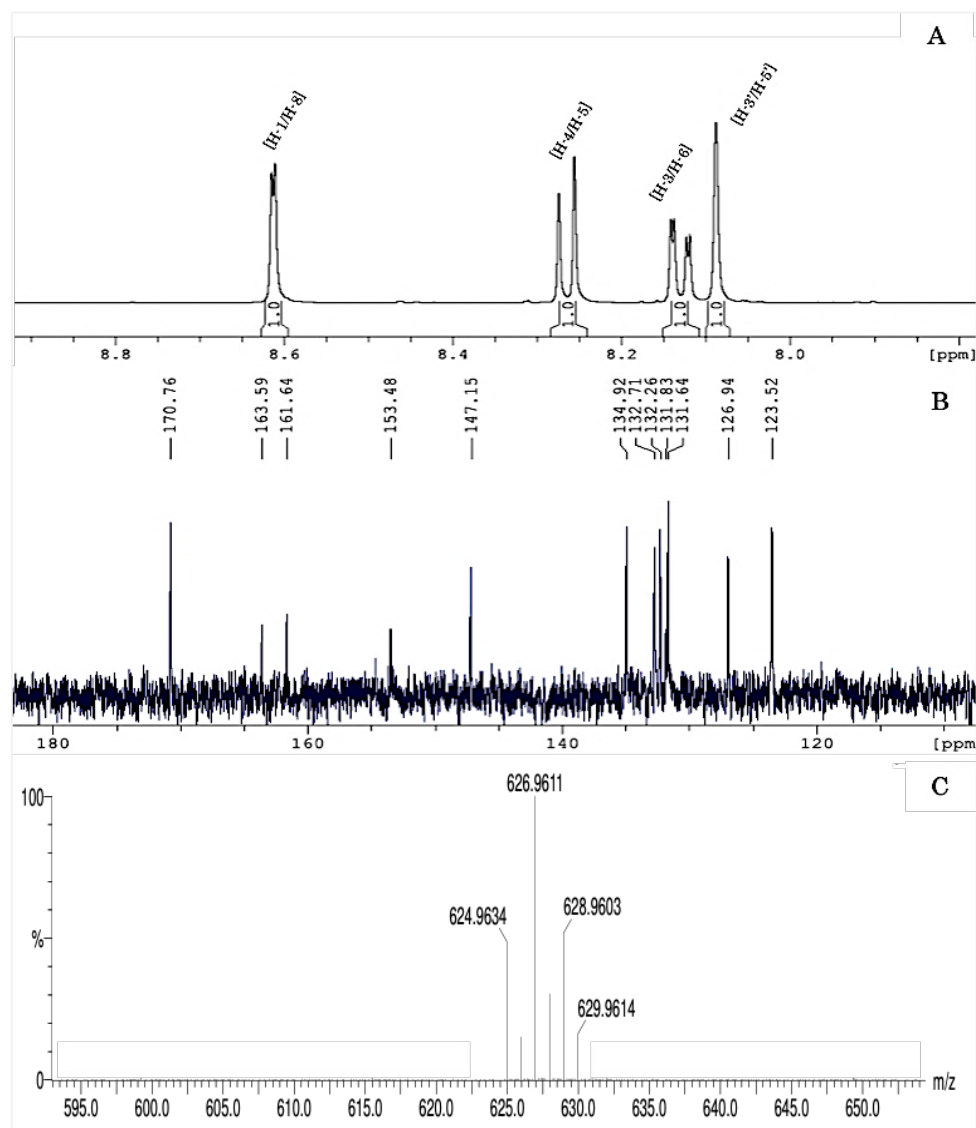
Figure 3. 28: The ^{1}H-NMR (A), ^{13}C-NMR (B) and mass spectra (C) of 4-(succinimidyloxycarbonyl)-2,6-dimethylphenyl 2,7-dibromoacridine-9-carboxylate (33by).

3.5.3 Synthesis of 4-(succinimidyloxycarbonyl)-2,6-dimethylphenyl 2,7-dibromo-10-methylacridinium-9-carboxylate trifluoromethanesulfonate (34by).
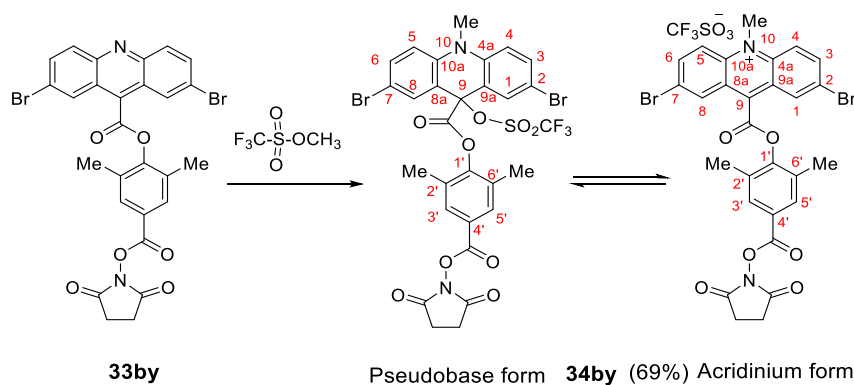
*Figure 3. 29: Synthesis of dibromoacridinium ester **34by** illustrating pseudo-base acridinium equilibrium.*

The final step of the synthesis of compound **34by** was methylation using methyl trifluoromethanesulfonate and worked satisfactorily to give the product, albeit as its pseudo-base form, in reasonable yield using a procedure similar to that used for the synthesis of compound **34bx**. Details are given below.

Methyl trifluoromethanesulfonate (0.26 mL, 394 mg, 2.4 mmol) was added to a stirred solution of **33by** (0.15 g, 0.240 mmol) in dry dichloromethane (40 mL). The mixture was heated to reflux under nitrogen and stirred at reflux for 8 days. The mixture was cooled to room temperature and then filtered. The yellow solid obtained was washed with diethyl ether (10 mL x 5) then with a mixture of DCM and diethyl ether (1:1, 10 mL) and dried under reduced pressure to give the pseudo-base of **34by** in 69% yield (0.13 g, 0.16 mmol).
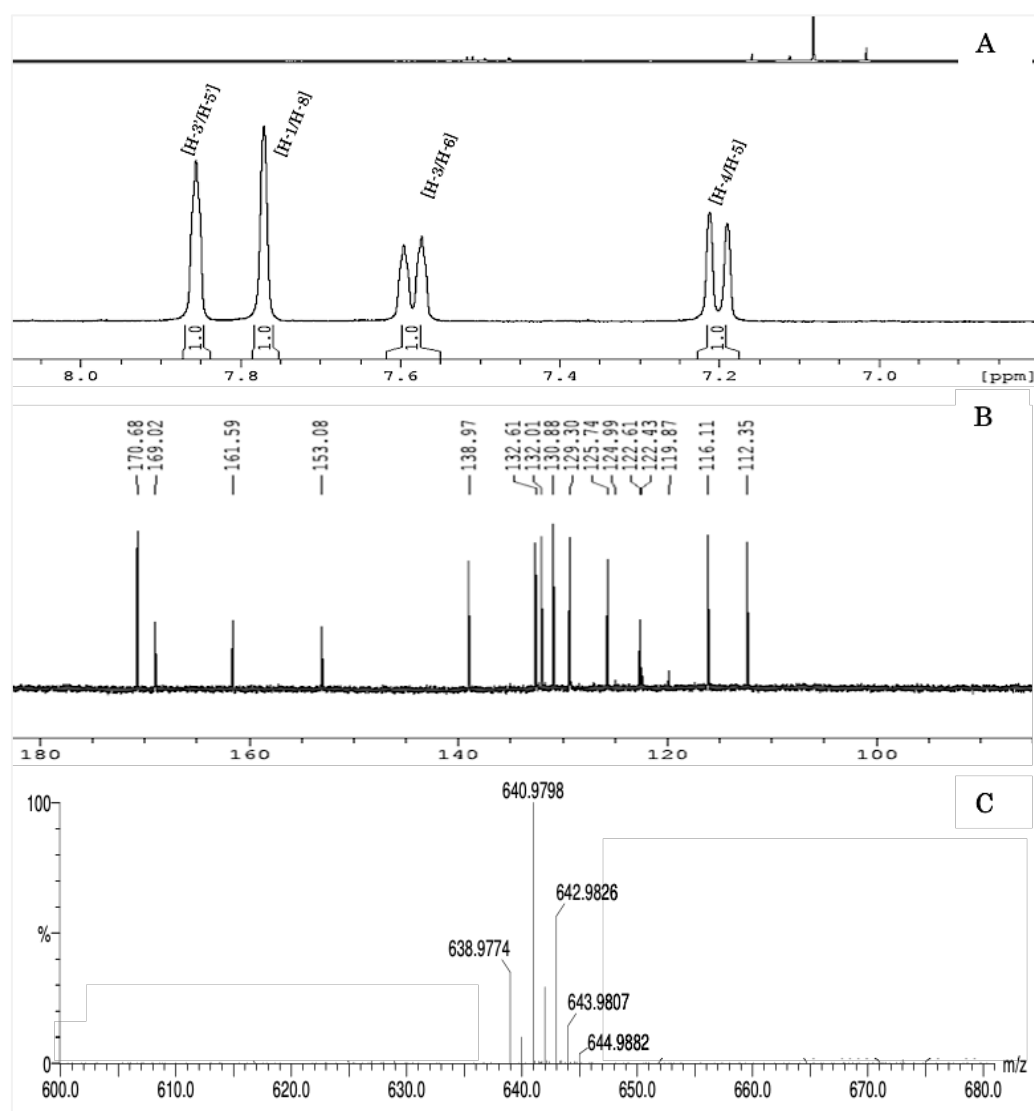
Figure 3. 30: The ^{1}H-NMR (A), ^{13}C-NMR (B) and mass spectra (C) of 4-(succinimidyloxycarbonyl)-3,5-dimethylphenyl 2,7-dibromo-10-methylacridinium-9-carboxylate trifluoromethanesulfonate (34by)

Mp; 297-298ºC, IR ν_{max}: 2910, 2293, 2252, 1747, 1614, 1425, 1375, 1166, 1109 cm^{-1}. ^{1}H-NMR spectroscopy (500 MHz; DMSO-d_6): δ =7.85 (s, 2H, H-3'/H-5'), 7.76 (s, 2H, H-1/H-8), 7.58 (d, *J* = 8.8 Hz, 2H, H-3/H-6), 7.20 (d, *J* = 8.8 Hz, 2H, H-4/H-5), 3.45 (s, 3H N-Me), 2.87 (s, 4H, CH₂CH₂), 1.69 (s, 6H, 2Me). ^{13}C NMR spectroscopy (125 MHz; DMSO-*d6*): δ = 170.7 (s, N-C=O), 169.0 (s, Acrid-C=O), 161.6 (s, Ar-C=O), 153.1 (s, C-1'), 139.0 (s, C-4a/C-10a), 132.3 (d, C-1/C-8), 132.0 (s, C-8a/C-9a), 130.9 (d, C-3/C-6),

95

129.3 (s, C-2'/C-6'), 125.7 (d, C-3'/C-5'), 122.5 (s, C-4'), 116.1 (d, C-4/C-5), 112.3 (s, C-2/C-7), 72.3 (s, C-9), 34.0 (q, N-Me), 26.0 (t, CH$_2$CH$_2$), 15.1 (q, Ar-Me). MS ES$^+$ spectrometry m/z (%): 639 (35), 641 (100), 643 (54), 644 (14), 645 (1). HRMS ES$^+$ spectrometry calc for C$_{28}$H$_{21}$^{79}Br$_2$N$_2$O$_6$ (M$^+$ - CF$_3$SO$_3$): 638.9766 found 638.9774.

3.6   Synthesis of 4-(succinimidyloxycarbonyl)-3,5-dimethoxyphenyl 2,7-dibromo-10-methylacridinium-9-carboxylate trifluoromethanesulfonate (34bz).

Synthesis of **34bz** was conducted in three steps, using 3,5-dimethoxy-4-hydroxybenzoic acid as starting material in a manner similar to that used for the synthesis of **34by**.

3.6.1   Synthesis of succinimidyl 3,5-dimethoxy-4-hydroxybenzoate (36z)

The final member of the series of 2,7-dibromoacridinium esters wanted for our studies involved a dimethoxy-substituted leaving group, and the first step of the synthesis was therefore to prepare succinimidyl 3,5-dimethoxy-4-hydroxybenzoate (**36z**) (Figure 3.30). This was achieved in a straightforward manner using conditions similar to those used for the synthesis of compound **36x**, details of which are given below.

To a stirred cold (0ºC) solution of 3,5-dimethoxy-4-hydroxybenzoic acid (4.95 g, 25 mmol) in tetrahydrofuran (150 mL), 1,3-dicyclohexylcarbodiimide (DCC) (5.78 g, 28 mmol) was added and the mixture was stirred for 10 min. *N*-Hydroxysuccinimide (4.38 g, 38 mmol) was added, and the mixture was stirred under nitrogen at 0ºC for 2 h and then at room temperature for 30 h. The mixture was filtered to remove the insoluble dicyclohexylurea and the filtrate was evaporated to dryness under reduced pressure.
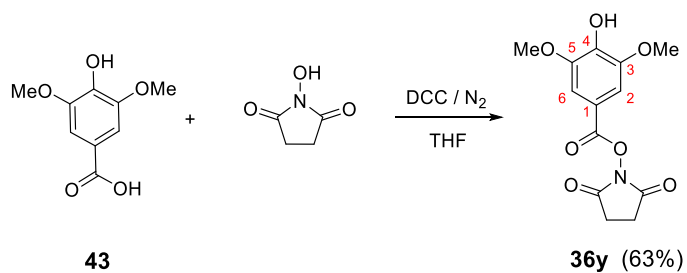
Figure 3. 31: Synthesis of succinimidyl 3,5-dimethoxy-4-hydroxybenzoate (36z).
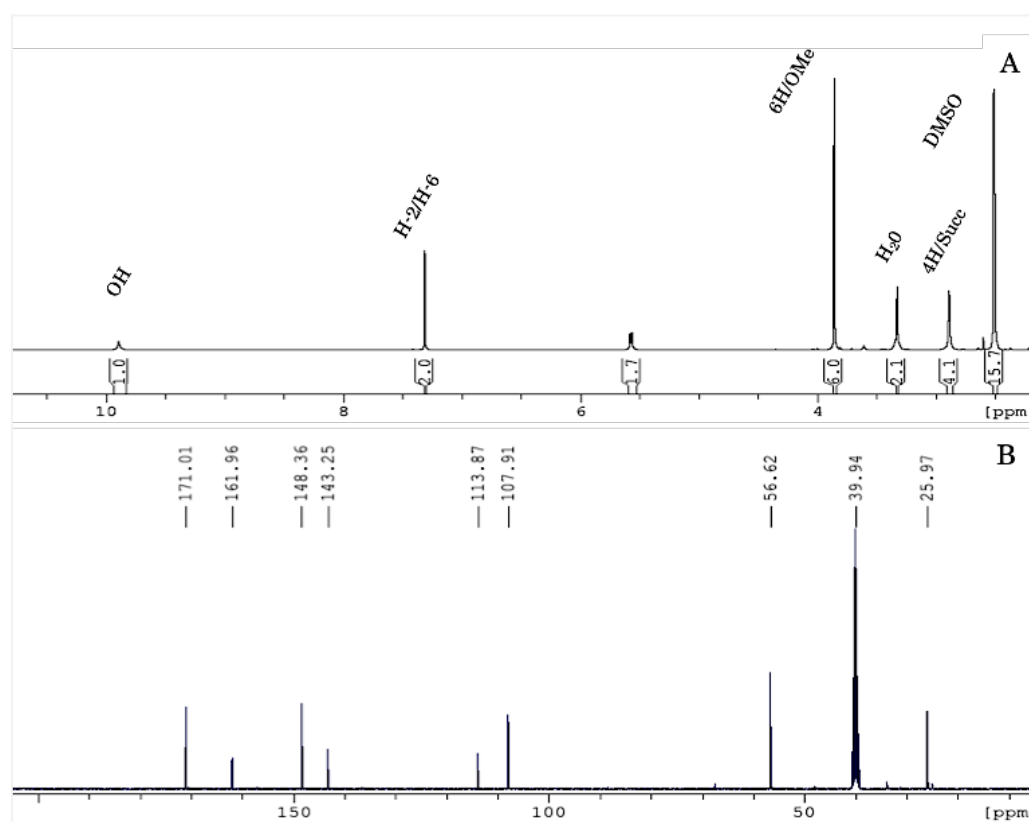
Figure 3. 32: The ^{1}H NMR (A) and ^{13}C NMR (B) of succinimidyl 3,5-dimethoxy-4-hydroxybenzoate (36z).

The residue obtained was washed with diethyl ether (2 × 30 mL) and then suspended in boiling ethyl acetate (100 mL). The suspension was allowed to cool and then filtered, and the filtrate was washed with saturated sodium bicarbonate solution followed by water

97

and dried over anhydrous magnesium sulfate. The solvent was concentrated, diethyl ether

(30 mL) was added, and the mixture was left at room temperature. The white powder

obtained was filtered to give **36z** (6.25 g, 15.7 mmol, 63% yield). Mp: 208-210ºC, IR ν_{max}:

3340, 2927, 2848, 1697, 1622, 1317, 1165 cm^{-1}. ^{1}H-NMR spectroscopy (400 MHz,

DMSO-d_6) δ = 9.94 (s, exch., 1 H, OH), 7.32 (s, 2 H, H-2/H-6 of Ar), 3.86 (s, 6 H, 2 OMe),

2.89 (s, 4 H, CH$_2$CH$_2$). ^{13}C-NMR spectroscopy (100 MHz, DMSO-$d6$) 171.0 (s, N-C=O),

162.0 (s, O=C-O), 148.4 (d, C-2/C-6 of Ar), 143.3 (s, C-4 of Ar), 113.9 (s, C-1 of Ar),

107.9 (s, C-3/C-5 of Ar), 56.5 (q, 2 OMe), 26.0 (t, CH$_2$CH$_2$). MS: = 295 (100), 296 (28),

397 (5).

3.6.2 Synthesis of 4-(succinimidyloxycarbonyl)-2,6-dimethoxyphenyl 2,7-dibromoacridine-9-carboxylate (33bz)

Esterification of 2,7-dibromoacridine-9-carbonyl chloride with the phenol **36z** (Figure

3.32) occurred smoothly according to the standard procedure, as detailed below.
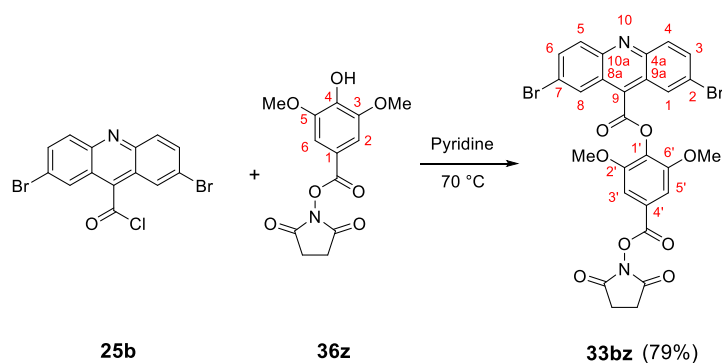
*Figure 3. 33: Synthesis of 4-(succinimidyloxycarbonyl)-2,6-dimethoxyphenyl 2,7-dibromoacridine- 9-carboxylate (**33bz**).*

A solution of succinimidyl 3,5-dimethoxy-4-hydroxybenzoate (**36z**, 0.83 g, 2.8 mmol)

in anhydrous pyridine (10 mL) was added to a stirred solution of 2,7-dibromoacridine-9-

carbonyl chloride (1.12 g, 2.8 mmol) in anhydrous pyridine and the mixture was stirred

under nitrogen for 48 h. The mixture was then poured into 1 M HCl (80 mL) containing

ice (50 g) and then filtered. The product was washed with acetone then DCM (15 mL) and

evaporated to dryness to give **33bz** (1.58 g, 2.4 mmol, 86% yield). Mp 295-297ºC. IR

ν_{max}: 3000, 1774, 1732, 1471, 1238, 1502, 1602, 1338, 1055.
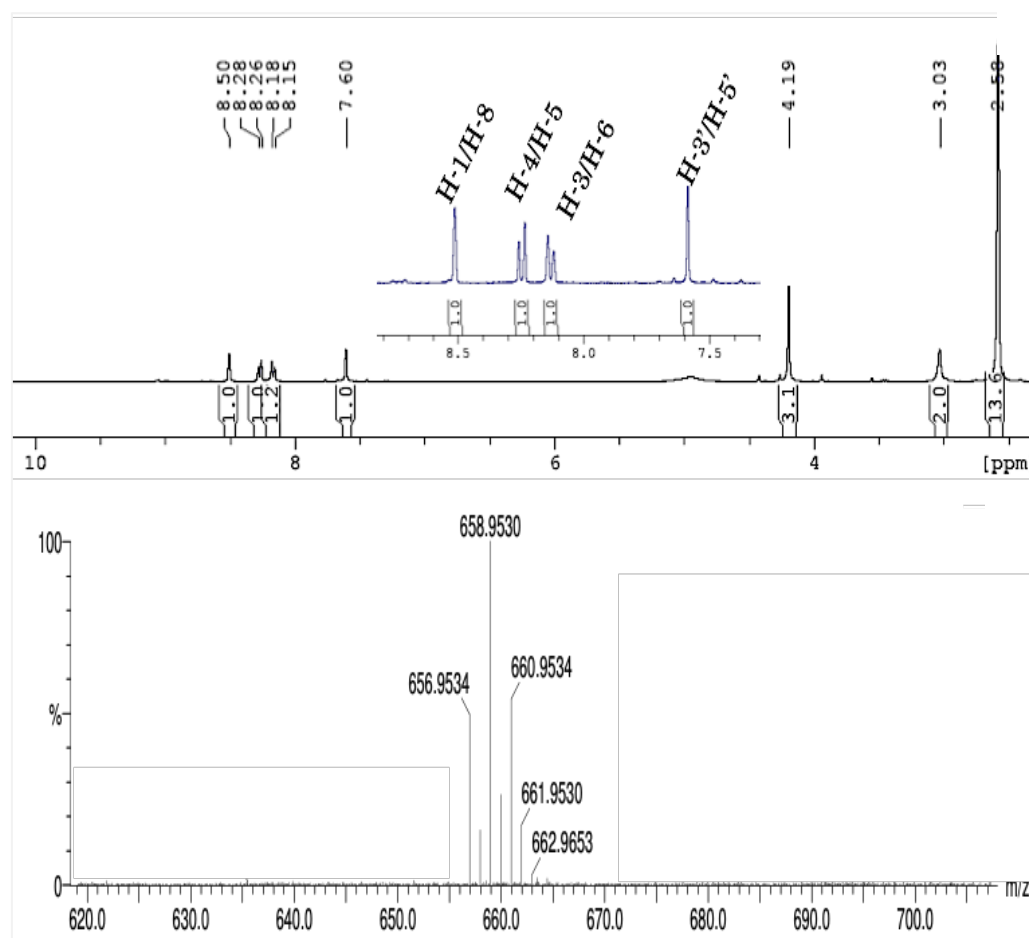
*Figure 3. 34: The ^1H NMR (A) and mass spectra (B) of 4-(succinimidyloxycarbonyl)-2,6-dimethoxyphenyl 2,7-dibromoacridine- 9-carboxylate (**33bz**).*

^{1}H-NMR spectroscopy (400 MHz; DMSO-d_6): δ = 8.51 (s, 2H H-1/H-8), 8.25 (d, J = 8Hz, 2H H-3/H-6), 8.14 (d, J = 8Hz, 2H, H-4/H-5), 8.59 (s, 2H H-3'/H-5'), 4.06 (s, 6H/

OMe), 2.95 (s, 4H CH$_2$CH$_2$). ^{13}C-NMR spectroscopy (100 MHz; DMSO-d_6): 135.1 (d, 2C C-3/C-6), 132.3 (d, 2C C-4/C-5), 127.0 (d, 2C C-1/C-8), 107.4 (d, 2C, C-3'/C-5'), 57.3 (q, 2C OMe), 26.1 (t, 2C CH$_2$CH$_2$) [the singlet signals were not identified]. MS-ES+: 663 (2), 662 (15), 661 (51), 659 (100%), 657 (49). HRMS ES$^+$ spectrometry calc for C$_{27}$H$_{19}$^{79}Br$_2$N$_2$O$_8$ (MH$^+$): 656.9508 found 656.9534.

3.6.3 Synthesis of 4-(succinimidyloxycarbonyl)-2,6-dimethoxyphenyl 2,7-dibromo-10-methylacridinium-9-carboxylate trifluoromethanesulfonate (34bz).

The final step in the synthesis of compound **34bz** was methylation of **33bz** with methyl trifluoromethanesulfonate, in a manner similar to that used for the other acridinium esters **34bx** and **34by**, which had led in both cases almost exclusively to the pseudo-base forms instead of the acridinium forms of the products.
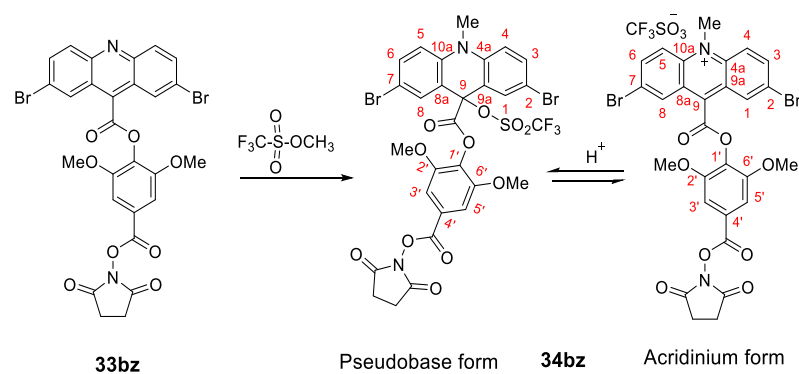
*Figure 3. 35: Synthesis of dibromoacridinium ester **34bz** illustrating pseudo-base acridinium equilibrium.*

The process was conducted in the same way as for the other two cases and the reaction worked smoothly, as described below, but this time the product was a mixture (approx.

60:40) of the two species, acridinium ester and its pseudo-base isomer. Methyl trifluoromethanesulfonate (0.25 mL, 377 mg, 2.3 mmol) was added to a stirred solution of **33bz** (0.15 g, 0.23 mmol) in dry dichloromethane (40 mL). The mixture was heated to reflux under nitrogen and stirred at reflux for 8 days. The mixture was cooled to room temperature and then filtered. The yellow solid obtained was washed with diethyl ether (10 mL x 5) then with a mixture of DCM and diethyl ether (1:1, 10 mL) and evaporated to dryness under reduced pressure to give a mixture of acridinium ester and its pseudobase isomer (collectively called **34bz**, 0.12 g, 0.15 mmol, 64% yield), Mp 287-289ºC. The H-NMR spectroscopy showed two sets of aromatic signals, one set corresponding to signals expected for the AE and one set being similar to the signals of the starting material; also, there were two distinct methyl signals, one at 3.47 and another at 4.99 ppm. Therefore, the crude product was a mixture of two components, the AE and another component that was assumed to be pseudobase based on the previous experience when producing compound **34bx**. However, attempted isolation of the AE form from the pseudobase form by crystallisation using many solvents was not successful, so the product was characterised as the mixture. ^{1}H NMR spectroscopy signals for the AE and pseudo-base are separately identified, but there were so many signals, all of them weak, in the ^{13}C NMR spectrum of the mixture that it was not possible to assign any of the signals. IR v_{max}: 3647, 3340, 2927, 2848, 2252, 1747, 1614, 1375, 1165, 1037 cm^{-1}. ^{1}H NMR spectroscopy (400 MHz; DMSO-d_6): δ = 8.95 (d, J = 8 Hz, 2H, H-4/H-5 AE), 8.80-8.76 (m, 4H, H-1/H-8 and H-3/H-6 AE), 7.70 (d, J = 2 Hz, 2H, H-1/H-8 pseudo-base), 7.67 (s, 2H, H-3'/H-5' AE), 7.58 (dd, J = 2, 9 Hz, 2H H-3/H-6 pseudo-base), 7.37 (s, 2H, H-3'/H-5' pseudo-base), 7.22 (d, J = 9 Hz, 2H, H-4/H-5 pseudo-base), 4.99 (s, 3H, N-Me AE), 4.24 (s, 6H, OMe AE) 3.86 (s, 6H, OMe pseudo-base) 3.48 (s, 3H, N-Me pseudo-base) 2.96 (s, 4H, CH$_2$CH$_2$ AE), 2.90 (s, 4H, CH$_2$CH$_2$ pseudo-base). MS AP$^+$ spectrometry m/z (%):677 (2), 676 (18), 675 (52),

673 (100), 671 (50). HRMS AP$^+$: spectrometry calc for $C_{28}H_{21}{}^{79}Br_2N_2O_8$ (M^+ - CF_3SO_3): 670.9665 found 670.9642.
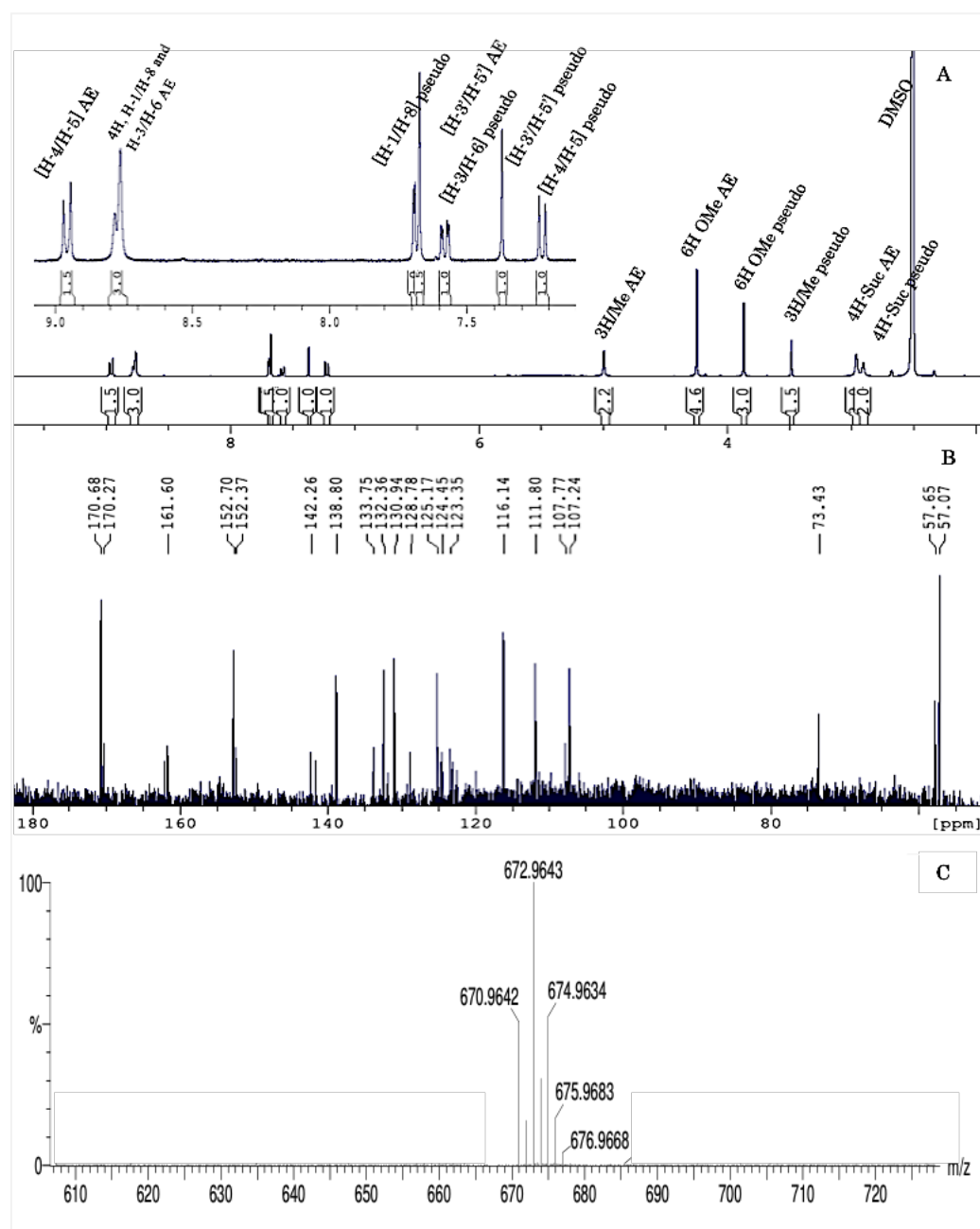
*Figure 3. 36: The ^1H NMR (A), ^{13}C NMR (B) and mass spectra (C) of dibromoacridinium ester **34bz** illustrating pseudobase-acridinium mixture*

3.7 Conclusion

In this part of our study, we have described the syntheses in reasonable yields of three 2,7-dibromo-*N*-methylacridinium esters (**34bx**, **34by** and **34bz**) having different aryloxy leaving groups with an NHS group for attachment to biological systems. During the course, we found difficulty in obtaining a good yield of compound **34bx** as part of the traditional route for the synthesis of AEs. We, therefore, developed an alternative approach (see Figure 3.17) involving fewer overall synthetic steps by making use of NHS esters of the appropriate hydroxybenzoic acids. We expect that the approach should be useful for the synthesis of other similar structures. There is a discussion in more detail in chapter 6. The immediate target was to synthesize AEs based on 2,7-dimethoxyacridine-9-carboxylic acid, and this is discussed in the following sections.

3.8 Synthesis of 4-(succinimidyloxycarbonyl)phenyl 2,7-dimethoxy-10-methylacridinium-9-carboxylate trifluoromethanesulfonate (34cx)

The synthesis of 2,7-dimethoxyacridinium esters was conducted using the new route developed in section 3.1 for the corresponding dibromo compounds (Figure 3.17). The first three stages of this route were based on Dr El-Hiti's procedures, and then an alternative route which is similar to that described in section 3.1 was applied. Briefly, a solution of *bis(*4-methoxyphenyl)amine in dichloromethane (DCM) was added dropwise to a stirred solution of oxalyl chloride in DCM and refluxed for 1.5 h under anhydrous conditions; the excess of oxalyl chloride was evaporated then aluminium chloride was added portion-wise to the residue in DCM and the mixture was refluxed under anhydrous conditions for 1.5 h to give **23**. Potassium hydroxide was added to a solution of **23** in water and heated to reflux for 72 h, then cooled to room temperature and poured into a mixture of hydrochloric acid and ice to give **24,** which was dissolved in thionyl chloride and heated to reflux under anhydrous conditions for 1 h to give **25**, which was evaporated to dryness under reduced pressure. The acid chloride (**25**) was then dissolved in anhydrous pyridine and stirred under anhydrous conditions with the appropriate 4-(succinimidyloxycarbonyl)phenol, prepared as described in section 3.1, to yield the corresponding ester (**33**). This approach involves fewer steps, and less vigorous reaction conditions and generally gives better yields than the standard route used to produce similar acridinium esters, as described by Weeks *et al.* and others. [80,123,131] Reactions of **33** with methyl trifluoromethanesulfonate in anhydrous DCM under nitrogen gave the corresponding acridinium esters **34**. Details of the individual steps are given in the following sections.

3.8.1 Synthesis of 1-(4-methoxyphenyl)-5-methoxyisatin (23c)
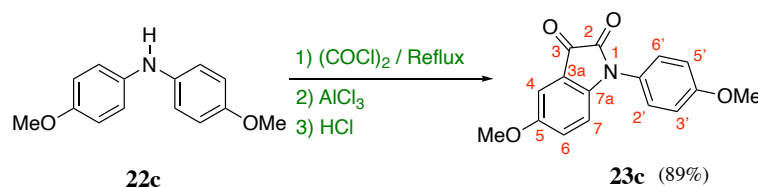
*Figure 3. 37: Synthesis of N-(4-methoxyphenyl)-5-methoxyisatin (**23c**).*

In an initial attempt at synthesis of **22c**, *bis*(4-methoxyphenyl)amine was reacted with oxalyl chloride and refluxed for 1 h to give an intermediate, which was cyclized in the presence of aluminium chloride (Figure 3.36) to give the corresponding isatin **23c** as a solid in 76% yield. Some by-product was obtained under the conditions tried. The structure of the by-product was confirmed by various spectroscopic techniques and by direct synthesis as 2-(*bis*(4-methoxyphenyl)amino)-2-oxoacetic (Figure 3.37).

3.8.1.1 Typical experimental procedure for the synthesis of 2-(bis(4-methoxyphenyl)amino)-2-oxoacetic acid (22d)
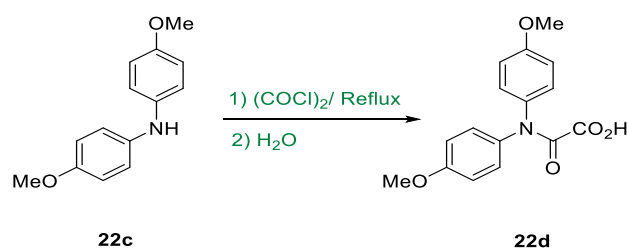
*Figure 3. 38: Synthesis of 2-(bis(4-methoxyphenyl)amino)-2-oxoacetic acid.(**22d**).*
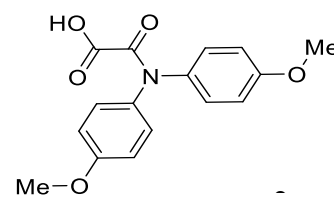
Equimolar quantities of oxalyl chloride and *bis*(4-methoxyphenyl)amine in DCM were stirred for 1.5 h and the organic layer was separated, dried over anhydrous magnesium sulfate and evaporated under reduced pressure to give 2-(*bis*(4-methoxyphenyl)amino)-2-oxoacetic acid **(22d)** in 46% yield. The product obtained from this experiment was identical in all respects to the one produced as a byproduct during the synthesis of **23c**. The low yield of **23c** could be explained by half of the amine acting as a base to abstract the hydrogen chloride evolved from the reaction. To confirm this possibility, the reaction was conducted between oxalyl chloride (1 mole equivalent) and *bis*(4-methoxyphenyl)amine (two mole equivalents). Following the aqueous work-up the crude product was obtained in 75% yield based on the oxalyl chloride.

The NMR spectra recorded at room temperature showed two sets of signals for the two aromatic rings, indicating restricted rotation about the C-N bond. ^{1}H NMR spectroscopy (400 MHz, DMSO-d_6): δ = 7.04, 6.96 (2 d, each J = 8.5 Hz, 4 H, H-2/H-6), 6.86, 6.69 (2 d, each J = 8.5 Hz, 4 H, H-3/H-5), 3.82, 3.71 (2 s, 6 H, OMe); ^{13}C NMR spectroscopy (100 Hz, DMSO-d_6):δ = 164.4 (s, CO_2H), 159.2 (s, C=O), 158.3 (s, C-4), 134.0, 132.8 (2 s, C-1), 129.8, 127.7 (2 d, C-2/C-6), 114.8 (d, C-3/C-5), 56.0, 55.8 (2 q, OMe). ES$^+$-MS: m/z (%) 302 (MH$^+$, 100), 288 (12); HRMS (ES) spectrometry: calc for $C_{16}H_{16}NO_5$ (MH$^+$): 302.1028; found: 302.1028. IR (FT): v_{max} 3300, 1740, 1713, 1665, 1500, 1366, 1167 cm^{-1}.

Crystallization using acetonitrile/hexane provided colourless crystals of the product. The structure of 2-(*bis*(4-methoxyphenyl)amino)-2-oxoacetic acid (Mp 122-123ºC) was confirmed by X-ray single crystal structure determination (Figure 3.38)(El-Hiti et al. 2017).

3.8.1.2   Crystal structure of 2-(bis(4-methoxyphenyl)amino)-2-oxoacetic acid (22d)

X-ray crystallography data for compound 22d			
Appearance	Colourless block	Radiation type	Mo Kα
Crystal size (mm)	0.30 x 0.22 x 0.17	μ (mm⁻¹)	0.10
Crystal system	Monoclinic	Diffractometer	Atlas
Space group	P2₁/n (no. 14)	No. measured reflections	15585
Temperature (K)	298	No. independent reflections	6846
a (A°)	6.7689 (5)	No. parameters	403
b (A°)	45.219 (3)	H atom treatment	Methyl C-H 0.96 A°; Aromatic C-H 0.93 A°; Hydroxyl O-H 0.82 A°
c (A°)	10.1102 (6)	Computer programs	CrysAlis, SHELX,
V (A°³)	3033.9 (4)	Chemical formula	$C_{16}H_{15}NO_5$
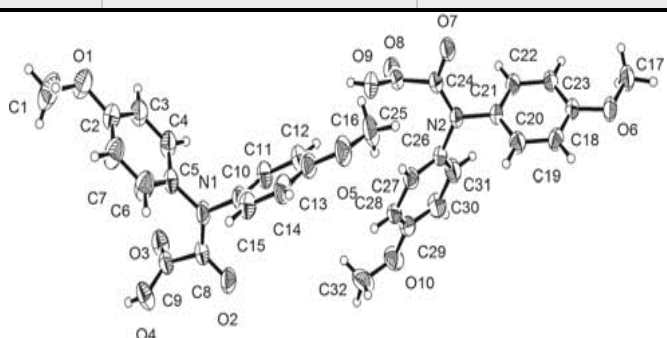
*Figure 3. 39: X-Ray crystal structure of 2-(bis(4-methoxyphenyl)amino)-2-oxoacetic acid (**22d**)*

Having established the structure of the byproduct, it was clear that it was the intermediate prior to cyclisation to give **23c**. Attempts were therefore made to increase the reaction time in the aluminium chloride activated step to see what effect this would have on the yield and the purity of the product. The yield of **23c** was increased to 89% when the reaction time was extended to 1.5 h. Also, no by-product was produced under such conditions, which were then used to synthesize sufficient of the product for the next step.
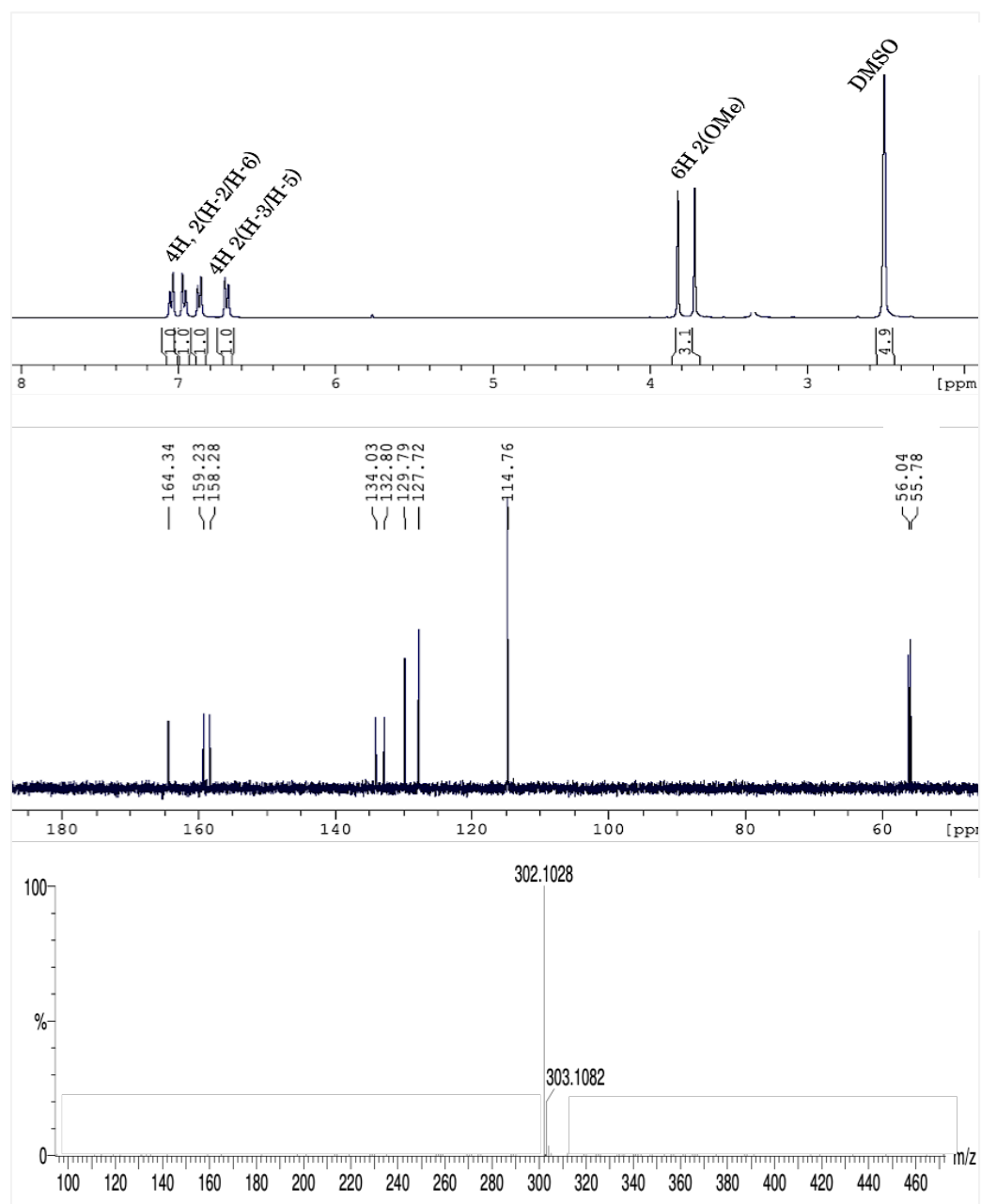
Figure 3. 40: The 1H NMR (A), 13C NMR (B) and Mass spectra (C) of 2-(bis(4-methoxyphenyl)amino)-2-oxoacetic acid (22d)

3.8.1.3 Experimental procedure for the synthesis of 23c.

A solution of *bis*(4-methoxyphenyl)amine **(**18.0 g, 22.4 mmol) in dichloromethane (DCM; 40 mL) was added dropwise to a stirred refluxing solution of oxalyl chloride (5.71 g, 45 mmol) in DCM (70 mL). The mixture was stirred under reflux for 1.5 h in anhydrous conditions. The excess of oxalyl chloride and DCM were removed under reduced pressure. Dichloromethane (150 mL) was added to the residue obtained followed by the addition of anhydrous aluminium chloride (6.0 g, 45 mmol) portion-wise over 10 min. The mixture was refluxed under anhydrous conditions for 1.5 h. The solvent was removed under reduced pressure and dilute hydrochloric acid (HCl, *ca*. 1 M, 60 mL) was added. The mixture was stirred for 30 min., the product was extracted with DCM (3×40 mL) and the combined extracts were dried over anhydrous magnesium sulfate (MgSO$_4$). The mixture was filtered, and the solvent was removed under reduced pressure to give the crude product as a brown solid. The solid was washed with diethyl ether (2×20 mL) and evaporated to dryness to give **23c** (4.58 g, 16.0 mmol) in 89% yield. Mp: 205-207ºC.(87Browne et al. 2011a) IR ν_{max}: 3125, 1740, 1725, 1602, 1283 cm^{-1}. ^{1}H NMR spectroscopy (400 MHz; CDCl$_3$): δ = 7.35 (d, J = 8.8 Hz, 2 H, H-2'/H-6'), 7.22 (d, J = 2.8 Hz, 1 H, H-4), 7.13 (dd, J = 2.8 and 8.6 Hz, 1 H, H-6), 7.10 (d, J = 8.8 Hz, 2 H, H-3'/H-5'), 6.70 (d, J = 8.6 Hz, 1.H, H-7), 3.80 (s, 3 H, OMe), 3.95 (s, 3 H, OMe). ^{13}C NMR spectroscopy (100 MHz; CDCl$_3$): δ = 183.5 (s, C-3), 159.5 (s, C-5), 157.7 (s, C-2), 156.7 (s, C-4'), 146.0 (s, C-7a), 127.3 (d, C-2'/C-6'), 125.6 (s, C-1'), 124.7 (d, C-6), 117.8 (s, C-3a), 115.0 (d, C-3'/C-5'), 112.2 (d, C-7), 109.0 (d, C-4), 56.0 (q, OMe), 55.6 (q, OMe). HRMS spectrometer (APCI) calc for C$_{16}$H$_{14}$NO$_4$ (MH+) 284.0923, found 284.0935.
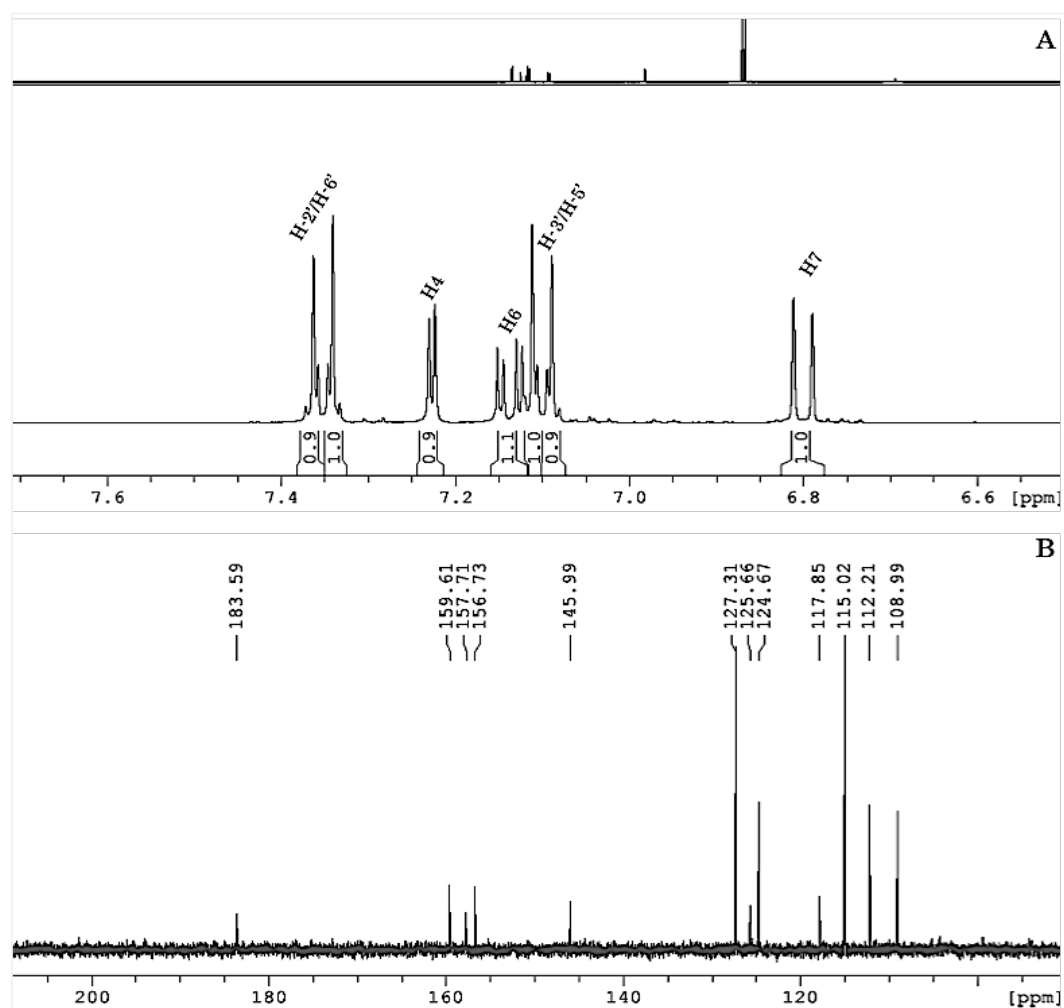
*Figure 3. 41: The ¹H NMR (A) and ¹³C NMR (B) of N-(4-methoxyphenyl)-5-methoxyisatin (**23c**)*

3.8.2 Synthesis of 2,7-dimethoxyacridine-9-carboxylic acid (24c)
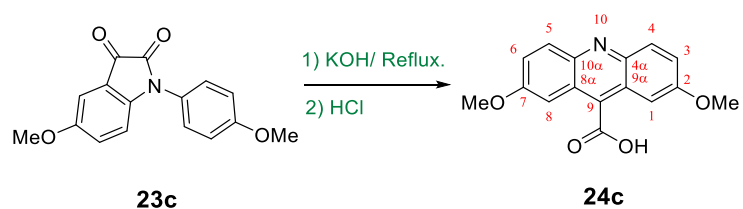
*Figure 3. 42: Synthesis of 2,7-dimethoxyacridine-9-carboxylic acid (**24c**).*

A mixture of **23c** (3.64 g, 12.8 mmol) and potassium hydroxide (KOH; 18.0 g, 320 mmol) in distilled water (200 mL) was stirred under reflux for 78 h (Figure 3.40). The hot green solution was allowed to cool in an ice bath for 20 min and then poured into a mixture of concentrated HCl (*ca*. 11 M, 70 mL) and ice (80 g). The yellowish green solid obtained was filtered and washed with water (3 × 40 mL) and methanol (2 × 40 mL). Residual solvent was removed under reduced pressure and the solid was then washed with DCM (2 ×30 mL) to give pure **24c** (3.41g, 12.1 mmol; 94% yield). ^{1}HNMR, ^{13}CNMR spectroscopy and MS spectrometry for 2,7-dimethoxyacridine-9-carboxylic acid have previously been reported in dimethyl sulfoxide solvent (DMSO-*d6*).
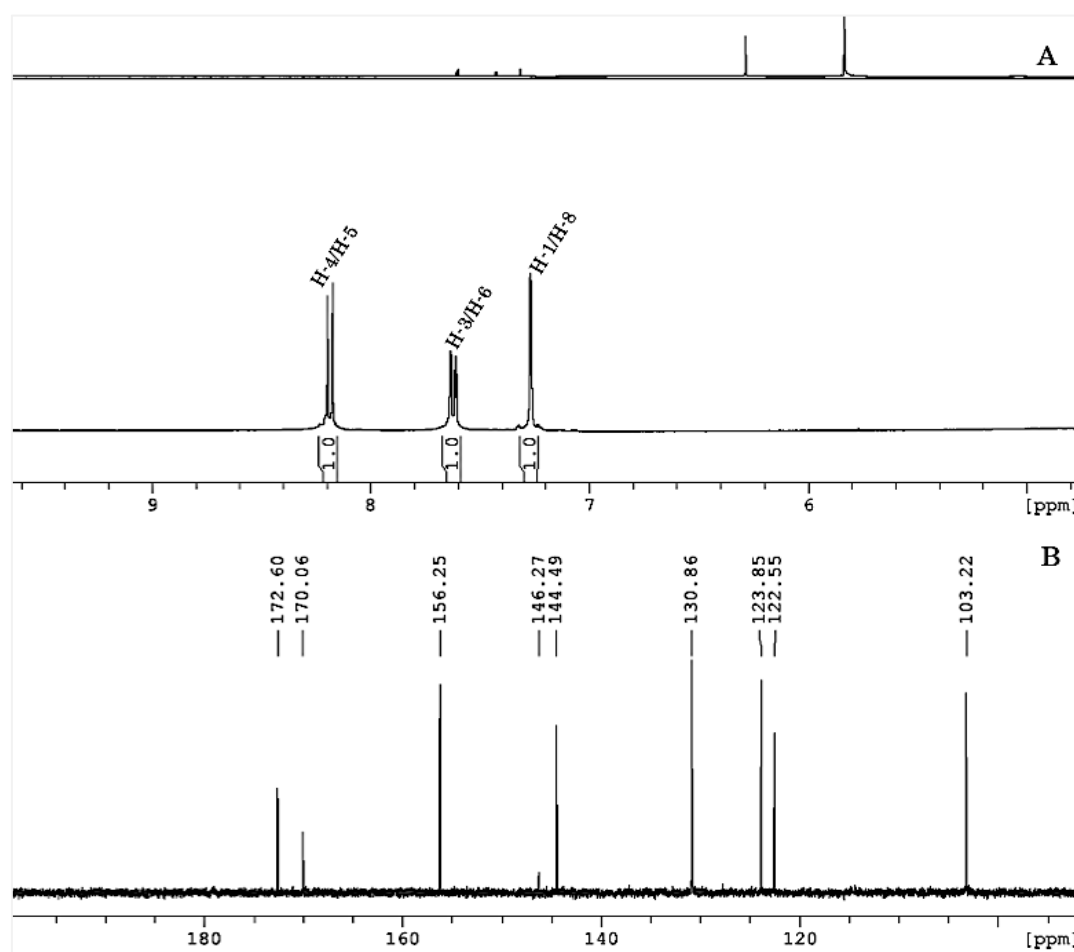
*Figure 3. 43: The ^{1}H NMR (A) and ^{13}C NMR (B) of N-(4-methoxyphenyl)-5-methoxyisatin (**34c**).*

The data for the sample prepared here (see Figure 3.41) are consistent with those in the literature.[65,132] Mp: 320–323ºC. IR ν_{max}: 3400-2500 (b), 1615, 1238 cm^{-1}. ^{1}H NMR spectroscopy(400 MHz; DMSO-d_6): δ = 8.07 (d, J = 9.4 Hz, 2 H, H-4/H-5), 7.5 (dd, J = 2.0 and 9.4 Hz, 2 H, H-3/H-6), 7.26 (d, J = 2.6, H-1/H-8), 3.93 (s, 6 H, 2 OMe). ^{13}C NMR spectroscopy(100 MHz; DMSO-d_6): δ = 172.6 (s, C=O), 170.1 (s, C-2/C-7), 156.2 (s, C-4a/C-10a), 144.5 (s, C-9), 130.8 (d, C-4/C-5), 123.8 (d, C-3/C-6), 122.5 (s, C-8a/C-9a), 103.2 (d, C-1/C-8), 55.7 (q, 2 OMe). EI-MS: m/z (%) = 283 (M$^+$, 100), 240 (27), 196 (12). HRMS (EI) spectrometry: calc for C$_{16}$H$_{13}$NO$_4$ [M$^+$]: 283.0845; found: 283.0845.

3.8.3   Synthesis of 2,7-dimethoxyacridine-9-carbonyl chloride (25c)
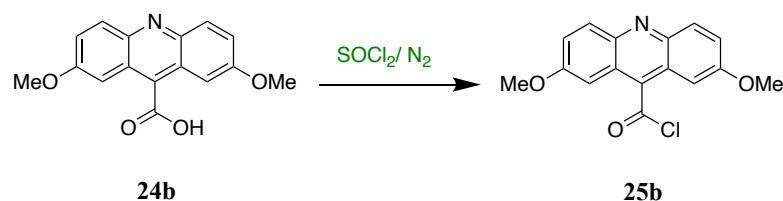
Figure 3. 44: Synthesis of 2,7-dimethoxyacridine-9-carbonyl chloride (25c).

A mixture of **24c** (3.10 g, 11 mmol) and freshly distilled thionyl chloride (40 mL) was refluxed under nitrogen for 1.5 h. The excess thionyl chloride was removed under reduced pressure to leave a yellowish green solid (3.31 g, 100% yield). The product was used immediately in the next step without purification or spectroscopic analysis.

3'/C-5'), 132.1 (d, C-4/C-5) 129.4 (s, C-9), 124.9 (d, C-3/C-6), 123.9 (d, C-2'/C-6'), 123.8 (s, C-4'), 123.3 (s, C-8a/C9a), 100.5 (d, C-1/C-8), 56.2 (q, 4 OMe), 26.1 (t, CH_2CH_2).

HRMS (ESP) spectrometry: calc for $C_{27}H_{21}N_2O_8$ [MH^+]: 501.1298; found 501.1309.
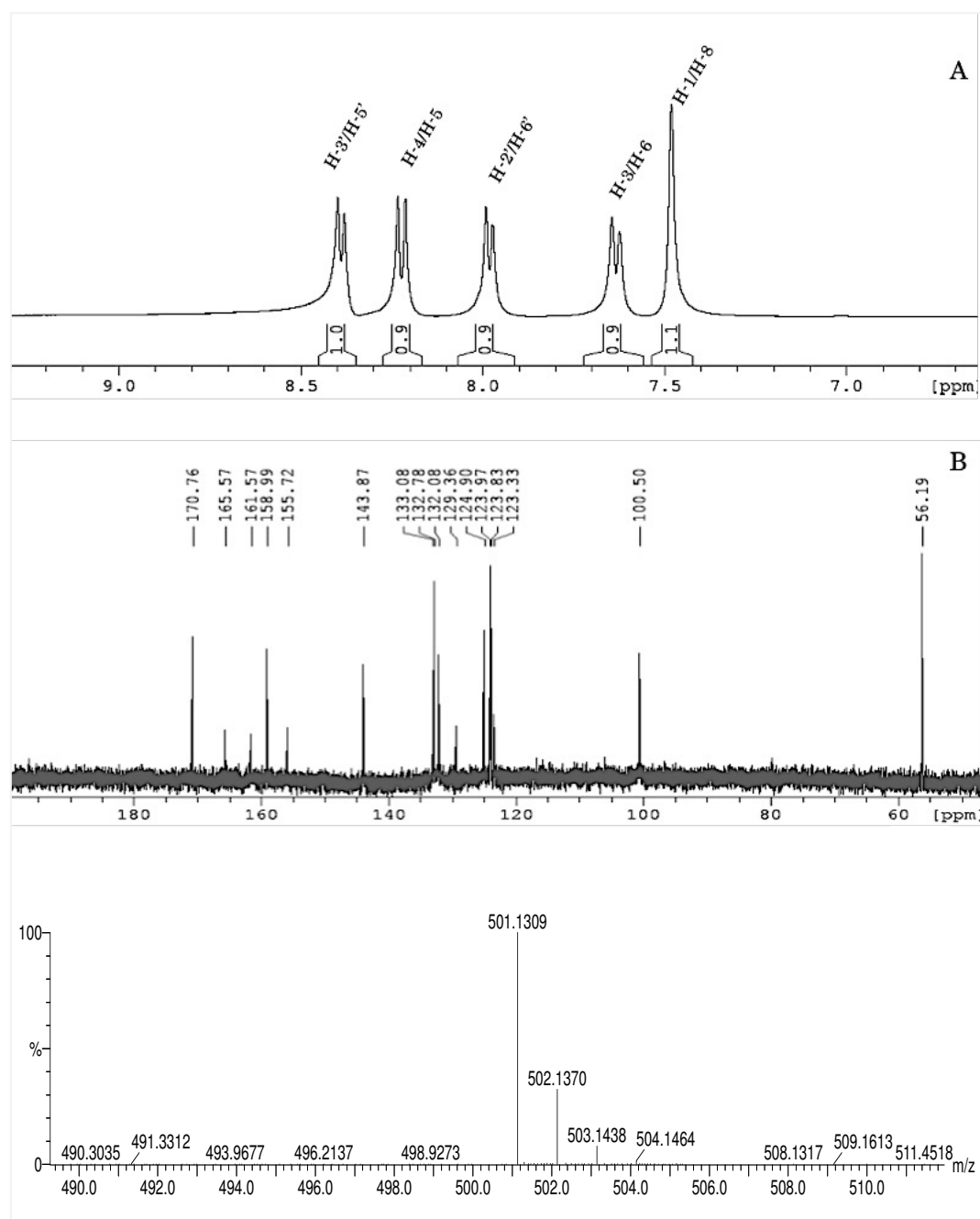
Figure 3. 46: The ^1H NMR (A), ^{13}C NMR (B) and mass spectra (C) of 4-(succinimidyloxycarbonyl)phenyl 2,7-dimethoxyacridine-9-carboxylate (33cx).

3.8.5 Synthesis of 4-(succinimidyloxycarbonyl)phenyl 2,7-dimethoxy-10-methylacridinium-9-carboxylate trifluoromethanesulfonate (34cx)
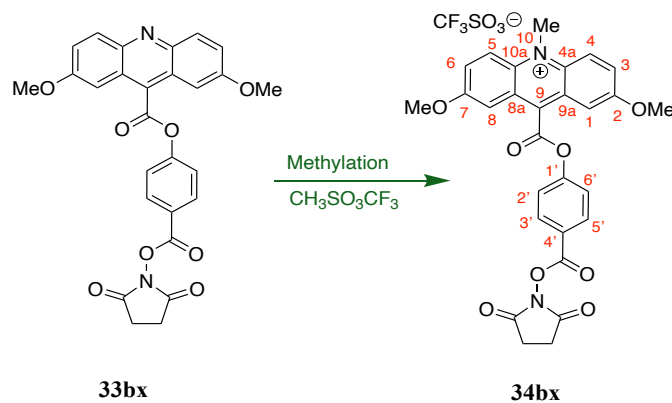
Figure 3. 47: Synthesis of 4-(succinimidyloxycarbonyl)phenyl 2,7-dimethoxy-10-methylacridinium-9-carboxylate trifluoromethanesulfonate (34cx)

Methyl trifluoromethanesulfonate (0.20 mL; 0.33 mg, 2.0 mmol) was added to a stirred solution of **33cx** (0.35 g, 0.70 mmol) in dry DCM (30 mL) under nitrogen. The mixture was stirred at room temperature for 36 h. The yellow solid obtained was filtered, washed with diethyl ether (3 × 10 mL) and dried under reduced pressure to give **34cx** (0.37 g, 0.56 mmol; 79% yield), Mp 192-194°C. In contrast to the situation with the dibromoacridine analogue, the product was exclusively the acridinium form and not the pseudo-base form. IR v_{max}: 3732, 2839, 1714, 1620 1128, 1062, 977 cm^{-1}. ^{1}H NMR spectroscopy (500 MHz, DMSO-d_6): δ = 8.87 (d, J = 10.0 Hz, 2 H, H-4/H-5), 8.37 (d, J = 8.7 Hz, 2 H, H-3'/H-5'), 8.14 (d, J = 2.6 and 10.0 Hz, 2 H, H-3/H-6), 8.02 (d, J = 8.7 Hz, 2 H, H-2'/H-6'), 7.57 (d, J = 2.6 Hz, 2 H, H-1/H-8), 4.95 (s, 3 H, Me), 4.13 (s, 6 H, 2 OMe), 2.94 (s, 4 H, CH$_2$CH$_2$). ^{13}C NMR spectroscopy (125 MHz, DMSO-d_6): δ = 170.7 (s, N-C=O), 163.4 (s, ArO-C=O), 161.5 (s, NO-C=O), 159.4, (s, C-2/C-7), 155.1 (s, C-1'), 139.6

(s, C9), 137.5 (s, C-4a/-C-10a), 132.9 (d, C-3'/C-5'), 131.9 (s, C-8a/C-9a), 125.3 (d, C-4/C-5), 123.8 (d, C-2'/C-6'), 122.5 (d, C-3/C-6), 102.4 (d, C-1/C-8), 57.0 (q, 2 OMe), 26.1 (t, CH_2CH_2). ES-MS spectrometry m/z (%): 515.14 (100), 516.15 (38), 517.15 (9), 514.95 (1), HRMS (ES$^+$) spectrometry: calc. for $C_{28}H_{23}N_2O_8$ (M$^+$ - CF$_3$SO$_3$): 515.1454 found: 515.1453.
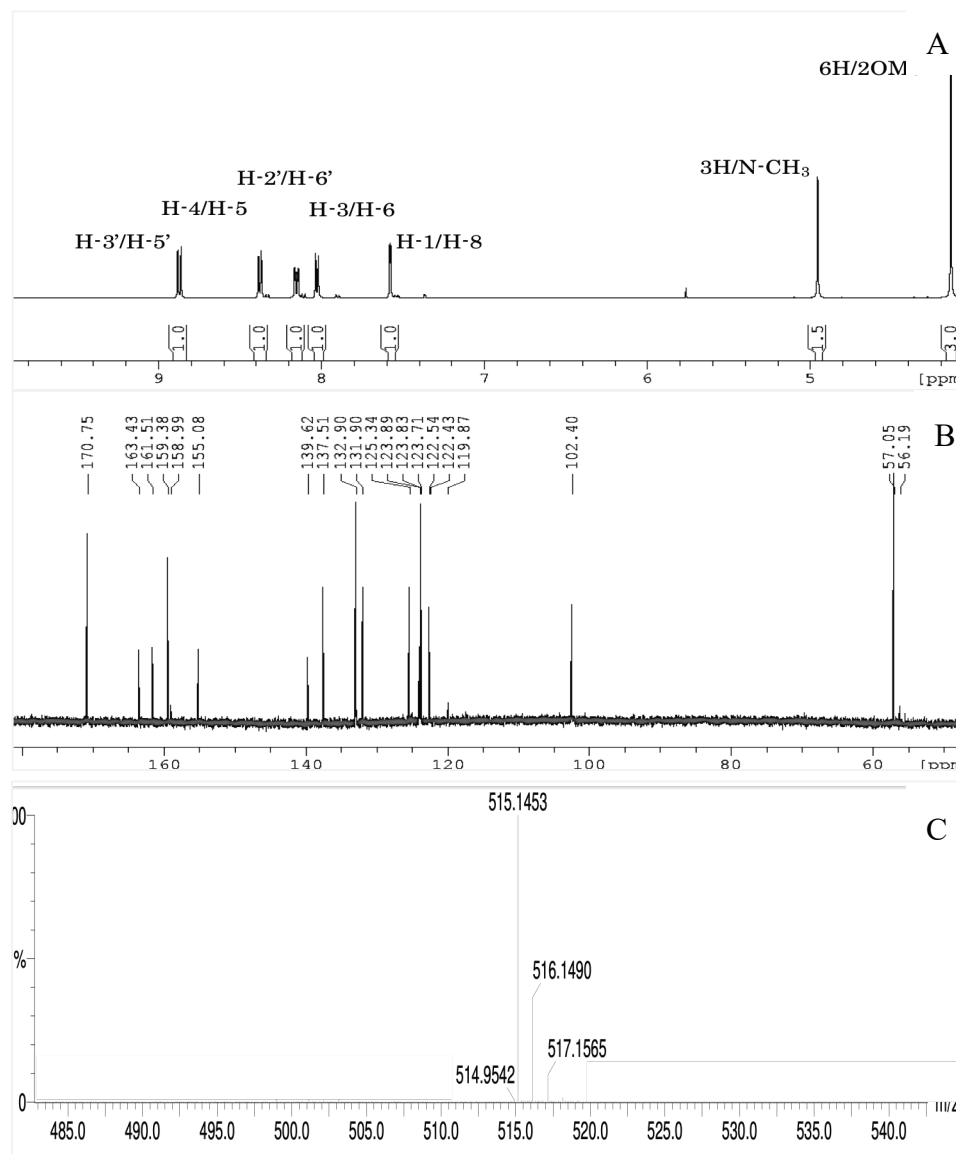
Figure 3. 48: The ^1H NMR (A), ^{13}C NMR (B) and mass spectra (C) of 4-(succinimidyloxycarbonyl)phenyl 2,7-dimethoxy-10-methylacridinium-9-carboxylate trifluoromethanesulfonate (34cx)

3.9 Synthesis of 2,6-dimethoxy-4-(succinimidyloxycarbonyl)phenyl 2,7-dimethoxy-10-methylacridinium-9-carboxylate trifluoromethanesulfonate (34cz).

Compound **34cz** was synthesized by a similar synthetic pathway to that used for compound **34cx**. The steps up to the synthesis of 2,7-dimethoxyacridine-9-carbonyl chloride (**25c**) were the same. Then **25c** was reacted with 2,6-dimethoxy-4-(succinimidyloxycarbonyl)phenol (**36z**)to give compound **33cz** (Figure 3.47), which on methylation would give **34cz**.

3.9.1 Synthesis of 2,6-dimethoxy-4-(succinimidyloxycarbonyl)phenyl 2,7-dimethoxyacridine-9-carboxylate (33cz)
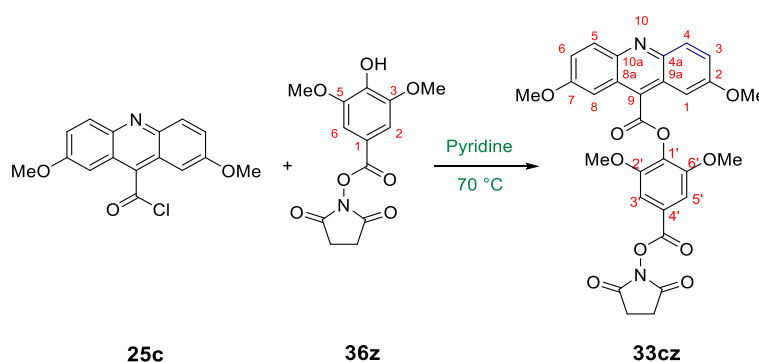
Figure 3. 49: Synthesis of (2,6-dimethoxy-4-(succinimidyloxycarbonyl))phenyl 2,7-dimethoxyacridine-9-carboxylate (33cz).

A solution of 2,7-dimethoxyacridine-9-carbonyl chloride (**25c**; 2.0 g, 6.6 mmol) in anhydrous pyridine (25 mL) was stirred at 40ºC for 10 min and allowed to cool down to room temperature. A solution of succinimidyl 3,5-dimethoxy-4-hydroxybenzoate (**36z**:1.57 g, 6.65 mmol) in anhydrous pyridine (10 mL) was added. The mixture was

stirred at 50ºC for 48 h under anhydrous conditions. The reaction mixture was cooled to

room temperature and poured into a mixture of dilute HCl (1 M, 80 mL) and ice (50 g).
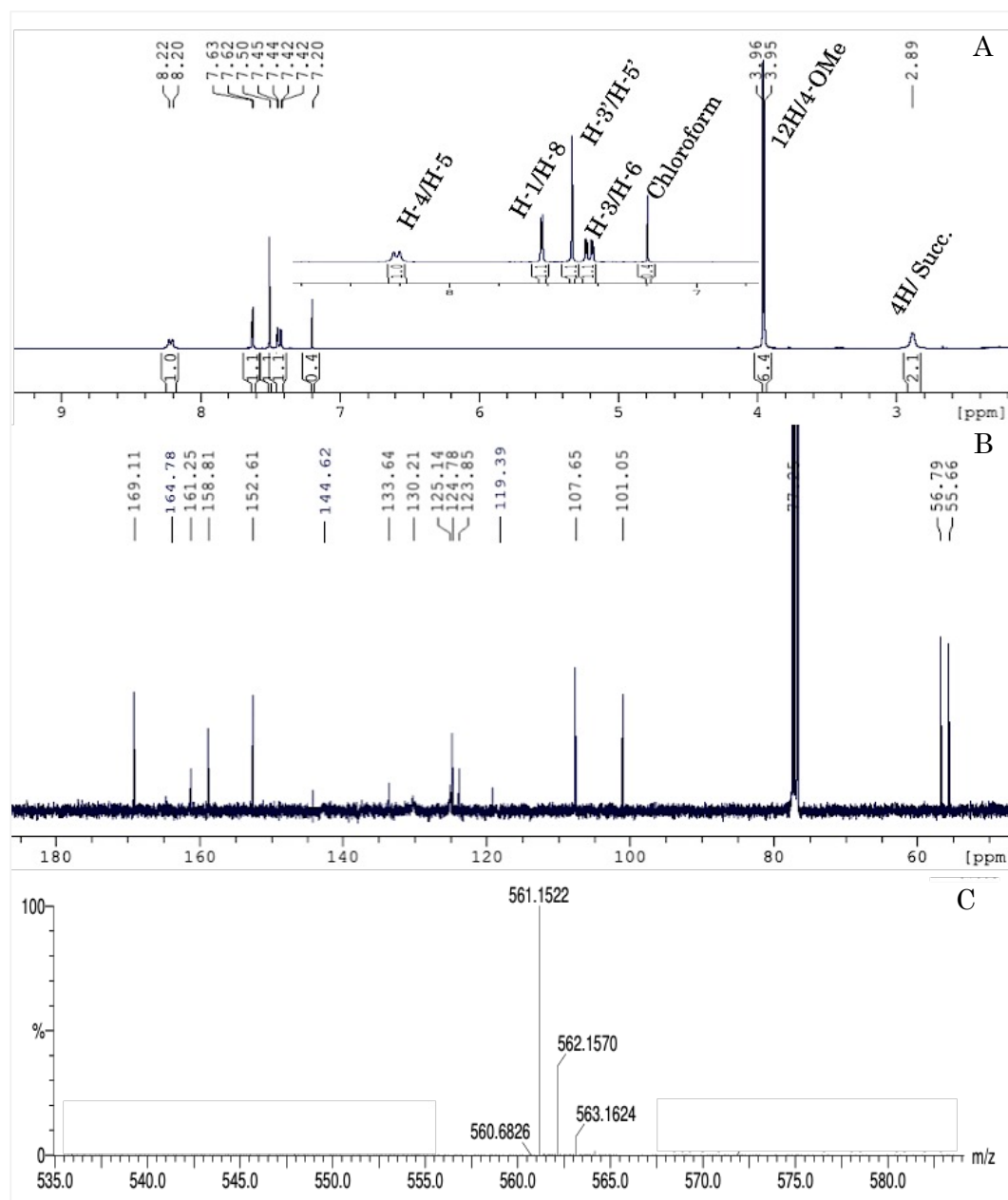
*Figure 3. 50: The 1H NMR (A), 13C NMR (B) and mass spectra (C) of 2,6-dimethoxy-4-
(succinimidyloxycarbonyl))phenyl 2,7-dimethoxyacridine-9-carboxylate (**33cz**).*

The solid was filtered and washed with a mixture of DCM and Et$_2$O (1:2 by volume, 30 mL) followed by Et$_2$O (2 × 15 mL) to give **33cz** (2.71 g, 5.42 mmol; 81% yield) as a yellowish solid, Mp: 157-158ºC. IR ν_{max}: 2949, 2839, 1734, 1604, 1463, 1288, 1070 cm^{-1}. ^{1}H NMR spectroscopy (400 MHz, DMSO-d_6): δ = 8.21 (d, J = 9.3 Hz, 2 H, H-4/H-5), 7.63 (d, J= 2.6, 2H, (H-1/H-8), 7.5 (s, (H-3'/H-5'), 7.4 (dd, J= 2.6, 9.3, H-3/H-6), 3.96 (s, 6H, 2 OMe), 3.95 (s, 6 H, 2 OMe), 2.89 (s, 4H, CH$_2$CH$_2$). ^{13}C NMR spectroscopy (100 MHz, DMSO-d_6): δ = 169.1 (s, N-C=O), 165.0 (s, ArO-C=O), 161.3 (s, NO-C=O), 158.8 (s, C-2/C-7), 152.6 (s, C-2'/C-6'), 144.1 (s, C-4a/C-10a), 133.6 (s, C-9), 130.5 (d, C-4/C-5), 125.1 (s, C-1'), 124.8 (s, C-8a/C9a), 123.9 (d, C-3/C-6), 123.7 (s, C-4'), 107.7, 101.1 (2 x d, C-3'/C-5' and C-1/C-8), 56.8 (q, OMe), 55.7 (q, OMe), 25.7 (t, CH$_2$CH$_2$). MS-ES spectrometry m/z (%): 561.15 (100, MH$^+$), 562.16 (36), 563.16 (8), 560.68 (1). HRMS (ES$^+$) spectrometry: calc. for C$_{29}$H$_{25}$N$_2$O$_{10}$: 561.1509; found: 561.1522. (Figure 3.50).

3.9.2 Synthesis of 2,6-dimethoxy-4-(succinimidyloxycarbonyl)phenyl 2,7-dimethoxy-10-methylacridinium-9-carboxylate trifluoromethanesulfonate (34cz)
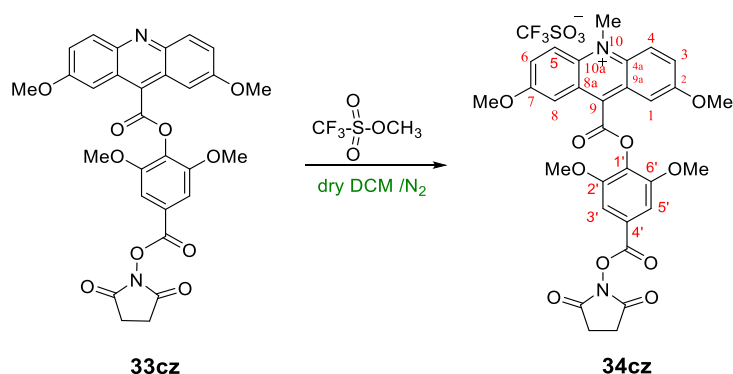
Figure 3. 51: Synthesis of 2,6-dimethoxy-4-(succinimidyloxycarbonylphenyl 2,7-dimethoxy-10-methylacridinium-9-carboxylate trifluoromethanesulfonate (34cz).

Methyl trifluoromethanesulfonate (0.33 mg, 2.0 mmol) was added to a stirred solution of **33cz** (0.20 g, 0.36 mmol) in dry DCM (30 mL) under nitrogen (Figure 3.49). The mixture was stirred at room temperature for 60 h. The yellow solid obtained was filtered, washed with diethyl ether (3 × 10 mL) and evaporated to dryness under reduced pressure to give **34cz** in 89% yield (0.23 g, 0.31 mmol) as a yellow solid product, Mp 167-169ºC.
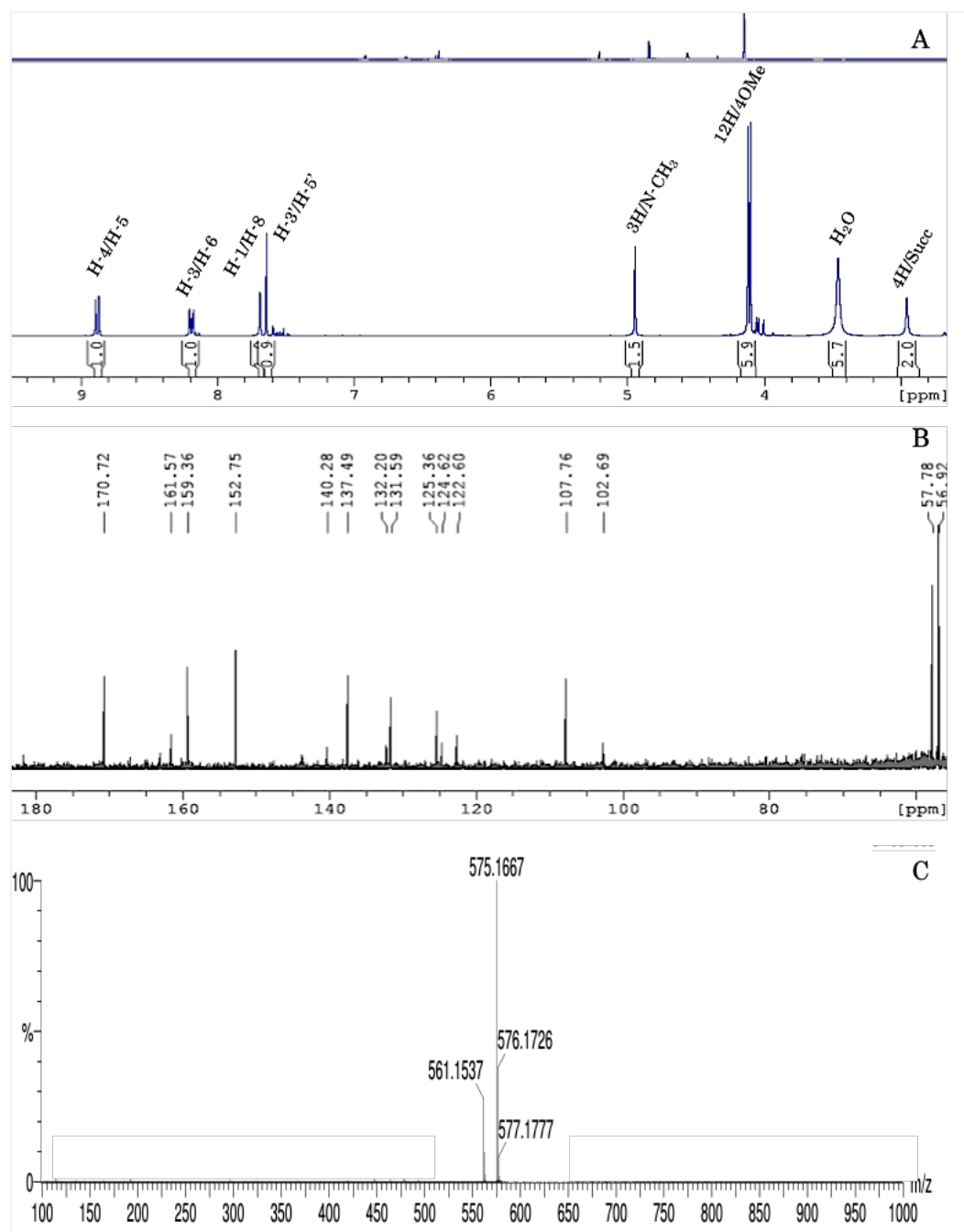
Figure 3. 52: The ^1H NMR (A), ^{13}C NMR (B) and mass spectra (C) of 2,6-dimethoxy-4-(succinimidyloxycarbonyl)phenyl 2,7-dimethoxy-10-methylacridinium-9-carboxylate trifluoromethanesulfonate (34cz).

Again, the product was exclusively in the acridinium form. IR ν_{max}: 3709, 2252, 1747, 1614, 1375, 1037, 918 cm^{-1}. ^{1}H NMR spectroscopy (400 MHz, DMSO-d_6): δ = 8.88 (d, J = 10.0 Hz, 2 H, H-4/H-5), 8.19 (dd, J = 2.7 and 10.0 Hz, 2 H, H-3/H-6), 7.68 (d, J = 2.7 Hz, 2 H, H-1/H-8), 7.64 (s, 2 H, H-3'/H-5'), 4.94 (s, 3 H, Me), 4.12 (s, 6 H, 2 OMe), 4.09 (s, 6 H, 2 OMe), 2.95 (s, 4 H, CH$_2$CH$_2$). ^{13}C NMR spectroscopy (100 MHz, DMSO-d_6): δ = 170.7 (s, N-C=O), 163.2 (s, ArO-C=O), 161.6 (s, NO-C=O), 159.4 (s, C-2/C-7), 152.8 (s, C-2'/C-6'), 140.3 (s, C-9), 137.5 (s, C-4a/C-10a), 132.2 (s, C-1'), 131.6 (d, C-4/C-5), 125.4 (s, C-8a/C-9a), 124.6 (s, C-4'), 122.6 (d, C-3/C-6), 107.8 (d, C-1/C-8), 102.7, (d, C-3'/C-5'), 57.8 (q, 2 OMe), 56.9 (q, 2 OMe), 40.9 (q, N-Me), 26.0 (t, CH$_2$CH$_2$) (CF$_3$ signal not observable). MS-ES m/z (%): 575 (100), 576 (38), 561 (27), 577 (9), HRMS (ES+) spectrometry, calc. for C$_{30}$H$_{27}$N$_2$O$_{10}$ (M$^+$ - CF$_3$SO$_3$): 575.1666; found: 575.1667 (Figure 3.52).

3.10 Conclusion

Two 2,7-dimethoxyacridinium esters have been synthesized using a modification of the method described by Weeks *et al.* and others.[53,80,131,133] The modified procedure, involving one fewer step overall, enabled the synthesis of the precursor acridinine esters in relatively high yield and in shorter times compared to the standard procedure. Whereas the standard procedure involves esterification of 2,7-dimethoxyacridine-9-carbonyl chloride with the appropriate 4-(benzyloxycarbonyl)phenol, followed by removal of the benzyl group and then formation of the NHS ester, the modified route involves the synthesis of the NHS ester of the appropriate 4-hydroxybenzoic acid and using this directly for esterifying the 2,7-dimethoxyacridine-9-carbonyl chloride.

The final step made use of an effective methylating reagent, namely methyl trifluoromethanesulfonate, under anhydrous conditions, to afford the target AEs. The chemical structures of the products were confirmed by mass spectrometry and NMR spectral data. In contrast to the dibromo derivatives, which had existed largely or exclusively in the pseudo-base form, the dimethoxyacridinium salts were indeed in the acridinium form. Both acridinium esters (**34cx** and **34cz**) showed high intensity chemiluminescence on treatment with alkaline hydrogen peroxide. The chemiluminescent properties of **34cx** and **34cz** along with those of other AEs prepared during this research project are discussed in detail in the next chapter.

3.11 Synthesis of the unsubstituted acridinium ester 34ax

The synthesis of 4-(succinimidyloxycarbonyl)phenyl *N*-methylacridinium-9-carboxylate trifluoromethanesulfonate (**34ax**) was conducted using the new route developed for the corresponding dibromo compounds (Figure 3.17).

3.11.1 Synthesis of 1-phenylisatin (23a)
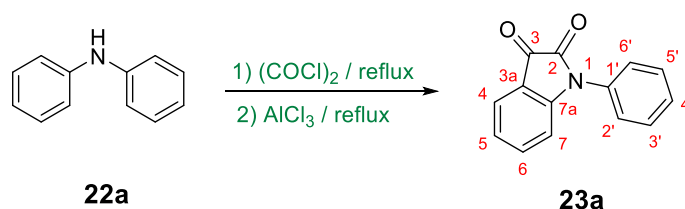
Figure 3. 53: Synthesis of 1-phenylisatin (23a)

Diphenylamine (**22a**, 2.9.g, 17.0 mmol) was dissolved in dichloromethane (DCM, 40 mL) and then added dropwise to stirred, refluxing oxalyl chloride (2.3 g, 18 mmol) in DCM (70 mL) (Figure 3.51). The mixture was heated under reflux with stirring for one hour. The excess of oxalyl chloride and DCM were evaporated under reduced pressure. To the residue, DCM (100 mL) was added followed by anhydrous aluminium chloride (AlCl$_3$, 2.40 g, 18 mmol) portion-wise over 10 min. The mixture was refluxed for one hour and the solvent was then removed under reduced pressure. Dilute hydrochloric acid (HCl, *ca.* 1 M, 60 mL) was added to the product and the mixture was stirred for 30 min, and then extracted with DCM (3 × 40 mL). The extract was dried over anhydrous magnesium sulfate and then filtered, and the organic layer was evaporated under reduced pressure. The orange solid obtained was washed with diethyl ether (20 mL) to give **23a** (3.50 g, 15.6 mmol) in

92% yield. ^{1}H NMR, ^{13}C NMR spectroscopy and mass analysis for 1-phenylisatin have appeared in a number of papers, which show data consistent with those obtained in this study[80,130,133]
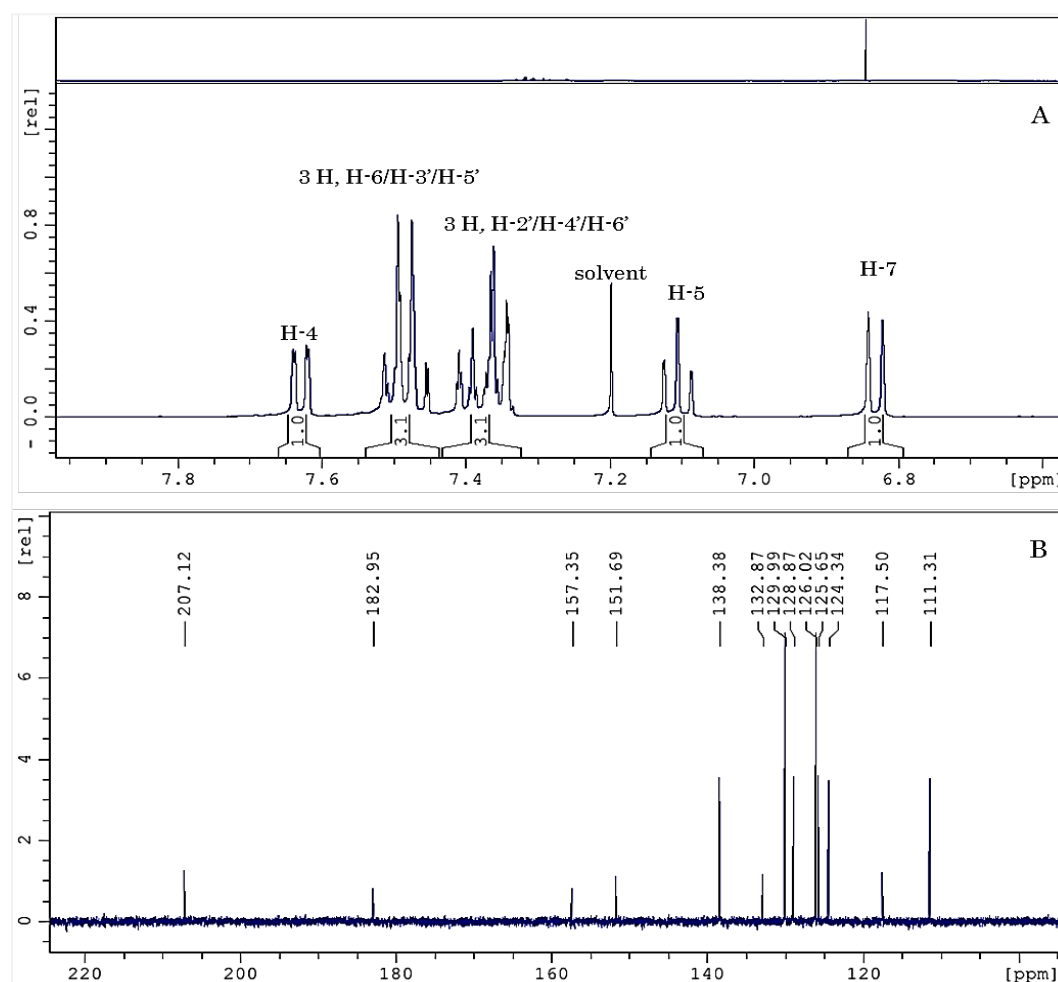
*Figure 3. 54: The ^{1}H NMR (A) and ^{13}C NMR (B) spectra of 1-phenylisatin (**23a**).*

Mp: 139-141ºC. IR ν_{max}: 3098, 1750, 1610, 1200 cm^{-1}. ^{1}H-NMR spectroscopy (400 MHz; CDCl$_3$): δ = 7.63 (d, J = 7.5 Hz, 1 H, H-4), 7.52- 7.45 (m, 3 H, H-6/H-3'/H-5'), 7.41- 7.34 (m, 3 H, H-2'/H-4'/H-6'), 7.11 (app. t, J = 7.5 Hz, 1 H, H-5), 6.83 (d, J = 8.0 Hz, 1 H, H-7). ^{13}C-NMR spectroscopy (100 MHz; CDCl$_3$): δ = 182.9 (s, C-3), 157.4 (s, C-2), 151.7 (s, C-7a), 138.4 (d, C-6), 132.9 (s, C-1'), 130.0 (d, C-3'/C-5'), 128.9 (d, C-7), 126.0 (d, C-2'/C-6'), 125.6 (d, C-4), 124.3 (d, C-5), 117.5 (s, C-3a), 111.3 (d, C-4'). EI-MS: *m/z* (%):

223 (100), 224 (18), 225 (2.8). HRMS (EI) spectrometry: calc for $C_{14}H_9NO_2$ (M$^+$): 223.0633; found: 223.0612.

3.11.2 Synthesis of acridine-9-carboxylic acid (24a)
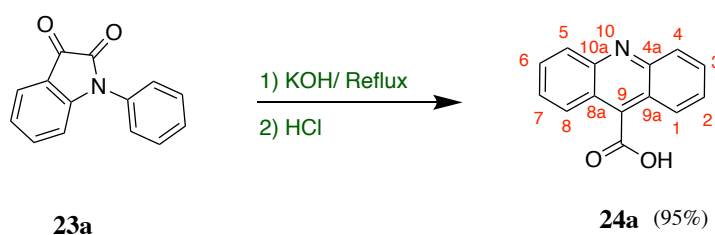
Figure 3. 55: Synthesis of acridine-9-carboxylic acid (24a).

A mixture of **23a** (2.0 g, 9 mmol) and potassium hydroxide (KOH; 12.6 g, 225 mmol) (Figure 3.53) in water (280 mL) was refluxed for 72 h. The resulting mixture, after cooling, was poured into a mixture of conc. HCl (ca. 11 M, 20 mL) and ice (50 g). The yellow solid obtained was collected by filtration, washed with water (3 × 50 mL), methanol (2 × 40 mL) and diethyl ether (40 mL), then dried to give **24a** as a yellow solid (1.9 g, 8.5 mmol, 95% yield). Syntheses of 1-phenylisatin have been reported[80,131,134] the data obtained shows consistency with those that were obtained in this study. Mp: 289-291ºC. IR ν_{max}: 3434, 2920, 1660, 1460, 1320, 1290 cm^{-1}. ^{1}H-NMR spectroscopy (400 MHz; DMSO-d_6): δ = 8.25 (d, J = 8.7 Hz, 2 H, H-4/H-5), 8.11 (d, J = 8.7 Hz, 2 H, H-1/H-8), 7.95 (J = ca. 8 Hz, 2 H, H-3/H-6), 7.75 (app. t, J = ca. 8 Hz, 2 H, H-2/H-7). ^{13}C-NMR spectroscopy (400 MHz; DMSO-d_6): δ = 167.7 (s, C=O), 147.2 (s, C-4a/C-10a), 134.8 (s, C-9), 134.8 (d, C-3/C-6), 132.3 (d, C-4/C-5), 127.5 (d, C-1/C-8), 122.8 (s, C-8a/C-9a), 122.1 (d, C-2/C-7).

EI-MS: *m/z* (%) = 223 (100), 224 (20), 225 (3.2). HRMS (EI) spectrometry: calc for

$C_{14}H_9NO_2$ [M$^+$]: 223.0633; found: 223.0610.
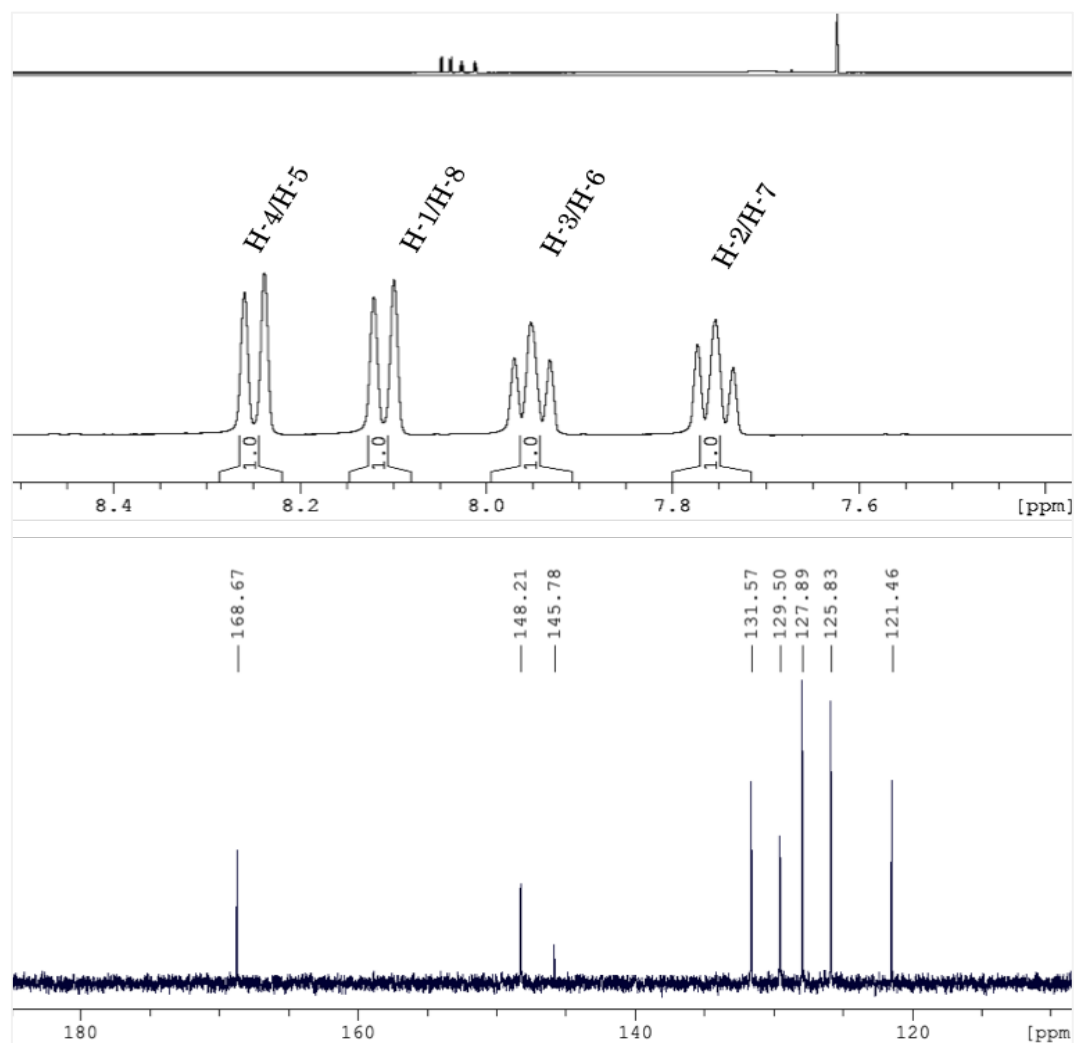
Figure 3. 56: The ^1H NMR and ^{13}C NMR spectra of acridine-9-carboxylic acid (24a).

3.11.3 Synthesis of acridine-9-carbonyl chloride (25a).
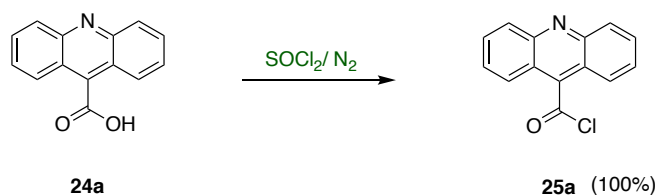
Figure 3. 57: Synthesis of acridine-9-carbonyl chloride (25a).

Acridine-9-carbonyl chloride (**25a**) was prepared according to the procedure reported by M. Rauhut and other later studies. [53,131] Acridine-9-carboxylic acid (**24a**; 2.20 g, 10.0 mmol) was dissolved in freshly distilled thionyl chloride (30 mL) and the solution was refluxed under anhydrous conditions for 1.5 h (Figure 3.55). Thionyl chloride was removed under reduced pressure to leave a yellow solid **25a** (*ca*. 2.41 g, 10 mmol), which was used for the next step without any further purification or spectroscopic analysis.

3.11.4 Synthesis of 4-(succinimidyloxycarbonyl)phenyl acridine-9-carboxylate (33ax)
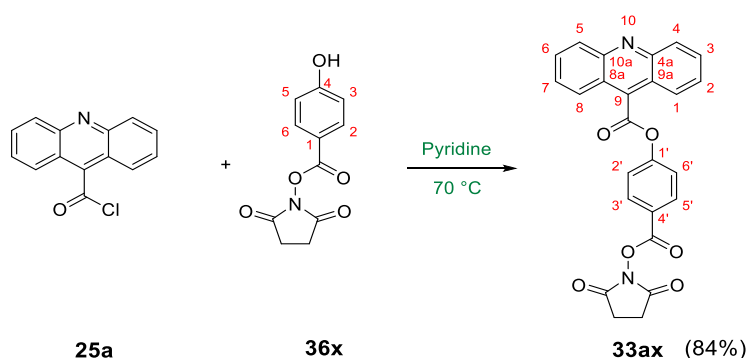
*Figure 3. 58: Synthesis of 4-(succinimidyloxycarbonyl)phenyl acridine-9-carboxylate (**33ax**).*

A solution of acridine-9-carbonyl chloride (**24a**; 1.9 g, 8.5 mmol) and 4-hydroxybenzoic acid 2,5-dioxopyrrolidin-1-yl ester (**36x**; 2.0 g, 8.5 mmol) in anhydrous pyridine (35 mL) was stirred at 70ºC overnight under anhydrous conditions (Figure 3.56). The mixture was cooled to room temperature then poured into a mixture of HCl (1 M, 80 mL) and ice (50 g), then filtered to give a crude product, which was washed with a mixture of DCM and diethyl ether (1:1, 30 mL) and then with an excess of diethyl ether to give a solid bright yellow product **33ax** (3.4g, 7.7 mmol, 90% yield). Mp; 242-243ºC, ^{1}H-NMR spectroscopy (400 MHz; DMSO-d_6): δ = 8.37-8.30 (m, 6 H, H-4/H-5, H-3'/H5', H-3/H-6), 8.04-7.96 (m, 4 H, H-2'/H-6', H-1/H-8), 7.85 (app. t, $J = ca.$ 7 Hz, 2 H, H-2/H-7), 2.94 (s, 4 H, CH_2CH_2).
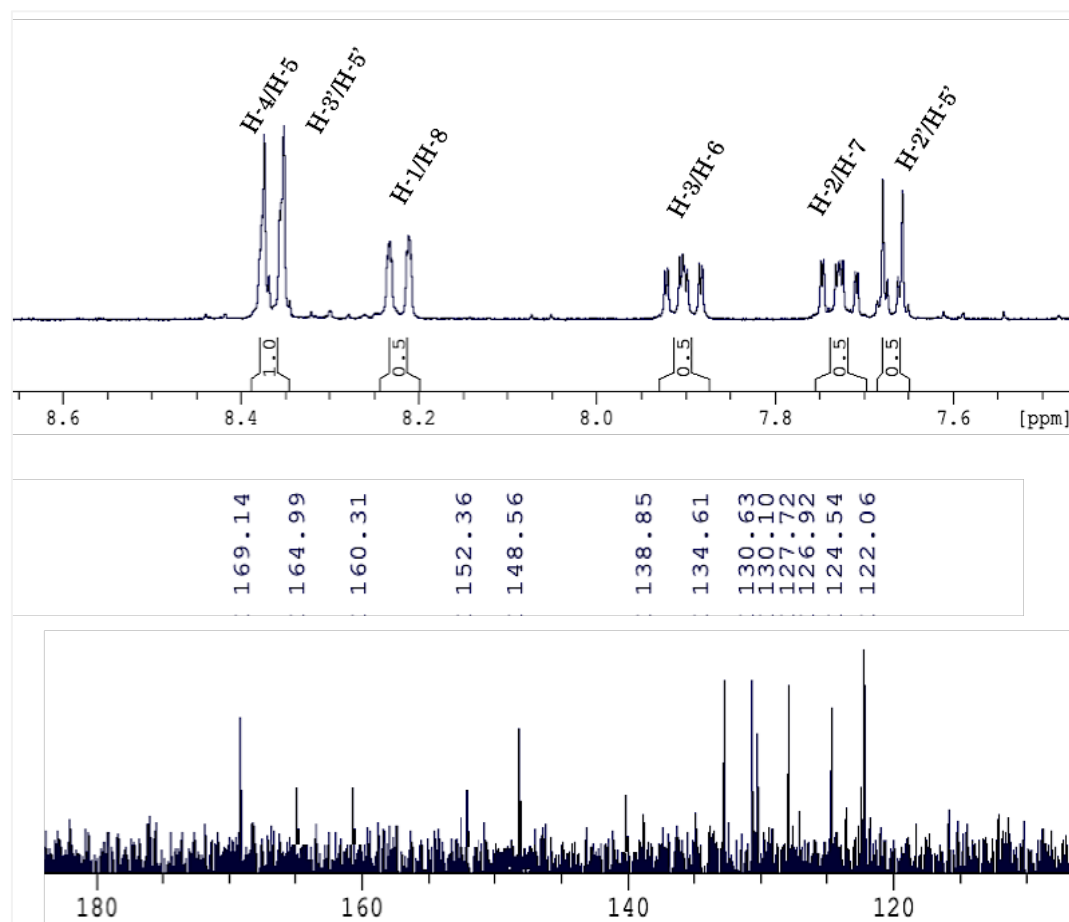
*Figure 3. 59: NMR spectra of 4-(succinimidyloxycarbonyl)phenyl acridine-9-carboxylate (**33ax**).*

^{13}C-NMR spectroscopy (400 MHz; DMSO-d_6): δ = 169.1 (s, N-C=O NHS), 165.0 (s, ArO-C=O), 160.3 (s, O=C-O-NHS), 152.4 (s, C-1'), 148.6 (s, C-4a/C10a), 138.8 (s, C-9), 134.6 (d, C-3'/C-5') 130.6 (d, C-3/C-6), 130.1, (d, C-4/C-5), 127.7 (d, C-2/C-7), 126.9 (s, C-4'), 124.5 (d, C-1/C-8), 123.5 (s, C-8a/C-9a), 122.1 (d, C-2'/C-6'), 25.8 (t, CH$_2$CH$_2$). TOF MS EI spectrometry m/z (%) = 440 (100), 441 (33), 442 (5). HRMS (EI) spectrometry: calc. for C$_{25}$H$_{16}$N$_2$O$_6$ (M$^+$): 440.1008; found: 440.1011.

3.11.5 Synthesis of 4-(succinimidyloxycarbonyl)phenyl 10-methylacridinium-9-carboxylate trifluoromethanesulfonate (34ax)
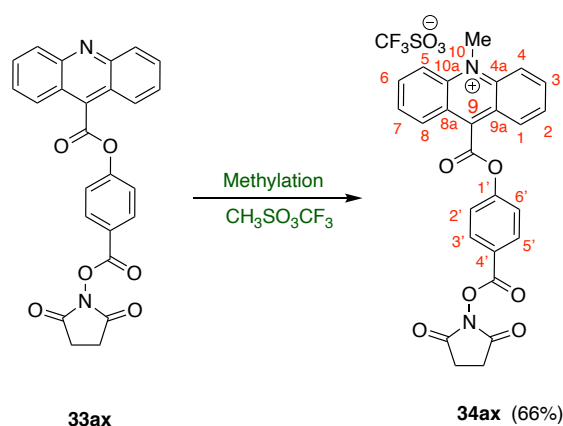
*Figure 3. 60: Synthesis of 4-(succinimidyloxycarbonyl)phenyl 10-methylacridinium-9-carboxylate trifluoromethanesulfonate (**34ax**).*

Methyl trifluoromethanesulfonate (0.20 mL; 0.33 mg, 2 mmol) was added to a stirred solution of **33ax** (0.10 g, 0.23 mmol) in dry dichloromethane (40 mL) under nitrogen (Figure 3.58). The mixture was stirred under reflux for 3 days. The reaction mixture was cooled to room temperature and the yellow solid obtained was filtered, washed with diethyl ether (5 × 10 mL) and finally a mixture of DCM and diethyl ether (1:1 in volume; 10 mL)

and evaporated under reduced pressure to give **34ax**, which was seen to be in the acridinium

form, in 76% yield (0.090 g, 0.15 mmol). Mp: 283-284ºC.
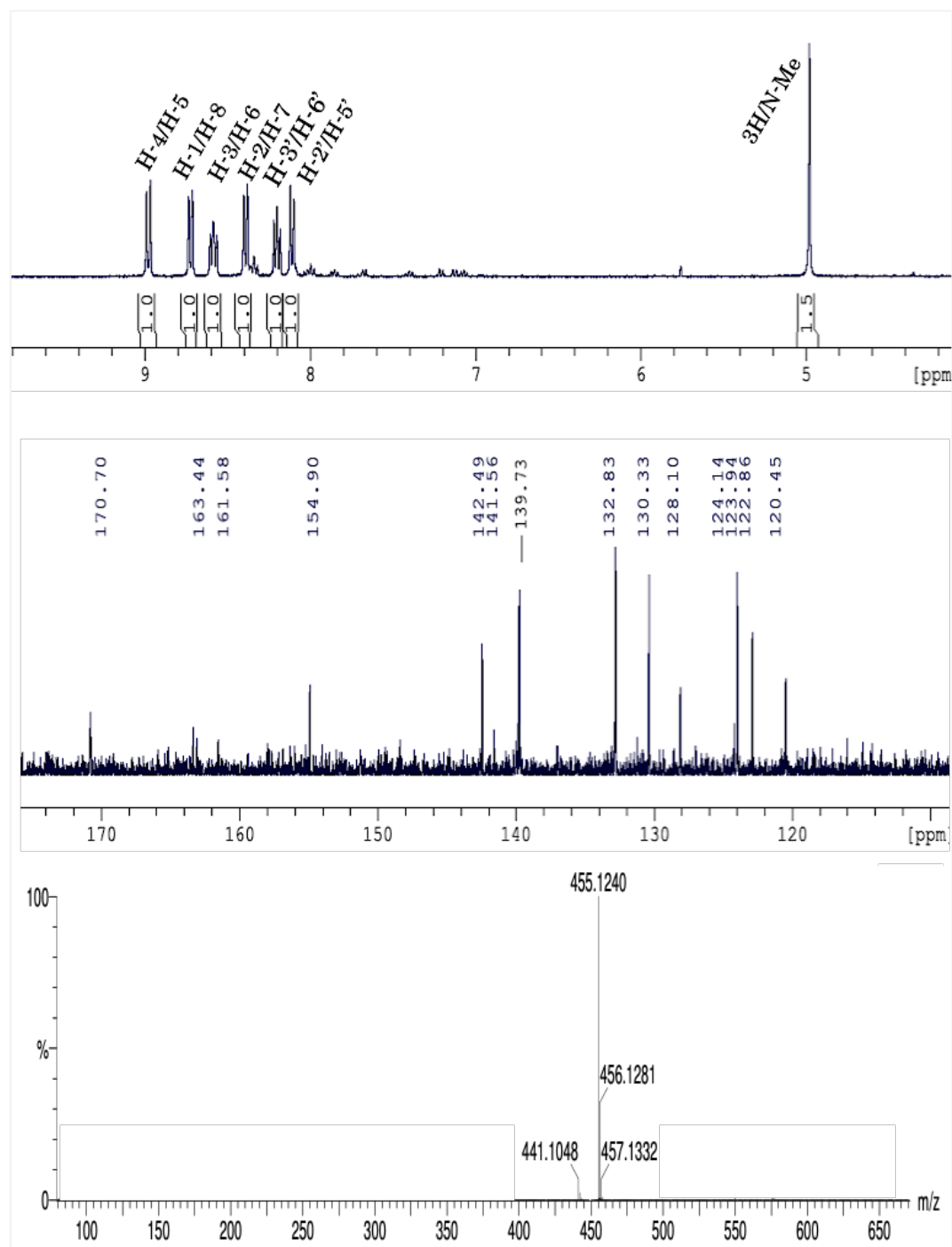
Figure 3. 61: The ^1H NMR (A), ^{13}C NMR (B) and mass spectrum (C) of 4-(succinimidyloxycarbonyl)phenyl 10-methylacridinium-9-carboxylate trifluoromethanesulfonate (34ax).

^{1}H NMR spectroscopy (400 MHz; DMSO-d_6): δ = 8.98 (d, J = 9.3 Hz, 2 H, H-4/H-5), 8.70 (d, J = 8.6 Hz, 2 H H-1/H-8), 8.58 (app. t, J = ca. 8 Hz, 4 H H-3/H-6), 8.39 (d, J = 8.6 Hz, 2 H H-3'/H-5'), 8.20 (app. t, J = ca. 8 Hz, 2 H, H-2/H-7), 8.11 (d, 2H, J = 8.6 Hz, 2H, H-2'/H-6'), 4.98, (s, 3H, N-CH$_3$), 2.94 (s, CH$_2$ CH$_2$). ^{13}C-NMR spectroscopy (400 MHz; DMSO-d_6): δ = 170.7 (s, O=C-N), 163.5 (s, O=C-OAr), 161.6 (s, O=C-N-Succ), 154.9 (s, C-1'), 142.4 (s, C-4a/10a), 141.5 (s, C-9), 139.7 (d, C-3/C-6), 132.8 (d, C-3'/C-5'), 130.3 (d, C-1/C-8), 128.1 (d, C-2/C-7), 124.1 (d, C-2'/C-6'), 123.9 (s, C-4'), 122.9 (s, C-8a/C-9a), 120.4 (d, C-4/C-5), 40.4 (q, N-CH$_3$), 26.1 (t, CH$_2$CH$_2$). TOF MS ES$^+$ spectrometry (*m/z*) (%): 455.1 (100), 456.1 (32), 457.1 (8), 441.1 (2). HRMS (ES) spectrometry: calc for C$_{26}$H$_{19}$N$_2$O$_6$ (M$^+$ - CF$_3$SO$_3$): 455.1243; found: 455.1240.

3.12 Conclusion

Similar synthetic pathways were used to create a number of unsubstituted acridinium ester derivatives as the relevant compounds at the beginning of this chapter (figure 3.17). All compounds were successfully synthesised, isolated in high yields, and identified using mass spectrometry, ^{1}HNMR, and ^{13}CNMR spectroscopy.

The data presented shows a consistent with the data reported in a number of literatures for compounds **23a** and **24a**.[80,131] Compound **34ax** was used to compare the chemiluminescence characteristics (kinetics and efficiency of emission, stability), to STD AE (**15**), which had previously been characterized, as well as with produced compounds (**34bx**, **34by**, **34bz**, **34ca** and **34cz**).[135] The two additional unsubstituted AE derivatives, which differ in structure by having methyl or methoxy groups in the 2 and 6-positions of the phenyl ester, were the subject of numerous attempts to synthesise, but these efforts were unsuccessful due to the difficulty in obtaining pure compounds or hydrolysis during the extraction.

Chapter 4

Characterization of the emission properties of modified acridinium esters.

4 Characterization of the emission properties of modified acridinium esters.

4.1 Introduction

4.1.1 Impact on chemiluminescent properties of the modified acridinium esters

This study focuses on a series of acridinium esters with different substituent groups on the C-2 and C-7 position of the acridinium ring (Figure 4.1). This series of acridinium esters compounds was synthesized as described in Chapter 3. The aim was to determine whether substitution on the acridinium ring had properties sufficiently different from those of the most commonly used, commercially available acridinium ester (4-(2-succinimidyloxycarbonylethyl)-phenyl-10-methylacridinium-9-carboxylate trifluoromethanesulfonate, which we will refer to as 'standard' or 'STD' AE (**15,** Figure 4.1) which has an unsubstituted acridinium ring and a longer coupling leaving group.

The purpose of this comparison is to determine whether two AE compounds could be measured simultaneously, and individual signals resolved. If this could be achieved, it would allow a dual measurement assay to be developed that would have many potential benefits and applications for clinical diagnostics. For example, a dual assay would facilitate a clinically relevant measurement to be determined together with simultaneous quantification of an internal or external reference. This would improve sample processing efficiency and reduce error since internal standardisation can be performed simultaneously with target analyte measurement in a homogenous assay format. Moreover, the instrumentation required for detection would be rapid, robust, cost effective and consume low quantities of reagents and it would be fully compatible with both homogeneous or

heterogeneous assay formats. Dual analyte assays are used widely in both medical and environmental diagnostics; however, there are only a small number of examples of this approach utilising chemiluminescent endpoints. Nelson *et al*. [88] exploited the contrasting kinetic properties of two AE reporters, with the two molecules emitting their light output over distinct time periods post chemical activation, allowing the resolution of the two measurements which formed the basis of a successful clinical assay.

There are a number of factors that can affect the light output. Studies have focused on the influence of both the leaving group and the functionalisation of the acridinium ring evaluating both the impact on chemiluminescence emission wavelength and overall light output (quantum yield). The impact on the emitted chemiluminescence when substituting the acridinium ring with an electron donating group (ie. OCH_3) and an electron accepting (ie. Br) group depending on the precise location of these modifications, with suggestions that C-3, C-6 or C-1, C-8 substituents have a higher quantum yield than *2,7*-substituents. [66,135] Moreover, despite several studies and patents describing the application of acridinium esters in novel analytical procedures, [41,136] limited research has focused on the physiochemical properties of AE with activated groups on the acridinium ring or the phenyl ring of a leaving group. Those studies that have explored these relationships have revealed that the efficiency of the light emitted by the action of peroxide and the kinetics of the resulting chemiluminescence is influenced by the chemical characteristics of the leaving groups. while the overall light output is also markedly affected by the structure of AE.[131,137] More recent, parallel studies have reported the synthesis of compounds with additional functional groups at the C-2, C-7 position of the acridinium ring, the effect of the substituent groups on the wavelength of light emission and the effect on the quantum yields.[60,68,134,138] The latter aspect of these studies seems to be important, as the substitution of the acridinium ester bearing an electron donating and an electron accepting

group, alter the physical properties of the chemiluminescent and the excited derivative emitters. Law *et al*. synthesized acridinium esters with different substituents on the acridinium ring and describe a novel, long-emission compounds and found only a 37 nm increase in peak emission wavelength in an acetonitrile solution. He also extended their studies to include fused benzacridinium system to additional aromatic rings and reported that the excited *N*-methylbenzacridone from the angular benz[a]acridinium ester derivative increased peak emission by only 11 nm while the excited *N*-methylbenzacridone from the linear benz[b]AE derivative increased peak emission wavelength by 95 nm in acetonitrile solutions.[126]

Natrajan *et al*. examine the impact of a single methoxy group at various places of the acridinium ring in a series of *N*-sulfopropyl-AEs.[108,138] This study found that either a single methoxy group at C-2 or two methoxy groups at C-2 and C-7 of the acridinium ring, increased the quantum yield, while the addition of methoxy group at other positions on the acridinium ring did not enhance the quantity of light emission. These changes caused slight shifts in wavelength, by 8 nm at the acridinium ring 3 position, while a substituent at position 2 or 4 led to increases in the emission wavelength by 32 and 52 nm respectively. They also found that the 2,7-dimethoxy substitution of their *N*-sulfopropyl shifted by 58 nm in the emission wavelength.

Browne and his co-workers synthesised a substituent acridinium ester that involved two methoxy groups at the C-2 and C-7 positions of the acridinium ring. Peak emissions from 2,7-dimethoxyAE-labeled probes shift bathochromatically by ~58 nm from those of AE-labelled probes, which emitted light present at 484 and 485 nm in water and dimethylformamide respectively but they present slower emission decay rate because of slower dark reactions of AE.[65] These differences in emission wavelengths and time decayed advantageously support the simultaneous spectral-temporal separation of signal

from two probes in a dual wavelength luminometer. Moreover. These studies show that some stabilisation towards hydrolysis can be achieved by incorporating bulky groups at the 2 and 6 positions of the phenol.

Therefore, there is good evidence to suggest that substitution at the C-2, C-7 positions on the acridinium ring may alter the wavelength and enhance the quantum yield of the acridinium compound. Ideally, the different substitutions of the acridinium ester compounds or conjugates should emit light of different wavelengths under an identical chemical stimulus. It may be anticipated that the six different chemiluminescence compounds, including unsubstituted AE and five novels modified AE in different substituents on the 2,7 positions of acridinium ring and on 2, 6 positions of phenyl ester as shown in Figure 4.1, may impact on the emission properties. To establish which compounds could be deployed in a novel clinical assay which supports dual analyte measurement, it was important to discover and characterise AE derivatives by testing the following: i) stability in aqueous solution; ii) the ability to initiate the chemiluminescence using hydrogen peroxide in an alkaline environment; and, iii) either an emission wavelength that can be distinguished from that of STD-AE (ideally a minimum shift of ~ 30-40 nm or an emission kinetic profile distinct from that of STD-AE (**15**).
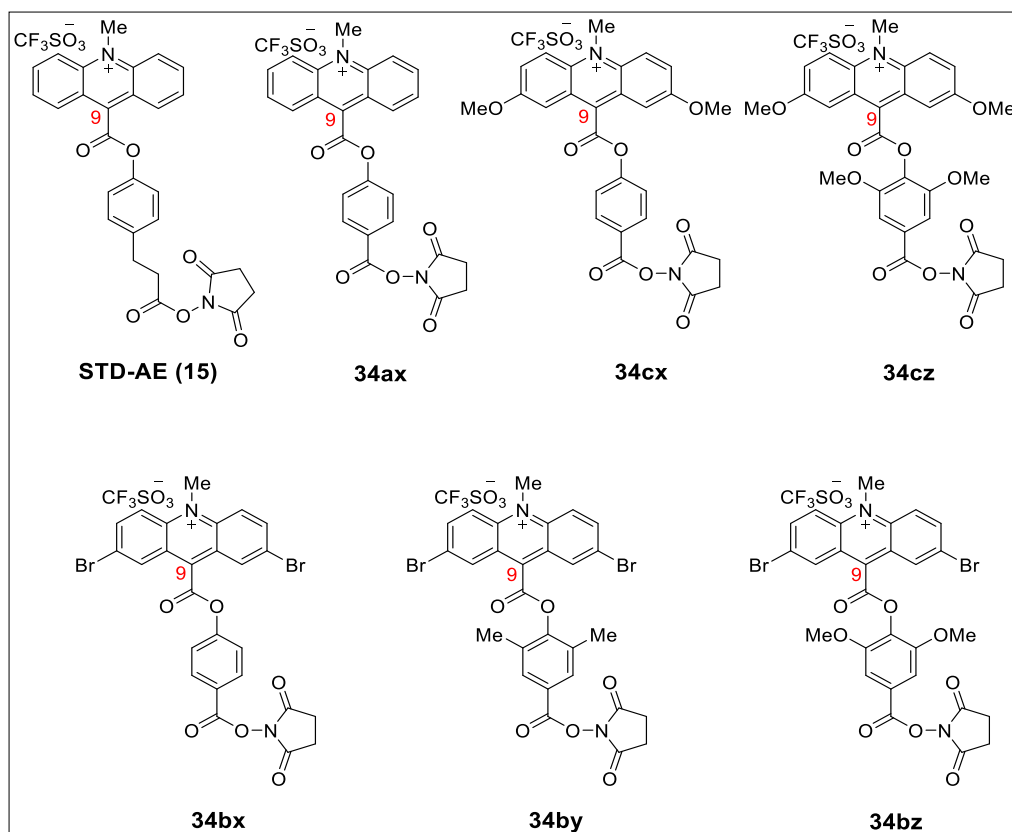
*Figure 4. 1: Structures of STD-AE (**15**) and modified acridinium ester compounds used for emission analysis. Acridinium ester with no substitution on the acridinium ring with a phenyl-ester leaving group (**15**: 4-(2-succinimidyloxycarbonylethyl)-phenyl 10-methylacridinium-9-carboxylate trifluoromethanesulfonate: Acronym: STD-AE), compared to un-substituted (**34ax**: 4-(succinimidyloxycarbonyl)phenyl -10-methylacridinium-9-carboxylate trifluoromethansulfonate: Chapter 3.3), (**34cx**: 4-(succinimidyloxycarbonyl)phenyl 2,7-dimethoxy-10-methylacridinium-9-carboxylate trifluoromethanesulfonate, (**34cz**: 4-(succinimidyloxycarbonyl)-2,6-dimethoxphenyl 2,7-dimethoxy-10-methylacridinium-9-carboxylate trifluoromethanesulfonate: Chapter 3.2) and dibromo substituted (**34bx**: 4-(succinimidyloxycarbonyl)phenyl 2,7-dibromo-10-methylacridinium-9-carboxylate trifluoromethanesulfonate: Chapter 3.1), (**34by**: 4-(succinimidyloxycarbonyl)-2,6-dimethylphenyl 2,7-dibromo-10-methylacridinium-9-carboxylate trifluoromethanesulfonate and (**34bz**: 4-(succinimidyloxycarbonyl)-2,6-dimethoxphenyl 2,7-dibromo-10-methylacridinium-9-carboxylate trifluoromethanesulfonate (Chapter 3.)*

4.1.2   Mechanism of light emission from acridinium esters

According to several studies [54,55,73,80] that have investigated the mechanism of acridinium ester chemiluminescence, light emission is generated when an electron returns to the ground state from its excited state. The chemiluminescence spectrum recorded should correspond to the fluorescence spectra of acridone present in the reaction mixture. The fast light emitting chemiluminescence from acridinium esters and their derivatives is usually generated in two steps. First, the acid converts any non-chemiluminescent pseudobase (**37**, Figure 4.2) to the chemiluminescent acridinium ester in the acidic form (**39**, Figure 4.2). Second, treatment of the acidic form (**39**) with alkaline hydrogen peroxide triggers light emission which is rapid and complete within 5 s forming an electronically excited state. Excited state acridone (**3**) is believed to be the light emitting species, which is formed in one of four processes,[52,139] from the decomposition of a high energy dioxetanone intermediate (**42**, Figure 4.2), or indirectly from the formation from dioxetane (**40**, Figure 4.2), or decomposition of dioxetane intermediate (**40**), or occurs by electron transfer from the acridine nitrogen to the peroxide bond by a chemically initiated electron exchange luminescence mechanism.

Hydroperoxide ion addition to C-9 followed by a series of intermediate reactions that ultimately lead to excited state acridone or substituted acridones which are the primary emitters. Dioxtanes and dioxitanones have been proposed as the reaction intermediate in the overall reaction pathway of acridinium ester leading to chemiluminescence light emissions, see figure 4.2 below.
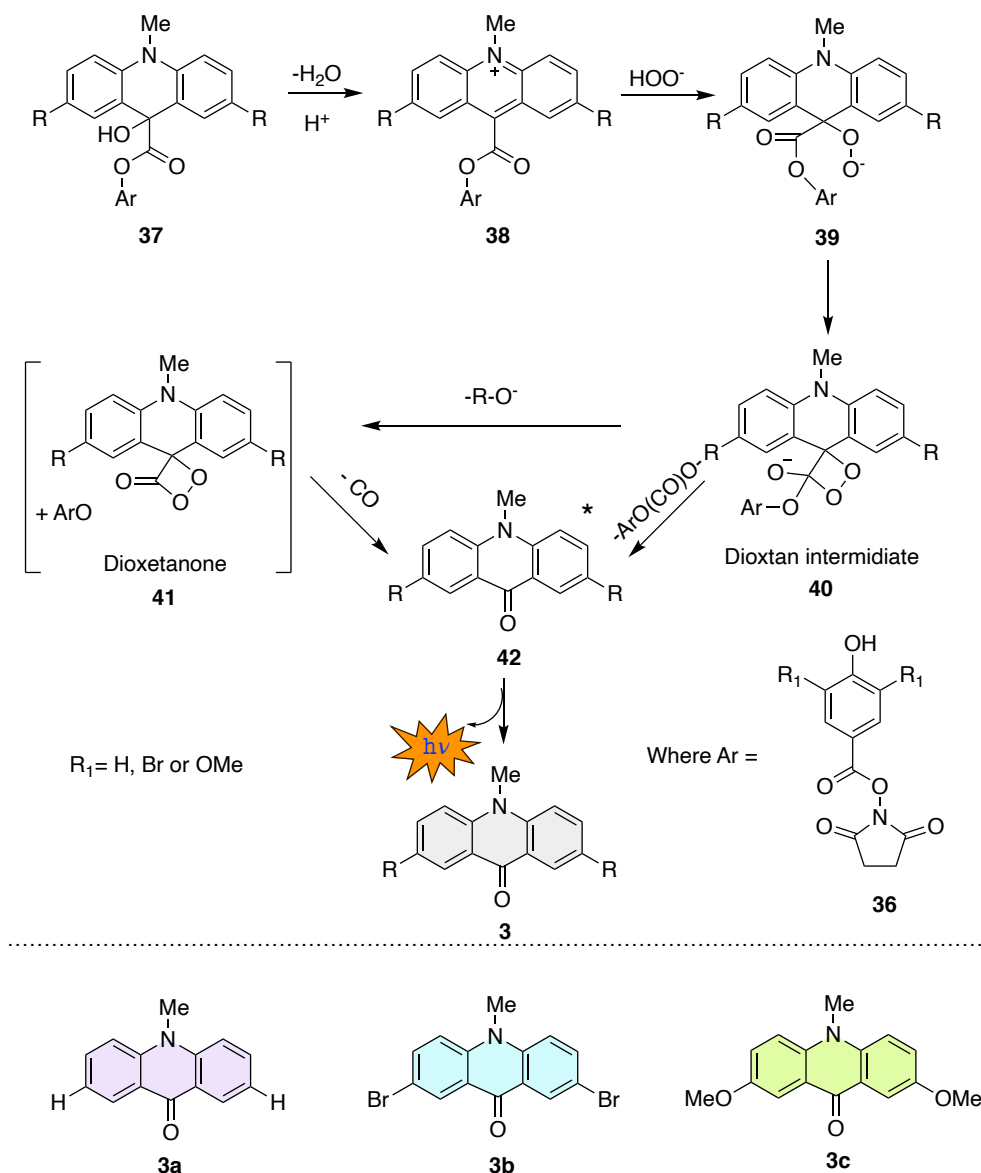
Figure 4. 2: General reaction pathway of chemiluminescence acridinium esters. Light emission is triggered by sequential addition of 0.1mM nitric acid containing 32mM hydrogen peroxide, followed by 1.5 M sodium hydroxide; the acid converts the non-chemiluminescent state to a chemiluminescent one (38) which then reacts with an alkaline peroxide to produce exited state acridone (41). Compounds 39 and 40 are unstable intermediates. 3a: N-methylacridone, 3b: 2,7-dibromo-10-methyl-9-acridone, 3c: 2,7-dimethoxy-10-methyl-9-acridone(McCapra et al. 1965)

4.1.3   Light emission of acridinium esters

The direct measurement of the chemiluminescent spectra of the modified acridinium esters would require a hyperspectral luminometer that could resolve the various wavelengths of light output immediately after chemical stimulation. Such equipment's were not available; however, the intermediate responsible for the light production, the excited state acridone can be produced by oxidizing phenyl esters to generate the substituted *N*-methylacridone (**3a**) (see 4.2 above) and using light to subsequently generate the excited state emission species. Thus, the photoluminescence properties of the acridone derivatives would reflect the emission properties of the chemiluminescent parent compounds from which they were derived.

To obtain an accurate measurement of fluorescence spectra, we must consider some important requirements inherent in the emission measurement: i) potential interference resulting from constituents of the sample buffer; ii) the excitation wavelength required to generate the maximum emission; and iii) the wavelength of emission and any impact of the chemical environment.

4.2   Material and Methods

4.2.1   Generation of acridone derivatives from acridinium esters

To determine the spectral properties of the chemiluminescent compounds we first oxidized the phenyl esters to generate the emission species, the acridone, as illustrated in Figure 4.2. More specifically, the chemiluminescent reaction was initiated from 50 mM of each compound in DMSO with the addition of Detection Reagent 1 ((R1, 0.1 M) nitric acid, (32 mM) hydrogen peroxide) and Detection Reagent 2 (R2, 1.5 M, sodium hydroxide)

to generate the acridone. The subsequent reaction mixture (100 µL) was diluted in DMSO/methanol (1000 µL). The fluorescence then was measured using 50 µL of each reaction for all compounds (see Section 4.3.3).

4.2.2   Measurements of Acridones Absorption

An absorption spectrum can be defined as a spectrum obtained by transmitting electromagnetic radiation through a substance. When the electron at the lower level absorbs the photon's energy, the energy of the electron is increased, leading the electron to be promoted to a higher level. If the energy between the two levels is not equal to the photon energy, then this can only occur; otherwise, the photon is not absorbed. Following radiation transmission through the medium, coloured bands corresponding to the unabsorbed photons and black lines indicating the absorbed photons are produced. The photon's energy is given as;

$$E = hc / \lambda$$

Where E: energy of the photon (Jmole-1), c: speed of radiation (ms-1)
h: Plank's constant, λ: wavelength (m).

According to the Beer-Lambert rule, the amount of light that a substance absorbs is exactly proportional to the substance's amount and the length of the light's passage through the solution. For example, isoquinoline and acridine fluoresce much more strongly in protic solvents than in hydrocarbon solvents.[140] The traditional explanation for these observations are that the lowest excited singlet state for many nitrogen heterocycles is of n,π^* character in hydrocarbon solvents but of π,π^* character in alcohols and other hydrogen-bond donors, and the n,π^* state is nonfluorescent because of efficient intersystem crossing and/or internal conversion. [140] The ground state is less well solvated in an aprotic

solvent than the excited state, and changes in the solvent's hydrogen-bond donor properties typically have little effect on the energies of the π-π* transitions.

In this study, a series of new chemiluminescent molecules based on substitution at 2,7-psition of acridinium rings [(2,7-dibromoacridinium ester (**34bx**, **34by** and **34bz**), 2,7-dimethoxyacridinium esters (**34cx**, **34cz**) and unsubstituted acridinium ester (**34ax**)] were synthesized. The identities of all new compounds were confirmed by several characterizations such as ^{1}H-NMR, ^{13}C-NMR, IR spectroscopy methods and Mass spectrometers (Chapter 3). From these new compounds, three methyl acridones compounds were obtained. Their absorption properties were studied in DMSO/methanol solvents, on Cary-60 UV-Vis spectrophotometer instrument (Agilent Technologies, Cheshire, UK), using quartz cuvettes, while the emissions were studied using a set of proportional solutions (DMSO/hybridization buffer) in different polarity to examine the effect of the buffer polarity on the photophysical properties as described in the next section. Samples were prepared by taking 10 μL of each chemiluminescent reaction solution separately and diluting it to 1000 μL in DMSO. An aliquot (10 μL) was then transferred to 1000 μL of methanol (HPLC grade) before absorbance spectra were recorded. A blank solution (1:100 DMSO/methanol) was used as a background. Data were collected at a scan rate of 2400 nm/min over a scanning wavelength range (200-650 nm); each spectrum was recorded in triplicate.

4.2.3   Excitation and emission spectra

The excitation and emission wavelengths were obtained on a SpectraMax Gemini EM, (Molecular Devices, Wokingham, U.K). The instrument parameters used were bandwidth slit: 2 nm, temperature 25ºC. All measurements were performed in a 96-well plate with a

50 µL sample volume. The wavelength of emitted light from acridinium compounds and their acridone counterparts should be in the region of 400-500 nm which corresponds to ca. 70 kcal/mole of energy, the reaction being exothermic by at least this amount. By comparison, peroxide compounds, with their weak O-O bond requires only 33 kcal/mole for cleavage. Thus, the emission spectra of the acridone were determined at a temperature of 25 ±1°C in the range of 350-650 nm under various excitation conditions and in contrasting chemical environments as described below.

4.2.4   Evaluation of spectral interference

Preliminary analysis using 'blank' samples consisting of a 1:1 ratio of aqueous solution and the solvent using an excitation λ_{max} of 380-410 nm, yielded no emission up to wavelength 620 nm.

4.3   Results

4.3.1   Acridones Absorption Spectra

The three acridones **3a**, **3b**, and **3c** were formed by the alkaline reaction of their parent chemiluminescent molecules **15**, **34bx**, **34cx**, and **34cz** (Figure 4.3; Panels B, D, E, F respectively). Since the spectra were determined without purification of the acridones, it was important to determine the absorption of other products of the alkaline reaction, therefore spectra were derived separately for the phenolic leaving group **36x** (Figure 4.3; Panel C) and a purified unsubstituted acridone **3a** (Figure 4.3; Panel A).

Initial analysis of the phenolic leaving group (succinimidyl 4-hydroxybenzoate (**36x**)) absorption spectra revealed a broad peak around 280 nm (data not shown) associated

with the phenoxy and the NHS groups comparable with data reported in publications.[141,142]

A further 1/1000 dilutions were then prepared in DMSO/Methanol solution and a fresh spectrum was acquired. The results obtained shows a broad peak around λ_{max} 294 nm. (Figure 4.3; Panel C). These peaks were observed in all impure acridones generated from their parent chemiluminescent molecules. The purified 10-methyleacridone (**3a**) showed two absorption maxima at 379 and 398 nm due to (π-π*) transition (Figure 4.3; Panel A), the spectral data being equivalent to that reported in literatures.[143] Acquisition of the spectra of **3a** derived from the parent chemiluminescent molecule (**15,** Figure 4.3; Panel B) showed a wide saturated absorption peak between 250-360 nm associated with the phenolic leaving group and NHS together with minor peaks at 379 and 398 nm associated with the acridone component establishing that this weaker absorption could be observed within the reaction mixture.

Compound 2,7-dibromo-10-methylacridone (**3b**), which was produced from compounds **34bx**, **34by**, and **34bz**, displayed a green shift of 15-20 nm in comparison to compound **3a** together with acridone absorption at 418 nm (Figure 4.3; Panel D). In addition to the phenolic absorption, 2,7-dimethoxy-10-methylacridone (**3c**), which was produced by the alkaline oxidation of **34cx** and **34cz**, showed a further green shift in absorption at 438 nm. The intermolecular charge transfer linked to the alkoxy donating groups may explain why the maximum absorption of acridone shifted from the unsubstituted **3a** (379–398 nm) to the OMe substituted **3c** (438 nm).
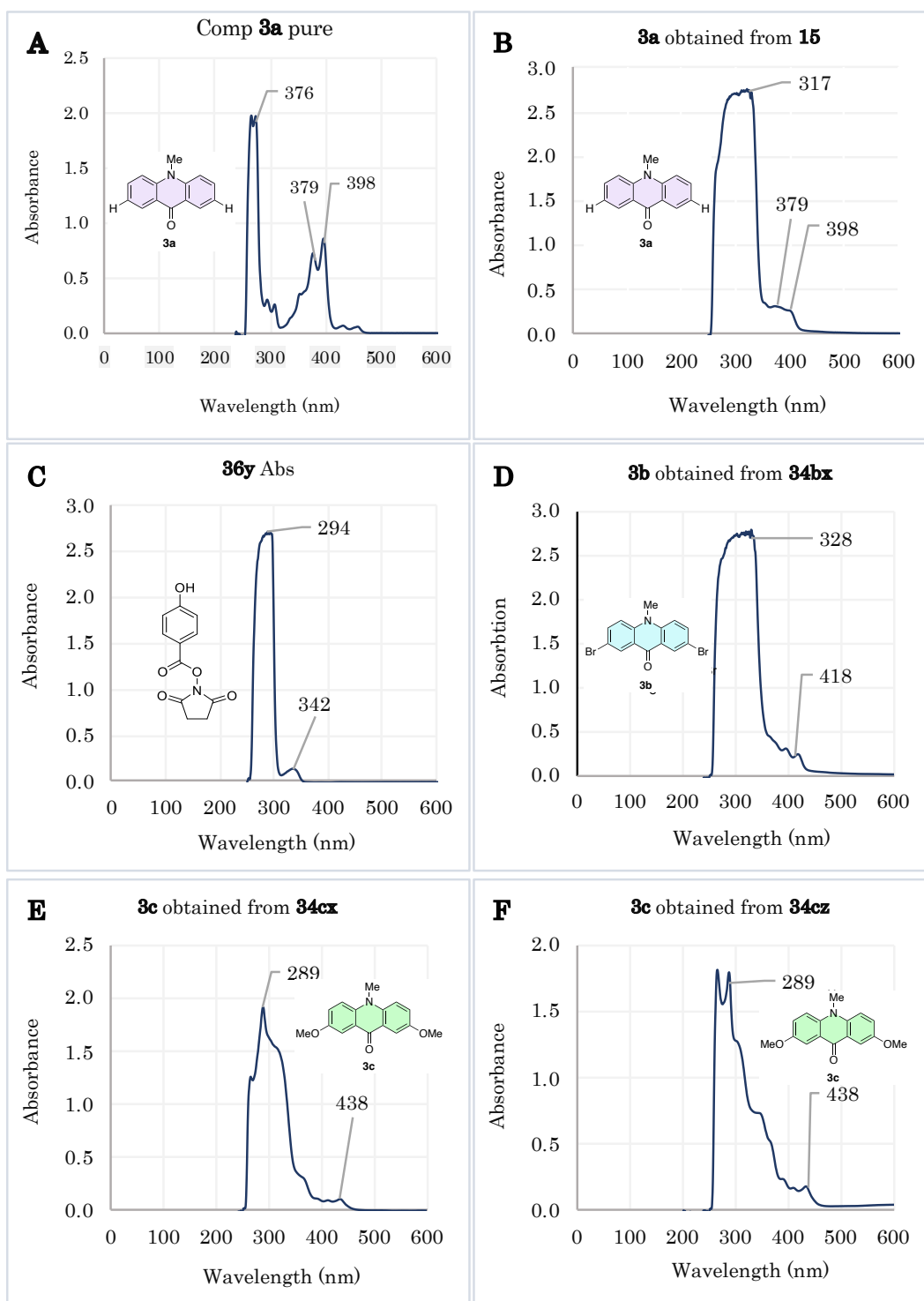
Figure 4. 3: Absorption spectra of acridone derivatives obtained in DMSO/Methanol solution.

4.3.2 Determination of maximal excitation wavelength for emission analysis of acridone derivatives.

A monochromator was used to scan the fluorescence emission between 400-600 nm under a range of excitations at 20 nm intervals across the maximal absorption wavelength (350-410 nm) associated with the series of derived acridones (Figure 4.4). The significant emission was recorded between 380-410 nm excitation for **3a, 3b** and 440 nm excitation for **3c**. Since there was a small Stokes' shift between excitation and emission we recorded the emission spectra starting from 400 nm independent of the excitation wavelength this resulted in incident light from the excitation beam creating an aberrant signal ~20 nm above the excitation wavelength. The excitation of **3a** and **3b** were chosen at 390 nm and 410 nm for **3c**. The maximal wavelength of emission resulting from the compounds investigated was observed at 430, 445 and 480 nm for *N*-methylacridone (**3a**) derived from **34ax** (unsubstituted AE), 2,7-dibromo-10-methyl-9-acridone (**3b**) derived from compounds **34bx**, **34by** and **34bz** and 2,7-dimethoxy-10-methyl-9-acridone (**3c**) derived from compounds **34cx** and **34cz,** independent of the excitation wavelength (indicative spectra are given in Figure 4.4)

The spectra thus generated (Figure 4.4) indicate that the unsubstituted acridones reach a maximal emission when excited at 390 nm whilst the dimethoxy substituted acridone and bromo substituted continue to generate increased yields up to 410 nm. A closer comparison of the emission of dibromo-10-methyl-9-acridone (**3b**) derived from the three-contrasting parent acridinium compounds **34bx**, **34by** and **34bz** (Figure 4.1; Panel B, C & D) reveals subtle differences in yield but comparable spectra.

The emission profile for 2,7-dimethoxy-10-methyl-9-acridone (**3c**) derived from compounds **34cx** and **34cz** exhibited a consisted profile ranging between 440-590 nm with maxima at 480 nm. The amplitude of the **3c**'s emission increased as the excitation

increased from 350 to 410 nm, although the emission associated with the estimated

absorption peak of the acridone 438 nm was not acquired.
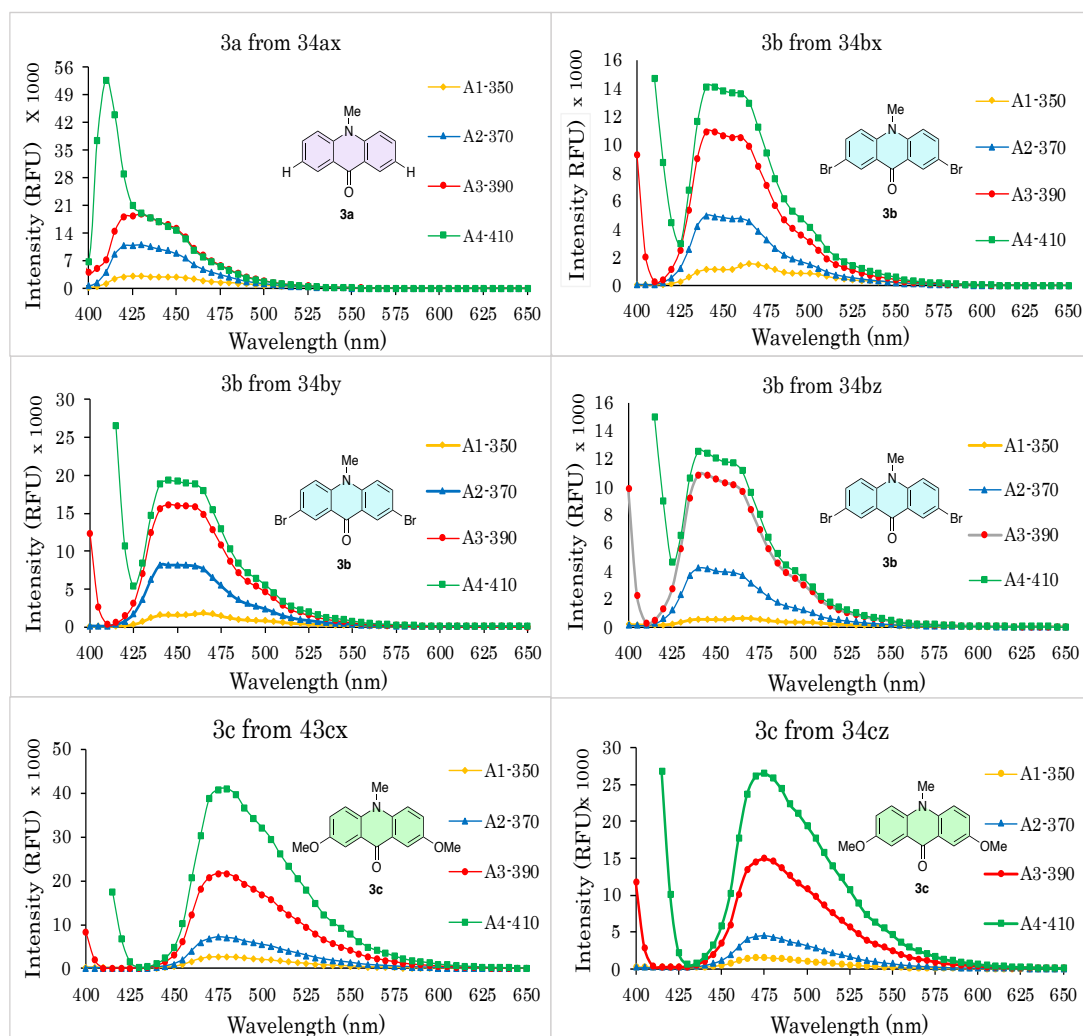
*Figure 4. 4: Optimisation of excitation wavelength. Excitation was performed at wavelengths 350 (yellow line), 370 (blue line), 390 (red line) and 410 nm (green line) and emission was acquired between 350-410 nm for the following compounds: Panel A: 10-methyl-9-acridone short tail (**3a**); Panel B, C and D: 2,7-dibromo-10-methyl-9-acridone (**3b**); and Panel E and F: 2.7-dimethoxy-10-methyl-9-acridone **(3c)***

.

4.3.3   Emission wavelength measurements

To determine the emission profile of acridone derivatives for the five acridinium esters generated (Figure 4.2), a spectrum was derived under the excitation wavelength that generated the maximal emission for each compound and where no interference from incident light was observed (Figure 4.4). Therefore, an excitation of 390 nm was used when studying **3a** and **3b** whilst 410 nm was used when measuring the emission from **3c**. To investigate the influence of the chemical environment on the spectral properties of the acridones, their emission spectra were recorded in a series of solutions from a highly hydrophobic solvent (DMSO) to a hydrophilic solution resulting from the mixture of the hybridisation buffer and detection reagents (R1 and R2) used when stimulating the chemiluminescent reaction in an HPA reaction (Section 4.2.1). The precise composition of these six solutions is provided in Table 4.1 below. In addition, a blank solution was prepared to contain all ingredients except acridone. The emission spectra were recorded over the range of 400-620 nm.

The emission of a commercially supplied unsubstituted *N*-methylacridone (**3a**) equivalent of that generated from compound **15** was measured and used as a reference (data not shown) whilst the same acridone derived from **34ax** yielded an equivalent spectral profile with a maximal emission at 430 nm (Figure 4.5). The emission from the 2,7-dibromo-10-methyl-9-acridone (**3b**) derived from all parent compounds, **34bx, 34by** and **34bz** generated equivalent spectra, with a maximal emission at 445 nm (Figure 4.4; Panel B-D), therefore we used a single compound, 3b derived from **34by**, to investigate emission profile under the different chemical environments (Figure 4.6). Similarly, the 2,7-dimethoxy-10-methyl-9-acridone (**3c**) derived from compound **34cx** or **34cz** showed equivalent emission profiles, with a maximal emission at 480 nm (Figure 4.4; Panels E & F), so we selected a single compound, **3c** derived from **34cx,** to study the impact on

emission on the change in hydrophobicity. For each of the compounds derived from a parent acridinium ester a spectral analysis was performed on the supernatant from the oxidation reaction. These supernatants revealed a negligible quantity of luminescence confirming that the precipitate represented the majority of the acridone.

Table 4. 1: Composition of mixtures used for spectral analysis. The acridones were prepared as described in Section 4.2.1 to yield a concentration of 0.1 mM. The proportion of DMSO solvent to aqueous components (Hyb. Buffer, and detection reagents 1 and 2) was varied to generate samples 1 to 5 in the proportions shown below.

Sample no	A	B	C	D	E
Sample vol (µL).	20	20	20	20	20
DMSO (µL)	180	135	90	45	0
Hyb/R1+R2 (µL)	0	45	90	135	180
Total volume (µL)	200	200	200	200	200
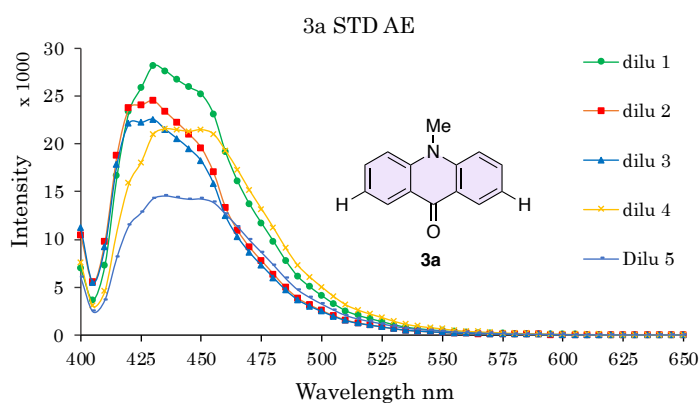
*Figure 4. 5: Emission spectra of N-methyl-9-acridone obtained from compound **34ax** in different proportion of aqueous solution to solvent. The composition solution used to record emission indicated by A-E, is provided in Table 4.1. The compound was excited at 390 nm. Each spectrum shown is an average from 5 independent aliquots acquired over triplicate readings.*

The results in Figure 4.5, 4.6 and 4.7 suggests that the chemical environment has little impact on the maximal wavelength of emission and although variation was observed in the quantum yield of the emission as the chemical environment polarity changed, with a consistent trend that was determined between hydrophobicity and yield.
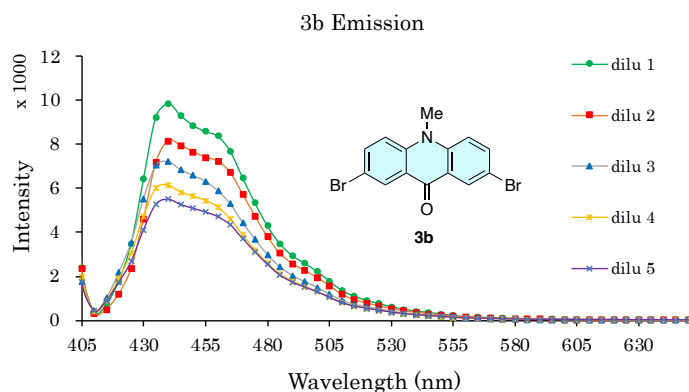
*Figure 4. 6: Emission spectra of 2,7-dibromo-10--methyl-9-acridone obtained from compound **34bx** in different proportion of aqueous solution to solvent. The composition solution used to record emission indicated by A-E, is provided in Table 4.1. The compound was excited at 410 nm. Each spectrum shown is an average from 5 independent aliquots acquired over triplicate readings.*
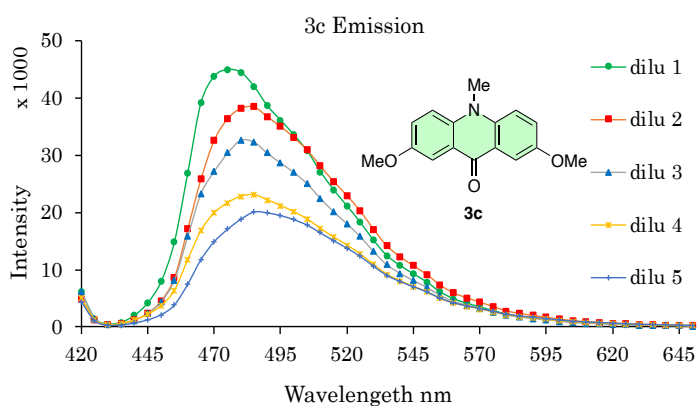
Figure 4. 7: Emission spectra of 2,7-dimethoxy-10--methyl-9-acridone obtained from both compounds 34cx and 34cz in different proportion of aqueous solution to solvent. The composition solution used to record emission indicated by A-E, is provided in Table 4.1. both compounds were excited at 410 nm the maxima emission were recorded at 480 nm. Each spectrum shown is an average from 5 independent aliquots acquired over triplicate readings.

4.4 Results and discussions

The chemiluminescent acridinium ester technology has improved over the years and the factors that affect light emission are starting to be understood including the reaction kinetics, the emission wavelength, and the quantum yield. Generally, the substituents on the acridinium ring have a strong influence on the emission wavelength while any substituent on the phenoxy leaving groups can influence the rate of chemiluminescence reaction. To allow application in clinical assays, it is important to synthesise AE derivatives that have stability in an aqueous solution, the ability to initiate the chemiluminescence reaction and the ideal to display emission maxima that differ by 40 nm, therefore, allowing discrimination between compounds.

Several studies have evaluated the effect of activating groups on various positions of acridinium esters (for details see 4.1.1). For example, in a recent study, Natrajan and his co-workers evaluated the effect of structural features in acridinium esters that led to an increase in the light output; the study concluded maximum light yield was observed with methoxy groups at the C-2 and C-7 position.[144] Also, the placement of electron donating groups at these positions enhances the aqueous solubility of the AE-label leading to lower nonspecific binding.

We have synthesized novel substituted acridinium esters that generate a different spectral profile than that of the unsubstituted acridinium ester, STD-AE (**15**). An experiment was conducted to determine the emission maxima as well as the quantity of the light emitted from a standard amount of acridone (0.01 mM) of the unsubstituted and the two substituted acridones. In summary, the maximal wavelength of emission for *N*-methylacridone (**3a**), 2,7-dibromo-10-methyl-9-acridone (**3b**) and 2,7-dimethoxy-10-methyl-9-acridone (**3c**) were observed at 430, 445 and 480 nm respectively (Figure 4.8).

The wavelength shifts between the STD-AE (**15**) and the 2,7-dibromo-10-methyl-9-acridone (**3b**) are not as significant as that between the 2,7-dimethoxy-10-methyl-9-acridone (**3c**), this is clearly illustrated when a pairwise comparison of the normalised emission spectra is performed (Figure 4.8: Panel A and C). Even given the overlapping spectrum, it should be possible to use a 20 nm bandwidth filter that is centred over the emission maxima of the fluorescence spectra to resolve the signals generated by the modified acridones from that of STD-AE (**15**) (Figure 4.8: Panel D – hypothetical 20 nm bandwidth filters are shown by shaded boxes).
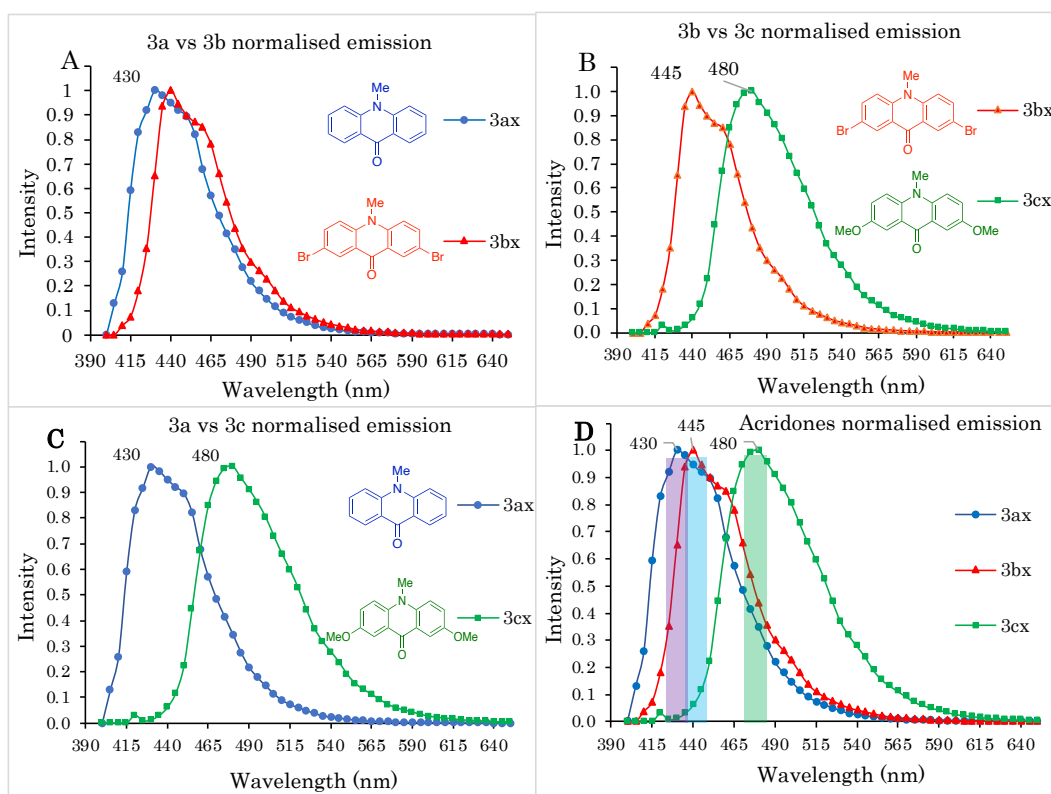
*Figure 4. 8: Comparison of emission spectra, **panel A** shows the N-methyl-9-acridone (3a) vs 2,7-dibromo-10-methyl-9-acridone (3b) at an excitation of 390 nm. Emission **3a** (blue circle) and **3b** (red triangles) are shown together with the wavelength of the maximal emission. **Panel B** shows 2,7-dibromo-10-methyl-9-acridone (3b) vs 2,7-dimethoxy-10-methyl-9-acridone (3c) at an excitation of 390 nm and 410 nm respectively. Emission **3b** (red triangles) and **3c** (green square) are shown together with the wavelength of the maximal emission. **Panel C** shows the N-methyl-9-acridone (3a) vs 2,7-dimethoxy-10-methyl-9-acridone (3c) at an excitation of 390 nm and 410 nm respectively. **Panel D** shows all acridone derivatives emissions together (3a, 3b and 3c) with a wavelength of the maximal emission.*

Although overlapping between the STD-AE (**15**) and 2,7-dibromo-10-methyl-9-acridone, (**3b**) it would be theoretically feasible to separate the signal of the 2,7-dibromo-10-methyl-9-acridone from STD-AE (**15**) would provide a basis for a dual analyte assay.

An evaluation of the profiles presented in Figure 4.5-4.7 enables the emission of the modified acridones to be compared in various media, differing in terms of the ratio of aqueous buffer to solvent (DMSO). These exhibited very similar spectra concerning the wavelength of emission; however, a consistent relationship between the chemical environment and quantum yield was evidence showing increased light output as the proportion of hydrophobic solvent (DMSO) increased. This relation was maintained for all compounds tested (Figures 4.5-4.7).

The data collected by fluorimetry indicates that the *N*-methylacridone (**3a**) and 2,7-dimethoxy-10-methyl-9-acridone (**3c**) have much higher emission light yield than the 2,7-dibromo-10-methyl-9-acridone (**3b**). A summary is given in Table 4.2. The light intensity of **3b** measured in this experiment was only 10.6% of that generated by **3a**. This may reflect the structure of the compound as the methylation of bromo compounds gives rise to a pseudobase which may hinder the chemiluminescence reaction.

Table 4. 2: *Fluorescence intensity of acridone derivatives, the maxima wavelength emission at the maxima excitation at 0.01 mM concentration. Such that, 3a is N-methylacridone, 3b is the 2,7-dibromo-10-methyl-9-acridone and 3c is the 2,7-dimethoxy-10-methyl-9-acridone*

Compound	Conc. mM	Ex. (nm)	Em (nm)	Intensity
STD-Ac 3a	0.01	390	430	50,065
Compound 3a	0.01	390	430	31,100
Compound 3b	0.01	410	445	10,947
Compound 3c	0.01	410	480	46,698

Initial characterisation of the chemiluminescent light emission obtained from acridones generated from the dibromo series of acridinium esters was markedly lower when compared with those generated from STD-AE which we hypothesised is due to the quantity of pseudobase present in the dibromo acridinium esters (Chapter 3). A range of acidic environments was tested to promote the conversion of the pseudobase to the acridinium ester form prior to oxidization resulting in the optimised conditions employed for the conversion to the acridone (Section 4.3.1). This enabled the effective conversion of dibromo acridinium ester pseudobase and enabled photoluminescent measurement of the acridone (data not shown).

In summary, the emission spectra profile of 2,7-dibromo-10-methyl-9-acridone (**3b**) shows a slight shift in wavelength by only 10 nm toward the red/ blue region, compared with the result obtained from unsubstituted acridone (**3a**) which had a maximal emission of 445 nm. The emission profile of 2,7-dimethoxy-10-methyl-9-acridone (**3c**) showed a significant red shift by ~50 nm toward the green emission region centred at 480 nm. In conclusion, functionalization of the acridinium ring plays a major effect on the chemiluminescent properties due to the severe steric hindrance of the donating or withdrawing group on position C-2, C-7 of the acridinium ring.

Chapter 5

Application of acridinium esters (AE) in DNA diagnostics

5 Application of acridinium esters (AE) in DNA diagnostics

5.1 Introduction

Several reviews clearly describe the advantages of acridinium esters (AE), particularly their high quantum efficiency, a wide linear dynamic range which can be achieved in a simple instrument, and the fact that they do not need a catalyst for the oxidation process. [61,127,144–146] These advantages are exploited for use in number of formats for clinical applications. The most common applications involve the use of AE as a 'marker' or 'label' for antibodies or DNA oligonucleotides, forming the backbone of assays designed to quantitatively measure clinically relevant endpoints such as RNA, DNA or protein.[11,80,93]

The acridinium esters have been used extensively as endpoint labels in ligand binding assays, such as immunoassay and nucleic acid hybridisation assays.[11,93,147,148] The initial study of the application of acridinium esters as labels in immunoassay was reported by Simpson.[78] AE-based chemiluminescence has become the main clinical and immunological analysis approach due to its wide dynamic range, high sensitivity, and low background.[84,149] Another common application of AE was based on labelling DNA oligonucleotides to form 'probes' used in clinical assays to quantify RNA or DNA targets.

The methodology of the nucleic acid-based assays can be broadly classified as heterogeneous or homogeneous. The heterogeneous assay depends on the physical separation of hybridised probes from the unhybridised probe. In the homogeneous hybridisation assay, hybridised and unhybridised probes exhibit distinct properties that make the separation unnecessary.

For example, in one version of these heterogeneous methods, Smith *et al.* [94] used cationic magnetic microspheres to capture the hybridised AE Probe collecting the solid

obtained on the side of the tube after the application of a magnetic field. At the same time, the removal of the solution also removed the unhybridised AE probe. An example of a homogenous assay format, Arnold, and his co-workers[11] developed a method for discriminating the hybridised probe from an unhybridised probe by using a chemical hydrolysis reaction without any physical separation step; the simple approach is entirely performed in solution and is based on chemical hydrolysis of the ester bond of the AE molecule. They found that the cleavage of the AE rendered it permanently non-chemiluminescent, and they developed a method by controlling the reaction conditions under which the hydrolysis of the ester bond is rapid for the unhybridised AE probe but slow for the hybridised AE probe (differential hydrolysis). Stopping the reaction at a specific time by rapidly lowering the temperature allows a significant signal to noise ratio, with only a small amount of the measured chemiluminescence coming from the unbound probe. This format was called the 'Hybridisation Protection Assay' (HPA) and is an important development in AE labelled DNA probe-based assays. The method takes place in solution, without a physical separation step and exploits chemical differences between the hybridised and unhybridised probe and target sequence. Initially, it was used to measure ribosomal RNA but has been adapted and expanded to measure messenger RNA [57,120,150] HPA is a detection methodology that can be adapted to detect virtually any target nucleic acid, provided the sequence is known.

In the HPA format, an oligonucleotide, with the reverse complement sequence to the target of interest, is labelled via an internal non-nucleotide linker with acridinium ester to form the probe, HPLC purified and then combined with the sample of interest. One of two possible options occurs (Figure 5.1): if the specific target is present, the probe will hybridise and form a protective double helix as the planar section of the AE will intercalate into the minor groove.[151] If there is no target present in the sample, the probe cannot bind,

leaving the AE unprotected. After the hybridisation step, a selective chemical reagent is used to eliminate any unprotected AE via a hydrolysis reaction that irreversibly destroys the chemiluminescent marker, which can no longer emit light during the next step of the assay. The remaining AE molecules, protected by the double helix environment, emit light measured by a luminometer. This is the basis of the quantitative measurement; as the amount of hybridised probe increases, the amount of protected AE molecule increases, and so the amount of light generated with the addition of the detection reagents increases. The hydrolysis step is critical to ensuring accurate results and reducing the risk of false positives. It allows the HPA to distinguish between targets that differ by only one nucleotide. It does not require an amplification step or the need for catalysts and allows the assay to be performed in a single tube or well, making it rapid and easy to perform. Using the HPA format, target sequences of 10^{-16} mole or less can be measured quickly and accurately.

In this chapter, the properties of acridinium derivatives containing electron donating and/or withdrawing groups were characterised by labelling a DNA oligonucleotide with the modified AE molecules (compounds **15**, **34ax**, **34bx**, **34cx**) that were synthesised, purified, and characterised as described in the previous chapters. The oligonucleotide chosen for this study was based on an earlier study by Nelson [88] that looked at the ability of HPA technology to distinguish between two targets with only a single base pair difference using standard AE whilst still retaining the homogenous format. This study aimed to use this characterised system to determine if the novel AE derivatives synthesised and described in earlier chapters had the required properties to be the basis of an HPA assay.

1- Hybridization   **2- Differential Hydrolysis**   **3- Detection**
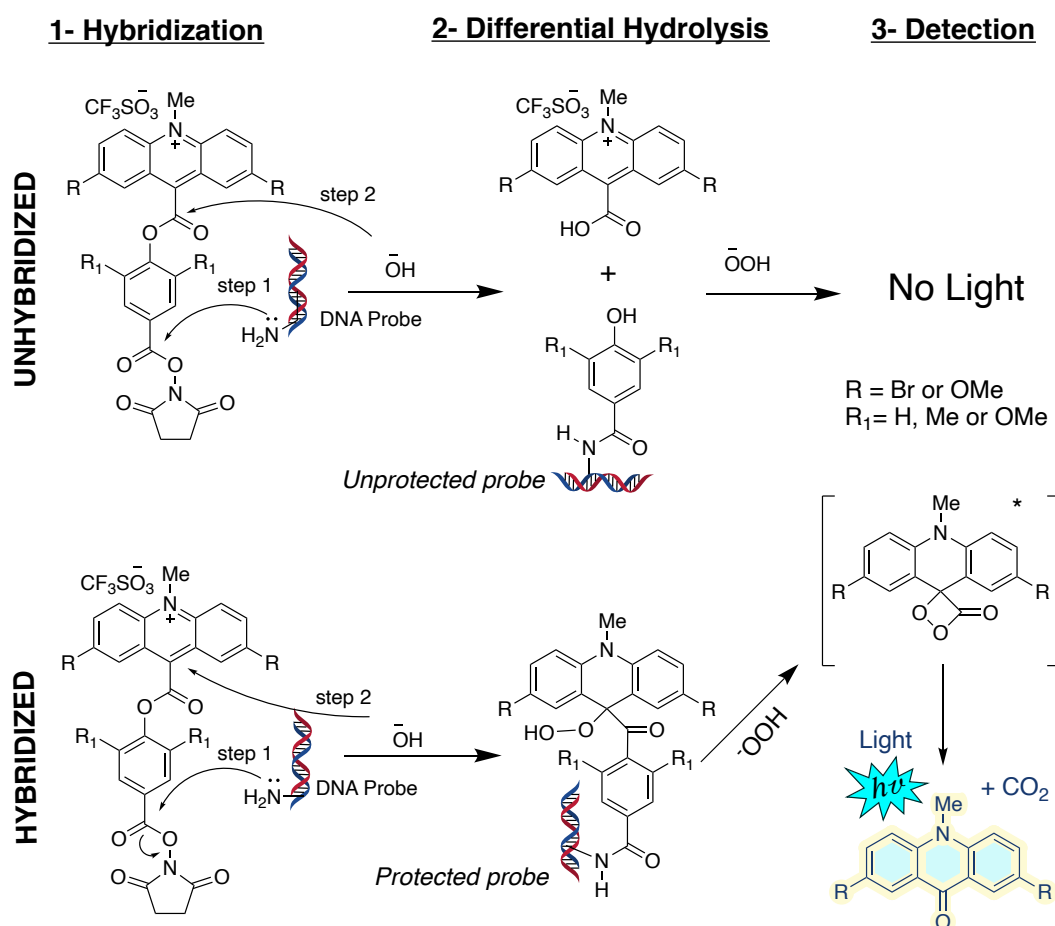
Figure 5. 1: Depiction of the three basic steps of the HPA assay. In step 1, the AE probe is hybridised with its specific nucleic acid target. In step 2, the unhybridised AE probe is rapidly hydrolysed, while the hybridised AE is protected from hydrolysis. Finally, in step 3, the AE associated with the hybridised probe produces chemiluminescence. In contrast, the AE associated with an unhybridised probe cannot generate light (adapted from Nelson et al., 1996).

5.2 Material and Methods

5.2.1 Materials

The sequences of both the modified oligonucleotide and its reverse complementary sequences are shown in Table 5.1. The modified DNA oligonucleotide (HIV-WT) was synthesised and HPLC purified by Integrated DNA Technologies (IDT, Coralville, IA, USA) with a non-nucleotide, amine-terminated linker in a central position within the

160

oligonucleotide. This provided an attachment site for a chemiluminescent acridinium ester. (# indicates the position of the linker). The unmodified oligonucleotide (HIV-WT Target) was synthesised and HPLC purified by Eurofins MWG Operon (Ebersberg, Germany).

Table 5. 1: HIV oligonucleotide sequence used for AE-labelling (HIV-WT) and of the reverse complementary sequence of the target.

NAME	SEQUENCE
HIV-WT	5'CAT CCA TGT ATT GAT # AGA TAA CTA TGT CTG G3'
HIV WT TARGET	5' CCA GAC ATA GTT ATC TAT CAA TAC ATG GAT G3'

5.2.2   Labelling of DNA oligonucleotides to AE.

The HIV-WT oligonucleotide was resuspended in HEPES (0.125 M, pH 8.0) to a concentration of 100 pmol/μL. A 50 mM (3.32 mg) stock solution of NHS-modified-AE (compounds; **34ax**, **34bx**, and **34cx**) was prepared in anhydrous DMSO (100 μL) each. Labelling of HIV-WT oligonucleotide with NHS-modified-AEs (Figure 5.2) was made for all compounds using the same route, initiated by adding 10 nmol of oligonucleotide (10 μL) to 5 mM of acridinium ester (10 uL) in a centrifuge tube; the tube was capped, and the mixture was centrifuged briefly in a microcentrifuge (to bring the contents to the bottom of the tube), then incubated in a water bath at 37ºC for 20 minutes. The excess of *N*-hydroxysuccinimide ester on the AE was deactivated by adding lysine (5 μL, 0.125 M in HEPES buffer, pH 8) in an ice slurry. The mixture was purified by precipitation by adding sodium acetate buffer (30 μL, 3 M, pH 5), water (240 μL) and glycogen (20 mg/mL, 10 μL) as an inert carrier.   The mixture was vortexed briefly, and then chilled absolute ethanol (640 μL) was added. The mixture was vortexed briefly and put at -70˚C for 10- 20 minutes, followed by centrifugation at 13,500 rpm at 0˚C for 10 minutes to pellet the nucleic acid.

Then, the supernatant was aspirated, and the pellet was washed with ethanol (400 μL, 70%) and centrifuged at 13,500 rpm at 0˚C for 5 minutes. The labelled probe was separated from the unlabelled probe and breakdown products using gradient elution ion-exchange HPLC chromatography (IE-HPLC), a 4.0 x 125 mm Nucleogen-DEAD 60-7 column pre-equilibrated with 75% of Buffer A (20 mM potassium dihydrogen phosphate (pH 7.0), 20% (*v/v*) acetonitrile) and 25% of Buffer B (20 mM potassium dihydrogen phosphate (pH 7.0), 20% (*v/v*) acetonitrile, 0.1 M potassium chloride) at a flow rate of 1.0 mL/min.

A mixture of Buffer A (60 μL) and Buffer B (20 μL) was added to 20 μL of resuspended pellet in storage buffer reagent (0.1 M sodium acetate buffer, pH 5.0, containing 0.1% SDS; *w/v* 20 μL) and vortexed to mix. An amount (10-20 μL) of the sample was loaded onto the column via the HPLC injector using an autosampler; the sample was eluted with a linear gradient from 25 to 80% Buffer B over 25 min at a flow rate of 1.0 mL/min. UV absorbance was monitored at a wavelength of 260 nm, and 0.5 mL fractions were collected into centrifugation tubes (1.5 mL) containing aqueous sodium dodecyl sulfate (SDS; 5 μL of 10%; *w/v*).
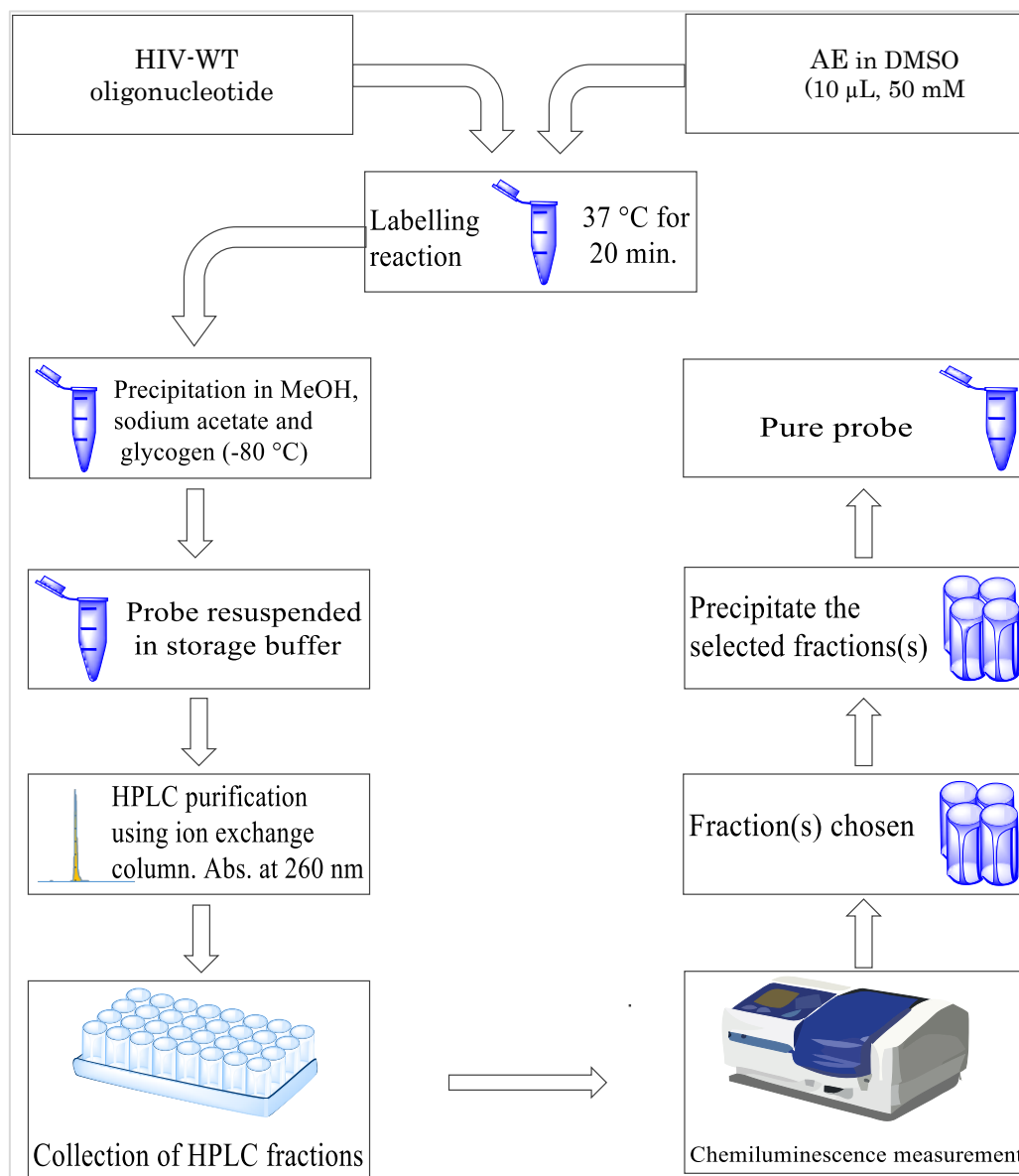
Figure 5. 2: Steps involved in labelling the DNA oligonucleotide with AE (1) Mixing excess AE with oligonucleotide and incubating for 20 min. (2) Precipitation of the nucleic acid (3) pellet resuspension. (4) Purifying the AE-labelled probe using an ion-exchange HPLC column and measuring the absorbance at 260 nm. (5) collection of HPLC fractions. (6) Testing the fractions collected for chemiluminescence (7) choosing the highest chemiluminescence signals fractions. (8) Precipitation of the chosen fraction(s) to give (9) the pure probe.

The fractions were collected over 15 min and measured with a luminometer to choose the highest chemiluminescence yield. First, fractions were selected based on containing both peaks of absorbance at 260 nm and chemiluminescence which demonstrated both the presence of nucleic acid and AE; this was found generally through the period 5.5 –7.0 mins (fractions 10, 11, and 12). Next, these fractions were precipitated and pooled, as described in section 5.2.4. Figure 5.3 shows an example of an absorbance profile at 260 nm, confirming nucleic acid's presence in the corresponding fractions.
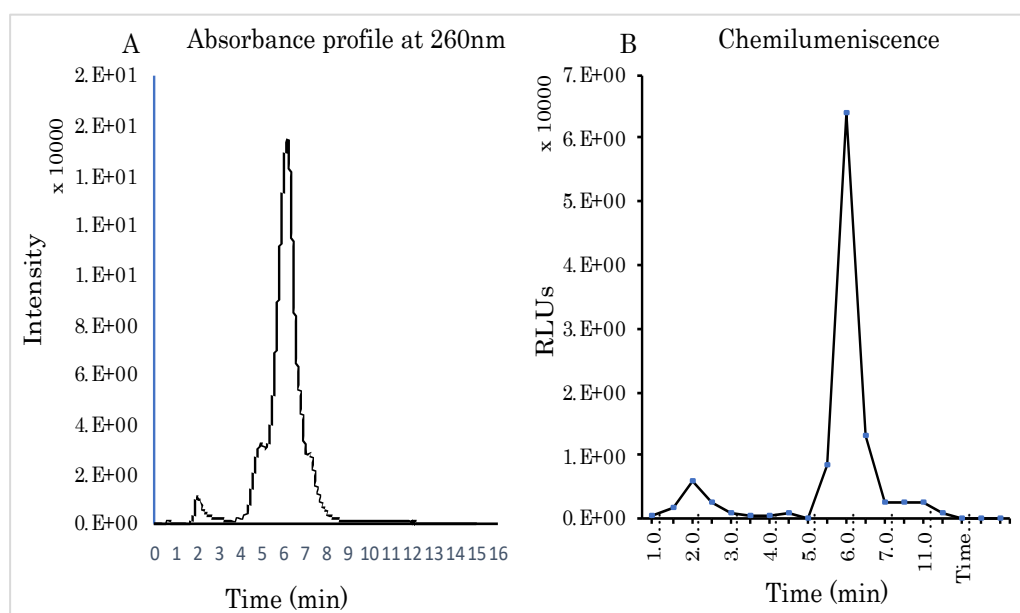
*Figure 5. 3: A typical example of the absorbance profile at 260 nm (A) and the associated chemiluminescence (B) of the collected fractions (section 5.2.4). Panel A shows the purification of the labelling reaction of HIV-WT oligonucleotide and **34cx** using ion exchange HPLC. The resultant profile presents a peak with two shoulders as described previously by Nelson et al. (1995): an unlabelled probe at 4.80 minutes (left), AE-labelled probe at 6.20 minutes (middle) and a peak at 7.3 minutes (right) consisting of the AE-probe after ester hydrolysis. Panel B: a high peak of chemiluminescence is measured in fractions (10, 11 and 12). The presence of nucleic acid, as detected by absorbance at 260 nm together with the high peak of chemiluminescence in fraction 6 indicates the presence of the labelled AE-probe.*

5.2.3   Measurement of chemiluminescence

The chemiluminescence signal for each fraction was measured in a LEADER 50i luminometer (Gen-Probe, San Diego, USA). Briefly, an aliquot (1 µl) of each fraction was added to aqueous SDS solution (100 µL of 0.1%; *w/v*), and then 1 µl was transferred into a 12 x 75 mm polystyrene tube. The chemiluminescence was measured in the luminometer using an automatic injection of 200 µL of Detection Reagent 1 (R1, 0.032 M hydrogen peroxide, 1 mM nitric acid) followed by 200 µl of Detection Reagent (R2, 1.5 M sodium hydroxide). The light output was integrated over 10 s. time intervals and data are expressed as Relative Light Units (RLU).

5.2.4   AE-probe precipitation

The fractions were collected separately in centrifugation tubes (1.5 mL) and precipitated by adding aqueous sodium acetate buffer (30 µL, 3 M, pH 5.0), glycogen (10 µL, 20 mg/mL), 240 µL nuclease-free water and 640 µL chilled 100% ethanol. The mixture was subjected to cooling at −70ºC for 10-20 min, then centrifuged at 14,000 rpm at 0ºC for 10 min using a Beckman Coulter Allegra 21R Centrifuge with the F2402H Rotor. Under these conditions, the nucleic acid precipitates as a pellet bringing any attached AE with it. Next, the supernatant was removed from the pellet. Finally, the probe storage buffer (20 µL, 0.1 M sodium acetate, pH 5, containing 0.1% sodium dodecyl sulphate, (SDS; *w/v*) was added to the pellet, the pellet resuspended and stored at -20ºC.

5.2.5   Chemiluminescence kinetic profile

Kinetic profiles, i.e. chemiluminescence intensity versus time, were recorded using a Tristar plate luminometer (Berthold Technologies UK, Harpenden, UK). Stock solutions

of labelled AE probes were diluted to a final concentration of 0.2 pmol / µL in a hybridisation buffer. Aliquots (2 µL) of these dilutions in triplicate were placed in a white hard shell 96-well microplate (Berthold Technologies UK, Harpenden, UK). To trigger the chemiluminescence reaction, detection Reagent 1 (200 µL) was injected, followed by Detection Reagent 2 (200 µL) after a 1 second delay (0.5 second delay, followed by 0.5 second shake). The chemiluminescence intensity in Relative Light Units (RLU) was obtained over 5 seconds. The intensity values obtained were normalised to the maximum value obtained from each compound. (Figure 5.4).

5.2.6 Differential hydrolysis experiments

A desired dilution of the probe was prepared (1 pmole/µL). Two replicates (1 µL each) of probe dilution were transferred to a 12 x 75 polystyrene tube to confirm the RLUs before continuation of the experiment. The chemiluminescence was measured in a luminometer, as described in Section 5.2.2. The experiment was established by combining the components in a 1.5 mL microcentrifuge tube, as shown in Table 5.2 below. The three reactions were as follows: "Hybrid" reaction consisted of AE-probe, which would hybridise with the complementary target oligo present; "Control" reactions contained AE-probe but no target with which to hybridise; and "Blank" reactions contained target but no AE-probe. The hybrid mixture, control mixture, and the blank were vortexed to mix and then incubated in a circulating water bath at 60˚C for 30 min; each reaction was diluted by adding 300 µL of hybridisation buffer (0.1 M lithium succinate, 2 mM EDTA, 2 M EGTA, 10% lithium dodecyl sulphate, pH 5.2).

Table 5. 2: Preparation of three reactions were prepared: "Hybrid" reaction that consisted of AE-probe, which would hybridise with the complementary target oligo present, "Control" reaction, which contained AE-probe but no target with which to hybridise; and the "Blank" reaction contained target but no AE-probe.

	Conc. (pmol/µL)	Hybrid (µL)	Control (µL)	Blank (µL)
Hybridization Buffer	-	15	15	15
AE-probe	0.1	5	5	0
Target	1.0	10	0	10
H2O	-	0	10	5
Final	-	30	30	30
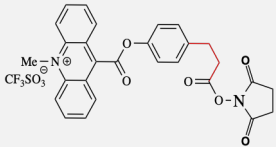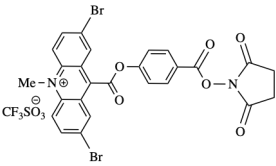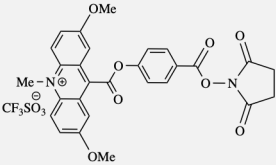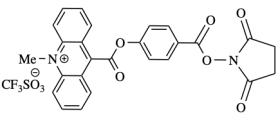
The experimental time points were prepared by pipetting an aliquot (10 µL) in duplicate from each reaction mixture described in Table 5.2 into a 12 x 75 mm polystyrene Sarstedt tube for each time point, i.e. 22 for each reaction. Hydrolysis Buffer (100 µL of 150 mM sodium tetraborate, 5% Triton X102 (*v/v*)) of varying pH (pH 8.5, 9.2, 9.4, 9.6, 9.8 and 10) was added to each tube, and the reactions were transferred to a circulated water bath at 60°C before being removed at the desired time points (1, 2, 3, 4, 5, 10, 20, 30, 40, 50 and 60 min) and placed in an ice bath to stop the hydrolysis reaction. An additional pair of duplicate tubes were prepared as the time zero (T_0) control for the hybrid, control and blank reactions; these were read immediately after the addition of the hydrolysis buffer (i.e. not placed in the water bath). The chemiluminescence of each reaction was measured by injecting Detection Reagent 1 followed by Detection Reagent 2 and measuring the emitted light for 5 seconds using the Leader 50i luminometer.

5.3 Results

5.3.1 The specific activity of the AE-labelled probes

All AE compounds were synthesised as described in Chapter 3, with the exception of STD-AE (**15**), which was sourced from CatCelt (Swansea, UK). This compound was included as a control measurement as it is the most often used in clinical diagnostic assays. The HIV-WT DNA oligonucleotide was labelled with four different AE compounds (**15, 34ax, 34bx, 34cx**) (Table 5.3). The labelled probes were purified using ion exchange HPLC as described in sections 5.2.2, 5.2.3 and 5.2.4 to generate AE-probes.

Table 5. 3: List of modified AEs used to label the HIV-WT DNA oligonucleotide: the structure of each AE, its associated acronym, plus the section in Chapter 3 which describes its synthesis.

Acronym	Structure of AE.	Chapter 3
STD-AE (15)		N/A
34bx		3.1
34cx		3.2
34ax		3.3

For each purified AE-probe, the nucleic acid concentration was estimated by measuring the absorbance at 260 nm with a Nanodrop spectrophotometer as described in Chapter 2 (section 2.2.5) and converted to pmol/µL using the following equation:

$$pmol\ (DNA) = \mu g\ (DNA) * \frac{pmol}{660\ pg} * \frac{10^6\ pg}{1\ \mu g} * \frac{1}{N}$$

N is the number of nucleotides (in kb), 660 pg/pmol is the average molecular weight of the nucleotide pair.

The chemiluminescence per µL of the undiluted probe was measured as described in section 5.2.3. Table 5.4 gives a summary of the efficacy of the probe labelling for each experiment. In general, 1 pmol of the probe was labelled with >1 x 10^6 RLU, which gives a specific activity of >1 x 10^6 RLU/pmole.

Table 5. 4: Summary of the properties of the AE-labelled probes. RLU denotes Relative Light Units

AE-probe	pmole/ µl	Volume (µl)	RLU *10^6	Specific Activity (RLU/pmol)* 10^6
HIV-WT-STD-(15)	0.10	1	0.92	9.2
HIV-WT-34ax	0.10	1	1.03	10.30
HIV-WT-34cx	0.10	1	3.76	37.6
HIV-WT-34bx	0.10	1	0.185	1.85

5.3.2 Kinetic profiles

Kinetic profiles, i.e. chemiluminescence intensity measured over time, were recorded using a Tristar plate luminometer as described in section 5.2.5 and Chapter 2. Stock solutions of three labelled AE probes, HIV-WT-**34ax**, HIV-WT-**34bx**, and HIV-WT-**34cx,** were diluted to a final concentration of 0.2 pmol / μL in hybridisation buffer and the light output from triplicates (2 μL) was measured for 5 seconds at 0.1 second intervals. Kinetic profiles are normalised to the maximum light reading for each AE (Figure 5.4).

The dilutions of each acridinium ester probe in the hybridisation reagent were used for chemiluminescence measurements, and the hybridisation reagent (containing no AE probe) was used to determine the presence of any background readings and the measurement of chemiluminescence in triplicate was taken place to obtain the average. The average of these background values was calculated and subtracted from the average of the chemiluminescent values. Finally, the results were drawn as a kinetic curve to represent the relative time over which chemiluminescence is emitted during the chemiluminescent reaction for the three different AE probes tested (Figure 5.4).

The kinetic curves show a difference in the speed with which the majority of light is emitted from the three probes tested. The probe labelled with **34ax** generated the majority of its light within the first 0.3 seconds with the peak intensity at 0.1 s, whereas the HIV-WT-**34bx** and HIV-WT-**34cx** probes were relatively slower, with the majority of their light output being over the first 0.5 seconds with the peak of intensity at 0.2 and 0.3 s respectively after the chemiluminescent reaction is triggered. The dibromo- and methoxy-substituted probes had similar kinetic outputs with broader peaks; the HIV-WT-**34bx** probe was only marginally faster. However, the light output was faster for all three probes than that previously reported for compound **15,** where the peak intensity of the flash was at 0.5 s.

However, the significant overlap between the 3 AE probes tested suggests it would be difficult to resolve the individual signals in a multiplexed assay based on this parameter.
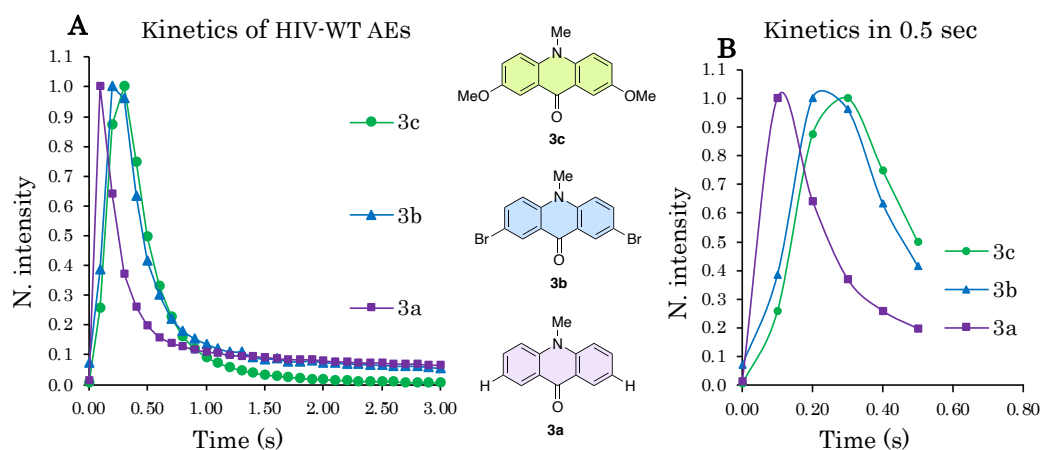
Figure 5. 4: Kinetic profiles collected over 5 seconds for HIV-WT-AE probes diluted in hybridisation buffer. Chemiluminescence was triggered using H₂O₂/NaOH, as described in Section 5.2.5. Kinetic profiles are normalised to the maximum light reading for each AE Panel A and Panel B shows the same data over 5 and 0.5 seconds, respectively.

5.3.3   Differential hydrolysis of HIV-34cx-labelling probe.

The hybridisation protection assay (HPA) was carried out as described (Arnold et al., 1989) with acridinium-ester-labelled DNA probes, which are added to a solution containing the target nucleic acid, and the mixture is incubated. The length of time required for this step is dependent on many factors, including temperature, buffer and hydrolysis conditions, the kinetics of the particular probe used, the concentration of the hybridising nucleic acid strands, i.e. the hydrolysis time that can minimise the background RLU emitted from the unhybridised or 'free' probe while not diminishing the signal from the probe that has hybridised to target therefore maximising the signal to noise ratio.

The HIV-WT-**34cx** probe was chosen for further investigation based on previous results, as its wavelength shift and good quantum yield suggested it may have advantages from the perspective of the HPA format. The HIV-WT-**34cx** probe was evaluated in an adaptation of the hybridisation protection assay format, which has a hydrolysis step based on selective chemical degradation of the unhybridised probe. In summary, the HIV-WT-**34cx** probe was tested in the presence and absence of its complementary single-stranded target, and during the hydrolysis step, the chemiluminescence associated with the unhybridised probe should be lost in a few minutes by the chemical environment provided by the hydrolysis reagents while the chemiluminescence associated with hybridised probe should be minimally affected. The difference between the chemiluminescence associated with the unhybridised and hybridised probe is known as the 'differential hydrolysis ratio. Initial results suggested that the HIV-WT-**34cx** probe was resistant to hydrolysis under conditions routinely used for the probes labelled with **15** (i.e. 15 -20 minutes hydrolysis at pH 7.5 to 8.5. The stability of hybridised versus unhybridised probes was tested using a Hydrolysis Buffer adjusted to a range of different pH (pH 8.5, 9.2, 9.4, 9.6, 9.8 and 10.0) as described in 5.2.6. The chemiluminescence measurement was obtained for each pH point by automatic injection of Detection Reagent 1 followed by Detection Reagent 2, as described in section 5.2.6. As expected from the preliminary results, both the hybridised and the unhybridised HIV-WT-**34cx** probe were relatively resistant to hydrolysis at pH 8.5 (Figure 5.6, Panel C and D). In particular, the rate of hydrolysis of the unhybridised probe, as shown by the gradient of the slope of -0.66, is slow compared to the rate of hydrolysis of the unhybridised STD-AE probe (HIV-**15**), which had a gradient of -0.0187 (Table 5.5). In an HPA assay, this would translate to considerable chemiluminescence remaining from the unhybridised probe even after 60 minutes at 60ºC and a low signal to noise ratio. As the pH increased, the hybridised probe remained resistant to hydrolysis when subjected to

a Hydrolysis Reagent of pH 8.5, 9.2, 9.4 and 9.6, as shown by the stable gradients of -0.0015, -0.0019, -0.0051 and -0.0044 respectively (Table 5.5), presumably due to protection from the formation of a DNA:DNA hybrid. Only when the pH reaches 9.8 does the AE associated with the hybridised probe start to decrease more rapidly, evidenced by a steeper slope of -0.032. At pH 10.0, this is significant with a gradient of -0.114, and the rate of hydrolysis of the hybridised is approaching that of the unhybridised probe (-0.199). After 20 minutes of hydrolysis at pH 10, there is little chemiluminescence signal remaining from the hybridised HIV-**34cx** probe. For the HPA format to be effective, there needs to be a rapid rate of hydrolysis of the unhybridised probe while the chemiluminescent signal for the hybridised probe stays stable during the time of the hydrolysis step. This experiment suggests there is a window of pH values over which this is the case: pH 9.2, 9.4 and 9.6. During hydrolysis at these pH values, the rate of hydrolysis of the unhybridised probe increases slowly from -0.0187 at pH 8.5 to -0.031, -0.051 and -0.063 (Table 5.5), while the rate of hydrolysis of the hybridised probe remains relatively stable. This suggests that it could be possible to use the HIV-**34cx** probe in an HPA format with hydrolysis conditions of pH 9.2-9.6 for 60 minutes at 60°C.
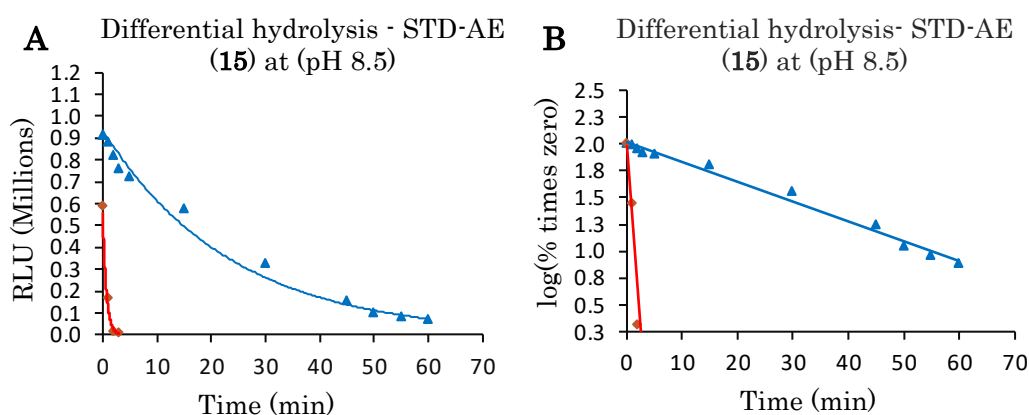
*Figure 5. 5: Rate of hydrolysis curve for the hybridised (blue) and unhybridised (red) HIV-WT-**15** probe at pH 8.5. Panel A shows the RLU values plotted against time (minutes). Panel B shows the log of a percentage of time zero chemiluminescence versus time (minutes).*

C — Differential hydrolysis (**34cx**) at (pH 8.5)

D — Differential hydrolysis (**34cx**) at (pH 8.5)

E — Differential hydrolysis (**34cx**) at (pH 9.2)

F — Differential hydrolysis (**34cx**) at (pH 9.2)

G — Differential hydrolysis (**34cx**) at (pH 9.4)

H — Differential hydrolysis (**34cx**) at (pH 9.4)

I — Differential hydrolysis (**34cx**) at (pH 9.6)

J — Differential hydrolysis (**34cx**) at (pH 9.6)
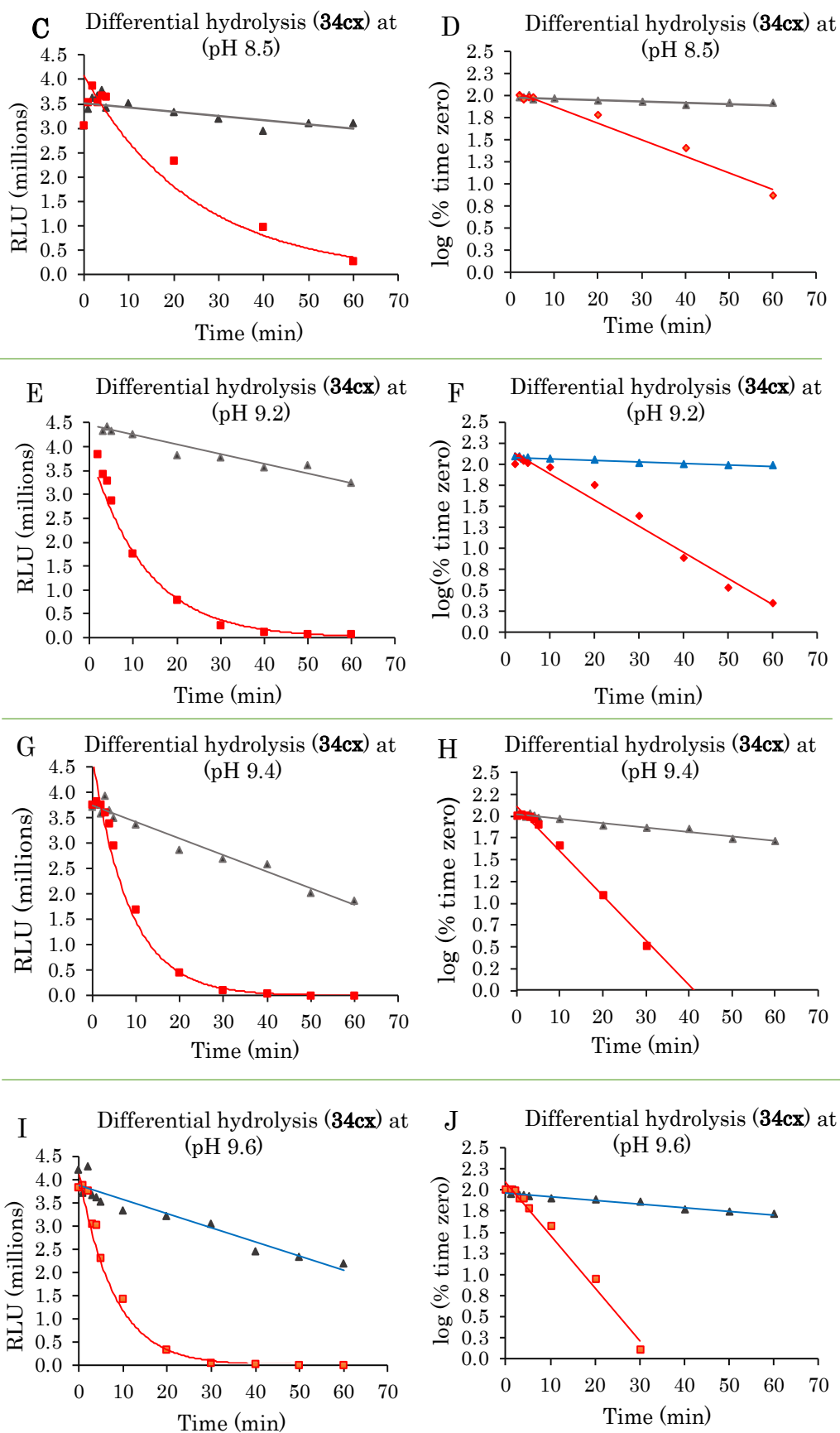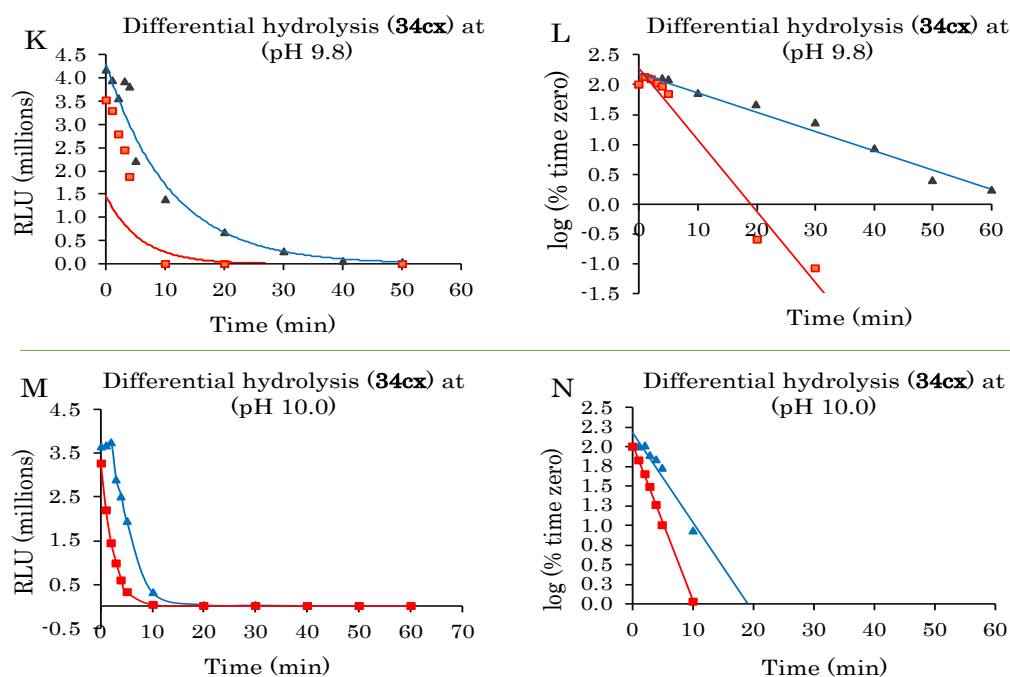
Figure 5. 6: Rate of hydrolysis curves for the hybridised (blue) and unhybridised (red) HIV-WT-34cx probe at pH 8.5, 9.2, and 9.4. 9.6, 9.8 and 10.0. Panels, C, E, G, I, K, M and O show the RLU values plotted against time (minutes). Panels D, F, H, J, L and N show the log of a percentage of time zero chemiluminescence versus time (minutes).

Table 5. 5: Summary of the hydrolysis characteristics of HIV-WT-STD-AE (15) with Hydrolysis reagent at pH 8.5 and HIV-WT-34cx over a range of pH values.

Probe	pH	R2 (Hyb)	R2 (Unhyb)	Gradient (log/min) (Hyb)	Gradient (log/min) (Unhyb)
HIV-WT-15	8.5	0.989	0.929	-0.018	-0.661
	8.5	0.779	0.977	-0.0015	-0.0187
	9.2	0.93	0.989	-0.0019	-0.031
HIV-WT-34cx	9.4	0.975	0.993	-0.0051	-0.051
	9.6	0.933	0.987	-0.0044	-0.0631
	9.8	0.98	0.966	-0.0322	-0.1195
	10.0	0.979	0.998	-0.1143	-0.1991

5.4 Discussion

The rate of hydrolysis is an essential component of the HPA format, as this step determines the discrimination between the hybridised and unhybridised probe by degrading the latter. The rate of hydrolysis of the HIV-**34cx** probe, when hybridised to or unhybridised to its reverse complementary target, was characterised by a chemical hydrolysis environment at a range of pH values (pH 8.5, 9.2, 9.4, 9.6, 9.8 and 10). Whereas degradation of both the hybridised and unhybridised probe was not significant at pH 8.5, the optimal pH value for hydrolysis of probes labelled with **15,** a range of pH values between pH 9.2 to 9.6 was found to degrade the free probe rapidly, whilst the hybridised probe was protected by the presence of its specific DNA target. This differential hydrolysis characteristic could allow the use of this AE in the HPA format, with a more alkaline chemical hydrolysis step than **15**.

Theoretically, these differential properties of dimethoxy-substituted AE DNA probes, the shift in emission wavelength and the hydrolysis at pH 9.2-9.6, which can discriminate between the hybridised and the free probe, are sufficiently different from **15** to form the basis of an HPA format capable of distinguishing two targets present in the same reaction.

Chapter 6

Discussion and Conclusion

6 Discussion and Conclusion

Chemiluminescence is the conversion of chemical energy into the emission of light (luminescence) as a result of an oxidation or hydrolysis reaction. The emission of light can be observed over a range of wavelengths, including the ultraviolet, visible, or infrared spectrum. Such chemiluminescent compounds are employed as detection reagents in clinical diagnostics and are particularly applied in the areas of immunoassays and nucleic acid assays. The advantage of their high quantum yields is that it supports detection in the attomole range. This thesis details the preparation of a series of novel chemiluminescent acridinium esters derivatives with an NHS group for attachment to biological systems which have been synthesised, characterised, and covalently attached to an oligonucleotide complementary to a sequence within the wild type of HIV virus.

A significant part of this study focused on the synthesis of a family of novel chemiluminescent compounds that have different properties by inserting a different activated group into both the acridinium rings and the phenyl ester (leaving group) on the position 2,7 and 2,6, respectively. We evaluated the effect of two different activated groups, the presence of strong electron donating methoxy- groups and withdrawing bromo- groups at the C-2 and C-7 position of the acridinium ring. Furthermore, we inserted methyl and methoxy groups to C-2 and C-6 of the phenyl ester (leaving group) to generate unique and stable acridinium esters.

To summarise, six chemiluminescent compounds were synthesised with reasonable yields using our modified route and isolated in a pure form (> 80% yield). Electronic absorption and emission, ^{1}H-NMR, ^{13}C-NMR spectroscopy, LRMS, HRMS, X-ray and computational methods were employed to determine the various features of the compound investigated.

In Chapter 3.6, the synthesis of 2,7-dibromo-*N*-methylacridinium esters yielded a pseudobase as the final product for all three compounds (**34bx**, **34by** and **34bz**), which had different aryloxy leaving groups. The formation of pseudobase can be predicted as it was described more than 20 years ago. [60,72] During the study, we had difficulty obtaining a good yield of compound **33bx** as part of the traditional route for the synthesis of AEs. We, therefore, developed an alternative approach (see Figure 3.18) involving fewer overall synthetic steps by making use of NHS esters of the appropriate hydroxybenzoic acids. We expect that the approach should be helpful for the synthesis of other similar structures.

The methylation of the acridine nitrogen with triflate reagents (the final step of the synthesis) was found to be remarkably challenging. Several attempts to introduce the methyl group to the *N*-atom of acridinium esters directly using methyl trifluoromethanesulfonate faced no success under normal conditions, even when changing the reaction environment, using aprotic polar solvents, or concentrating the reagent. For example, acetonitrile, which has a higher boiling point than DCM, was observed to react with the methyl triflate reagent. Destruction of the NHS ester occurred when the compounds were heated to 70ºC in a mixture of dimethylformamide and dichloromethane and in some other cases. However, success was achieved by the use of refluxing with DCM for eight days, giving the acridinium esters in reasonable yields.

These acridinium esters, which have both electron-withdrawing bromo groups on the acridinium ring and an electron-withdrawing carbonyl group attached to the phenolic part of the ester, showed a strong tendency to exist as isomeric pseudo-base adducts rather than as the relatively pure acridinium esters usually seen with many other acridinium esters prepared in the past. The reactions gave different proportions of the pseudo-base and acridinium forms of the product, depending on the nature of the esterifying phenol. Compound **34bz**, with two methoxy groups *ortho* to the phenolic group, gave the highest

proportion (about 50%) of the acridinium ester form of the product, possibly because the electron-donating effect of the methoxy groups counteracted to some extent the electron-withdrawing nature of the succinimidyloxycarbonyl group, resulting in lower electron deficiency at position 9. The other two compounds were mainly in the form of pseudo-base, but a small amount of AE was seen in the case of compound **34bx**. Compound **34bz** showed no discernible quantity of AE, which may also reflect the difficulty of forming a planar arrangement of the acridine ring and the attached carbonyl group with such bulky groups as bromo and methyl groups trying to compete for the same region of three-dimensional space.

In Section 3.8, two 2,7-dimethoxy-N-methylacridinium esters (**34cx**, **34cz**) were synthesised using a modification of the method described by Weeks *et al*. and others. [80,131] The modified procedure, involving one fewer step, enabled the synthesis of the precursor acridine esters in relatively high yield and in shorter times compared to the standard procedure. Whereas the standard procedure involves esterification of 2,7-dimethoxyacridine-9-carboxyl chloride with the appropriate 4-(benzyloxycarbonyl)phenol, followed by removal of the benzyl group and then the formation of the NHS ester, the modified route involves the synthesis of the NHS ester of the appropriate 4-hydroxybenzoic acid and using this directly for esterifying the 2,7-dimethoxyacridine-9 carboxyl chloride. The final step made use of an effective methylating reagent, namely, methyl trifluoromethanesulfonate under anhydrous conditions, to afford the target AEs. The chemical structures of the products were confirmed by mass spectrometry and NMR spectral data. Both acridinium esters (**34cx** and **34cz**) showed high intensity chemiluminescence on treatment with alkaline hydrogen peroxide. The nitrogen atom on the acridine ring was alkylated by methyl triflate because *N*-methylation takes place more rapidly and gives a better yield. The chemiluminescent kinetic reaction is

known to be independent of the nature of the group attached to the nitrogen of the acridine ring.[152]

Characterisation of compounds **34bx**, **34by**, **34bz**, **34cx** and **34cz** included consideration of optimal excitation wavelength, emission spectra, chemiluminescence efficiency and once linked to a DNA oligonucleotide, the kinetics of light output and the rate of hydrolysis of the modified acridinium esters. The analysis of the spectra of light emission accompanying the oxidation product of the selected compound is presented in chapter 4 and includes the fluorescence spectrum of the *N*-methyl-9-acridone (**3a**), 2,7-dibromo-10-methyl-9-acridone (**3b**) and 2,7-dimethoxy-10-methyl-9-acridone (**3c**). (Figure 6.1).

*Figure 6. 1: Normalised fluorescence spectra of acridone derivatives recorded at an excitation of 390 nm. Emission spectra for N-methyl-9-acridone (**3c**, blue circles), 2,7-dibromo-10-methyl-9-acridone (**3b**, red triangles) and 2,7-dimethoxy-10-methyl-9-acridone (**3c**, green squares) are displayed. The wavelength of maximal emission for each compound is shown above the relevant spectra. The boxes indicate 20nm bandwidth as an example of the transmission bandwidth of a filter centred on the emission maxima.*

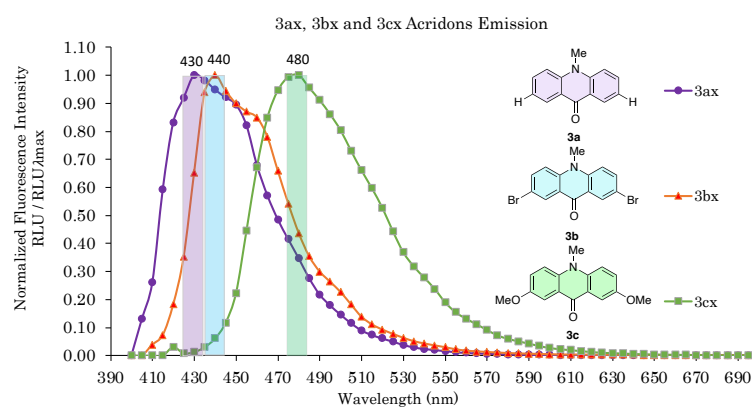The emission of *N*-methyl-9-acridone (**3a**), 2,7-dibromo-10-methyl-9-acridone (**3b**) and 2,7-dimethoxy-10-methyl-9-acridone (**3c**) were measured and shown to reach a maxima emission at 430, 440, and 480 nm, respectively. The emission obtained from *N*-methyl-9-acridone (**3a**) was used as a reference for the comparison of the other compounds. We can see the effect of the donating and the withdrawing group on the emission spectra. The addition of the two bromo- groups shifted the emission maxima by about 10 nm from 430 nm to 440 nm. The data also shows a significant difference in the emission maxima between the 2,7-dimethoxy-10-methyl-9-acridone and the unsubstituted acridone by ~50 nm. The time resolved chemiluminescent emission spectra are similar to the unsubstituted acridone, but it has a substantially slower emission decay rate. These results correspond to a shift of 58 nm demonstrated by Browne *et al*. [65] for 2,7 dimethoxy labelled HICS probes which also had a slower emission decay rate. Based on the result illustrated in Figure 6.1, we can conclude that it would be theoretically feasible to separate the signal of the 2,7-dimethoxy-10-methyl-9-acridone (**3c**) from that of *N*-methyl-9-acridone (**3a**), suggesting a possible mechanism for a dual analyte assay.

As an example of our six novel chemiluminescence compounds, 4-(succinimidyloxycarbonyl)phenyl 2,7-dimethoxy-10-methylacridinium-9-carboxylate trifluoromethanesulfonate (**34ca**, Table 5.3) was used to label a single-stranded DNA oligonucleotide of 31 nucleotides (HIV-WT). The labelling experiments were successfully applied, and the pure probe was obtained using ion-exchange HPLC purification. The AE-labelled probe (HIV-WT-**34cx**-AE) was hybridised to an oligonucleotide with the reverse complementary sequence, and any unhybridised probe was degraded with alkaline Hydrolysis Reagent while the hybridised probe was protected from hydrolysis, presumably by the formation of a double helix.

The difference between the rate of hydrolysis of the hybridised and unhybridised AE-probe is known as 'differential hydrolysis', and it is an essential parameter of the HPA format. Differential hydrolysis of HIV-WT-**34cx**-AE for the bound versus free probe was evaluated by the addition of Hydrolysis Reagent and incubation at 60ºC for 60 minutes. The chemiluminescence was measured in a luminometer using two sequential injections of hydrogen peroxide and sodium hydroxide. The data were collected and plotted as the log of the percentage of the time zero chemiluminescence to show the rate of hydrolysis of hybridised and unhybridised probes. The differential hydrolysis process was applied over a range of pH between pH 8.5 to pH 10 and compared to the hydrolysis of HIV-WT-**34ax**-AE at pH 8.5. The results are illustrated in Chapter 5 (Figure 5.5), which illustrates the loss of chemiluminescence with time due to ester hydrolysis. As shown in Figure 5.5, the chemiluminescence associated with the unhybridised HIV-WT-**34ax**-AE probe is rapidly reduced to a low level, whereas chemiluminescence associated with the hybridised probe is minimally affected over the usual time of the hydrolysis step in an assay (~15-20 minutes). However, both the hybridised and the unhybridised HIV-**34cx** probe were relatively resistant to hydrolysis at pH 8.5 (Figure 5.6).

The rate of hydrolysis is an important component of the HPA format, as this step determines the discrimination between the hybridised and unhybridised probe by degrading the latter. The data shows that there are several pH values (pH 9.2 to 9.6) at which the rate of the hydrolysis of the unhybridised and hybridised HIV-WT-**34ax**-AE probes are different. This 'differential hydrolysis' rate has the advantage that this compound could be used to label probes for use in the HPA format, though the assay would need a higher hydrolysis pH than is used for **15**-AE labelled probes.

There are two interesting characteristics of the dimethoxy-modified AE that might be exploitable in a dual-label assay. The shift in the peak of the emission wavelength spectra

of 2,7-dimethoxy-10-methyl-9-acridone (**3c**) was 50 nm from that of the unsubstituted acridone. This difference in emission wavelength maxima may allow the ability to distinguish between two or more analytes in a dual wavelength luminometer. The second characteristic of this modified AE is the resistance to hydrolysis at pH 8.5 but increased hydrolysis at higher pH. The differential hydrolysis experiments show that as the pH increases, the rate of hydrolysis of the unhybridised probe increases relative to the rate of hydrolysis of the hybridised probe between pH 9.2 to 9.6. At higher pH, the rate of hydrolysis of the hybridised probe also becomes affected; this would have the effect of reducing the signal-to-noise ratio and adversely affecting the performance in an HPA type assay. For future experiments, the optimal pH for an HPA with the HIV-WT-**34cx** AE probe would be 9.4, the pH at which the difference between the signal emitted from the unhybridised and the hybridised probe was maximal. This data suggests that the HIV-WT-**34cx** AE could be utilised in an HPA format with a more alkaline hydrolysis reagent.

When combined with the wavelength shift of ~50 nm and the ability of the Tristar luminometer to resolve different wavelength spectra, this could potentially allow for a dual analyte assay format based on two probes for two different analytes, one labelled with **15-AE** and the other with 2,7-dimethoxy-AE (**34cx**). The initial hydrolysis step could be done with a hydrolysis reagent of pH 7.5-8.5, causing hydrolysis of the unhybridised STD-AE (**15**) probe but not the hybridised **15**-AE probe or either the unhybridised or hybridised **34cx**-AE labelled probe. Part of the reaction could be removed and read on the Tristar luminometer, which is capable of measuring chemiluminescence output at different wavelengths. A filter of 405-445 nm would allow the light from the unsubstituted AE to be measured with little contamination from light from the **34cx**-AE probe- giving effective measurement and quantitation of the first analyte. A second hydrolysis reagent at pH 9.4 could be added to the reaction for 30-60 minutes, causing the unhybridised **34cx**-AE probe

to be hydrolysed and, potentially, the **15-**AE hybrid to be destroyed. The light emitted at the end of this hydrolysis step would be from the hybridised **34cx-**AE probe, potentially with little contamination from the **15-**AE probe or the unhybridised **34cx-**AE probe. The exact assay conditions need to be optimised and tested, but theoretically, these two characteristics and the capability of the Tristar luminometer to measure selective wavelength ranges could be used as the basis of a dual analyte format.

In conclusion, theoretically, these properties of the **34cx-**substituted AE probes, the shift in emission wavelength and the differential hydrolysis of the hybridised and unhybridised probes at pH 9.2-9.6 are sufficiently different from those of probes labelled with **15-**AE to form the basis of an HPA format capable of distinguishing two targets present in the same reaction. Figure 6.2 and table 6.1 shows summary of the results which obtained from synthesis of series of novel acridinium esters include part of characterisations, emission, kinetic profiles, and the other physical properties.

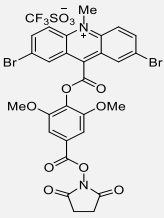*Figure 6. 2: shows a summary of the charactrization study, three types of acridones (3a, 3b, 3c) were obtained from 6 novel compounds (34ax, 34bx, 34by, 34bz, 34ca and 34cz). Including the emission and/or the kinetic profiles, the ester hydrolysis kinatics of hybridized and unhybridized probe. (HPA assay).*
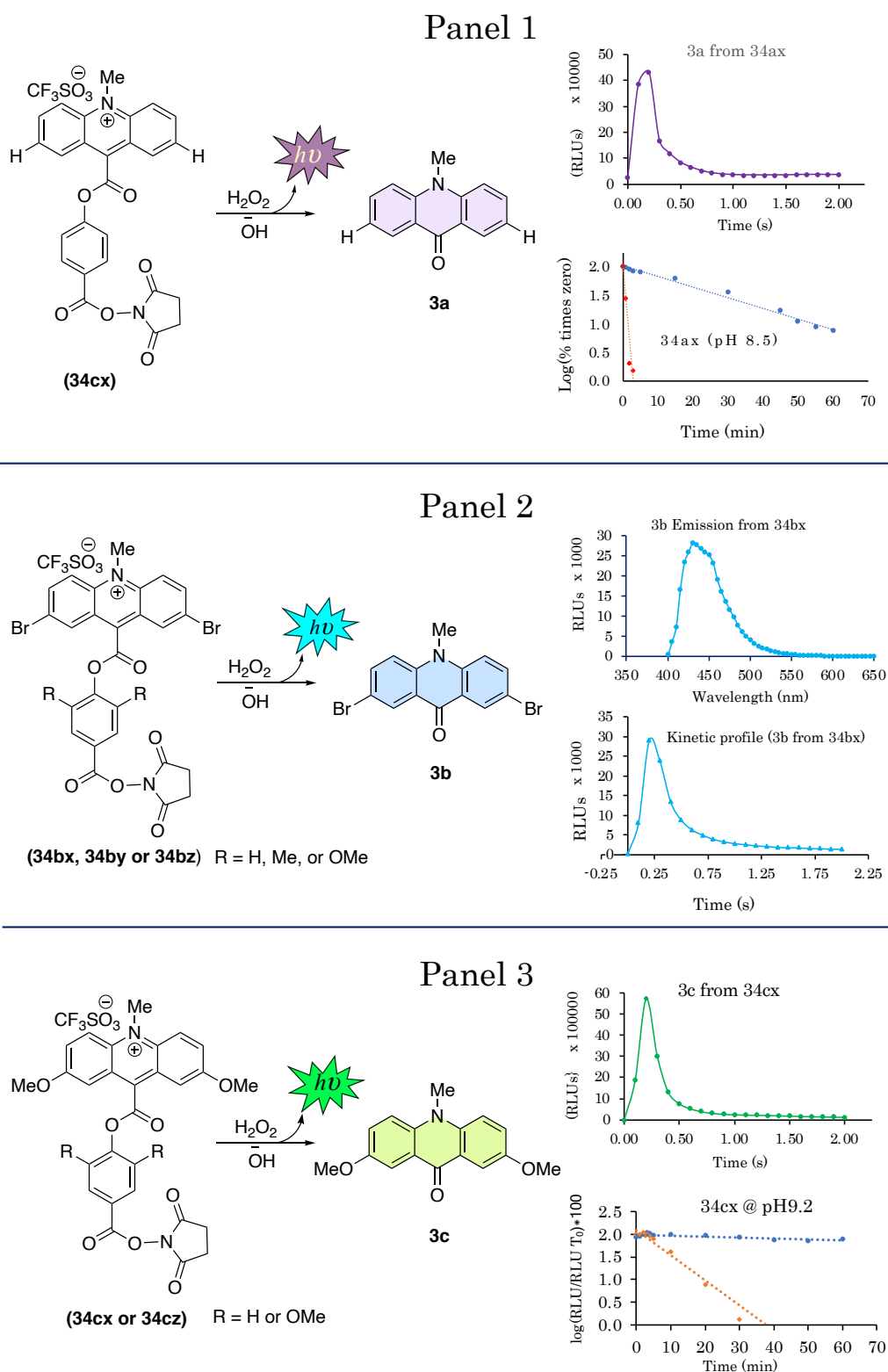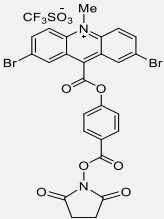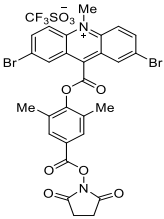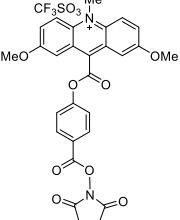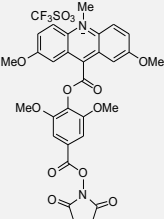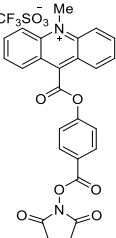
Table 6. 2:The table shows a summary of the physical properties of the final compounds based on the synthetic route including compound ID, chemical structure, and the reference pages.

No.	Chem.ID & Structure	Physical Properties	Ref. Page
1	ID:34bx	Product yield: 72% Melting point: (Mp; 283-285°C). Absorption (λ_{max}): 418 nm. Emission (λ): 440 nm. M.Wt: $C_{26}H_{17}{}^{79}Br_2N_2O_6$ (M$^+$ - CF$_3$SO$_3$): 610.9454; found: 610.9456.	85
2	ID:34by	Product yield: 69% Melting point: (Mp; 297-298°C). Absorption (λ_{max}): 418 nm Emission (λ): 440 nm. M.Wt: $C_{28}H_{21}{}^{79}Br_2N_2O_6$ (M$^+$ - CF$_3$SO$_3$): 638.9766 found 638.9774.	94
3	ID:34bz	Product yield: 64%. Melting point: (Mp, 287-289 °C). Absorption (λ_{max}): 418 nm. Emission (λ): 440 nm. M.Wt: $C_{28}H_{21}{}^{79}Br_2N_2O_8$ (M$^+$ - CF$_3$SO$_3$): 670.9665 found 670.9642.	100
4	ID:34cx	Product yield: 79% Melting point: (MP: 192-194°C). Absorption (λ_{max}): 438 nm. Emission (λ): 480 nm. M.Wt: $C_{28}H_{23}N_2O_8$ (M$^+$ - CF$_3$SO$_3$): 515.1454 found: 515.1453.	115
5	ID:34cz	Product yield: 89% Melting point: Mp 167-169°C Absorption (λ_{max}): 438 nm. Emission (λ): 480 nm. M.Wt: $C_{30}H_{27}N_2O_{10}$ (M$^+$ - CF$_3$SO$_3$): 575.1666; found: 575.1667	119
6	ID:34ax	Product yield: 76%. Melting point: (Mp; 283-284°C). Absorption (λ_{max}): 390 nm. Emission (λ): 430 nm. M.Wt: $C_{26}H_{19}N_2O_6$ (M$^+$ - CF$_3$SO$_3$): 455.1243; found: 455.1240.	129

Chapter 7

Bibliography

7 Bibliography

1. Wiedemann, E. (1888). Ueber Fluorescenz und Phosphorescenz I. Abhandlung. *Annalen Der Physik*, *270*(7), 446–463. https://doi.org/10.1002/andp.18882700703

2. Ian Weeks and G. Svehla (ed). (1992). Chemiluminescence: the phenomenon. In *Comprehensive Analytical Chemistry* (Vol. 29, pp. 7–52). Elsevier. https://doi.org/https://doi.org/10.1016/S0166-526X(05)80068-6

3. Gundermann, K.-D., & McCapra, F. (1987). *Chemiluminescence in Organic Chemistry* (Vol. 23). Springer Berlin Heidelberg. https://doi.org/10.1007/978-3-642-71645-4

4. Montalti, M., Credi, A., Prodi, L., & Gandolfi, M. T. (2006). Handbook of Photochemistry. In *Handbook of Photochemistry*. CRC Press. https://doi.org/10.1201/9781420015195

5. Sharma, A., & Schulman, S. G. (1999). *Introduction to fluorescence spectroscopy* (Vol. 13). Wiley New York.

6. McCapra, F., & Beheshti, I. (1985). Selected chemical reactions that produce light. *Bioluminescence and Chemiluminescence: Instruments and Applications*, *1*, 9–42.

7. Hastings, J. G. M. (1987). Luminescence in clinical microbiology. *Bioluminescence and Chemiluminescence, New Perspectives*, 453.

8. Weeks, I., Sturgess, M., Brown, R. C., & Stuart Woodhead, J. (1986). Immunoassays Using Acridinium Esters. *Methods in Enzymology*, *133*(C), 366–387. https://doi.org/10.1016/0076-6879(86)33080-5

9. Berry, D. J., Clark, P. M., & Price, C. P. (1988). A laboratory and clinical evaluation of an immunochemiluminometric assay of thyrotropin in serum. *Clinical Chemistry*, *34*(10), 2087–2090. https://doi.org/10.1093/clinchem/34.10.2087

10. Bronstein, I. Y., & Voyta, J. C. (1989). *Methods of using chemiluminescent 1,2-dioxetanes*. https://patents.google.com/patent/CA1340070C/en

11. Arnold, L. J., Hammond, P. W., Wiese, W. A., & Nelson, N. C. (1989). Assay formats involving acridinium-ester-labeled DNA probes. *Clinical Chemistry*, *35*(8), 1588–1594.

12. Bronstein, I., Voyta, J. C., Lazzari, K. G., Murphy, O., Edwards, B., & Kricka, L. J. (1990). Rapid and sensitive detection of DNA in southern blots with chemiluminescence. *BioTechniques*, *8*(3), 310–314.

13. Lewis, J. S., Kranig-Brown, D., & Trainor, D. A. (1990). DNA probe confirmatory test for Neisseria gonorrhoeae. *Journal of Clinical Microbiology*, *28*(10), 2349–2350. https://doi.org/10.1128/jcm.28.10.2349-2350.1990

14. Dhingra, K., Talpaz, M., Riggs, M. G., Eastman, P. S., Zipf, T., Ku, S., & Kurzrock, R. (1991). Hybridization protection assay: A rapid, sensitive, and specific method for detection of Philadelphia chromosome- positive leukemias. *Blood*, *77*, 238–242. https://doi.org/https://doi.org/10.1182/blood.V77.2.238.238

15. Stockman, L., Clark, K. A., Hunt, J. M., & Roberts, G. D. (1993). Evaluation of commercially available acridinium ester-labeled chemiluminescent DNA probes for culture identification of Blastomyces dermatitidis, Coccidioides immitis, Cryptococcus neoformans, and Histoplasma capsulatum. *Journal of Clinical Microbiology*, *31*(4), 845–850. https://doi.org/https://doi.org/10.1128%2Fjcm.31.4.845-850.1993

16. McCapra, F., & Baldwin, T. O. (1990). Chemiluminescence and Bioluminescence. *Journal of Photochemistry and Photobiology, A: Chemistry*, *51*(1), 21–28. https://doi.org/10.1016/1010-6030(90)87037-C

17. Viviani, V. R. (2002). The origin, diversity, and structure function relationships of insect luciferases. *Cellular and Molecular Life Sciences*, *59*(11), 1833–1850. https://doi.org/10.1007/PL00012509/METRICS

18. White, E. H., McCapra, F., Field, G. F., & McElroy, W. D. (1961). The structure and synthesis of firefly luciferin. *Journal of the American Chemical Society*, *83*(10), 2402–2403. https://doi.org/10.1021/ja01471a051

19. Yagur-Kroll, S., Bilic, B., & Belkin, S. (2010). Strategies for enhancing bioluminescent bacterial sensor performance by promoter region manipulation. *Microbial Biotechnology*, *3*(3), 300–310. https://doi.org/https://doi.org/10.1111/j.1751-7915.2009.00149.x

20. Adam, W., Kazakov, D. v, & Kazakov, V. P. (2005). Singlet-Oxygen Chemiluminescence in Peroxide Reactions. *Chemical Reviews*, *105*(9), 3371–3387. https://doi.org/10.1021/cr0300035

21. Marques, S. M., & Esteves da Silva, J. C. G. (2009). Firefly bioluminescence: A mechanistic approach of luciferase catalyzed reactions. *IUBMB Life*, *61*(1), 6–17. https://doi.org/https://doi.org/10.1002/iub.134

22. Adamczyk, M., Mattingly, P. G., van Dyke, K., van Dyke, C., & Woodfork, K. (2002). *Luminescence Biotechnology Instruments and Applications (Chemiluminescent N-Sulfonylacridinum 9-Carboxamides and Their Application in Clinical Assays)*. CRC Press.

23. Hastings, J. W., & Johnson, C. H. (2003). Bioluminescence and chemiluminescence. In *Methods in Enzymology* (Vol. 360, pp. 75–104). Academic Press. https://doi.org/https://doi.org/10.1016/S0076-6879(03)60107-2

24. Poznyak, S. K., Talapin, D. v, Shevchenko, E. v, & Weller, H. (2004). Quantum dot chemiluminescence. *Nano Letters*, *4*(4), 693–698. https://doi.org/10.1021/nl049713w

25. Barnett, N. W., & Francis, P. S. (2005). CHEMILUMINESCENCE | Liquid-Phase. In *Encyclopedia of Analytical Science* (pp. 511–521). Elsevier. https://doi.org/10.1016/B0-12-369397-7/00070-4

26. Yamaguchi, S., Kishikawa, N., Ohyama, K., Ohba, Y., Kohno, M., Masuda, T., Takadate, A., Nakashima, K., & Kuroda, N. (2010). Evaluation of chemiluminescence reagents for selective detection of reactive oxygen species. *Analytica Chimica Acta*, *665*(1), 74–78. https://doi.org/10.1016/j.aca.2010.03.025

27. Czechowska, J., Kawecka, A., Romanowska, A., Marczak, M., Wityk, P., Krzymiński, K., & Zadykowicz, B. (2017). Chemiluminogenic acridinium salts: A comparison study.

Detection of intermediate entities appearing upon light generation. *Journal of Luminescence*, *187*, 102–112. https://doi.org/10.1016/j.jlumin.2017.02.068

28. Abou-Hatab, S., Spata, V. A., & Matsika, S. (2017). Substituent Effects on the Absorption and Fluorescence Properties of Anthracene. *The Journal of Physical Chemistry A*, *121*(6), 1213–1222. https://doi.org/10.1021/acs.jpca.6b12031

29. Skoog D, West D, Holler F, & Crouch S. (2018). *Principles of Instrumental Analysis: Edition 7*. Cengage Learning, Australia,.

30. Merényi, G., Lind, J., & Eriksen, T. E. (1990). Luminol chemiluminescence: Chemistry, excitation, emitter. *Journal of Bioluminescence and Chemiluminescence*, *5*(1), 53–56. https://doi.org/https://doi.org/10.1002/bio.1170050111

31. Isacsson, U., & Wettermark, G. (1974). Chemiluminescence in analytical chemistry. *Analytica Chimica Acta*, *68*(2), 339–362. https://doi.org/10.1016/S0003-2670(01)82590-3

32. Goldberg, M. C., & Weiner, E. R. (2009). *The Science of Luminescence*. https://doi.org/10.1021/bk-1989-0383.ch001

33. Trautz, M. S. P. P. (1905). *Z.Wiss. photogr* (Vol. 3, p. 121).

34. Albrecht, H. O. (1928). Chemiluminescence of aminophthalic hydrazide. *Z. Phys. Chem*, *136*, 321.

35. Drew, H. D. K., & Garwood, R. F. (1939). Chemiluminescent organic compounds. Part VII. Substituted phthalaz-1: 4-diones. Effect of substituents on the luminescent power. *Journal of the Chemical Society (Resumed)*, *0*, 836–837. https://doi.org/10.1039/JR9390000836

36. Roswell, D. F., & White, E. H. (1978). The chemiluminescence of luminol and related hydrazides. In *Methods in Enzymology* (Vol. 57, pp. 409–423). Academic Press. https://doi.org/10.1016/0076-6879(78)57038-9

37. Schroeder, H. R. (1982). Chemiluminescence immunoassay for serum thyroxine. In *Methods in Enzymology* (Vol. 84, pp. 303–317). Academic Press. https://doi.org/https://doi.org/10.1016/0076-6879(82)84025-1

38. Sarabia, J., Pérez-Martínez, C., Hernández del Rincón, J. P., & Luna, A. (2018). Study of chemiluminescence measured by luminometry and its application in the estimation of postmortem interval of bone remains. *Legal Medicine*, *33*, 32–35. https://doi.org/https://doi.org/10.1016/j.legalmed.2018.05.001

39. Rongen, H. A. H., Hoetelmans, R. M. W., Bult, A., & van Bennekom, W. P. (1994). Chemiluminescence and immunoassays. *Journal of Pharmaceutical and Biomedical Analysis*, *12*(4), 433–462. https://doi.org/10.1016/0731-7085(94)80027-8

40. Schroeder, H. R., & Yeager, F. M. (1978). Chemiluminescence yields and detection limits of some isoluminol derivatives in various oxidation systems. *Analytical Chemistry*, *50*(8), 1114–1120. https://doi.org/10.1021/ac50030a027

41. Dodeigne, C., Thunus, L., & Lejeune, R. (2000). Chemiluminescence as a diagnostic tool. A review. In *Talanta* (Vol. 51, Issue 3, pp. 415–439). https://doi.org/10.1016/S0039-9140(99)00294-5

42. Shimomura, O., Johnson, F. H., & Morise, H. (1974). Mechanism of the luminescent intramolecular reaction of aequorin. *Biochemistry*, *13*(16), 3278–3286. https://doi.org/10.1021/bi00713a016

43. Inoue, S., Sugiura, S., Kakoi, H., Hasizume, K., Goto, T., & Iio, H. (1975). Squid bioluminescence ii. Isolation from watasenia scintillans and synthesis of 2-(p-hydroxybenzyl)-6-(p-hydroxyphenyl)-3,7-dihydroimidazo[1,2-a]pyrazin-3-one. *Chemistry Letters*, *4*(2), 141–144. https://doi.org/10.1246/cl.1975.141

44. Teranishi, K. (2007). Luminescence of imidazo[1,2-a]pyrazin-3(7H)-one compounds. *Bioorganic Chemistry*, *35*(1), 82–111. https://doi.org/https://doi.org/10.1016/j.bioorg.2006.08.003

45. Sabnis, R. W. (2010). Handbook of Biological Dyes and Stains: Synthesisand Industrial Applications. *Handbook of Biological Dyes and Stains: Synthesisand Industrial Applications*. https://doi.org/10.1002/9780470586242

46. Roda, A., Pasini, P., Guardigli, M., Baraldini, M., Musiani, M., & Mirasoli, M. (2000). Bio- and chemiluminescence in bioanalysis. *Fresenius' Journal of Analytical Chemistry*, *366*(6–7), 752–759. https://doi.org/10.1007/s002160051569

47. Rauhut, M. M. (1969). Chemiluminescence from concerted peroxide decomposition reactions. *Accounts of Chemical Research*, *2*(3), 80–87. https://doi.org/10.1021/ar50015a003

48. Chandross, E. A. (1963). A new chemiluminescent system. *Tetrahedron Letters*, *4*(12), 761–765. https://doi.org/https://doi.org/10.1016/S0040-4039(01)90712-9

49. Capomacchia, A. C., Jennings, R. N., Hemingway, S. M., D'Souza, P., Prapaitrakul, W., & Gingle, A. (1987). Native peroxyoxalate chemiluminescence from the reaction of bis(2,4-dinitrophenyl) oxalate and hydrogen peroxide perturbed by nonfluorophores. *Analytica Chimica Acta*, *196*, 305–310. https://doi.org/https://doi.org/10.1016/S0003-2670(00)83101-3

50. Gleu, K., & Petsch, W. (1935). Die Chemiluminescenz der Dimethyl-diacridyliumsalze. *Angewandte Chemie*, *48*(3), 57–59. https://doi.org/10.1002/ange.19350480302

51. Beinlich, C. J., Piper, J. A., O'Neal, J. C., & White, O. D. (1985). Evaluation of dual-label simultaneous assays for lutropin and follitropin in serum. *Clinical Chemistry*, *31*(12), 2014–2018.

52. McCapra, F., Richardson, D. G., & Chang, Y. C. (1965). Chemiluminescence Involving Peroxide Decompositions. *Photochemistry and Photobiology*, *4*(6), 1111–1121. https://doi.org/10.1111/j.1751-1097.1965.tb09300.x

53. Rauhut, M. M., Sheehan, D., Clarke, R. A., Roberts, B. G., & Semsel, A. M. (1965). Chemiluminescence from the Reaction of 9-Chlorocarbonyl-10-methylacridinium Chloride with Aqueous Hydrogen Peroxide. *Journal of Organic Chemistry*, *30*(11), 3587–3592. https://doi.org/10.1021/jo01022a002

54. McCapra, F., & Richardson, D. G. (1964). The mechanism of chemiluminescence: A new chemiluminescent reaction. *Tetrahedron Letters*, *5*(43), 3167–3172. https://doi.org/10.1016/0040-4039(64)83128-2

55. McCapra, F. (1970). The chemiluminescence of organic compounds. *Pure and Applied Chemistry*, *24*(3), 611–630. https://doi.org/doi:10.1351/pac197024030611

56. McCapra, F. (1976). Chemical Mechanisms in Bioluminescence. *Accounts of Chemical Research*, *9*(6), 201–208. https://doi.org/10.1021/ar50102a001

57. Thomas-Jones, E., Walkley, N., Morris, C., Kille, P., Cryer, J., Weeks, I., & Woodhead, J. S. (2003). Quantitative measurement of fathead minnow vitellogenin mRNA using hybridization protection assays. *Environmental Toxicology and Chemistry*, *22*(5), 992–995. http://www.ncbi.nlm.nih.gov/pubmed/12729208

58. Zhang, F., Bartels, M. J., Brodeur, J. C., & Woodburn, K. B. (2004). Quantitative Measurement of Fathead Minnow Vitellogenin By Liquid Chromatography Combined With Tandem Mass Spectrometry Using a Signature Peptide of Vitellogenin. *Environmental Toxicology and Chemistry*, *23*(6), 1408. https://doi.org/10.1897/03-425

59. Natrajan, A., Sharpe, D., & Wen, D. (2012). Zwitterionic reagents for labeling, cross-linking and improving the performance of chemiluminescent immunoassays. *Organic & Biomolecular Chemistry*, *10*(9), 1883. https://doi.org/10.1039/c2ob06807a

60. Law, S. J., Miller, T., Piran, U., Klukas, C., Chang, S., & Unger, J. (1989). Novel poly-substituted aryl acridinium esters and their use in immunoassay. *Journal of Bioluminescence and Chemiluminescence*, *4*(1), 88–98. https://doi.org/10.1002/bio.1170040115

61. Natrajan, A., & Wen, D. (2015). A comparison of chemiluminescent acridinium dimethylphenyl ester labels with different conjugation sites. *Organic and Biomolecular Chemistry*, *13*(9), 2622–2633. https://doi.org/10.1039/c4ob02528h

62. Natrajan, A., Jiang, & Sharpe, D. (2003). *Acridinium ester labels having hydrophilic modifiers* (Patent No. US6664043B2). Google Patent. https://www.google.com/patents/US6664043

63. Mattingly, P. G. (1991). Chemiluminescent 10-methyl-acridinium-9-(N-sulphonylcarboxamide) salts. Synthesis and kinetics of light emission. *Journal of Bioluminescence and Chemiluminescence*, *6*(2), 107–114. https://doi.org/10.1002/bio.1170060208

64. Adamczyk, M., Chen, Y. Y., Mattingly, P. G., Moore, J. A., & Shreder, K. (1999). Modulation of the chemiluminescent signal from N10(3-sulfopropyl)-N- sulfonylacridinium-9-carboxamides. *Tetrahedron*, *55*(36), 10899–10914. https://doi.org/10.1016/S0040-4020(99)00624-9

65. Browne, K. A., Deheyn, D. D., El-Hiti, G. A., Smith, K., & Weeks, I. (2011). Simultaneous quantification of multiple nucleic acid targets using chemiluminescent probes. *Journal of the American Chemical Society*, *133*(37), 14637–14648. https://doi.org/10.1021/ja202221h

66. Brown, R. C., Li, Z., Rutter, A. J., Mu, X., Weeks, O. H., Smith, K., & Weeks, I. (2009). Development and application of a novel acridinium ester for use as a chemiluminescent emitter in nucleic acid hybridisation assays using chemiluminescence quenching. *Org. Biomol. Chem.*, *7*(2), 386–394. https://doi.org/10.1039/B811947C

67. Sato, N. (1996). Synthesis and properties of new luminescent 10-carboxymethylacridinium derivatives. *Tetrahedron Letters*, *37*(47), 8519–8522. https://doi.org/10.1016/0040-4039(96)01980-6

68. Natrajan, A., Sharpe, D., & Wen, D. (2012). Chemiluminescence from alkoxy-substituted acridinium dimethylphenyl ester labels. *Organic and Biomolecular Chemistry*, *10*(17), 3432–3447. https://doi.org/10.1039/c2ob00022a

69. Natrajan, A., & Sharpe, D. (2013). Synthesis and properties of differently charged chemiluminescent acridinium ester labels. *Organic & Biomolecular Chemistry*, *11*(6), 1026. https://doi.org/10.1039/c2ob27190g

70. Nakazono, M., Oshikawa, Y., Nakamura, M., Kubota, H., & Nanbu, S. (2017). Strongly Chemiluminescent Acridinium Esters under Neutral Conditions: Synthesis, Properties, Determination, and Theoretical Study. *Journal of Organic Chemistry*, *82*(5), 2450–2461. https://doi.org/10.1021/acs.joc.6b02748

71. Townshend, A. (1990). Solution chemiluminescence—some recent analytical developments. Plenary lecture. *The Analyst*, *115*(5), 495–500. https://doi.org/10.1039/AN9901500495

72. Hammond, P. W., Wiese, W. A., Waldrop, A. A., Nelson, N. C., Arnold, L. J., Hammond, P. W., Nelson, N. C., Wiese, W. A., & Waldrop, A. A. (1991). Nucleophilic addition to the 9 position of 9-phenylcarboxylate-10-methylacridinium protects against hydrolysis of the ester. *Journal of Bioluminescence and Chemiluminescence*, *6*(1), 35–43. https://doi.org/10.1002/bio.1170060108

73. Rak, J., Skurski, P., & Błazejowski, J. (1999). Toward an understanding of the chemilumineseence accompanying the reaction of 9-carboxy-10-methylacridinium phenyl ester with hydrogen peroxide. *Journal of Organic Chemistry*, *64*(9), 3002–3008. https://doi.org/10.1021/jo980566u

74. Yalow, R. S., & Berson, S. A. (1959). Assay of plasma insulin in human subjects by immunological methods. *Nature*, *184*(4699), 1648–1649. https://doi.org/10.1038/1841648b0

75. Sharma, J. D., Wynne Ahernet, G., & Marks, V. (1989). Enhanced chemiluminescent enzyme immunoassay for cannabinoids in urine. *The Analyst*, *114*, 1279–1282. https://doi.org/10.1039/AN9891401279

76. Darwish, I. A. (2006). Immunoassay methods and their applications in pharmaceutical analysis: Basic methodology and recent advances. *Int. J. Biomed. Sci.*, *2*(3), 217–235.

77. Campbell, A. K. (1988). *Chemiluminescence. Principles and applications in biology and medicine*. VCH Verlagsges. ,Weinheim, Germany, F.R. https://doi.org/https://doi.org/

78. Simpson, J. S. A., Campbell, A. K., Woodhead, J. S., Richardson, A., Hart, R., & McCapra, F. (1981). Chemiluminescent labels in immunoassay. In *"Bioluminescence and Chemiluminescence: Basic Chemistry and Analytical Applications"* (pp. 673–679). Academic Press New York.

79. Schroeder, H. R., Vogelhut, P. O., Carrico, R. J., Boguslaski, R. C., & Buckler, R. T. (1976). Competitive Protein Binding Assay for Biotin Monitored by Chemiluminescence. *Analytical Chemistry*, *48*(13), 1933–1937. https://doi.org/10.1021/ac50007a032

80. Weeks, I., Beheshti, I., McCapra, F., Campbell, A. K., & Woodhead, J. S. (1983). Acridinium esters as high-specific-activity labels in immunoassay. *Clinical Chemistry*, *29*(8), 1474–1479.

81. Sarrazin, C. (2002). Highly sensitive hepatitis C virus RNA detection methods: molecular backgrounds and clinical significance. *Journal of Clinical Virology*, *25*(SUPPL. 3), 23–29. https://doi.org/10.1016/S1386-6532(02)00195-6

82. King, D. W., Cooper, W. J., Rusak, S. A., Peake, B. M., Kiddle, J. J., O'Sullivan, D. W., Melamed, M. L., Morgan, C. R., & Theberge, S. M. (2007). Flow injection analysis of H2O2 in natural waters using acridinium ester chemiluminescence: Method development and optimization using a kinetic model. *Analytical Chemistry*, *79*(11), 4169–4176. https://doi.org/10.1021/ac062228w

83. Lai, Y., Qi, Y., Wang, J., & Chen, G. (2009). Using acridinium ester as the sonochemiluminescent probe for labeling of protein. *The Analyst*, *134*(1), 131–137. https://doi.org/10.1039/B813330A

84. Kricka, L. J. (2000). Application of bioluminescence and chemiluminescence in biomedical sciences. *Methods Enzymol.*, *305*, 333–345. https://doi.org/10.1016/S0076-6879(00)05498-7

85. Natrajan, A., Sells, T., Schroeder, H., Yang, G., & Sharpe, D. (2008). *Applications of acridinium compounds and derivatives in homogeneous assays* (Patent No. US-7319041-B2).

86. Nelson, N. C. (1998). Rapid detection of genetic mutations using the chemiluminescent hybridization protection assay (HPA): Overview and comparison with other methods. *Critical Reviews in Clinical Laboratory Sciences*, *35*(5), 369–414. https://doi.org/10.1080/10408369891234228

87. Nelson, N. C., Woodhead, J. S., Weeks, I., & Cheikh, A. ben. (1998). Labeled hybridization assay probes useful for the detection and quantification of multiple nucleic acid sequences. In *United States Patent and Trademark Office Granted Patent*.

88. Nelson, N. C., Cheikh, A. ben, Matsuda, E., & Becker, M. M. (1996). Simultaneous detection of multiple nucleic acid targets in a homogeneous format. *Biochemistry*, *35*(25), 8429–8438. https://doi.org/10.1021/bi960085+

89. Sayler, G. S., & Layton, A. C. (1990). Environmental Application of Nucleic Acid Hybridization. *Annual Review of Microbiology*, *44*(1), 625–648. https://doi.org/10.1146/annurev.mi.44.100190.003205

90. Wetmur, J. G., & Fresco, J. (1991). DNA probes: Applications of the principles of nucleic acid hybridization. *Critical Reviews in Biochemistry and Molecular Biology*, *26*(3–4), 227–259. https://doi.org/10.3109/10409239109114069

91. Carrino, J. J., & Lee, H. H. (1995). Nucleic acid amplification methods. *Journal of Microbiological Methods*, *23*(1), 3–20. https://doi.org/10.1016/0167-7012(95)00024-F

92. Chernesky, M. A. (1999). Nucleic acid tests for the diagnosis of sexually transmitted diseases. *FEMS Immunology & Medical Microbiology*, *24*(4), 437–446. https://doi.org/10.1111/j.1574-695X.1999.tb01316.x

93. Nelson, N. C., Reynolds, M. A., & Arnold, L. J. (1995). Detection of Acridinium Esters by Chemiluminescence. In *Nonisotopic Probing, Blotting, and Sequencing* (pp. 391–428). Elsevier. https://doi.org/10.1016/B978-012426291-1/50019-4

94. Smith, C. J., & Osborn, A. M. (2009). Advantages and limitations of quantitative PCR (Q-PCR)-based approaches in microbial ecology. *FEMS Microbiology Ecology*, *67*(1), 6–20. https://doi.org/10.1111/j.1574-6941.2008.00629.x

95. Arnold, Jr. et al., Mark Alan Reynolds, & Ram Saroop Bhatt. (1988). *Non-nucleotide linking reagents for nucleotide probes*. Google Patents. https://encrypted.google.com/patents/WO1989002439A1?cl=ja

96. Nelson, N. C., Woodhead, J. S., Weeks, I., & Cheikh, A. ben. (1998). Compositions and methods for the simultaneous detection and quantification of multiple specific nucleic acid sequences. In *United States Patent and Trademark Office Granted Patent*.

97. Kluytmans, J. A. J. W., Niesters, H. G. M., Mouton, J. W., Quint, W. G. v, Ijpelaar, J. A. J., van Rijsoort-Vos, J. H., Habbema, L., Stolz, E., Michel, M. F., & Wagenvoort, J. H. T. (1991). Performance of a nonisotopic DNA probe for detection of Chlamydia trachomatis in urogenital specimens. *Journal of Clinical Microbiology*, *29*(12), 2685–2689.

98. Iwen, P. C., Blair, T. M. H., & Woods, G. L. (1991). Comparison of the gen-probe PACE2(TM) system, direct fluorescent-antibody, and cell culture for detecting Chlamydia trachomatis in cervical specimens. *American Journal of Clinical Pathology*, *95*(4), 578–582.

99. Tyagi, S., & Kramer, F. R. (1996). Molecular Beacons: Probes that Fluoresce Upon Hybridization. *Nature Biotechnology*, *14*(3), 303–308. https://doi.org/10.1038/nbt0396-303

100. Becker, M., Lerum, V., Dickson, S., Nelson, N. C., & Matsuda, E. (1999). The double helix is dehydrated: Evidence from the hydrolysis of acridinium ester-labeled probes. *Biochemistry*, *38*(17), 5603–5611. https://doi.org/10.1021/bi9828066

101. Pachl, C., Todd, J. A., Kern, D. G., Sheridan, P. J., Fong, S. J., Stempien, M., Hoo, B., Besemer, D., Yeghiazarian, T., Irvine, B., Kolberg, J., Kokka, R., Neuwald, P., & Urdea, M. S. (1995). Rapid and precise quantification of HIV-1 RNA in plasma using a branched DNA signal amplification assay. *Journal of Acquired Immune Deficiency Syndromes and Human Retrovirology*, *8*(5), 446–454. https://doi.org/10.1097/00042560-199504120-00003

102. Bisceglie, A. M., Alter, H. J., Sanchez-Pescador, R., Urdea, M. S., Wilber, J. C., Shih, JamesW. W., Lagier, R. J., & Neuwald, P. D. (2007). Evaluation of branched DNA signal amplification for the detection of hepatitis C virus RNA. *Journal of Viral Hepatitis*, *2*(3), 121–132. https://doi.org/10.1111/j.1365-2893.1995.tb00017.x

103. Tsongalis, G. J. (2006). Branched DNA technology in molecular diagnostics. *American Journal of Clinical Pathology*, *126*(3), 448–453. https://doi.org/10.1309/90BU6KDXANFLN4RJ

104. Giachetti, C., Linnen, J. M., Kolk, D. P., Dockter, J., Gillotte-Taylor, K., Park, M., Ho-Sing-Loy, M., McCormick, M. K., Mimms, L. T., & McDonough, S. H. (2002). Highly sensitive multiplex assay for detection of human immunodeficiency virus type 1 and hepatitis C virus RNA. *Journal of Clinical Microbiology*, *40*(7), 2408–2419. https://doi.org/10.1128/JCM.40.7.2408-2419.2002

105. Compton, J. (1991). Nucleic acid sequence-based amplification. *Nature*, *350*(6313), 91–92. https://doi.org/10.1038/350091a0

106. Guatelli, J. C., Whitfield, K. M., Kwoh, D. Y., Barringer, K. J., Richman, D. D., & Gingeras, T. R. (1990). Isothermal, in vitro amplification of nucleic acids by a multienzyme reaction modeled after retroviral replication. *Proceedings of the National Academy of Sciences of the United States of America*, *87*(5), 1874–1878. http://www.ncbi.nlm.nih.gov/pubmed/2308948

107. Nelson, N. C., Hammond, P. W., Matsuda, E., Goud, A. A., & Becker, M. M. (1996). Detection of all single-base mismatches in solution by chemiluminescence. *Nucleic Acids Research*, *24*(24), 4998–5003. https://doi.org/10.1093/nar/24.24.4998

108. Natrajan, A., JIANG, Q., SHARPE, D., & Law, S.-J. (2002). Near Infrared Chemiluminescent Acridinium Compounds And Uses Thereof. *190-848-241-315-360*, *US*, B1–B1. https://lens.org/190-848-241-315-360

109. Goto, M., Oka, S., Okuzumi, K., Kimura, S., & Shimada, K. (1991). Evaluation of acridinium-ester-labeled DNA probes for identification of Mycobacterium tuberculosis and Mycobacterium avium-Mycobacterium intracellulare complex in culture. *Journal of Clinical Microbiology*, *29*(11), 2473–2476.

110. Lee, H. H., Morse, S. A., Olsvik, Ørjan., Orum, H., Kessler, C., Koch, T., Lee, H. H., Morse, S. A., & Olsvik, Ørjan. (2011). Nucleic Acid Amplification Technologies Application to Disease Diagnosis. In *Nucleic Acid Amplification Technologies Application to Disease Diagnosis*. Birkhäuser Boston. https://doi.org/10.1007/978-1-4612-2454-9

111. Jonas, V., Alden, M. J., Curry, J. I., Kamisango, K., Knott, C. A., Lankford, R., Wolfe, J. M., & Moore, D. F. (1993). Detection and identification of Mycobacterium tuberculosis directly from sputum sediments by amplification of rRNA. *Journal of Clinical Microbiology*, *31*(9), 2410–2416. http://www.ncbi.nlm.nih.gov/pubmed/8408564

112. Ichiyama, S., Iinuma, Y., Tawada, Y., Yamori, S., Hasegawa, Y., Shimokata, K., & Nakashima, N. (1996). Evaluation of gen-probe amplified mycobacterium tuberculosis direct test and roche PCR-microwell plate hybridization method (AMPLICOR MYCOBACTERIUM) for direct detection of mycobacteria. *Journal of Clinical Microbiology*, *34*(1), 130–133.

113. Collins, M. L., Irvine, B., Tyner, D., Fine, E., Zayati, C., Chang, C. A., Horn, T., Ahle, D., Detmer, J., Shen, L. P., Kolberg, J., Bushnell, S., Urdea, M. S., & Ho, D. D. (1997). A branched DNA signal amplification assay for quantification of nucleic acid targets below 100 molecules/ml. *Nucleic Acids Research*, *25*(15), 2979–2984. https://doi.org/10.1093/nar/25.15.2979

114. Crotchfelt, K. A., Pare, B., Gaydos, C., & Quinn, T. C. (1998). Detection of Chlamydia trachomatis by the Gen-Probe AMPLIFIED Chlamydia Trachomatis Assay (AMP CT) in urine specimens from men and women and endocervical specimens from women. *Journal of Clinical Microbiology*, *36*(2), 391–394. http://www.ncbi.nlm.nih.gov/pubmed/9466747

115. Matthews, J. A., & Kricka, L. J. (1988). Analytical strategies for the use of DNA probes. In *Analytical Biochemistry* (Vol. 169, Issue 1, pp. 1–25). https://doi.org/10.1016/0003-2697(88)90251-5

116. Mozola, M. A. (2000). Detection of microorganisms in foods using DNA probes targeted to ribosomal RNA sequences. *Food Biotechnology*, *14*(3), 173–194. https://doi.org/10.1080/08905430009549986

117. Arnold, Jr. et al. (1993). *Acridinium ester labelling and purification of nucleotide probes* (Patent No. US5185439A).

118. Morris, C. A., Owen, J. R., Thomas, M. C., El-Hiti, G. A., Harwood, J. L., & Kille, P. (2014). Intracellular localization and induction of a dynamic RNA-editing event of macro-algal V-ATPase subunit A (VHA-A) in response to copper. *Plant, Cell and Environment*, *37*(1), 189–203. https://doi.org/10.1111/pce.12145

119. Morris, C. A., El-Hiti, G., Weeks, I., Woodhead, S., Smith, K., & Kille, P. (2012). Utilising chemiluminescent methods for animal-free toxicology tests. *Toxicology Letters*, *211*, S104–S105. https://doi.org/10.1016/j.toxlet.2012.03.390

120. Morris, C. A., El-Hiti, G. A., Weeks, I., Woodhead, S., Smith, K., & Kille, P. (2017). Quantitative analysis of gene expression changes in response to genotoxic compounds. *Toxicology in Vitro*, *39*, 15–28. https://doi.org/10.1016/j.tiv.2016.11.004

121. Batmanghelich, S., Stuart Woodhead, J., Smith, K., & Weeks, I. (1991). Synthesis and chemiluminescent evaluation of a series of phenyl N-alkylacridinium 9-carboxylates. *Journal of Photochemistry and Photobiology A: Chemistry*, *56*(2–3), 249–254. https://doi.org/10.1016/1010-6030(91)80025-D

122. Browne, K. A., Deheyn, D. D., Brown, R. C., & Weeks, I. (2012). Spectrally resolved chemiluminescent probes for sensitive multiplex molecular quantification. *Analytical Chemistry*, *84*(21), 9222–9229. https://doi.org/10.1021/ac3017423

123. Zomer, G., & Stavenuiter, J. F. C. (1989). Chemiluminogenic labels, old and new. *Analytica Chimica Acta*, *227*(C), 11–19. https://doi.org/10.1016/S0003-2670(00)82640-9

124. Wang, S., & Natrajan, A. (2015). Synthesis and properties of chemiluminescent acridinium esters with different N-alkyl groups. *RSC Advances*, *5*(26), 19989–20002. https://doi.org/10.1039/c5ra00334b

125. Lyle J. Arnold, Jr. ; N. C., & Nelson Calif, both of S. D. (1994). *Homogeneous Protection Assay* (Patent No. WO/1989/002476).

126. Law et al., JIANG, Q., FISCHER, W., UNGER, J. T., & KRODEL, E. K. (1994). *Long emission wavelength chemiluminescent compounds and their use in test assays* (Patent No. WO/1994/021823).

127. Say-Jung Law Mass; Chariklia Sotiriou-Levenis Rolla Mo.; Anand Natrajan Manchester, W., N.H; Qingping Jiang, N., Mass_; Peter B_ Connolly' Walpole' Mass; John P. Kilroy Mass.;, B., & Constance R. McCudden Mass; Stephen M. 'l'irrell Franklin Mass., B. (1997). *Functionaized Hydrophilic Acridinium Esters*.

128. Natrajan, A., & Wen, D. (2011). Facile N-alkylation of acridine esters with 1,3-propane sultone in ionic liquids. *Green Chemistry*, *13*(4), 913. https://doi.org/10.1039/c0gc00758g

129. Bronstein, I., & Martin, C. (1993). Chemiluminescence immunoassay. Ian Weeks, Comprehensive Analytical Chemistry. Volume XXIX Elsevier Science Publishers, Amsterdam (1992), 294 pages, Dfl. 295.00, ISBN 0-444-89035-1. *Journal of Bioluminescence and Chemiluminescence*, *8*(6), 331. https://doi.org/10.1002/bio.1170080607

130. Smith, K., Li, Z., Yang, J. J., Weeks, I., & Woodhead, J. S. (2000). Synthesis and properties of novel chemiluminescent biological probes: Substituted 4-(2-succinimidyloxycarbonylethyl)phenyl 10-methylacridinium-9-carboxylate trifluoromethanesulphonate. *Journal of Photochemistry and Photobiology A: Chemistry*, *132*(3), 181–191. https://doi.org/10.1016/S1010-6030(00)00209-4

131. Smith, K., Yang, J.-J., Li, Z., Weeks, I., & Woodhead, J. S. (2009). Synthesis and properties of novel chemiluminescent biological probes: 2- and 3-(2-Succinimidyloxycarbonylethyl)phenyl acridinium esters. In *Journal of Photochemistry and Photobiology A: Chemistry*. https://doi.org/https://doi.org/10.1016/j.jphotochem.2008.12.020

132. Zomer et al. (2000). *Acridinium Compounds As Chemiluminogenic Label, [Patent]*.

133. Li, Z., Weeks, I., Woodhead, J. S., Yang, J.-J. J., Smith, K., Yang, J.-J. J., Li, Z., Weeks, I., & Woodhead, J. S. (2009). Synthesis and properties of novel chemiluminescent biological probes: 2- and 3-(2-Succinimidyloxycarbonylethyl)phenyl acridinium esters. *Journal of Photochemistry and Photobiology A: Chemistry*, *203*(1), 72–79. https://doi.org/10.1016/j.jphotochem.2008.12.020

134. Zadykowicz, B., Czechowska, J., Ozóg, A., Renkevich, A., & Krzymiński, K. (2016). Effective chemiluminogenic systems based on acridinium esters bearing substituents of various electronic and steric properties. *Organic and Biomolecular Chemistry*, *14*(2), 652–668. https://doi.org/10.1039/c5ob01798j

135. Krzymiński, K., Ozóg, A., Malecha, P., Roshal, A. D., Wróblewska, A., Zadykowicz, B., & Błazejowski, J. (2011). Chemiluminogenic features of 10-Methyl-9-(phenoxycarbonyl)acridinium Trifluoromethanesulfonates alkyl substituted at the benzene ring in aqueous media. *Journal of Organic Chemistry*, *76*(4), 1072–1085. https://doi.org/10.1021/jo1020882

136. Kricka, L. J. (2003). Clinical applications of chemiluminescence. *Analytica Chimica Acta*, *500*(1–2), 279–286. https://doi.org/10.1016/S0003-2670(03)00809-2

137. Roshal, A. D., Zadykowicz, B., & Białk-bielin, A. (2010). *Chemiluminogenic Properties of 10-Methyl-9- (phenoxycarbonyl) acridinium Cations in*. 10550–10562.

138. Natrajan, A., & Wen, D. (2014). Effect of branching in remote substituents on light emission and stability of chemiluminescent acridinium esters. *RSC Adv.*, *4*(42), 21852–21863. https://doi.org/10.1039/C4RA02516D

139. Guilbault, G. G. (1990). *Practical Fluorescence, Second Edition* (G. G. Guilbault, Ed.; 2nd Edition). CRC Press. https://doi.org/10.1201/9781003066514

140. B, L. S., & Berlman, I. B. (2002). Handbook of fluorescence spectra of aromatic molecules. In *Journal of Molecular Structure* (Vol. 13, Issue 1, p. 140). Academic Press. https://doi.org/10.1016/0022-2860(72)87041-8

141. Miron, T., & Wilchek, M. (1982). A spectrophotometric assay for soluble and immobilized N-hydroxysuccinimide esters. In *Analytical Biochemistry* (Vol. 126, Issue 2, pp. 433–435). Academic Press. https://doi.org/10.1016/0003-2697(82)90540-1

142. Sharma, B. K., Shaikh, A. M., Agarwal, N., & Kamble, R. M. (2016). *Synthesis, photophysical and electrochemical studies of acridone-amine based donor-acceptors for hole transport materials †*. https://doi.org/10.1039/c5ra25115j

143. Kricka, L. J. (1991). Chemiluminescent and bioluminescent techniques. *Clinical Chemistry*, *37*(9), 1472–1481. https://doi.org/10.1016/0731-7085(87)80101-2

144. Natrajan, A., Qingping Jiang, David Sharpe, & Say-Jong Law. (2005). *High quantum yield acridinium compounds and there uses in improving assay sensetivity* (Patent No. US20080014660A1).

145. Natrajan, A., Sharpe, D., Costello, J., & Jiang, Q. (2010). Enhanced immunoassay sensitivity using chemiluminescent acridinium esters with increased light output. *Analytical Biochemistry*, *406*(2), 204–213. https://doi.org/10.1016/j.ab.2010.07.025

146. Weeks, I., Campbell, a K., & Woodhead, J. S. (1983). Two-site immunochemiluminometric assay for human alpha 1-fetoprotein. *Clinical Chemistry*, *29*(8), 1480–1483.

147. Woodhead, J. S., & Weeks, I. (1991). Immunochemiluminometric assays based on acridinium labels with a microtiter plate luminometer. In *Clinical Chemistry* (Vol. 37, Issue 3, p. 472).

148. R. Rodriguez-Orozco, A., Ruiz-Reyes, H., & Medina-Serriteno, N. (2010). Recent Applications of Chemiluminescence Assays in Clinical Immunology. *Mini-Reviews in Medicinal Chemistry*, *10*(14), 1393–1400. https://doi.org/10.2174/138955710793564142

149. Thomas-Jones, E., Thorpe, K., Harrison, N., Thomas, G., Morris, C., Hutchinson, T., Woodhead, S., & Tyler, C. (2003). Dynamics of estrogen biomarker responses in rainbow trout exposed to 17β-estradiol and 17α-ethinylestradiol. *Environmental Toxicology and Chemistry*, *22*(12), 3001–3008. https://doi.org/10.1897/03-31

150. White, S., Szewczyk, J. W., Turner, J. M., Baird, E. E., & Dervan, P. B. (1998). Recognition of the four Watson-Crick base pairs in the DNA minor groove by synthetic ligands. *Nature*, *391*(6666), 468–471. https://doi.org/10.1038/35106

151. Batmanghelich, S., Brown, R. C., Stuart Woodhead, J., Weeks, I., & Smith, K. (1992). Preparation of a chemiluminescent imidoester for the non-radioactive labelling of proteins. *Journal of Photochemistry and Photobiology, B: Biology*, *12*(2), 193–201. https://doi.org/10.1016/1011-1344(92)85008-I
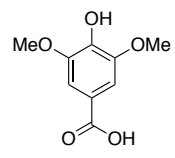
Chapter 8
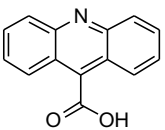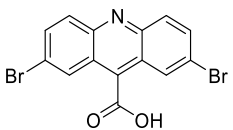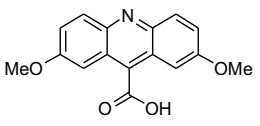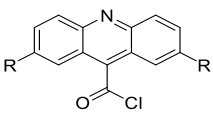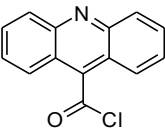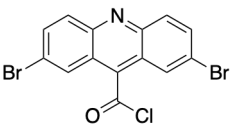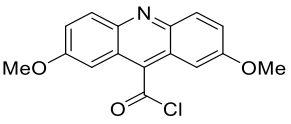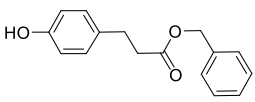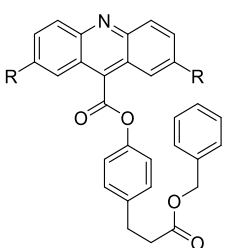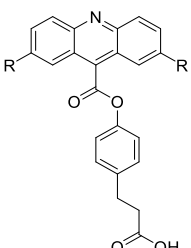
Appendix
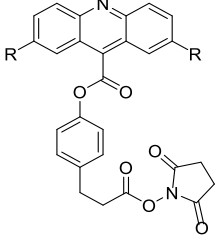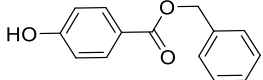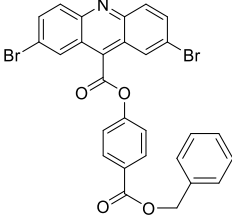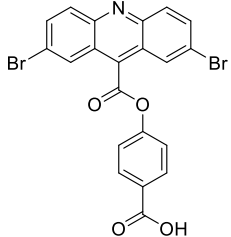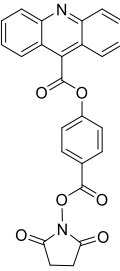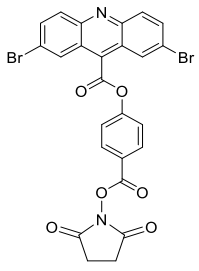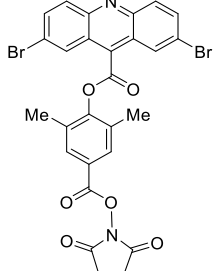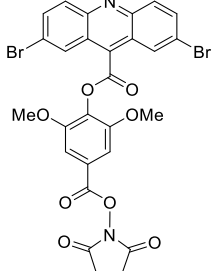
8 Appendix
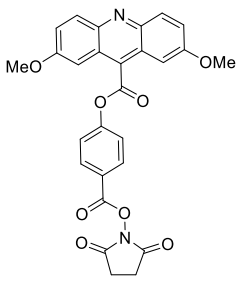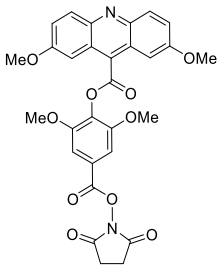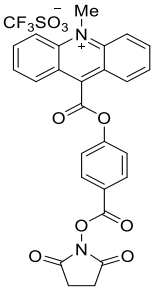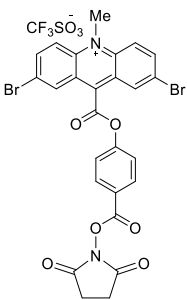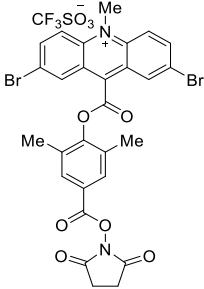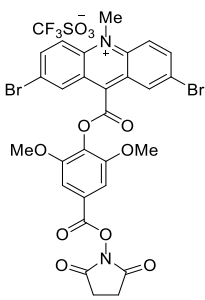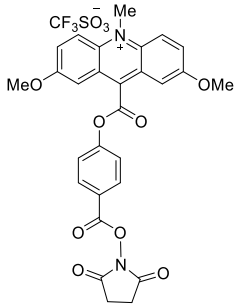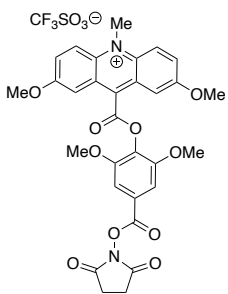
8.1 Compounds list
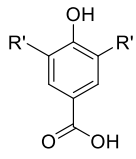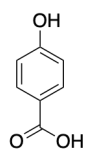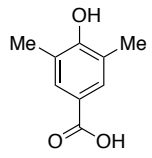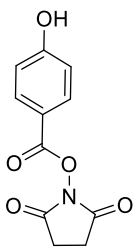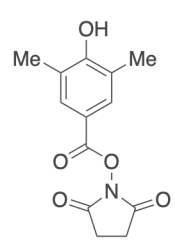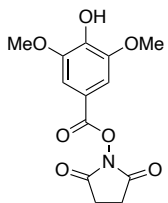
Comp. ID	Chemical structure	Comp. ID	Chemical structure
1		2	
3x		3b	
3c		4	
5		6	
7		8	
9		10	

Comp. ID	Chemical structure	Comp. ID	Chemical structure
11		12	
13		14	
15		16	
17		18	
19		20	
21		22	

Comp. ID	Chemical structure	Comp. ID	Chemical structure
24a		24b	
24c		25	
25a		25b	
25c		26	
27		28	

Comp. ID	Chemical structure	Comp. ID	Chemical structure
29		30x	
31bx		32bx	
33ax		33bx	
33by		33bz	

Comp. ID	Chemical structure	Comp. ID	Chemical structure
33cx		33cz	
34ax		34bx	
34by		34bz	
34cx		34cz	

Comp. ID	Chemical structure	Comp. ID	Chemical structure
35		35a	
35b		35c	
36x		36y	
36z		x	x